Unresolved Anomalies and Tensions in the Standard Cosmological Model

February 14th 2024
Nishinomiya-Yukawa Symposium
"General Relativity and Beyond"

Eleonora Di Valentino
Royal Society Dorothy Hodgkin Research Fellow
School of Mathematics and Statistics
University of Sheffield (UK)

University of Sheffield

THE ROYAL SOCIETY

The ΛCDM model

Out of various cosmological models proposed in literature,
the Lambda cold dark matter (ΛCDM) scenario has been chosen
as the standard model for its simplicity and ability to accurately describe
a wide range of astrophysical and cosmological observations.

However, ΛCDM still has many unknown areas and lacks the ability to explain
fundamental concepts related to the structure and evolution of the universe.
These concepts are based on three unknown ingredients that are not supported by
theoretical first principles or laboratory experiments
but are instead inferred from cosmological and astrophysical observations.

The three unknown ingredients are:
inflation, dark matter (DM), and dark energy (DE).
In ΛCDM, inflation is given by a single, slow-rolling scalar field;
DM is assumed to interact only through gravity,
be cold and pressureless, and lack direct evidence of its existence;
DE is represented by the cosmological constant term Λ,
without any strong physical explanation.

The ΛCDM model

Despite its theoretical shortcomings, ΛCDM remains the preferred model due to its ability to accurately describe observed phenomena.
However, the ΛCDM model with its six parameters is not based on deep-rooted physical principles and should be considered, at best, an approximation of an underlying physical theory that remains undiscovered.

Hence, as observations become more numerous and accurate, deviations from the ΛCDM model are expected to be detected.
And in fact, discrepancies in important cosmological parameters, such as H0, have already arisen in various observations with different statistical significance.

While some of these tensions may have a systematic origin, their recurrence across multiple probes suggests that there may be flaws in the standard cosmological scenario, and that new physics may be necessary to explain these observational shortcomings.

Therefore, the persistence of these tensions could indicate the failure of the canonical ΛCDM model.

What is H0?

The Hubble constant H0 describes the expansion rate of the Universe today.

This can be obtained in two ways:

1. measuring the luminosity distance and the recessional velocity of known galaxies, and computing the proportionality factor.

Hubble's Law

$$v = H_0\, D$$

This approach is model independent and based on geometrical measurements.

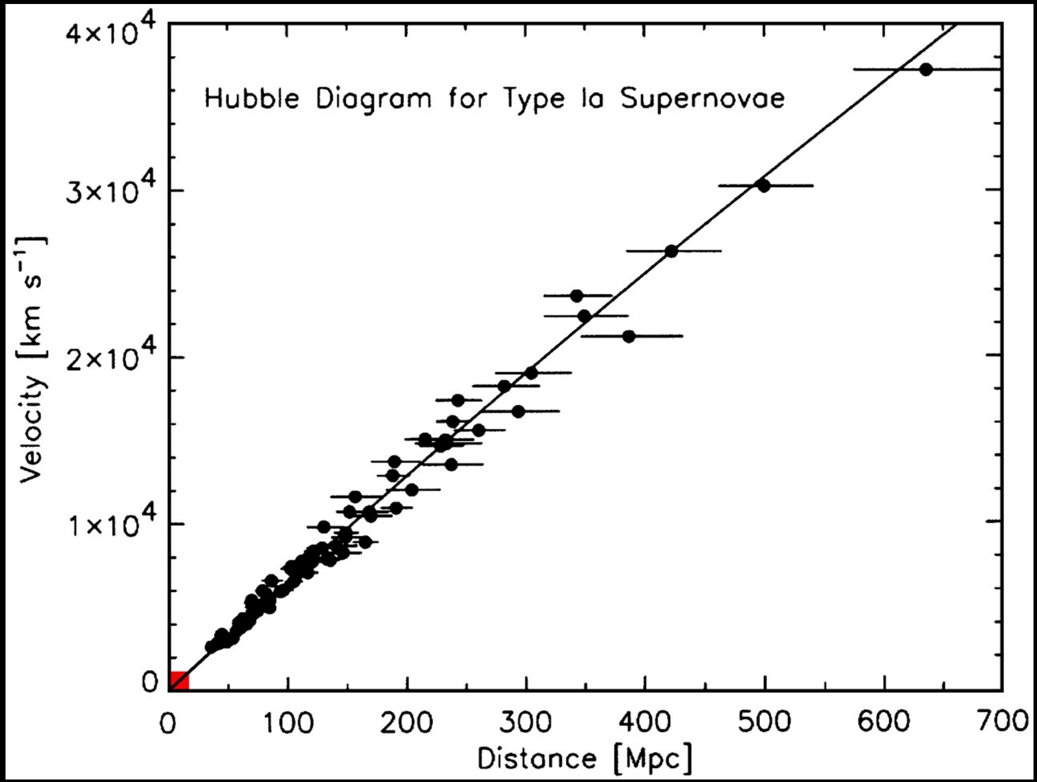

Jha, S. (2002) Ph.D. thesis (Harvard Univ., Cambridge, MA).

What is H0?

The Hubble constant H0 describes the expansion rate of the Universe today.

This can be obtained in two ways:

1. measuring the luminosity distance and the recessional velocity of known galaxies, and computing the proportionality factor.
2. considering early universe measurements, and assuming a model for the expansion history of the universe.

For example, we have CMB measurements and we assume the standard model of cosmology, i.e. the ΛCDM scenario.

1st Friedmann equations describes the expansion history of the universe:

$$H^2(z) = H_0^2 \left(\Omega_m(1+z)^3 + \Omega_k(1+z)^2 + \Omega_\Lambda\right).$$

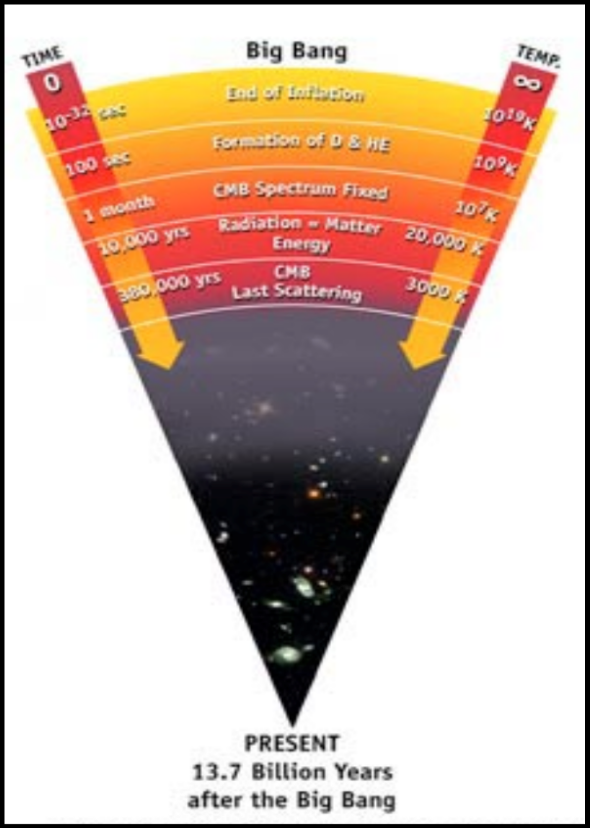

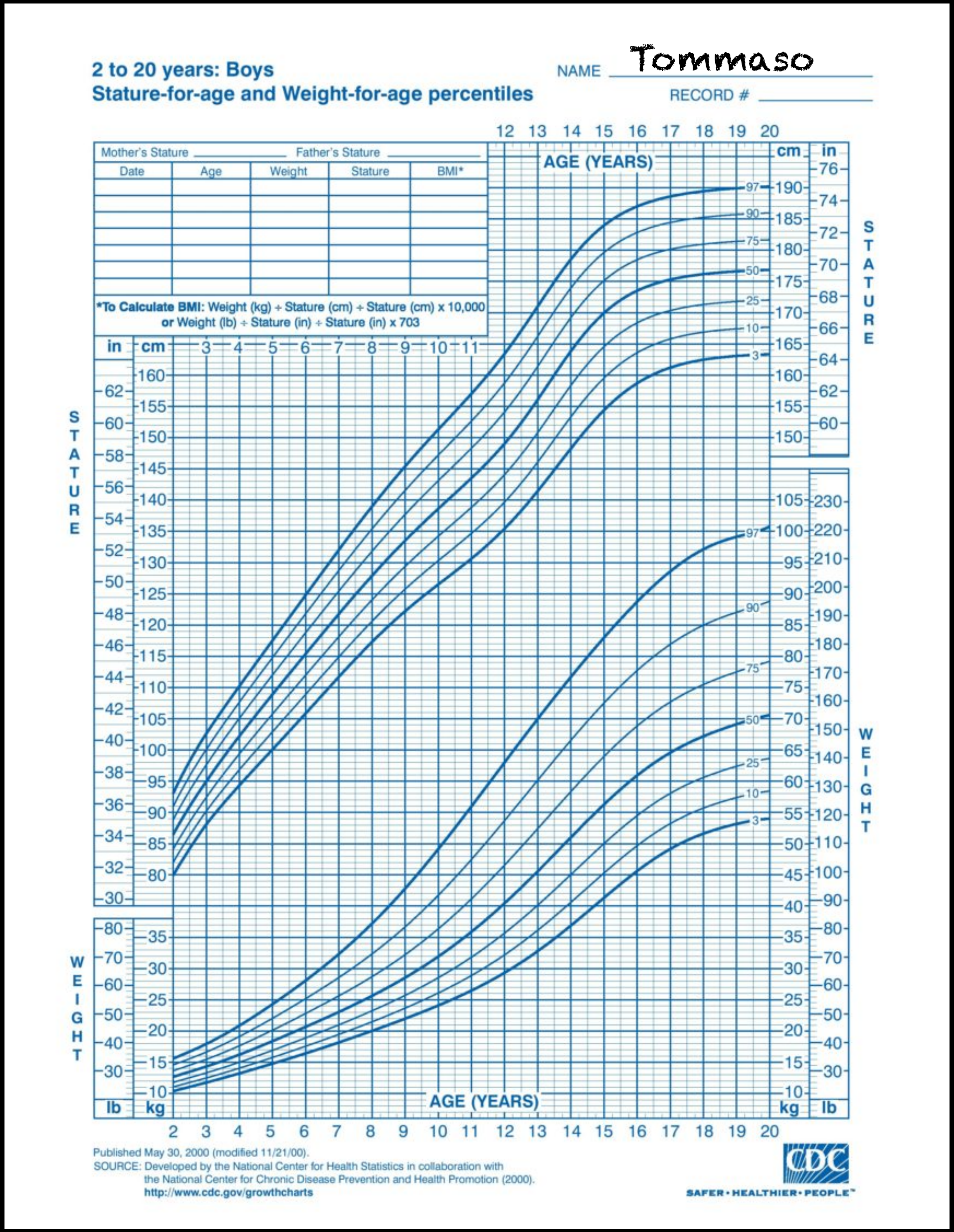
2 to 20 years: Boys
Stature-for-age and Weight-for-age percentiles
NAME Tommaso
RECORD #
Mother's Stature
Father's Stature
Date
Age
Weight
Stature
BMI*
*To Calculate BMI: Weight (kg) ÷ Stature (cm) ÷ Stature (cm) x 10,000
or Weight (lb) ÷ Stature (in) ÷ Stature (in) x 703
AGE (YEARS)
STATURE
WEIGHT
in
cm
kg
lb
Published May 30, 2000 (modified 11/21/00).
SOURCE: Developed by the National Center for Health Statistics in collaboration with
the National Center for Chronic Disease Prevention and Health Promotion (2000).
http://www.cdc.gov/growthcharts
CDC
SAFER · HEALTHIER · PEOPLE™

H0 tension

If we compare the H0 estimates using these 2 methods they disagree.

The Planck estimate assuming a "vanilla" ΛCDM cosmological model:
$H0 = 67.36 \pm 0.54$ km/s/Mpc

Planck 2018, Astron.Astrophys. 641 (2020) A6

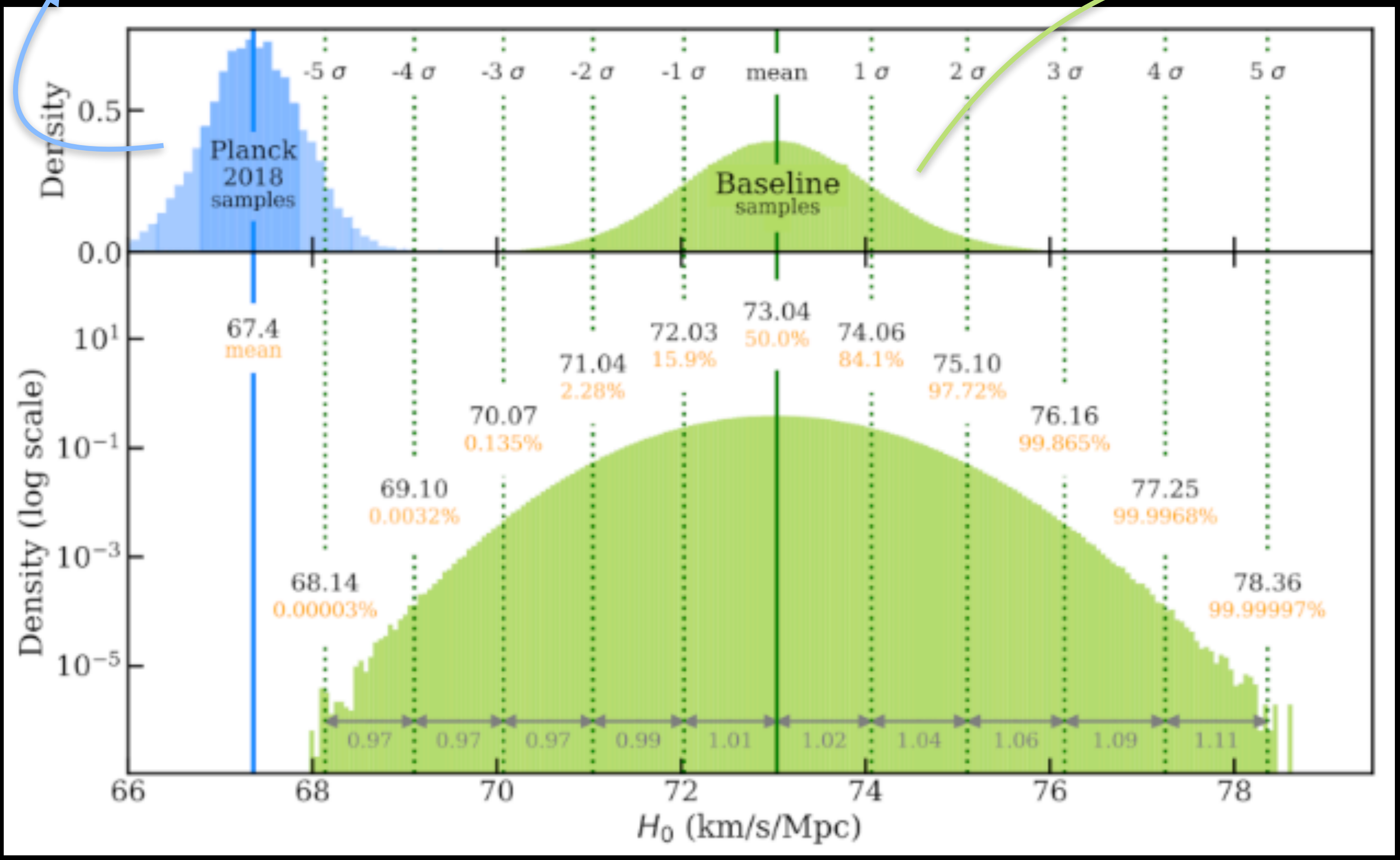

The latest local measurements obtained by the SH0ES collaboration

$H0 = 73.04 \pm 1.04$ km/s/Mpc

Riess et al. arXiv:*2112.04510*

5σ = one in 3.5 million implausible to reconcile the two by chance

The Planck estimate assuming a “vanilla" ΛCDM cosmological model:

$H0 = 67.36 \pm 0.54$ km/s/Mpc

Planck 2018, Astron.Astrophys. 641 (2020) A6

Distance Ladder

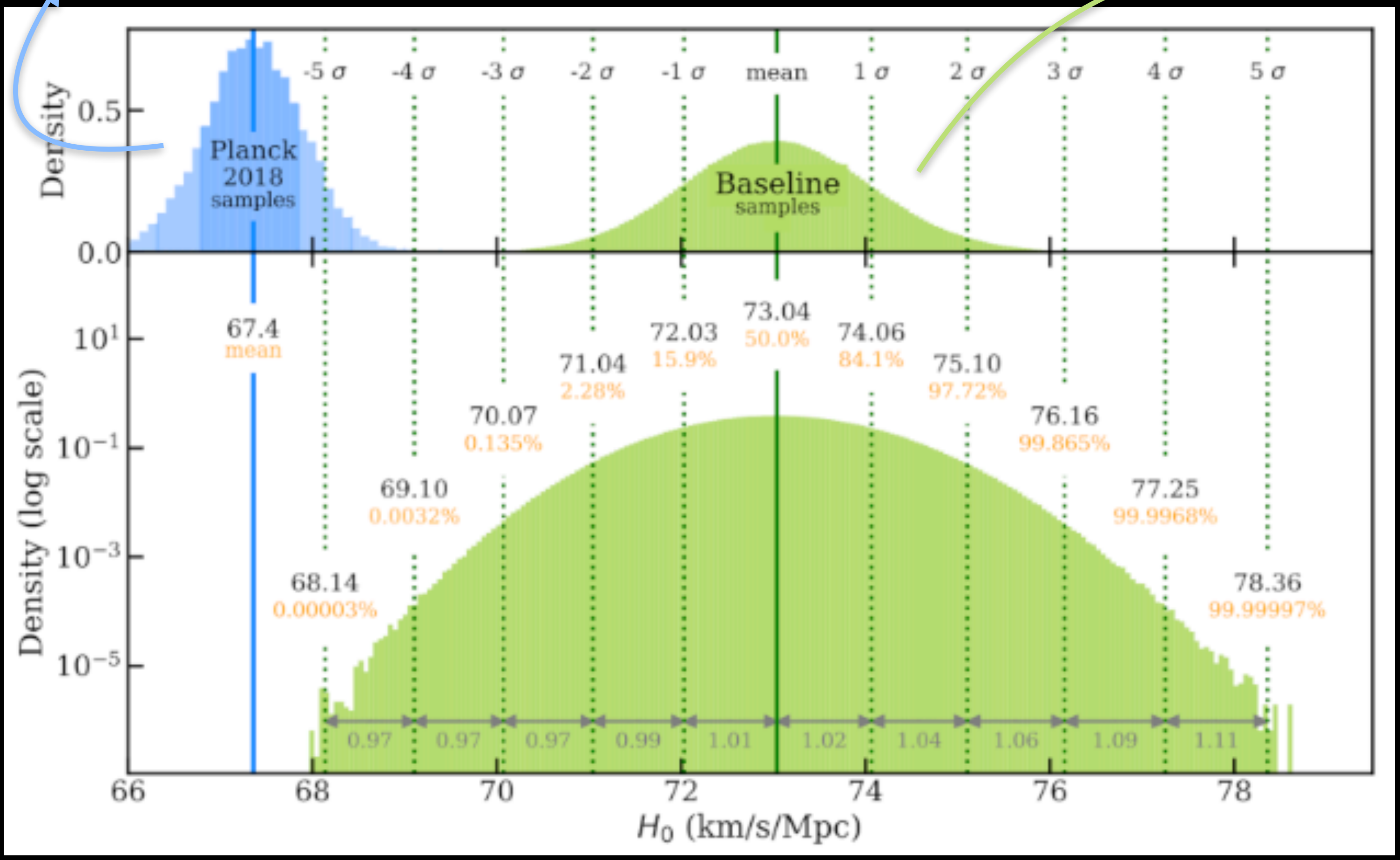

The latest local measurements obtained by the SH0ES collaboration

$H0 = 73.04 \pm 1.04$ km/s/Mpc

Riess et al. arXiv:*2112.04510*

Distance Ladder

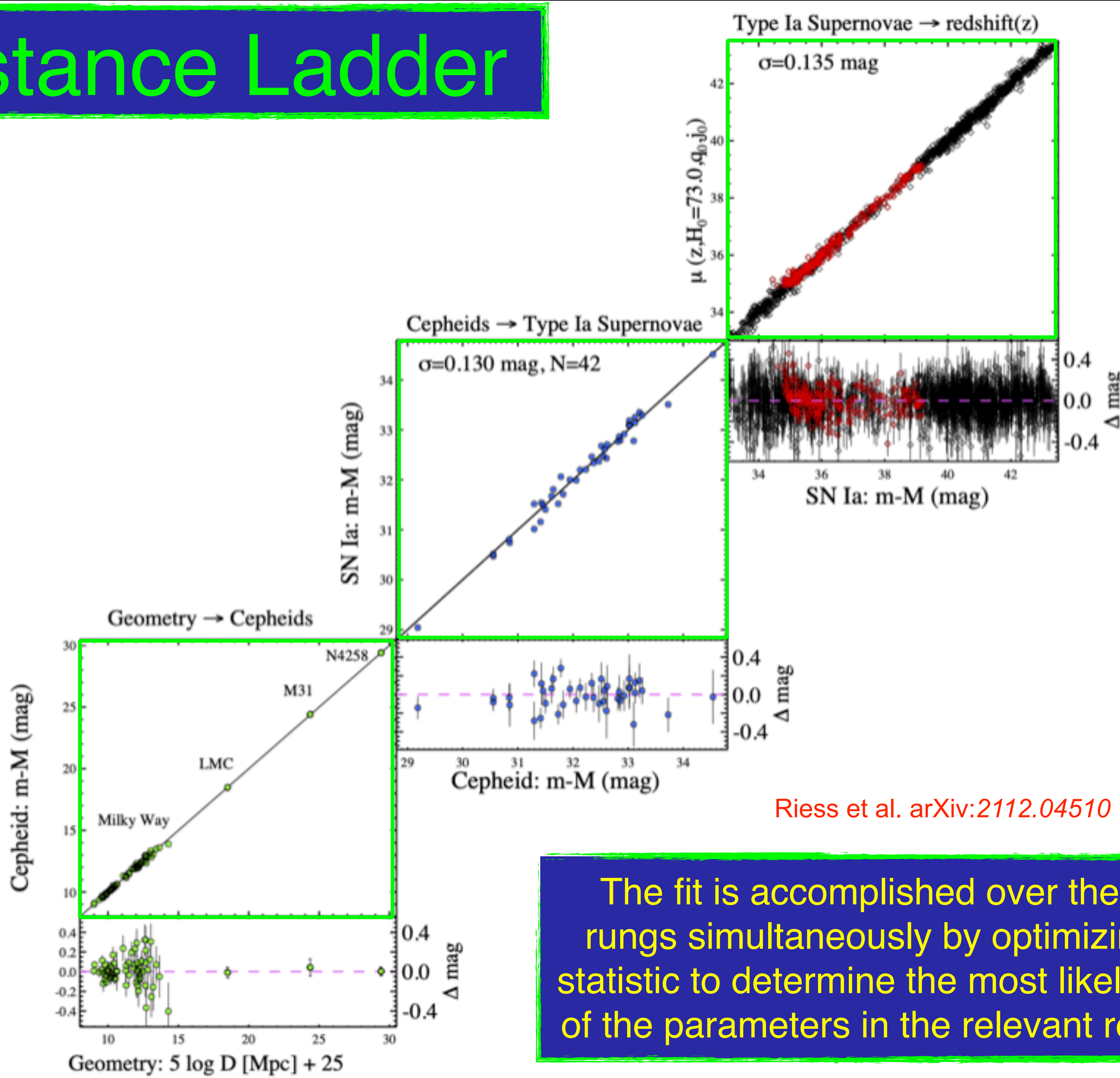

Riess et al. arXiv:*2112.04510*

The fit is accomplished over the three rungs simultaneously by optimizing a χ^2 statistic to determine the most likely values of the parameters in the relevant relations.

Distance Ladder

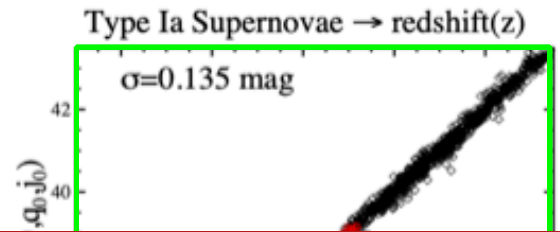

arXiv > astro-ph > arXiv:2306.00070

Search...

Help | Advanced

Astrophysics > Cosmology and Nongalactic Astrophysics

[Submitted on 31 May 2023]

Leveraging SN Ia spectroscopic similarity to improve the measurement of H_0

Yukei S. Murakami, Adam G. Riess, Benjamin E. Stahl, W. D'Arcy Kenworthy, Dahne-More A. Pluck, Antonella Macoretta, Dillon Brout, David O. Jones, Dan M. Scolnic, Alexei V. Filippenko

Recent studies suggest spectroscopic differences explain a fraction of the variation in Type Ia supernova (SN Ia) luminosities after light-curve/color standardization. In this work, (i) we empirically characterize the variations of standardized SN Ia luminosities, and (ii) we use a spectroscopically inferred parameter, SIP, to improve the precision of SNe Ia along the distance ladder and the determination of the Hubble constant (H_0). First, we show that the \texttt{Pantheon+} covariance model modestly overestimates the uncertainty of standardized magnitudes by $\sim$ 7%, in the parameter space used by the SH0ES Team to measure H_0 ; accounting for this alone yields $H_0 = 73.01 \pm 0.92$ km s^{-1} Mpc^{-1} . Furthermore, accounting for spectroscopic similarity between SNe~Ia on the distance ladder reduces their relative scatter to ~ 0.12 mag per object (compared to ~ 0.14 mag previously). Combining these two findings in the model of SN covariance, we find an overall 14% reduction (to ± 0.85km s^{-1} Mpc^{-1}) of the uncertainty in the Hubble constant and a modest increase in its value. Including a budget for systematic uncertainties itemized by Riess et al. (2022a), we report an updated local Hubble constant with $\sim 1.2\%$ uncertainty, $H_0 = 73.29 \pm 0.90$km s^{-1} Mpc^{-1} . We conclude that spectroscopic differences among photometrically standardized SNe Ia do not explain the ``Hubble tension." Rather, accounting for such differences increases its significance, as the discrepancy against ΛCDM calibrated by the *Planck* 2018 measurement rises to 5.7σ.

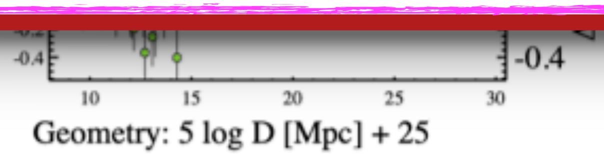

CMB constraints

The Planck estimate assuming a “vanilla"
ΛCDM cosmological model:
H0 = 67.36 ± 0.54 km/s/Mpc
Planck 2018, Astron.Astrophys. 641 (2020) A6

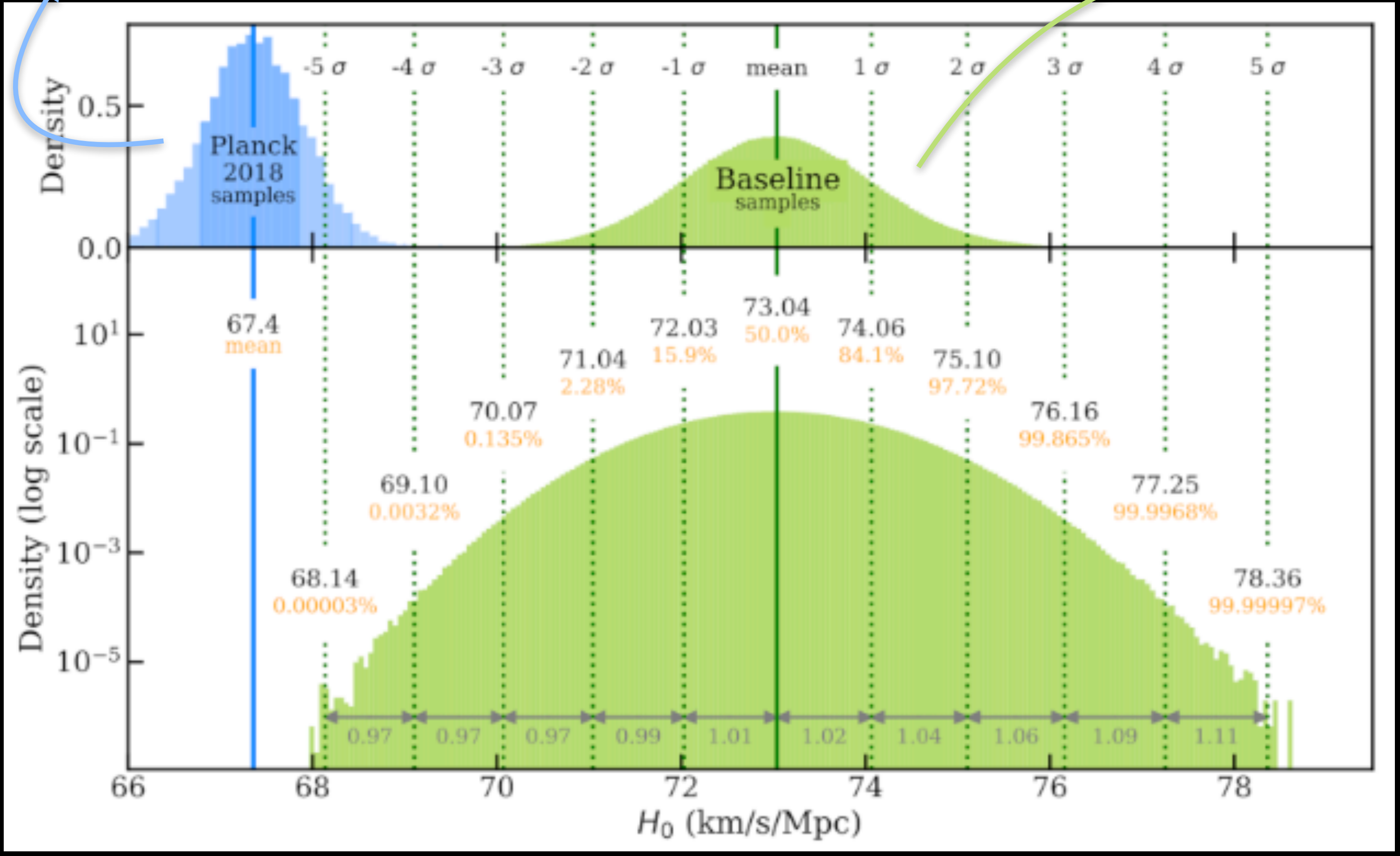

The latest local measurements obtained by the SH0ES collaboration

H0 = 73.04 ± 1.04 km/s/Mpc

Riess et al. arXiv:*2112.04510*

CMB constraints

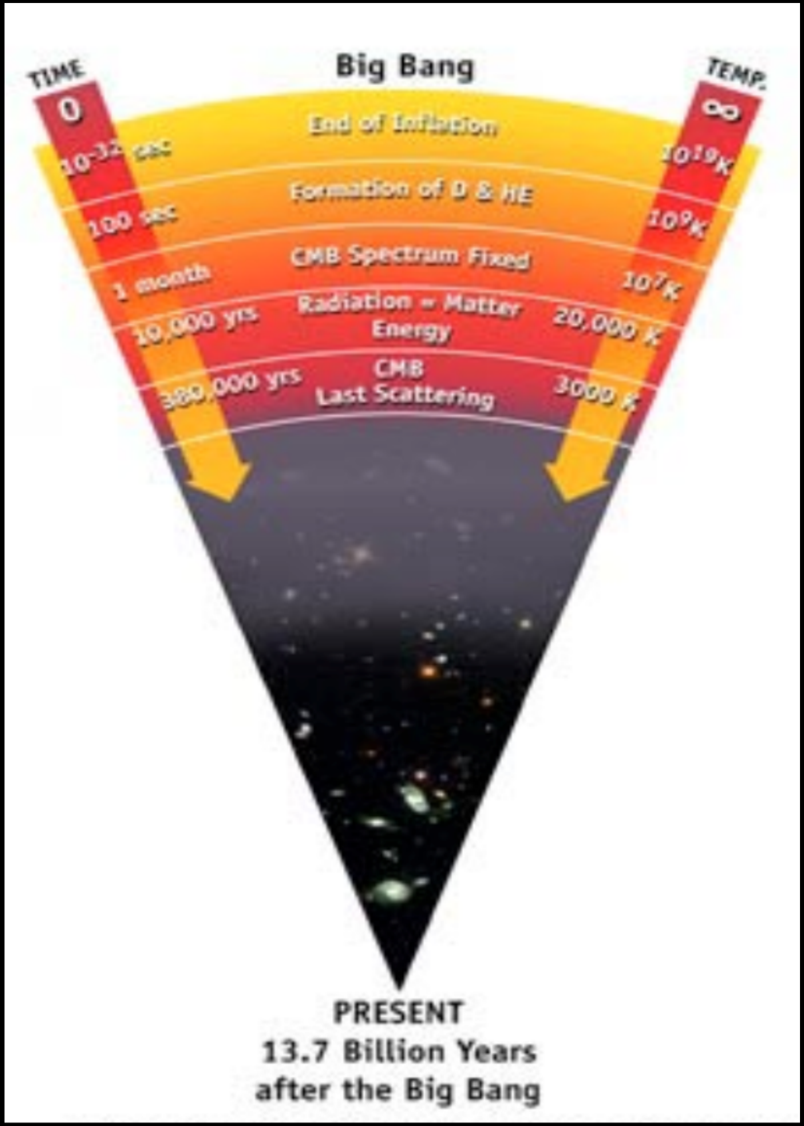

Figura: http://wmap.gsfc.nasa.gov

The Universe originates from a hot Big Bang.

The primordial plasma in thermodynamic equilibrium cools with the expansion of the Universe. It goes through the phase of recombination, where electrons and protons combine into hydrogen atoms, and decoupling, where the Universe becomes transparent to the motion of photons.

The Cosmic Microwave Background (CMB) is the radiation coming from recombination, emitted about 13 billion years ago, just 380,000 years after the Big Bang.

The CMB retains the shape of the primordial universe in which photons were in thermodynamic equilibrium, displaying a black-body spectrum that has cooled with the expansion of the universe, reaching a temperature of T=2.726K today.
This radiation coming from all directions is almost homogeneous, but also offers an image of the minuscule density differences present at recombination and bears witness to everything that happens to photons as they travel to us.
These effects result in small temperature variations among the photons themselves, on the order of 1/100000, known as anisotropies.

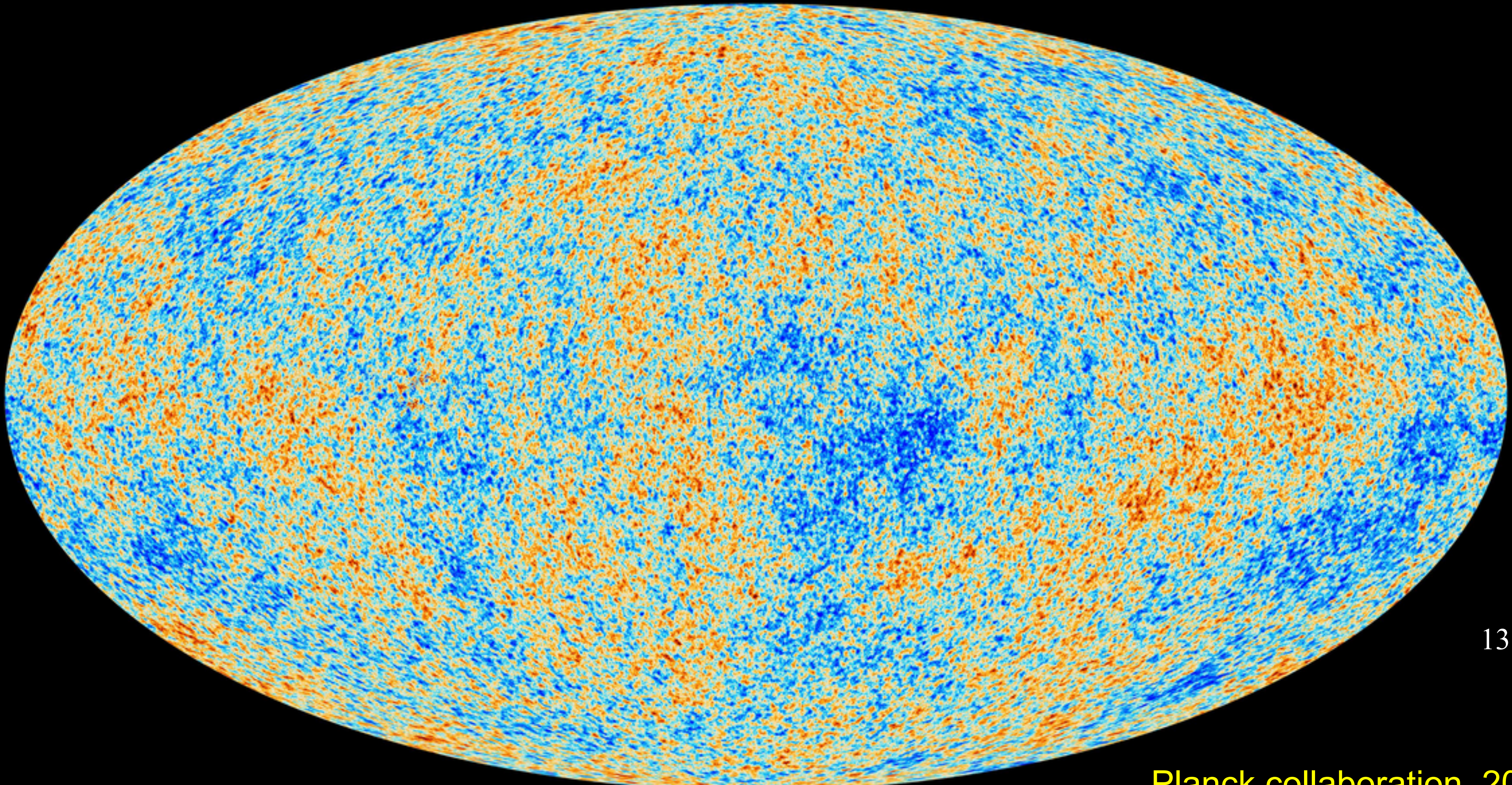

Planck collaboration, 2018

CMB constraints

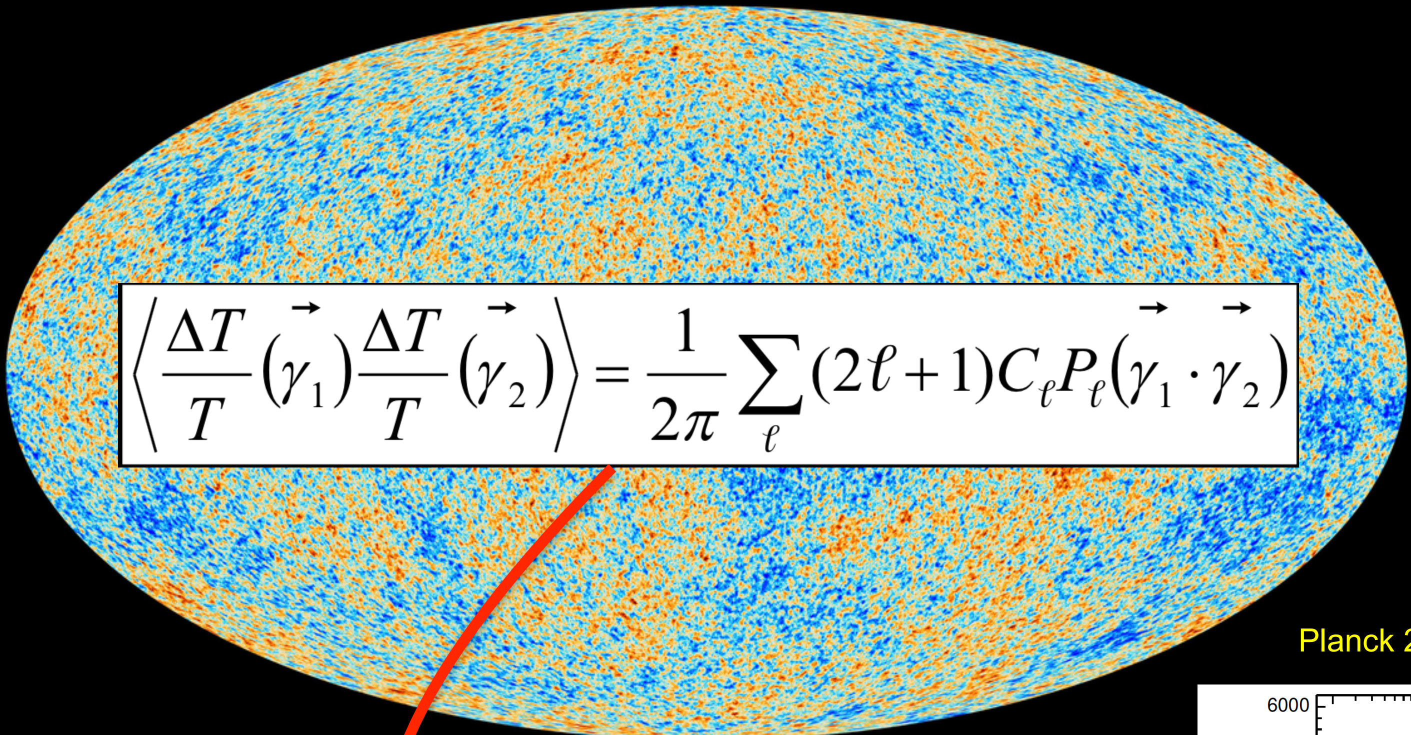

$$\left\langle \frac{\Delta T}{T}(\vec{\gamma}_1)\frac{\Delta T}{T}(\vec{\gamma}_2)\right\rangle = \frac{1}{2\pi}\sum_{\ell}(2\ell+1)C_\ell P_\ell(\vec{\gamma}_1\cdot\vec{\gamma}_2)$$

From the map of the CMB anisotropies we can extract the temperature angular power spectrum.

Planck 2018, Astron.Astrophys. 641 (2020) A6

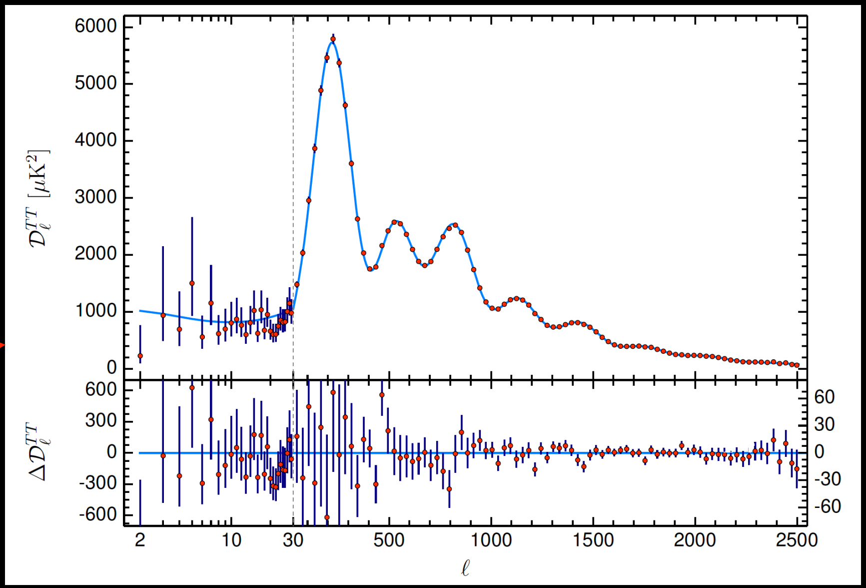

Cosmological parameters:
($\Omega_b h^2$, $\Omega_m h^2$, H0 , n_s , τ, As)

→ Theoretical model

We choose a set of cosmological parameters that describes our theoretical model and compute the angular power spectra. Because of the correlations present between the parameters, variation of different quantities can produce similar effects on the CMB.

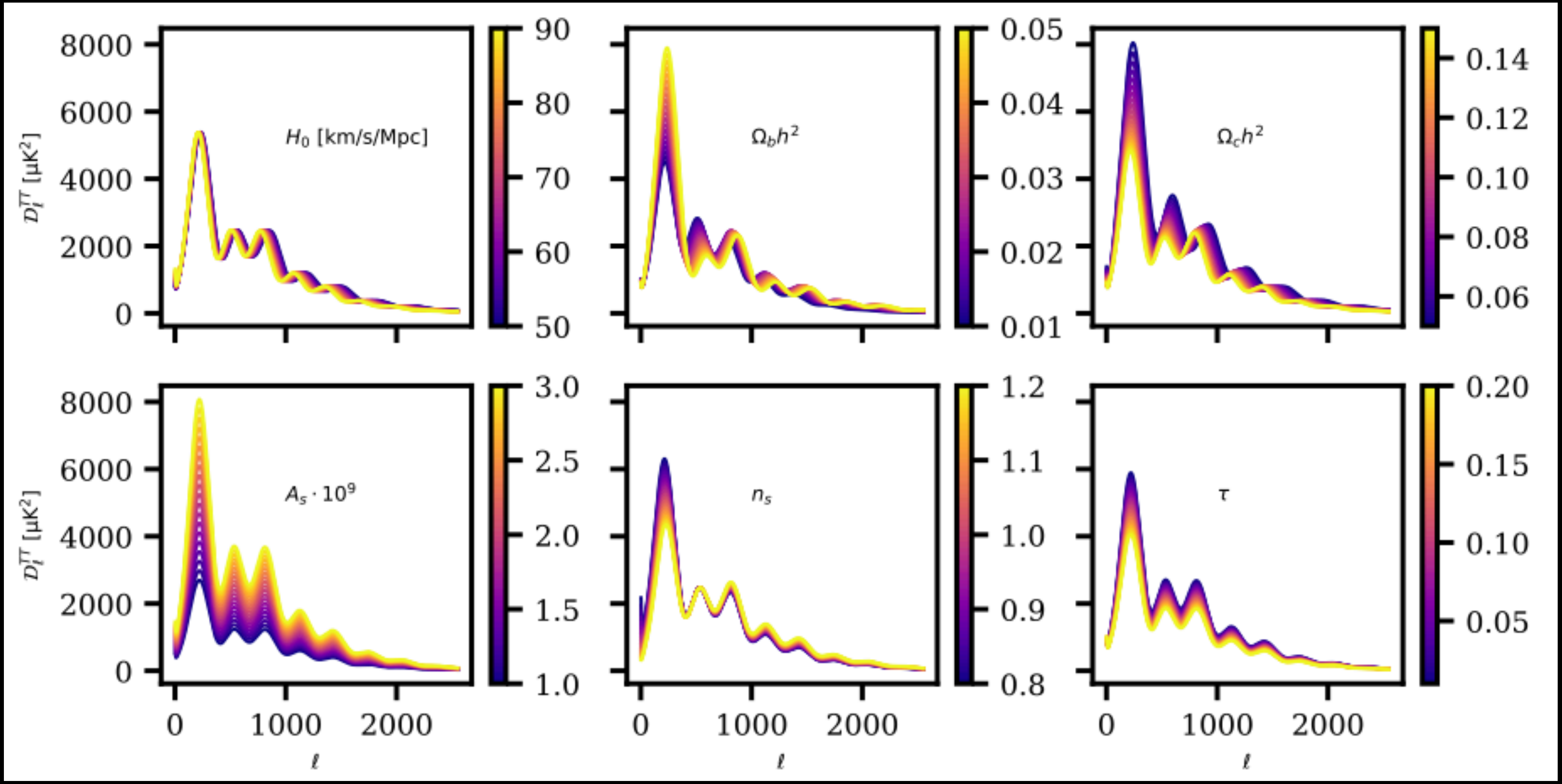

Lemos & Shah, arXiv:2307.13083

Cosmological parameters:
($\Omega_b h^2$, $\Omega_m h^2$, H0 , n_s , τ, As)

Theoretical model

We compare the angular power spectra we computed with the data and, using a bayesian analysis, we get a combination of cosmological parameter values in agreement with these.

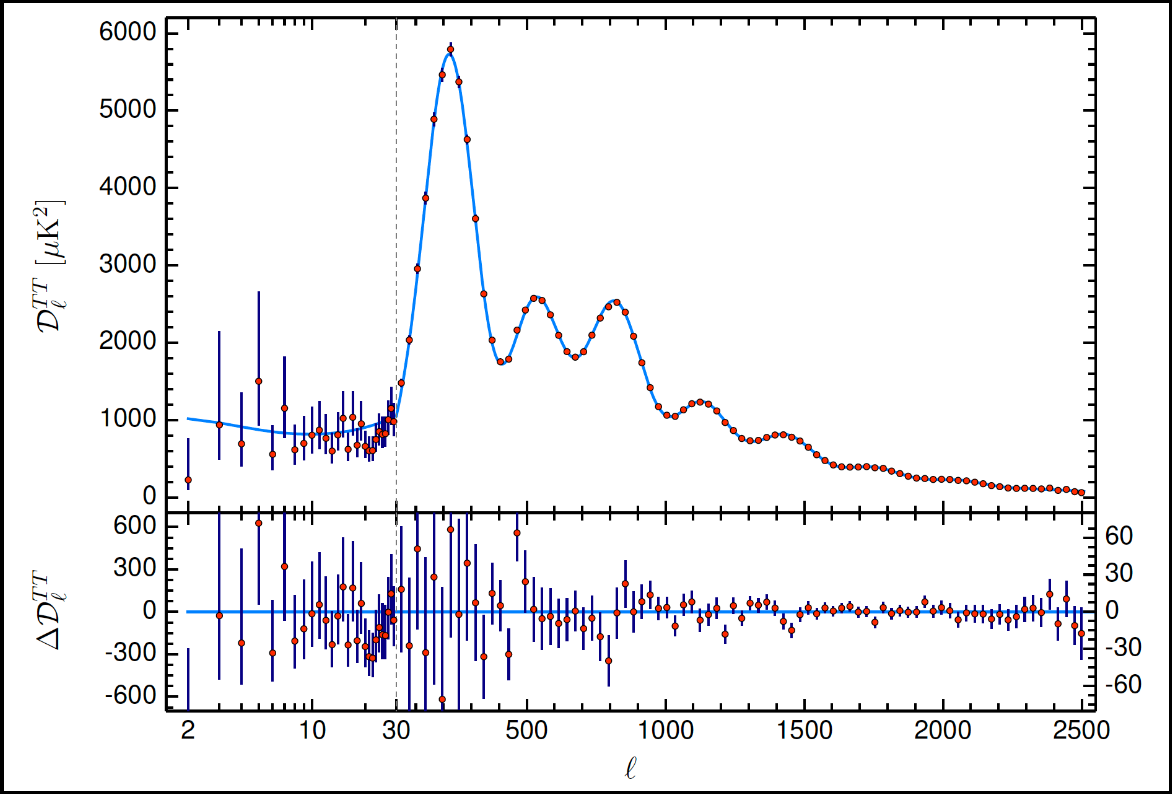

Planck 2018, Astron.Astrophys. 641 (2020) A6

Parameter constraints

CMB constraints

Parameter	TT+lowE 68% limits	TE+lowE 68% limits	EE+lowE 68% limits	TT,TE,EE+lowE 68% limits	TT,TE,EE+lowE+lensing 68% limits	TT,TE,EE+lowE+lensing+BAO 68% limits
$\Omega_b h^2$	0.02212 ± 0.00022	0.02249 ± 0.00025	0.0240 ± 0.0012	0.02236 ± 0.00015	0.02237 ± 0.00015	0.02242 ± 0.00014
$\Omega_c h^2$	0.1206 ± 0.0021	0.1177 ± 0.0020	0.1158 ± 0.0046	0.1202 ± 0.0014	0.1200 ± 0.0012	0.11933 ± 0.00091
$100\theta_{MC}$	1.04077 ± 0.00047	1.04139 ± 0.00049	1.03999 ± 0.00089	1.04090 ± 0.00031	1.04092 ± 0.00031	1.04101 ± 0.00029
τ	0.0522 ± 0.0080	0.0496 ± 0.0085	0.0527 ± 0.0090	$0.0544^{+0.0070}_{-0.0081}$	0.0544 ± 0.0073	0.0561 ± 0.0071
$\ln(10^{10} A_s)$	3.040 ± 0.016	$3.018^{+0.020}_{-0.018}$	3.052 ± 0.022	3.045 ± 0.016	3.044 ± 0.014	3.047 ± 0.014
n_s	0.9626 ± 0.0057	0.967 ± 0.011	0.980 ± 0.015	0.9649 ± 0.0044	0.9649 ± 0.0042	0.9665 ± 0.0038
H_0 [km s^{-1} Mpc^{-1}] . .	66.88 ± 0.92	68.44 ± 0.91	69.9 ± 2.7	67.27 ± 0.60	67.36 ± 0.54	67.66 ± 0.42
Ω_Λ	0.679 ± 0.013	0.699 ± 0.012	$0.711^{+0.033}_{-0.026}$	0.6834 ± 0.0084	0.6847 ± 0.0073	0.6889 ± 0.0056
Ω_m	0.321 ± 0.013	0.301 ± 0.012	$0.289^{+0.026}_{-0.033}$	0.3166 ± 0.0084	0.3153 ± 0.0073	0.3111 ± 0.0056
$\Omega_m h^2$	0.1434 ± 0.0020	0.1408 ± 0.0019	$0.1404^{+0.0034}_{-0.0039}$	0.1432 ± 0.0013	0.1430 ± 0.0011	0.14240 ± 0.00087
$\Omega_m h^3$	0.09589 ± 0.00046	0.09635 ± 0.00051	$0.0981^{+0.0016}_{-0.0018}$	0.09633 ± 0.00029	0.09633 ± 0.00030	0.09635 ± 0.00030
σ_8	0.8118 ± 0.0089	0.793 ± 0.011	0.796 ± 0.018	0.8120 ± 0.0073	0.8111 ± 0.0060	0.8102 ± 0.0060
$S_8 \equiv \sigma_8(\Omega_m/0.3)^{0.5}$.	0.840 ± 0.024	0.794 ± 0.024	$0.781^{+0.052}_{-0.060}$	0.834 ± 0.016	0.832 ± 0.013	0.825 ± 0.011

Planck 2018, Astron.Astrophys. 641 (2020) A6

2018 Planck results are a wonderful confirmation of the flat standard ΛCDM cosmological model, but are model dependent!

- The cosmological constraints are obtained assuming a cosmological model.
- The results are affected by the degeneracy between the parameters that induce similar effects on the observables.

CMB constraints

Parameter	TT+lowE 68% limits	TE+lowE 68% limits	EE+lowE 68% limits	TT,TE,EE+lowE 68% limits	TT,TE,EE+lowE+lensing 68% limits	TT,TE,EE+lowE+lensing+BAO 68% limits
$\Omega_b h^2$	0.02212 ± 0.00022	0.02249 ± 0.00025	0.0240 ± 0.0012	0.02236 ± 0.00015	0.02237 ± 0.00015	0.02242 ± 0.00014
$\Omega_c h^2$						0091
$100\theta_{MC}$						0029
τ						071
$\ln(10^{10} A_s)$						14
n_s						038
H_0 [km s^{-1} Mpc$^-$						42
Ω_Λ						056
Ω_m						056
$\Omega_m h^2$						0087
$\Omega_m h^3$						0030
σ_8						060
$S_8 \equiv \sigma_8(\Omega_m/0.3$						11

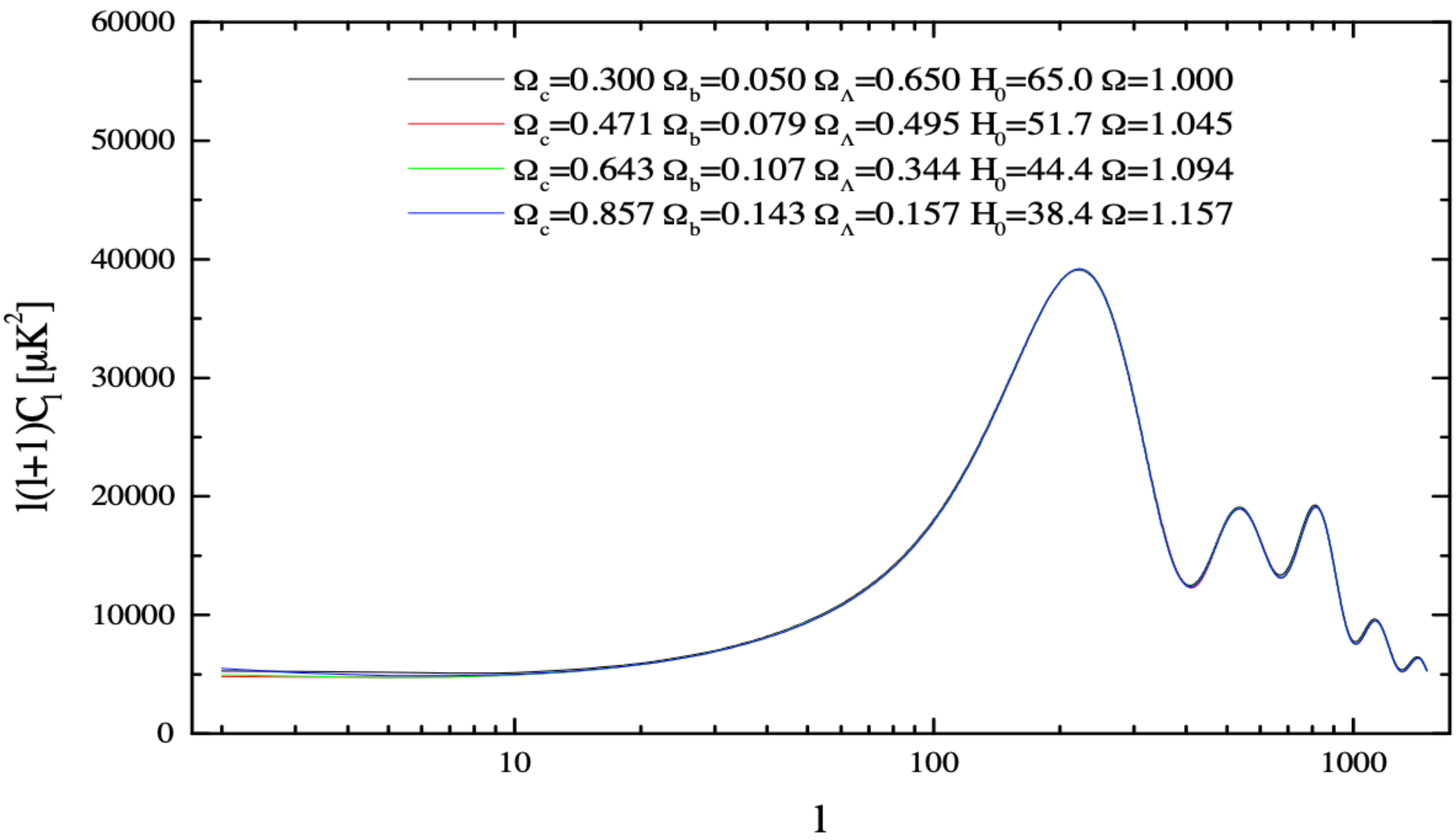

- The … del.
- The results are affected by the degeneracy between the parameters that induce similar effects on the observables.

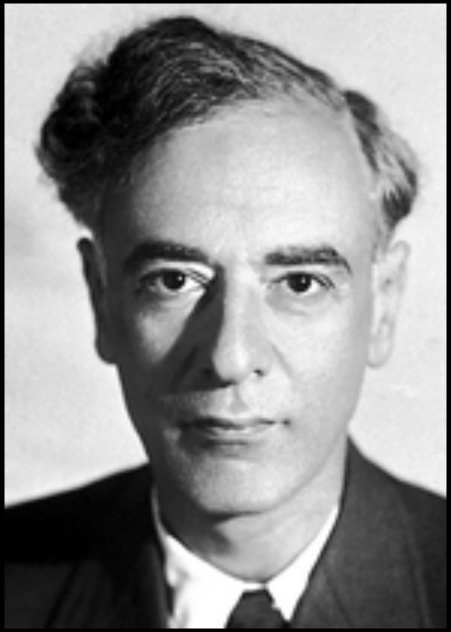

“Cosmologists are often in error but never in doubt”

Lev Landau

Are there other H0 estimates?

Latest H0 measurements

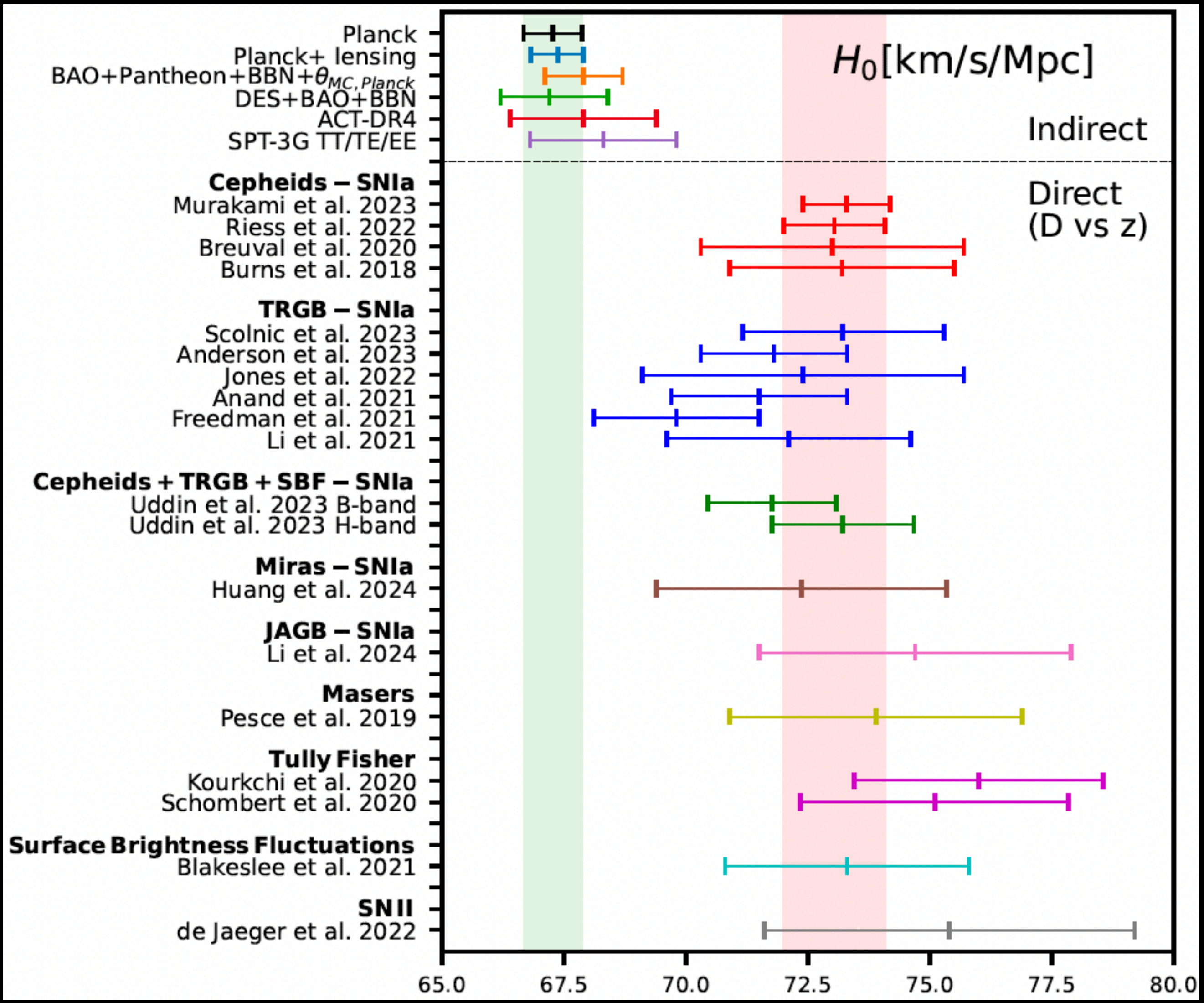

Hubble constant measurements made by different astronomical missions and groups over the years.

The red vertical band corresponds to the H0 value from SH0ES Team and the green vertical band corresponds to the H0 value as reported by Planck 2018 team within a ΛCDM scenario.

Di Valentino, *MNRAS* 502 (2021) 2, 2065-2073

On the same side of Planck, i.e. preferring smaller values of H_0 we have:

Ground based CMB telescope

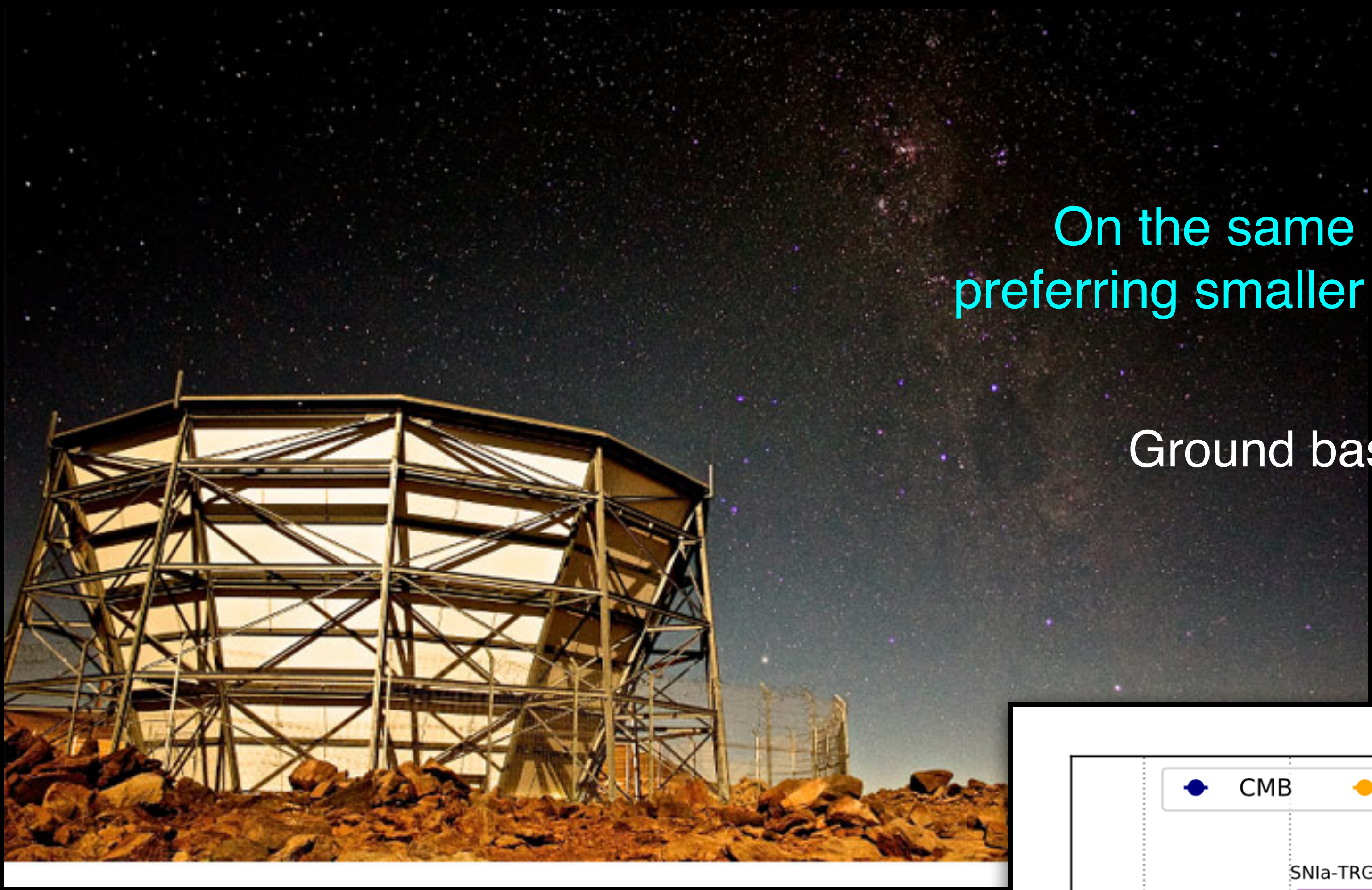

ACT-DR4:
H0 = 67.9 ± 1.5 km/s/Mpc in ΛCDM

ACT-DR4 + WMAP:
H0 = 67.6 ± 1.1 km/s/Mpc in ΛCDM

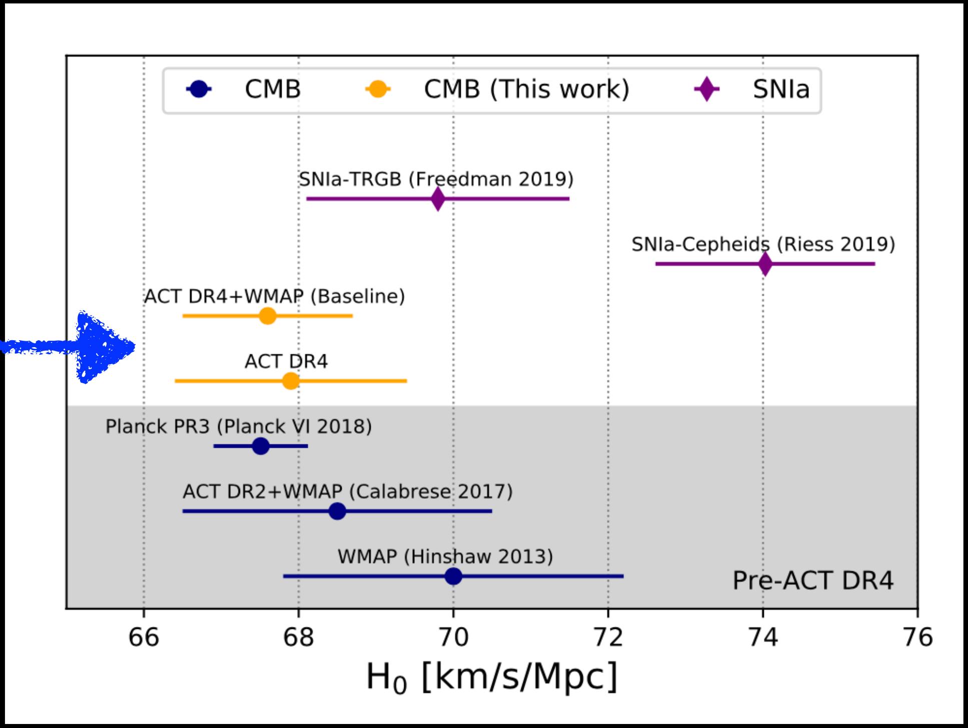

ACT-DR4 2020, *JCAP* 12 (2020) 047

ΛCDM - dependent

On the same side of Planck, i.e. preferring smaller values of H_0 we have:

Ground based CMB telescope

SPT-3G TT/TE/EE:
H0 = 68.3 ± 1.5 km/s/Mpc in ΛCDM

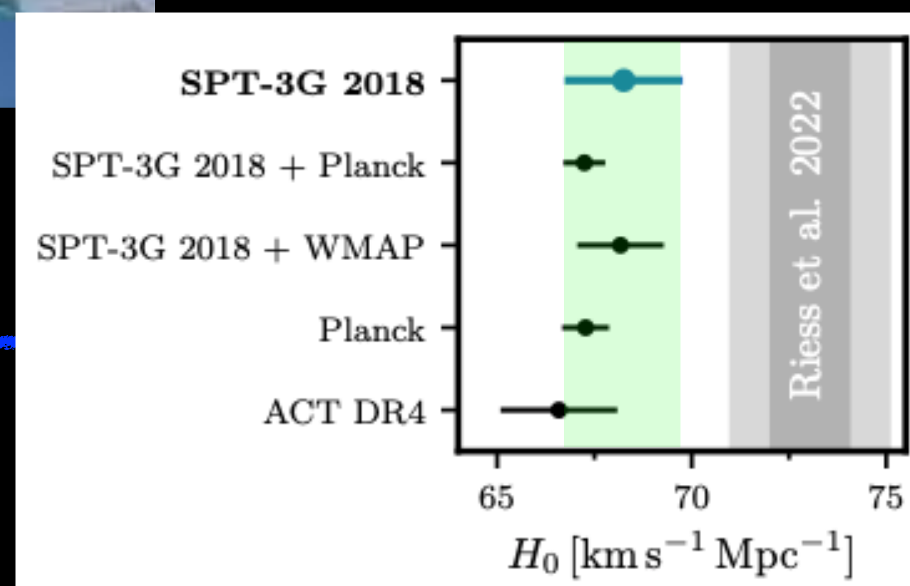

SPT-3G collaboration, arXiv:2212.05642

ΛCDM - dependent

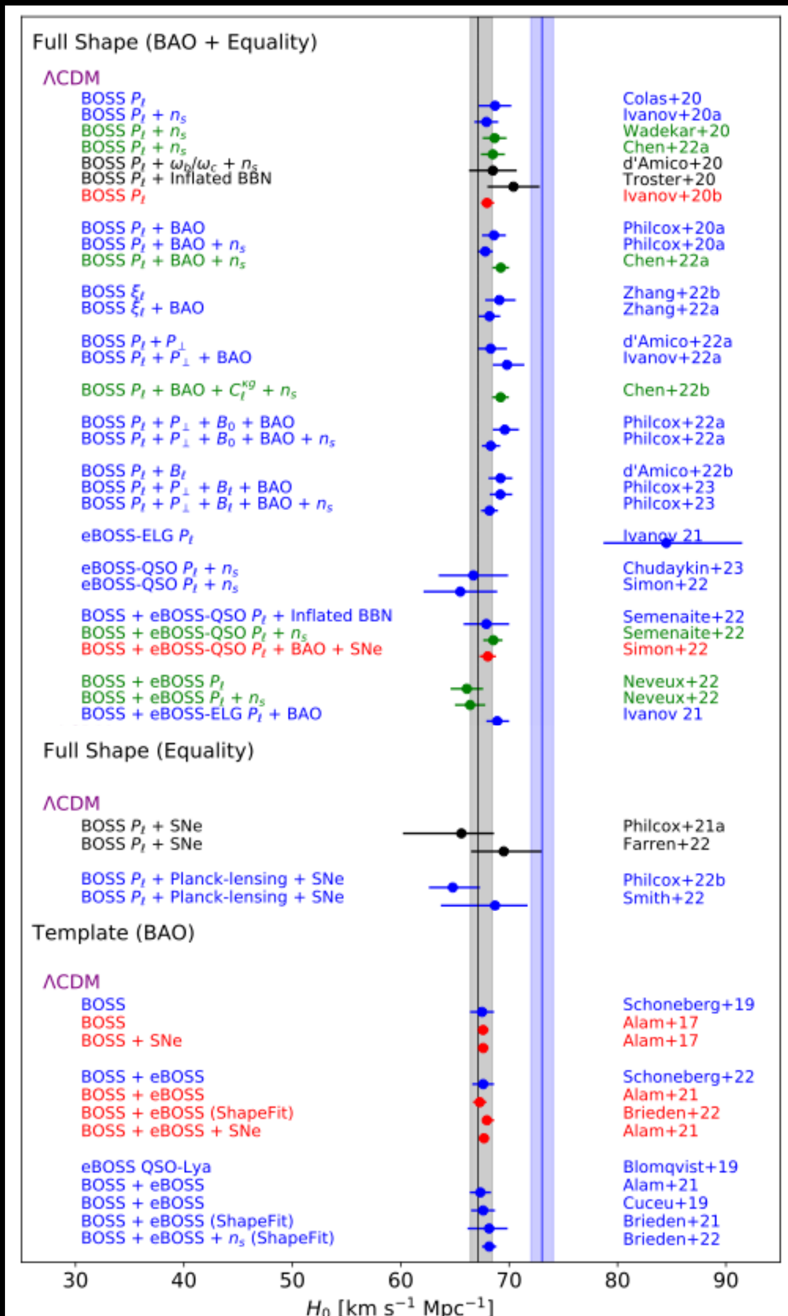

Ivanov and Philcox, arXiv:2305.07977

On the same side of Planck, i.e. preferring smaller values of H_0 we have:

Spectroscopic Surveys
BAO and Full Shape from BOSS and eBOSS

Results shown in blue include a BBN prior on ωb, in green use an ωb prior from *Planck*, in red are combined with the full *Planck* dataset.

ΛCDM - dependent

Latest H0 measurements

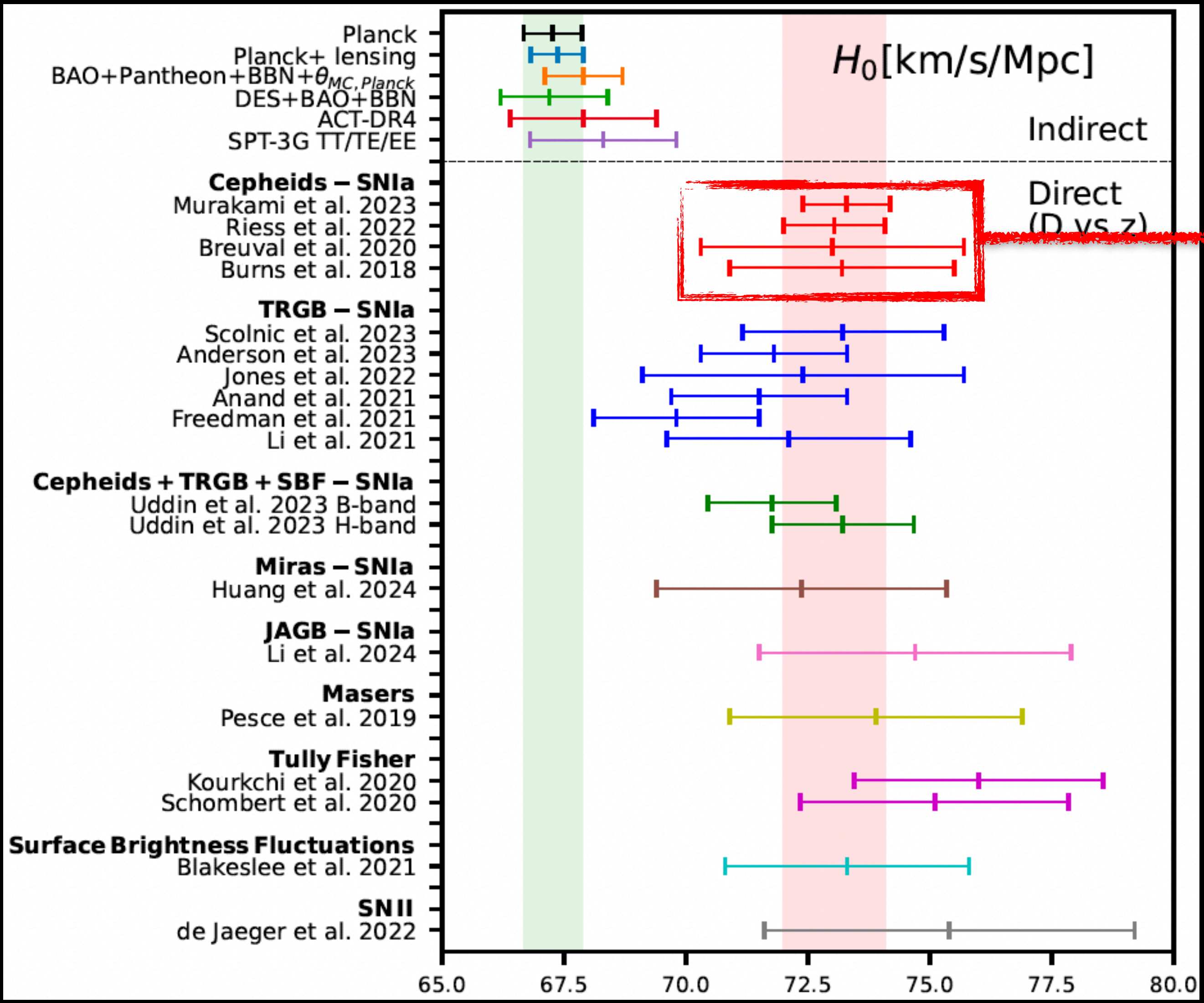

Di Valentino, *MNRAS* 502 (2021) 2, 2065-2073

Cepheids-SN Ia:

H0 = 73.29 ± 0.90 km/s/Mpc

Murakami et al., arXiv:*2306.00070*

H0 = 73.04 ± 1.04 km/s/Mpc

Riess et al., arXiv:*2112.04510*

Latest H0 measurements

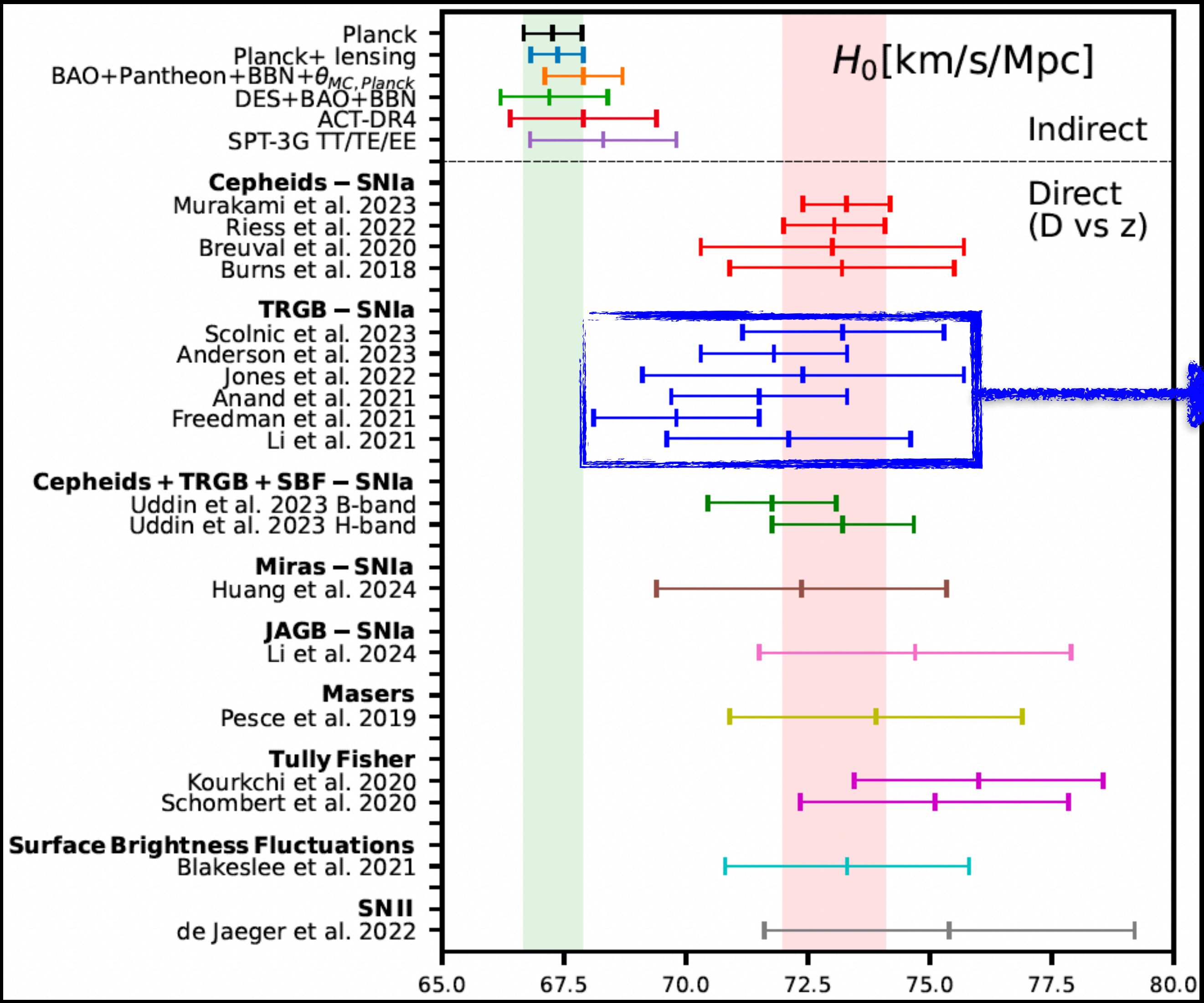

Di Valentino, *MNRAS* 502 (2021) 2, 2065-2073

The Tip of the Red Giant Branch (TRGB) is the peak brightness reached by red giant stars after they stop using hydrogen and begin fusing helium in their core.

H0 = 73.22±2.06 km/s/Mpc

Scolnic et al., arXiv:2304.06693

H0 = 71.8±1.5 km/s/Mpc

Anderson et al., arXiv:2303.04790

H0 = 72.4±3.3 km/s/Mpc

Jones et al., arXiv:2201.07801

H0 = 71.5±1.8 km/s/Mpc

Anand et al., arXiv:2108.00007

H0 = 69.8±1.7 km/s/Mpc

Freedman, arXiv:2106.15656

Latest H0 measurements

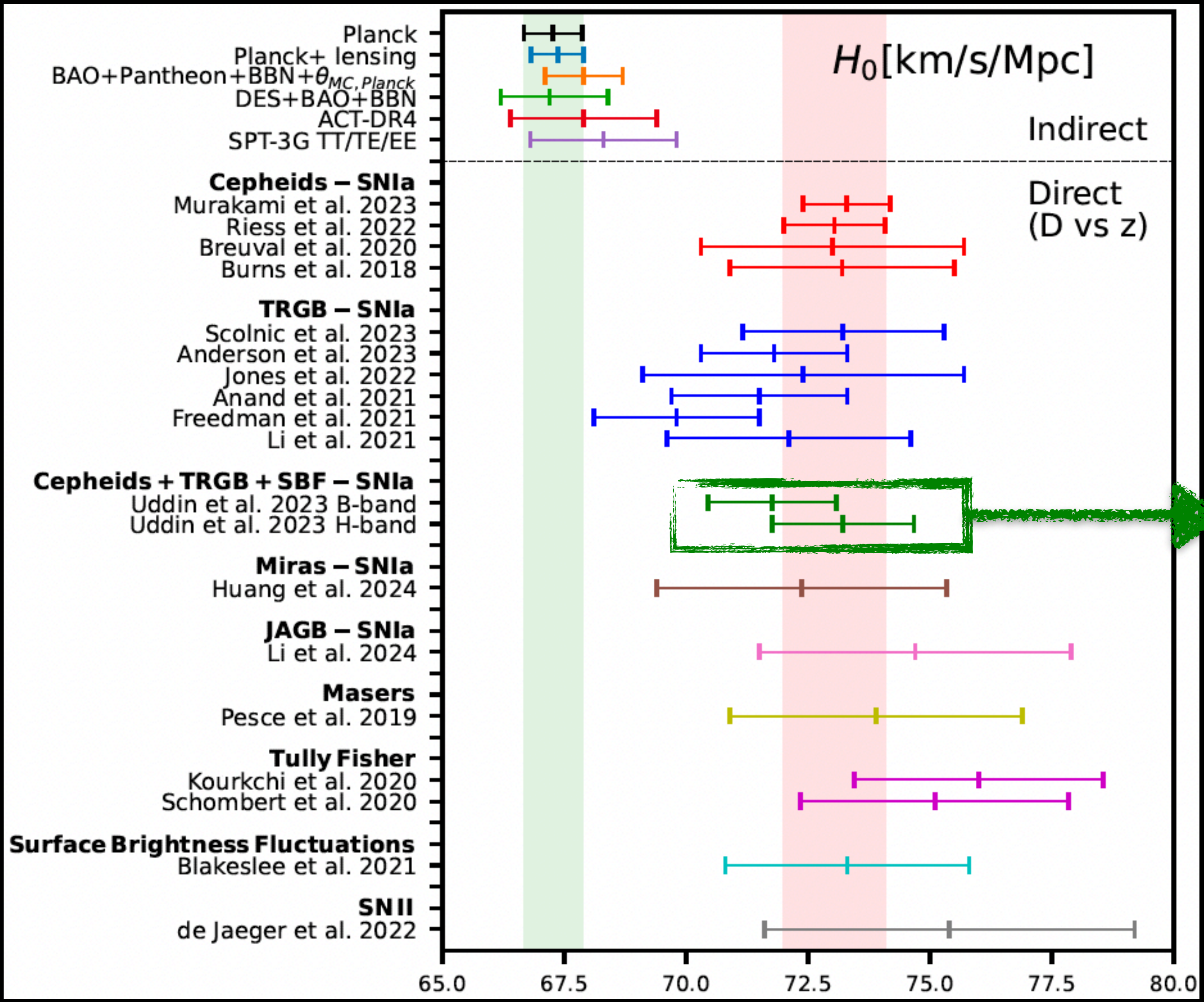

Carnegie Supernova Project:

Measurements of H0 using Cepheids, TRGB, and SBF Distance Calibration to Type Ia Supernovae

H0 = 71.76 ± 1.32 km/s/Mpc

H0 = 73.22 ± 1.45 km/s/Mpc

Uddin et al., arXiv:2308.01875 [astro-ph.CO]

Di Valentino, *MNRAS* 502 (2021) 2, 2065-2073

Latest H0 measurements

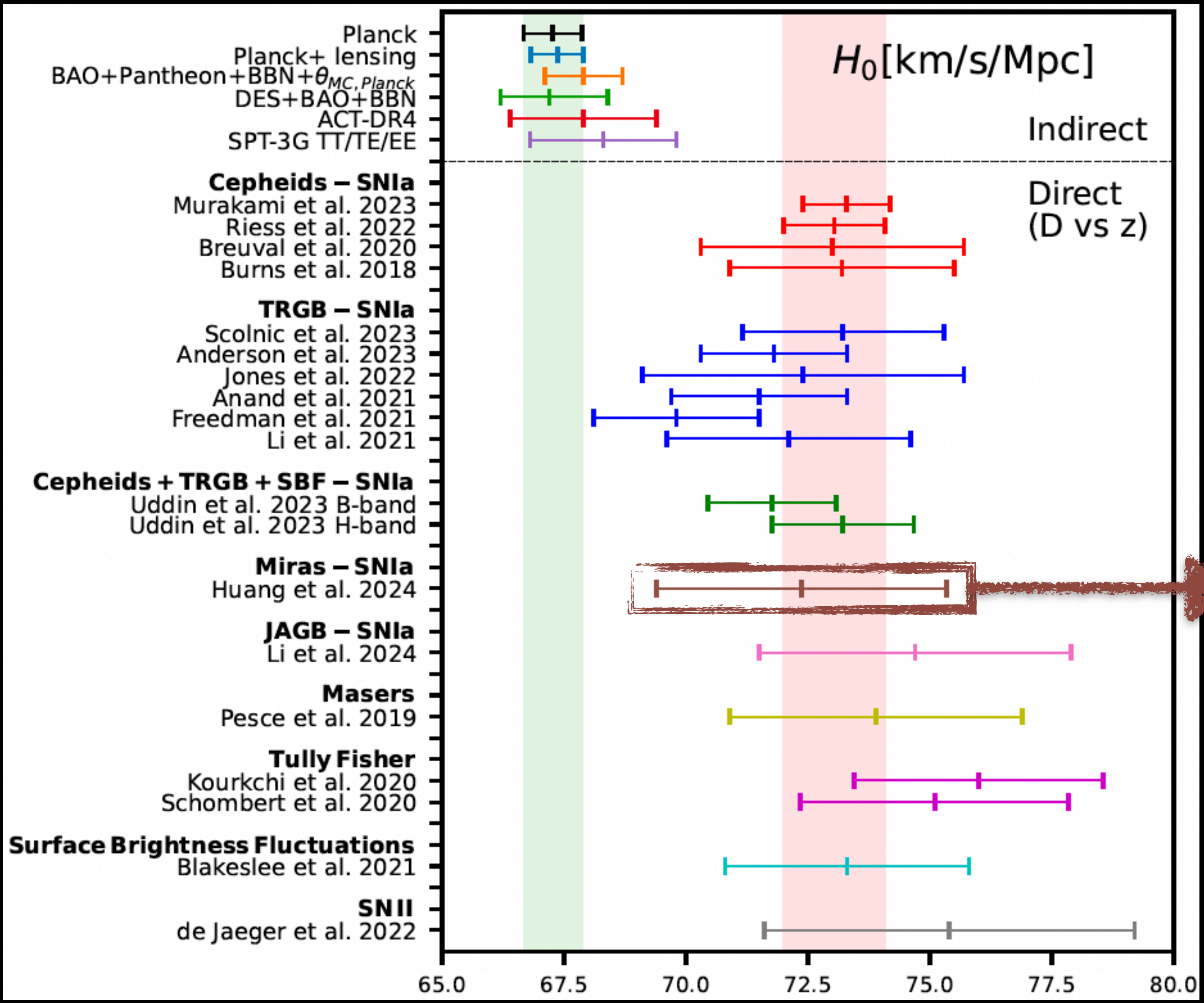

Di Valentino, *MNRAS* 502 (2021) 2, 2065-2073

MIRAS
variable red giant stars from older stellar populations

H0 = 72.37 ± 2.97 km/s/Mpc

Huang et al., arXiv:2312.08423 [astro-ph.CO]

Latest H0 measurements

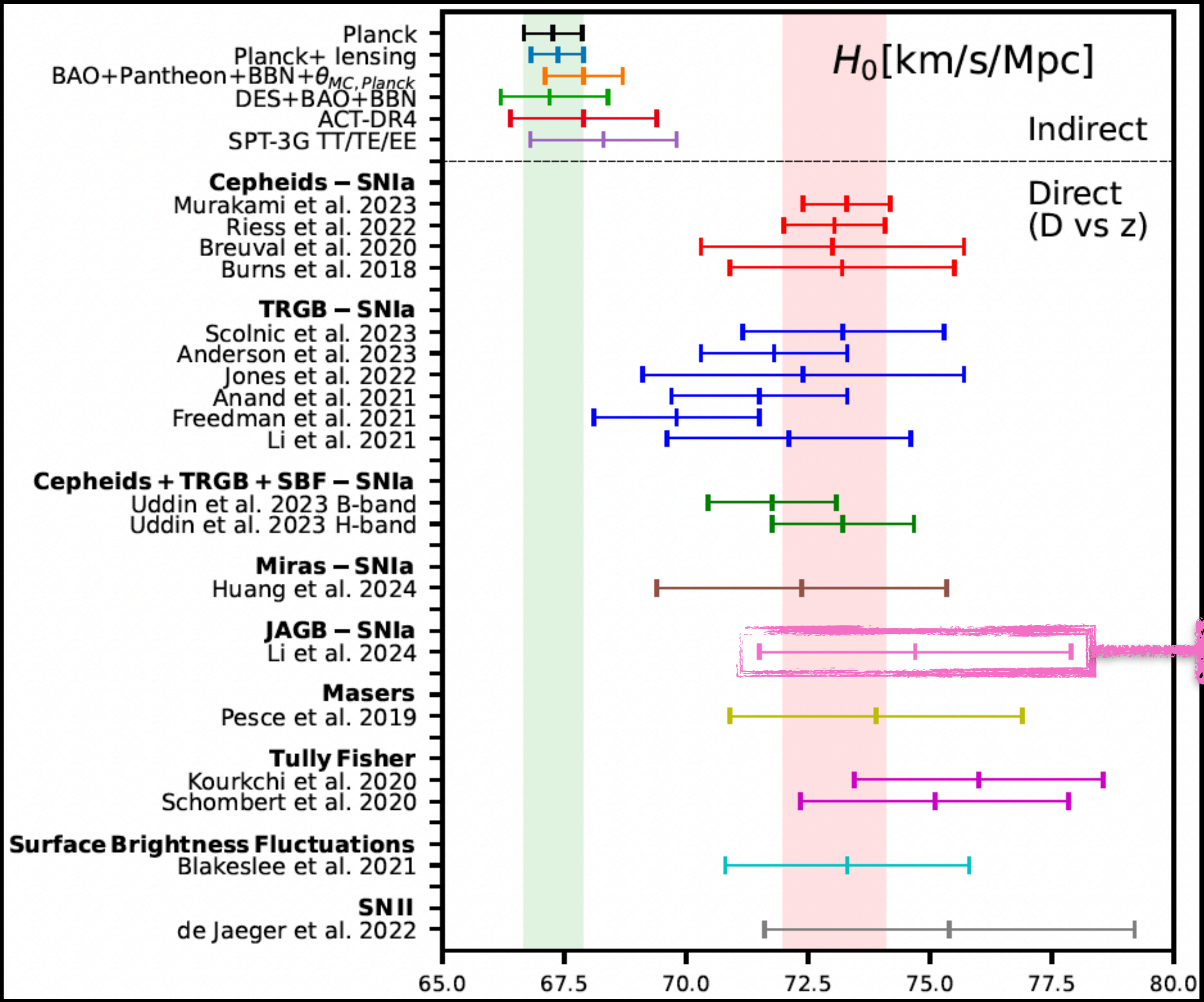

Di Valentino, *MNRAS* 502 (2021) 2, 2065-2073

JAGB
The J-regions of the Asymptotic Giant Branch is expected from stellar theory to be populated by thermally-pulsing carbon-rich dust-producing asymptotic giant branch stars.

H0 = 74.7 ± 3.2 km/s/Mpc

Li et al., arXiv:2401.04777 [astro-ph.CO]

Latest H0 measurements

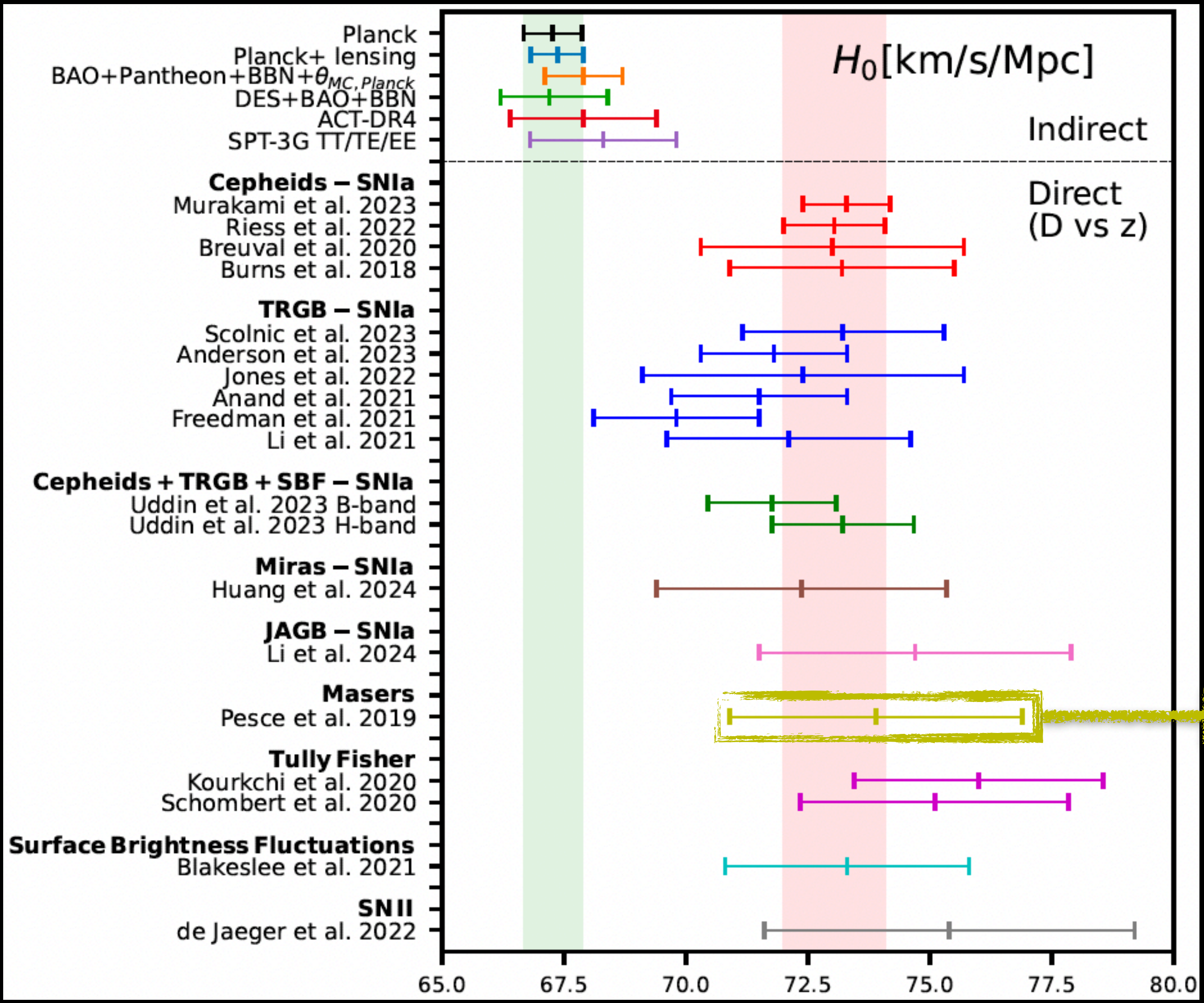

H0 = 73.9 ± 3.0 km/s/Mpc

Pesce et al. arXiv:2001.09213

The Megamaser Cosmology Project measures H0 using geometric distance measurements to six Megamaser - hosting galaxies. This approach avoids any distance ladder by providing geometric distance directly into the Hubble flow.

Di Valentino, *MNRAS* 502 (2021) 2, 2065-2073

Latest H0 measurements

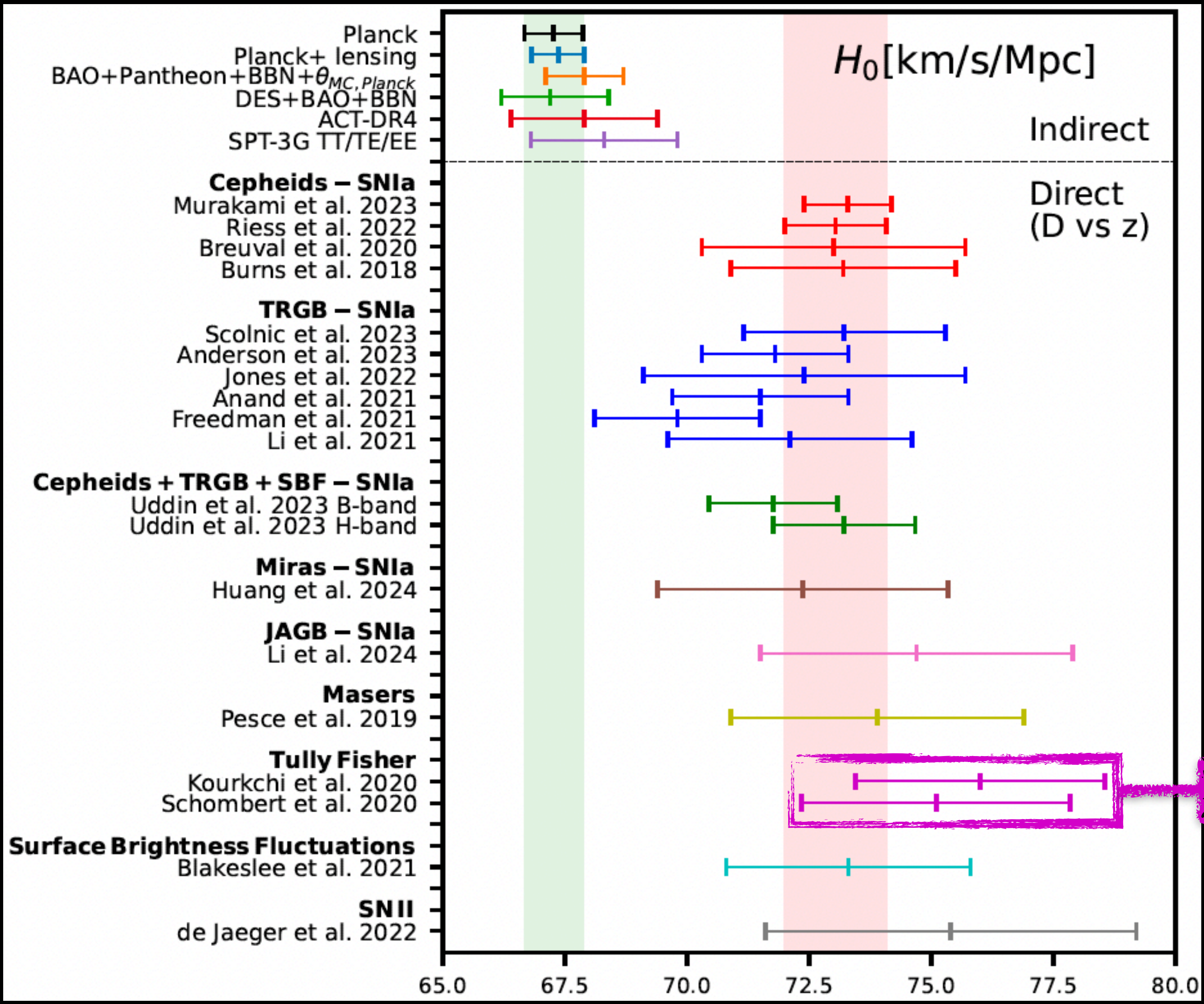

Di Valentino, *MNRAS* 502 (2021) 2, 2065-2073

H0 = 76.00 ± 2.55 km/s/Mpc

Kourkchi et al. arXiv:2004.14499

H0 = 75.10 ± 2.75 km/s/Mpc

Schombert et al. arXiv:2006.08615

Tully-Fisher Relation (based on the correlation between the rotation rate of spiral galaxies and their absolute luminosity, and using as calibrators Cepheids and TRGB)

Latest H0 measurements

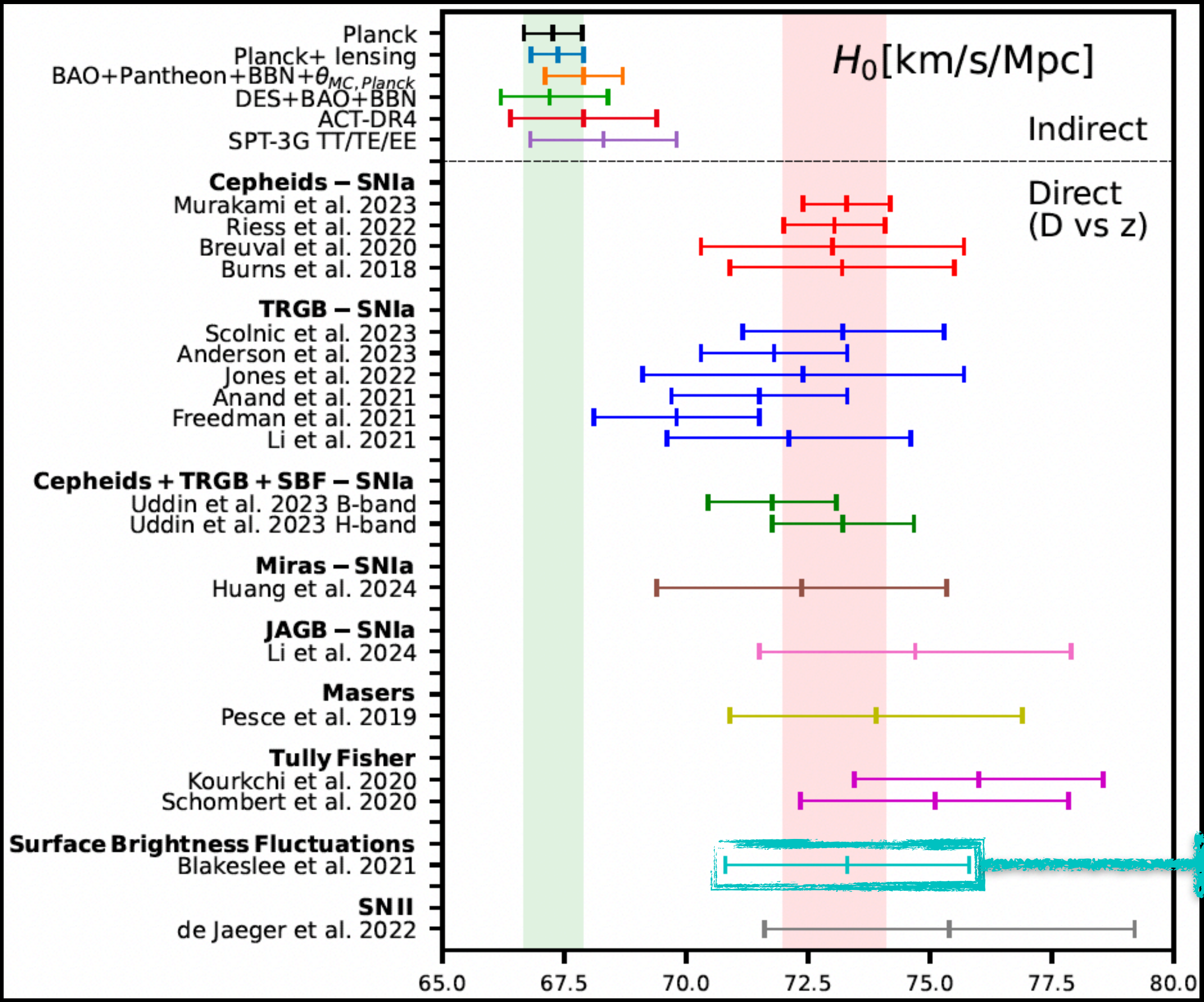

H0 = 73.3 ± 2.5 km/s/Mpc

Blakeslee et al., arXiv:2101.02221

Surface Brightness Fluctuations (substitutive distance ladder for long range indicator, calibrated by both Cepheids and TRGB)

Di Valentino, *MNRAS* 502 (2021) 2, 2065-2073

Latest H0 measurements

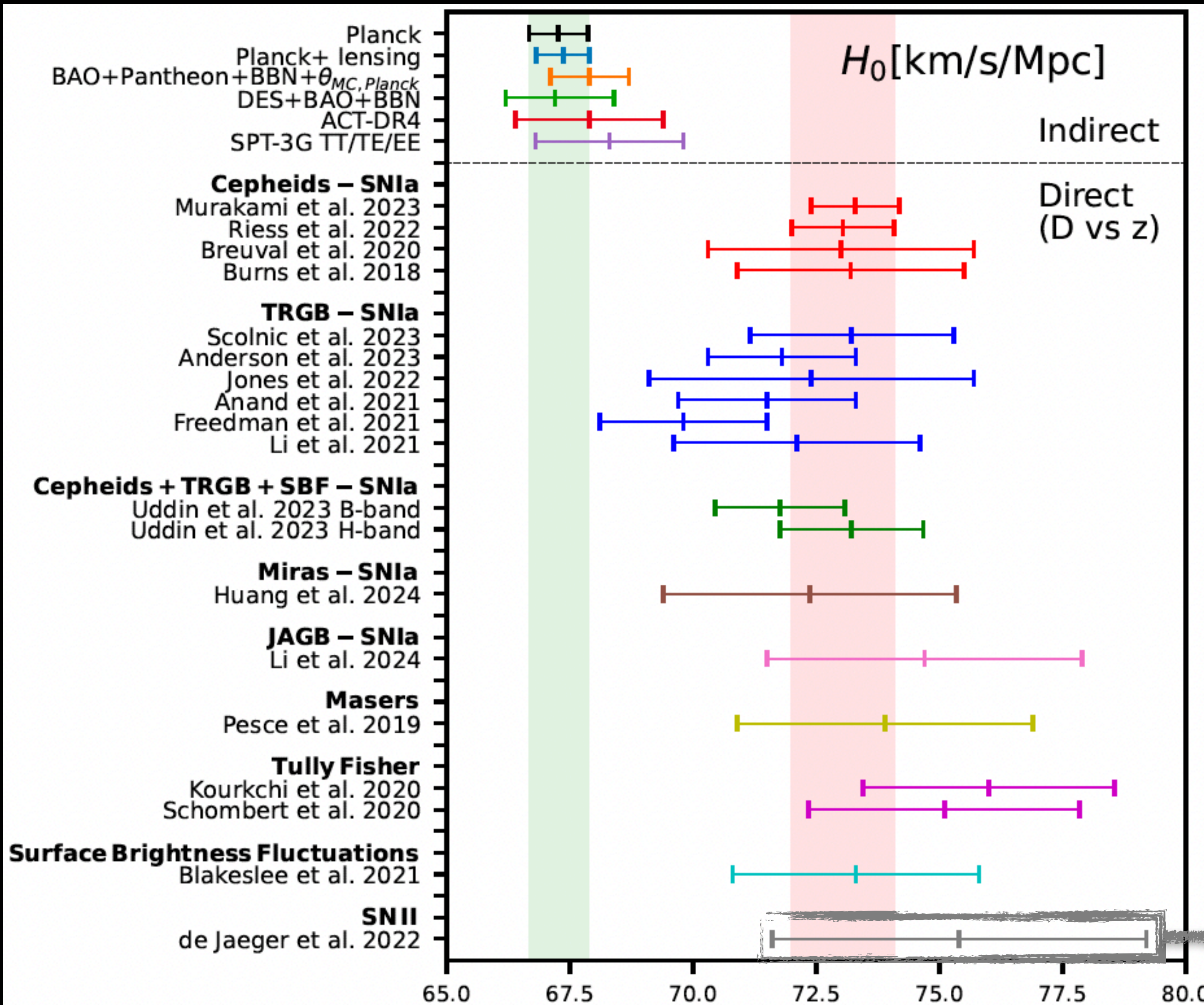

$H0 = 75.4^{+3.8}_{-3.7}$ km/s/Mpc

de Jaeger et al., arXiv:2203.08974

Type II supernovae used as standardisable candles and calibrated by both Cepheids and TRGB

Di Valentino, *MNRAS* 502 (2021) 2, 2065-2073

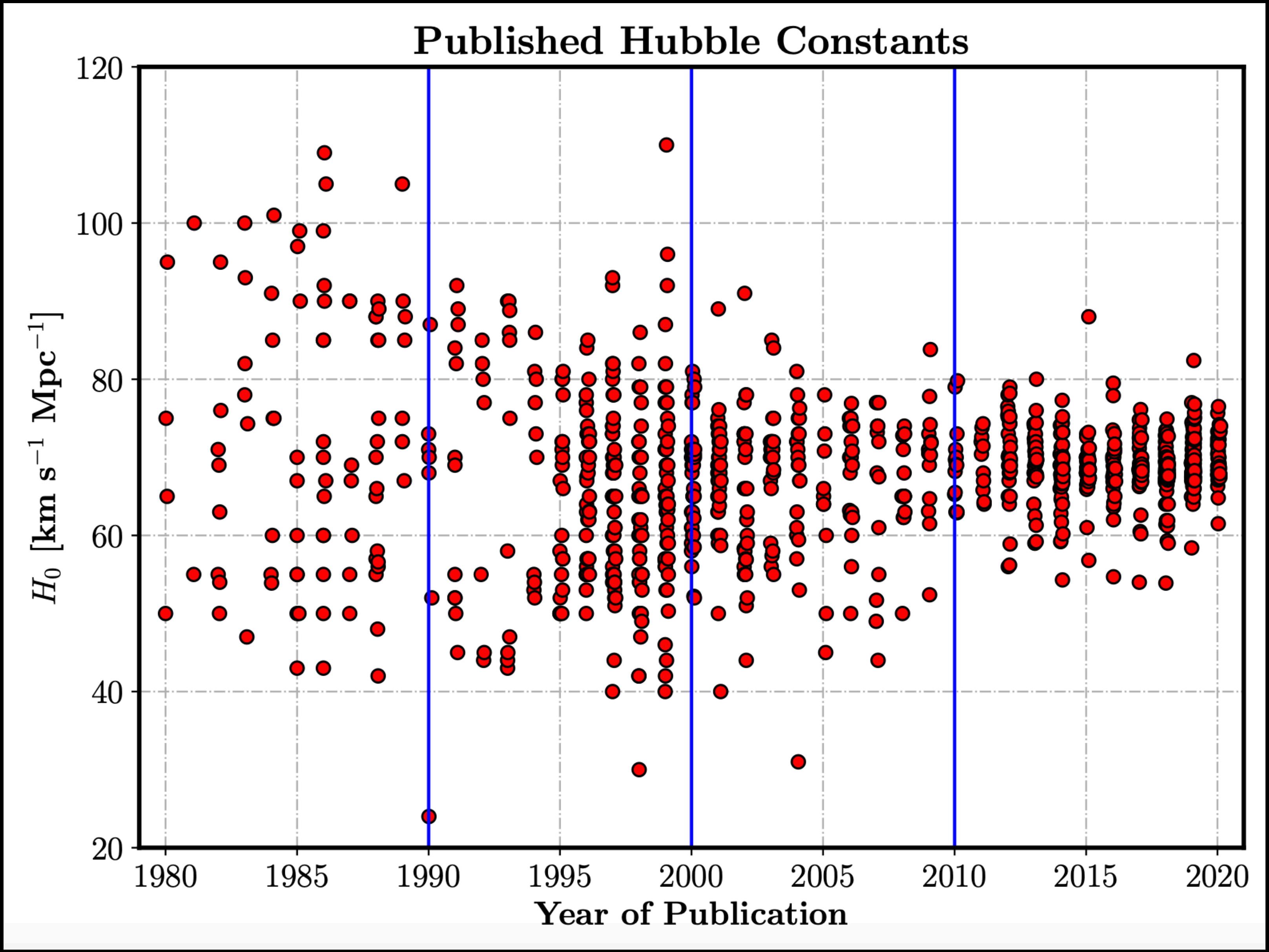

Freedman, *Astrophys.J.* 919 (2021) 1, 16

In the past the tension was within the same types of measurements and at the same redshifts and thus pointing directly to systematics.

Latest H0 measurements

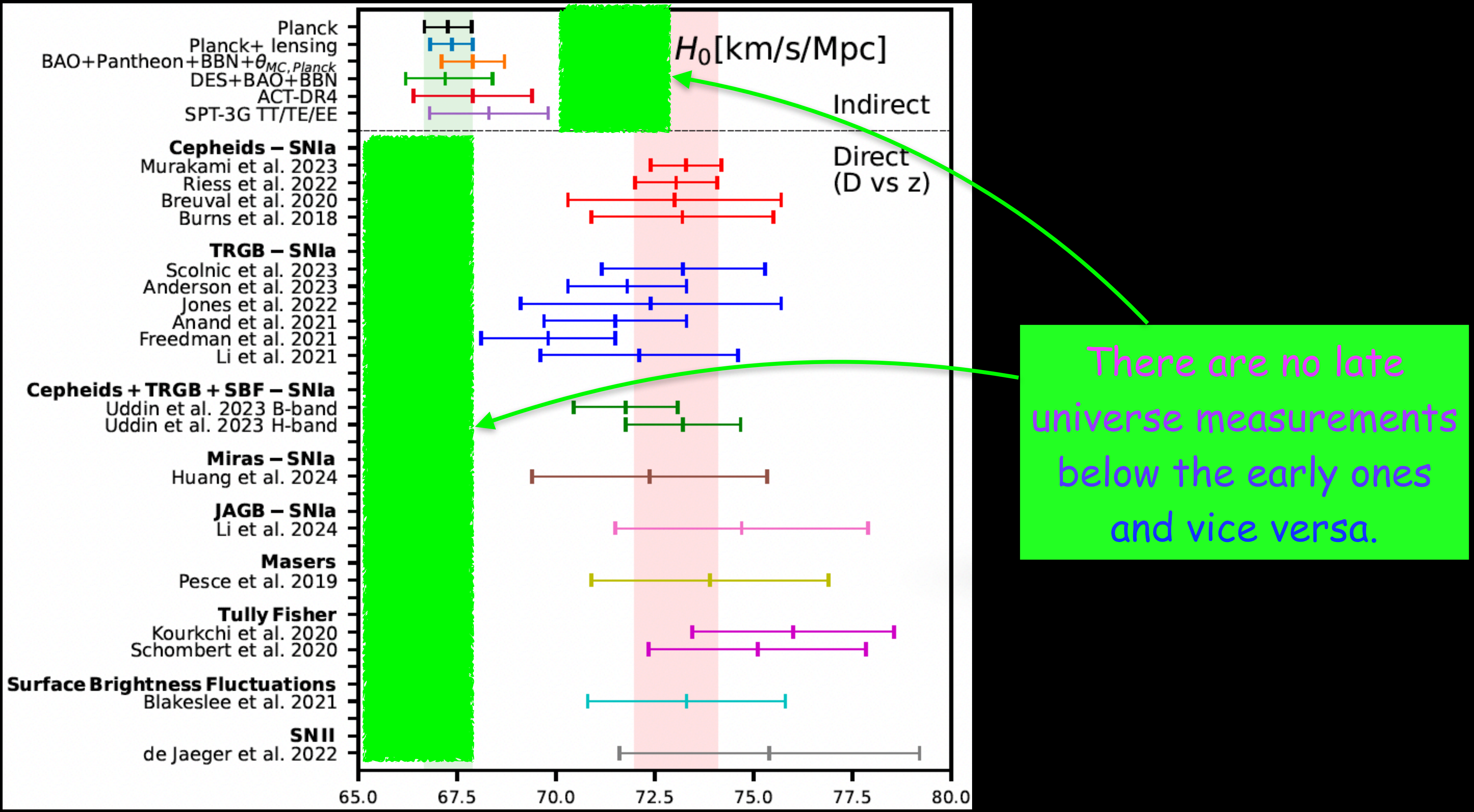

Di Valentino, *MNRAS* 502 (2021) 2, 2065-2073

It is difficult to imagine a single systematic error that would consistently explain the discrepancies observed in the diverse range of phenomena that we have encountered earlier, thereby resolving the Hubble constant tension.

Since this tension persists in the 5 - 6.3σ range

(Riess, Nature Reviews Physics (2019); Di Valentino, *MNRAS* 502 (2021) 2, 2065-2073; Di Valentino, Universe 2022, 8(8), 399)

even after eliminating the measurements of any individual type of object, team, or calibration, it is challenging to identify a single error that could account for it. While multiple independent systematic errors could offer more flexibility in resolving the tension, they are less likely to occur.

Given that the indirect constraints are model-dependent, we can explore the possibility of expanding the cosmological scenario and examining which extensions can resolve the discrepancies between the various cosmological probes.

Let's modify the ΛCDM model with a few example…

(Di Valentino et al. *Class.Quant.Grav.* 38 (2021) 15, 153001 and Abdalla et al., *JHEAp* 34 (2022) 49-211)

The Neutrino effective number

We can consider modifications in the
dark matter sector.

A classical extension is the
effective number of relativistic degrees of freedom,
i.e. additional relativistic matter at recombination,
corresponding to a modification of the expansion history
of the universe at early times.

The Neutrino effective number

The expected value is Neff = 3.044, if we assume standard electroweak interactions and three active massless neutrinos. If we measure a Neff > 3.044, we are in presence of extra radiation.

If we vary Neff, at 68% cl H0 is equal to 66.4 ± 1.4 km/s/Mpc, and the tension with SH0ES is still 3.9σ.

$$N_{\rm eff} = 2.92^{+0.36}_{-0.37} \quad (95\,\%, \textit{Planck}\ \text{TT,TE,EE+lowE}),$$

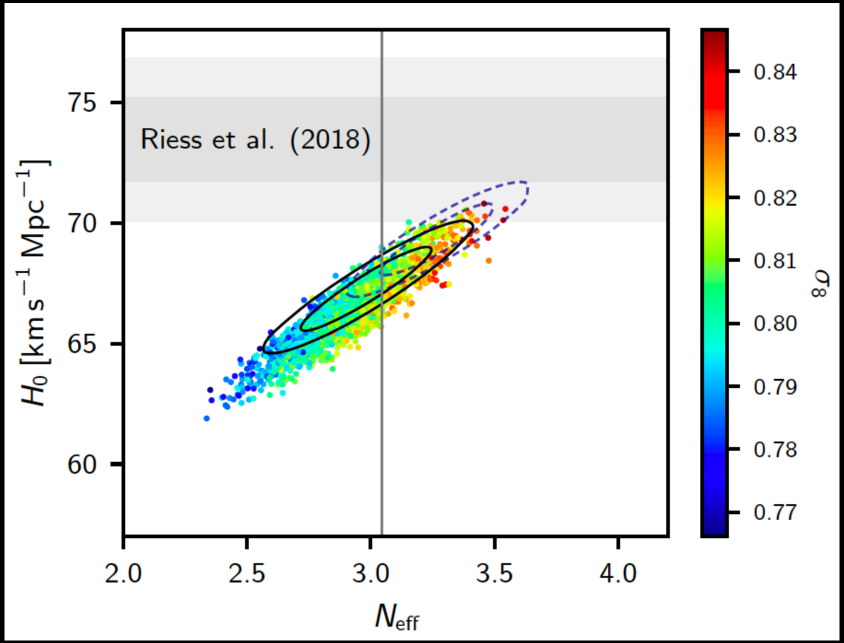

Planck 2018, Astron.Astrophys. 641 (2020) A6

The Dark energy equation of state

For example, we can consider modifications in the dark energy sector.

A classical extension is a varying dark energy equation of state, that is a modification of the expansion history of the universe at late times.

The Dark energy equation of state

If we change the cosmological constant with a Dark Energy with equation of state w, we are changing the expansion rate of the Universe:

$$H^2 = \left(\frac{\dot{a}}{a}\right)^2 = H_0^2 \left(\frac{\Omega_r}{a^4} + \frac{\Omega_m}{a^3} + \frac{\Omega_k}{a^2} + \Omega_\Lambda\right)$$

$$H^2 = H_0^2 \Big[\Omega_m(1+z)^3 + \Omega_r(1+z)^4 + \Omega_{\rm de}(1+z)^{3(1+w)} + \Omega_k(1+z)^2\Big]$$

w introduces a geometrical degeneracy with the Hubble constant that is almost unconstrained using the CMB data only, resulting in agreement with SH0ES.

We have in 2018 $w = -1.58^{+0.52}_{-0.41}$ with H0 > 69.9 km/s/Mpc at 95% c.l.

Planck data prefer a phantom dark energy, with an energy component with $w < -1$, for which the density increases with time in an expanding universe that will end in a Big Rip. A phantom dark energy violates the energy condition $\rho \geq |p|$, that means that the matter could move faster than light and a comoving observer measure a negative energy density, and the Hamiltonian could have vacuum instabilities due to a negative kinetic energy.

Formally successful models in solving H0

tension $\leq 1\sigma$ *"Excellent models"*	tension $\leq 2\sigma$ *"Good models"*	tension $\leq 3\sigma$ *"Promising models"*
Dark energy in extended parameter spaces [289]	Early Dark Energy [235]	Early Dark Energy [229]
Dynamical Dark Energy [309]	Phantom Dark Energy [11]	Decaying Warm DM [474]
Metastable Dark Energy [314]	Dynamical Dark Energy [11, 281, 309]	Neutrino-DM Interaction [506]
PEDE [392, 394]	GEDE [397]	Interacting dark radiation [517]
Elaborated Vacuum Metamorphosis [400–402]	Vacuum Metamorphosis [402]	Self-Interacting Neutrinos [700, 701]
IDE [314, 636, 637, 639, 652, 657, 661–663]	IDE [314, 653, 656, 661, 663, 670]	IDE [656]
Self-interacting sterile neutrinos [711]	Critically Emergent Dark Energy [997]	Unified Cosmologies [747]
Generalized Chaplygin gas model [744]	$f(\mathcal{T})$ gravity [814]	Scalar-tensor gravity [856]
Galileon gravity [876, 882]	Über-gravity [59]	Modified recombination [986]
Power Law Inflation [966]	Reconstructed PPS [978]	Super ΛCDM [1007]
$f(\mathcal{T})$ [818]		Coupled Dark Energy [650]

Table B1. Models solving the H_0 tension with R20 within the 1σ, 2σ and 3σ confidence levels considering the *Planck* dataset only.

Planck only

Di Valentino et al., Class.Quant.Grav. (2021), arXiv:2103.01183 [astro-ph.CO]

The state of the Dark energy equation of state

Dataset combination	w	H_0 [km/s/Mpc]
CMB	$-1.57^{+0.16}_{-0.36}$ $(-1.57^{+0.53}_{-0.42})$	> 82.4 (> 69.3)
CMB+BAO	-1.039 ± 0.059 $(-1.04^{+0.11}_{-0.12})$	68.6 ± 1.5 $(68.6^{+3.1}_{-2.8})$
CMB+SN	-0.976 ± 0.029 $(-0.976^{+0.055}_{-0.056})$	66.54 ± 0.81 $(66.5^{+1.6}_{-1.6})$

Escamilla, Giarè, Di Valentino et al., arXiv: 2307.14802

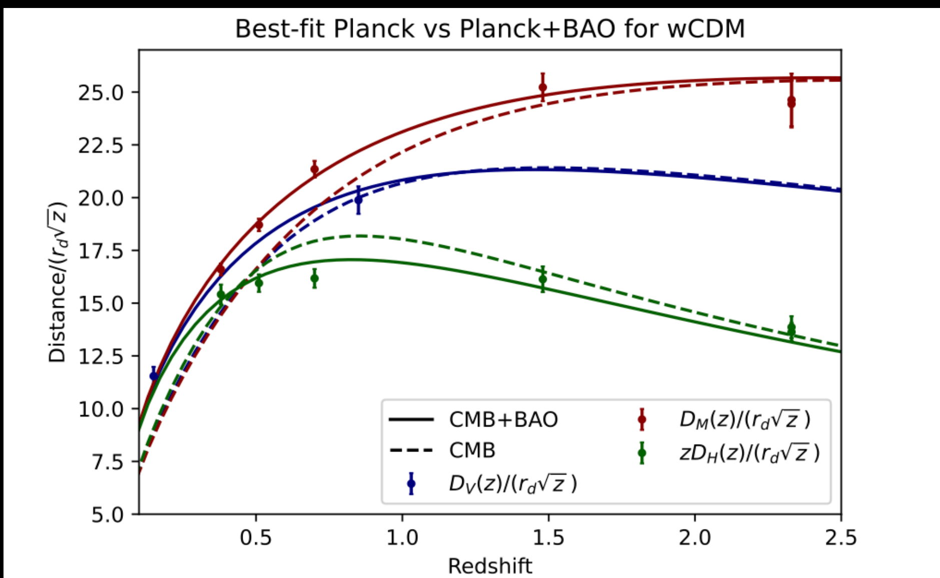

FIG. 5. Best-fit predictions for (rescaled) distance-redshift relations from a wCDM fit to *Planck* CMB data alone (dashed curves) and the CMB+BAO dataset (solid curves). These predictions are presented for the three different types of distances probed by BAO measurements (rescaled as per the y label), each indicated by the colors reported in the legend. The error bars represent $\pm 1\sigma$ uncertainties.

However, if BAO data are included, the wCDM model with w<-1 worsens considerably the fit of the BAO data because the best fit from Planck alone fails in recover the shape of H(z) at low redshifts. Therefore, when the CMB is combined with BAO data, the favoured model is again the LCDM one and the H0 tension is restored.

Complication:
the sound horizon problem

What about BAO+Pantheon?

BAO+Pantheon measurements constrain the product of H0 and the sound horizon r_s .

In order to have a higher H0 value in agreement with SH0ES, we need r_s near 137 Mpc. However, Planck by assuming ΛCDM, prefers r_s near 147 Mpc. Therefore, a cosmological solution that can increase H0 and at the same time can lower the sound horizon inferred from CMB data is the most promising way to put in agreement all the measurements.

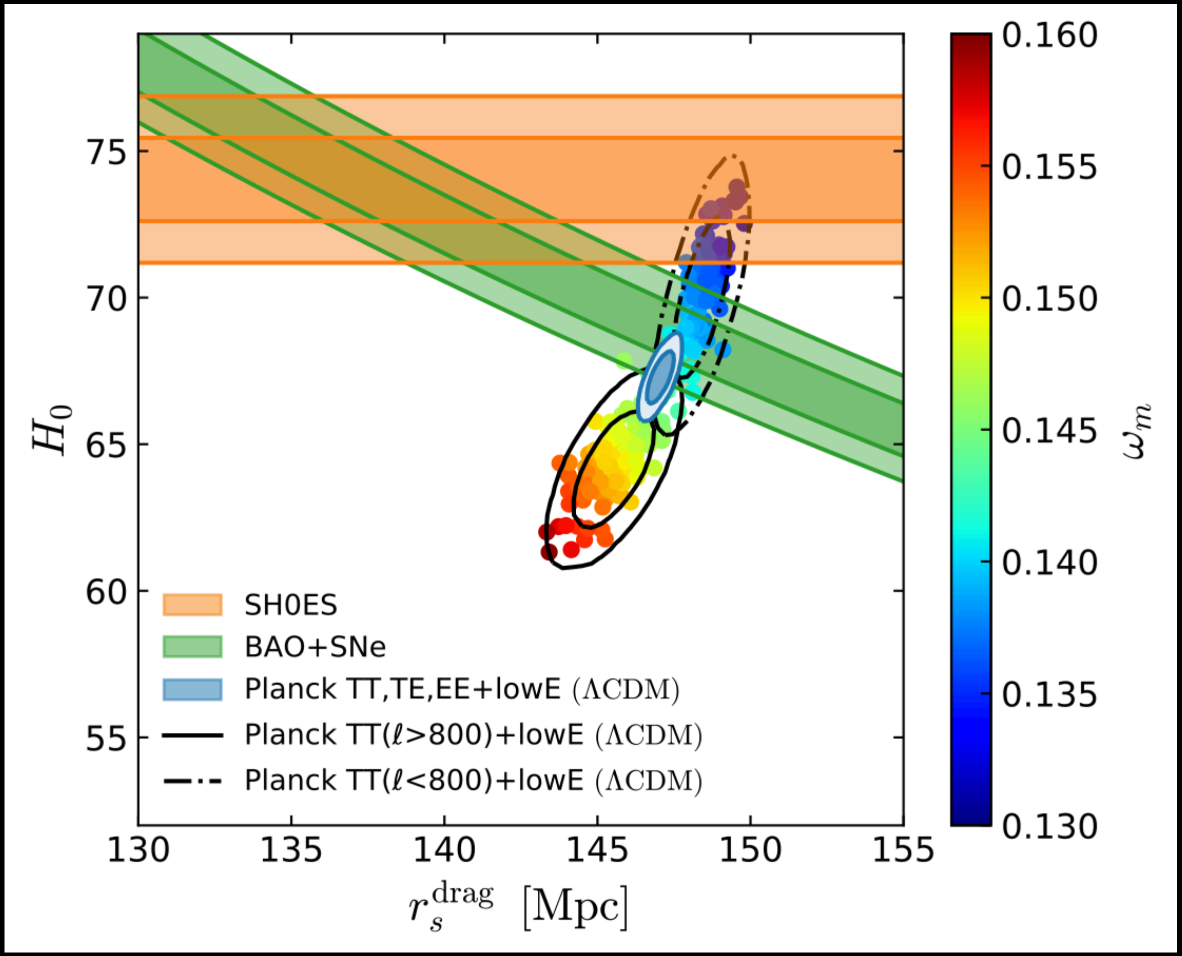

Knox and Millea, *Phys.Rev.D* 101 (2020) 4, 043533

Early vs late time solutions

Here we can see the comparison of the 2σ credibility regions of the CMB constraints and the measurements from late-time observations (SN + BAO + H0LiCOW + SH0ES).

We see that the late time solutions, as wCDM, increase H0 because they decrease the expansion history at intermediate redshift, but leave r_s unaltered.

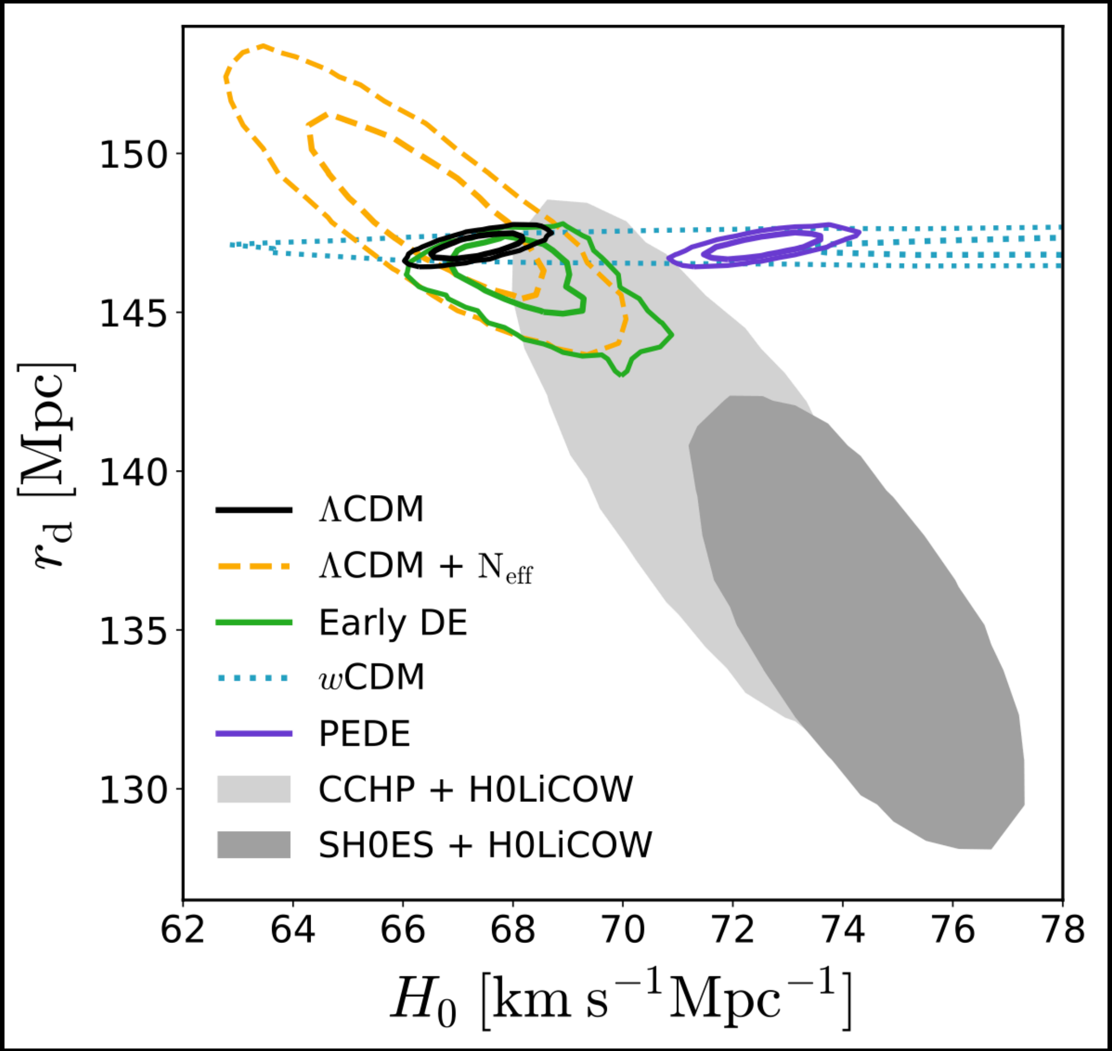

Arendse et al., Astron.Astrophys. 639 (2020) A57

Early vs late time solutions

Here we can see the comparison of the 2σ credibility regions of the CMB constraints and the measurements from late-time observations (SN + BAO + H0LiCOW + SH0ES).

However, the early time solutions, as Neff or Early Dark Energy, move in the right direction both the parameters, but can't solve completely the H0 tension between Planck and SH0ES.

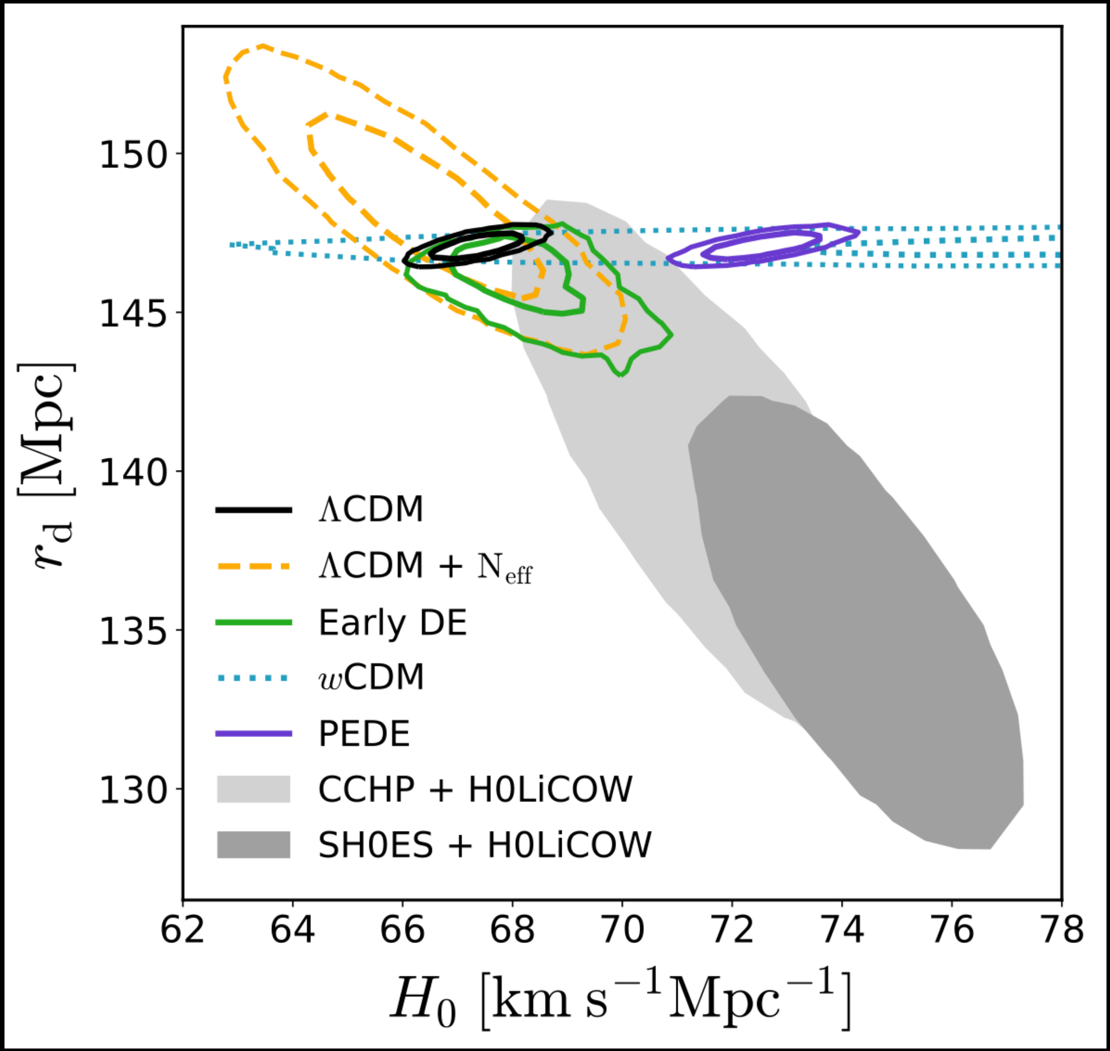

Arendse et al., Astron.Astrophys. 639 (2020) A57

Early Dark Energy

Early dark energy (EDE) scenario assumes that there is a new fundamental field that accelerates the cosmic expansion rate before recombination. This field contributes roughly 10-12% of the total energy density near the matter-radiation equality, but eventually dissipates like radiation or at a faster rate (depending on the shape of the potential).
In order to have an effect on the sound horizon we should have $H \sim T^2/M_{pl} \approx m$ just before the recombination, so the mass of the scalar field should be $m \approx 10^{-27}$ eV, similar to an axion particle:

$$V(\phi) = m^2 f^2 \left(1 - \cos(\phi/f)\right)^n$$

At the minimum of the potential the field oscillates yielding to an effective equation of state

$$w_\phi = (n-1)/(n+1)$$

If we take n = 1 (the standard axion potential) then $w_\phi = 0$ near the potential minimum, and the EDE energy density redshifts as matter creating problems in the late-time cosmology, therefore it does not work phenomenologically.
For n = 2 instead it decays away like radiation ($\propto a^{-4}$),
and for $n \to \infty$ like kinetic energy ($\propto a^{-6}$). However, values n > 5 are disfavored.

Karwal & Kamionkowski *PRD* 94 (2016) 10, 103523 and Poulin et al. *PRL* 122 (2019) 22, 221301)

Early Dark Energy

Constraints at 68% cl.

Constraints from *Planck* 2018 data only: TT+TE+EE

Parameter	ΛCDM	EDE ($n = 3$)
$\ln(10^{10} A_s)$	$3.044\,(3.055)\ \pm 0.016$	$3.051\,(3.056)\ \pm 0.017$
n_s	$0.9645\,(0.9659)\ \pm 0.0043$	$0.9702\,(0.9769)^{+0.0071}_{-0.0069}$
$100\theta_s$	$1.04185\,(1.04200)\ \pm 0.00029$	$1.04164\,(1.04168)\ \pm 0.00034$
$\Omega_b h^2$	$0.02235\,(0.02244)\ \pm 0.00015$	$0.02250\,(0.02250)\ \pm 0.00020$
$\Omega_c h^2$	$0.1202\,(0.1201)\ \pm 0.0013$	$0.1234\,(0.1268)^{+0.0031}_{-0.0030}$
τ_{reio}	$0.0541\,(0.0587)\ \pm 0.0076$	$0.0549\,(0.0539)\ \pm 0.0078$
$\log_{10}(z_c)$	–	$3.66\,(3.75)^{+0.28}_{-0.24}$
f_{EDE}	–	$< 0.087\,(0.068)$
θ_i	–	$> 0.36\,(2.96)$
H_0 [km/s/Mpc]	$67.29\,(67.44)\ \pm 0.59$	$68.29\,(69.13)^{+1.02}_{-1.00}$
Ω_m	$0.3162\,(0.3147)\ \pm 0.0083$	$0.3145\,(0.3138)\ \pm 0.0086$
σ_8	$0.8114\,(0.8156)\ \pm 0.0073$	$0.8198\,(0.8280)^{+0.0109}_{-0.0107}$
S_8	$0.8331\,(0.8355)\ \pm 0.0159$	$0.8393\,(0.8468)\ \pm 0.0173$
$\log_{10}(f/\mathrm{eV})$	–	$26.57\,(26.36)^{+0.39}_{-0.36}$
$\log_{10}(m/\mathrm{eV})$	–	$-26.94\,(-26.90)^{+0.58}_{-0.53}$

Hill et al. *Phys.Rev.D* 102 (2020) 4, 043507

Planck 2018 results shows no evidence for EDE
and H0 is in agreement with the value obtained assuming ΛCDM.

Formally successful models in solving H0

tension $\leq 1\sigma$ *"Excellent models"*	tension $\leq 2\sigma$ *"Good models"*	tension $\leq 3\sigma$ *"Promising models"*
Early Dark Energy [228, 235, 240, 250]	Early Dark Energy [212, 229, 236, 263]	DE in extended parameter spaces [289]
Exponential Acoustic Dark Energy [259]	Rock 'n' Roll [242]	Dynamical Dark Energy [281, 309]
Phantom Crossing [315]	New Early Dark Energy [247]	Holographic Dark Energy [350]
Late Dark Energy Transition [317]	Acoustic Dark Energy [257]	Swampland Conjectures [370]
Metastable Dark Energy [314]	Dynamical Dark Energy [309]	MEDE [399]
PEDE [394]	Running vacuum model [332]	Coupled DM - Dark radiation [534]
Vacuum Metamorphosis [402]	Bulk viscous models [340, 341]	Decaying Ultralight Scalar [538]
Elaborated Vacuum Metamorphosis [401, 402]	Holographic Dark Energy [350]	BD-ΛCDM [852]
Sterile Neutrinos [433]	Phantom Braneworld DE [378]	Metastable Dark Energy [314]
Decaying Dark Matter [481]	PEDE [391, 392]	Self-Interacting Neutrinos [700]
Neutrino-Majoron Interactions [509]	Elaborated Vacuum Metamorphosis [401]	Dark Neutrino Interactions [716]
IDE [637, 639, 657, 661]	IDE [659, 670]	IDE [634–636, 653, 656, 663, 669]
DM - Photon Coupling [685]	Interacting Dark Radiation [517]	Scalar-tensor gravity [855, 856]
$f(\mathcal{T})$ gravity theory [812]	Decaying Dark Matter [471, 474]	Galileon gravity [877, 881]
BD-ΛCDM [851]	DM - Photon Coupling [686]	Nonlocal gravity [886]
Über-Gravity [59]	Self-interacting sterile neutrinos [711]	Modified recombination [986]
Galileon Gravity [875]	$f(\mathcal{T})$ gravity theory [817]	Effective Electron Rest Mass [989]
Unimodular Gravity [890]	Über-Gravity [871]	Super ΛCDM [1007]
Time Varying Electron Mass [990]	VCDM [893]	Axi-Higgs [991]
ΛCDM [995]	Primordial magnetic fields [992]	Self-Interacting Dark Matter [479]
Ginzburg-Landau theory [996]	Early modified gravity [859]	Primordial Black Holes [545]
Lorentzian Quintessential Inflation [979]	Bianchi type I spacetime [999]	
Holographic Dark Energy [351]	$f(\mathcal{T})$ [818]	

Table B2. Models solving the H_0 tension with R20 within 1σ, 2σ and 3
Planck in combination with additional cosmological probes. D
datasets are discussed in the main text.

Combination of datasets

Di Valentino et al., Class.Quant.Grav. (2021), arXiv:2103.01183 [astro-ph.CO]

Additional complication:
the early solutions proposed to alleviate the H0 tension increase the S8 tension!

The S8 tension

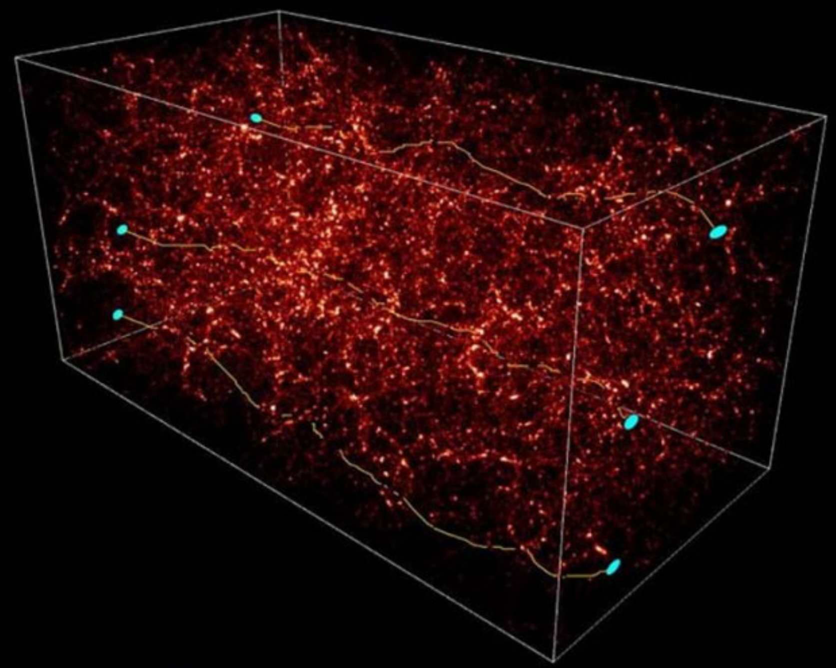

$$S_8 \equiv \sigma_8 \sqrt{\Omega_m / 0.3}$$

A tension on S8 is present between the Planck data in the ΛCDM scenario and the cosmic shear data.

The S8 tension

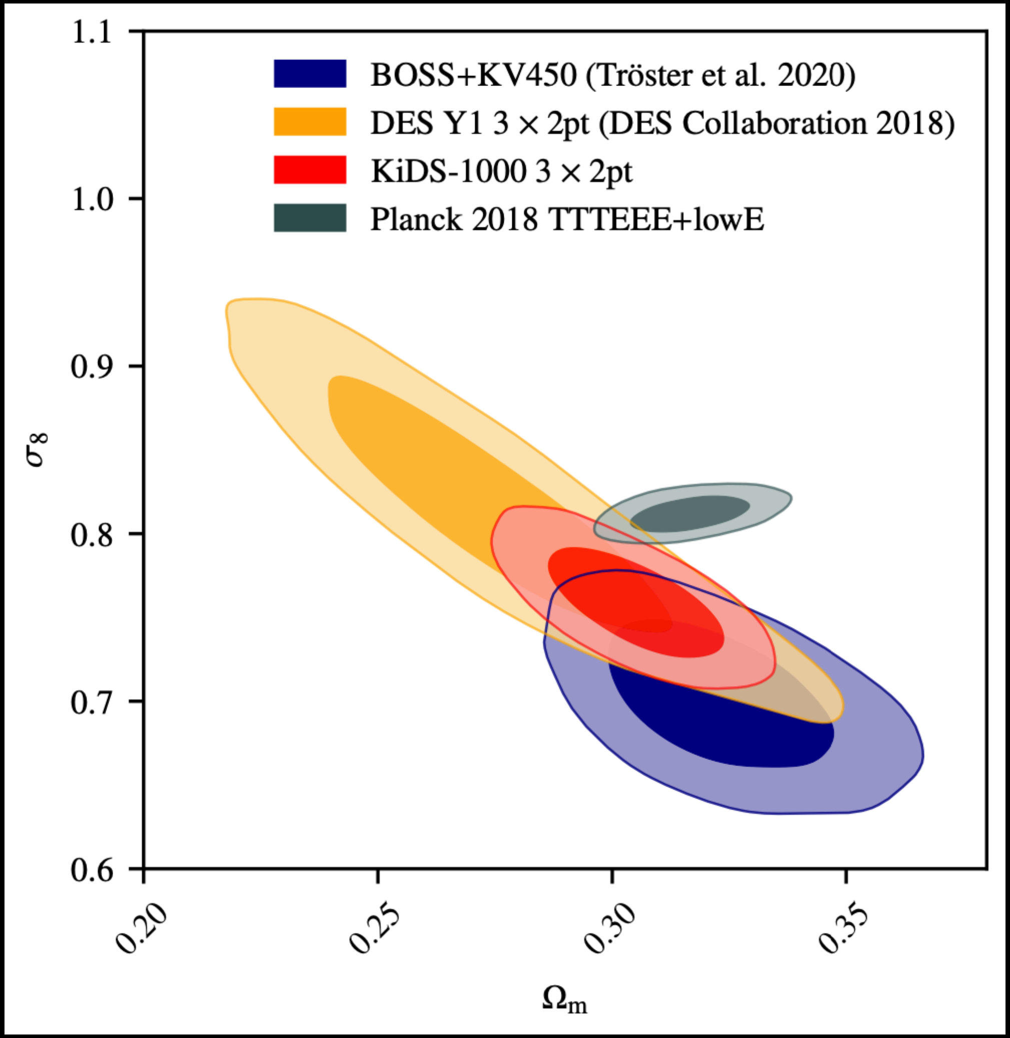

KiDS-1000, Heymans et al., arXiv:2007.15632 [astro-ph.CO]

The S8 tension is present at 3.4σ between Planck assuming ΛCDM and KiDS+VIKING-450 and BOSS combined together, or 3.1σ with KiDS-1000.

$S_8 = 0.834 \pm 0.016$

Planck 2018, Aghanim et al., arXiv:1807.06209 [astro-ph.CO]

$S_8 = 0.728 \pm 0.045$

Troster et al., arXiv:1909.11006 [astro-ph.CO]

$S_8 = 0.766^{+0.020}_{-0.014}$

KiDS-1000, Heymans et al., arXiv:2007.15632 [astro-ph.CO]

The S8 tension

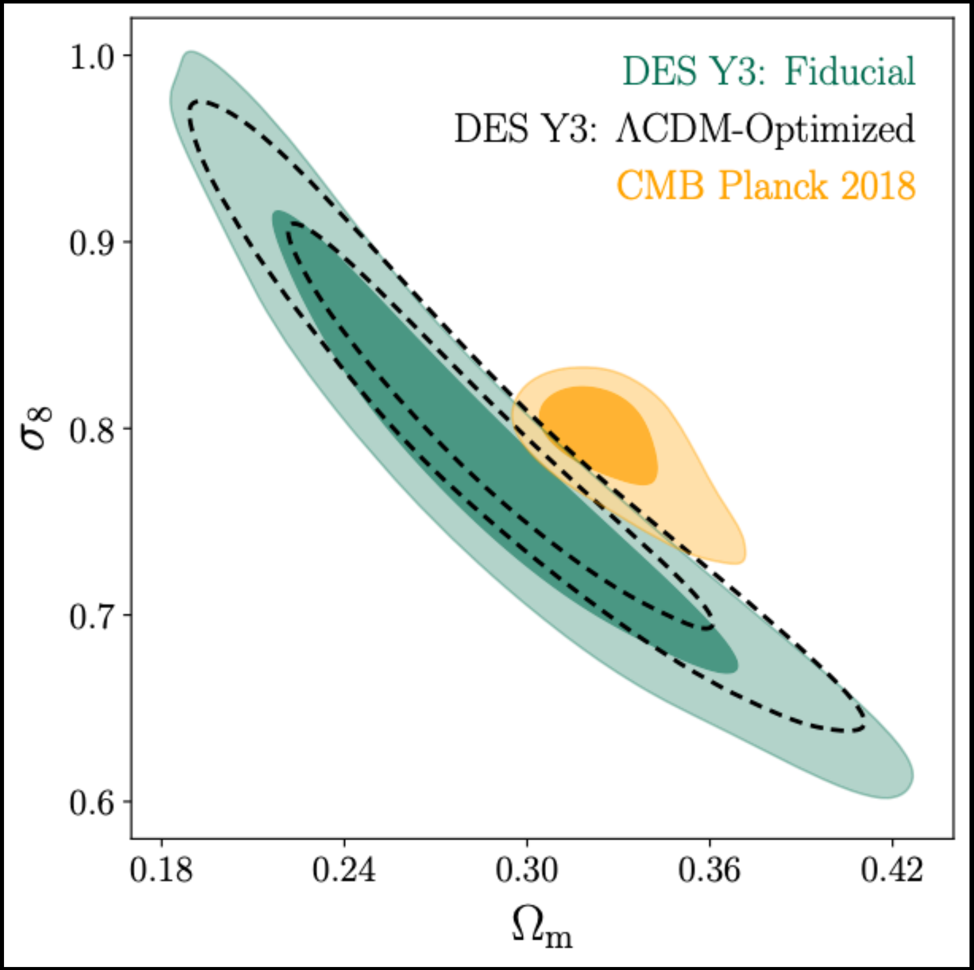

DES-Y3, Amon et al., arXiv:2105.13543 [astro-ph.CO]

The S8 tension is present at 2.5σ between Planck assuming ΛCDM and DES-Y3.

$S_8 = 0.834 \pm 0.016$

Planck 2018, Aghanim et al., arXiv:1807.06209 [astro-ph.CO]

$S_8 = 0.776^{+0.017}_{-0.017}$

DES-Y3, Abbott et al., arXiv:2105.13549 [astro-ph.CO]

$S_8 = 0.759^{+0.025}_{-0.025}$

DES-Y3 fiducial, Amon et al., arXiv:2105.13543 [astro-ph.CO]

The S8 tension

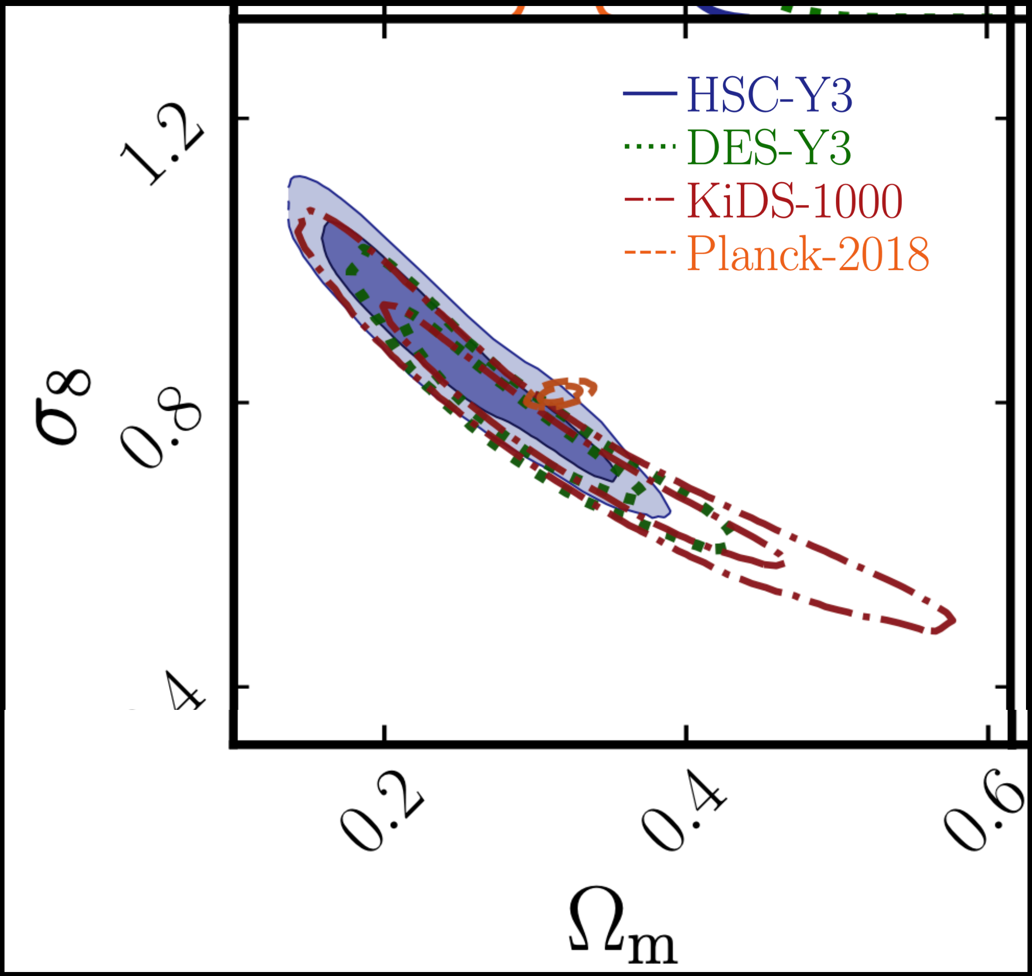

HSC-Y3, Dalal et al., arXiv:2304.00701 [astro-ph.CO]

The S8 tension is present at about 2σ between Planck assuming ΛCDM and HSC-Y3.

$S_8 = 0.834 \pm 0.016$

Planck 2018, Aghanim et al., arXiv:1807.06209 [astro-ph.CO]

$S_8 = 0.776^{+0.032}_{-0.033}$

HSC-Y3, Dalal et al., arXiv:2304.00701 [astro-ph.CO]

The S8 tension

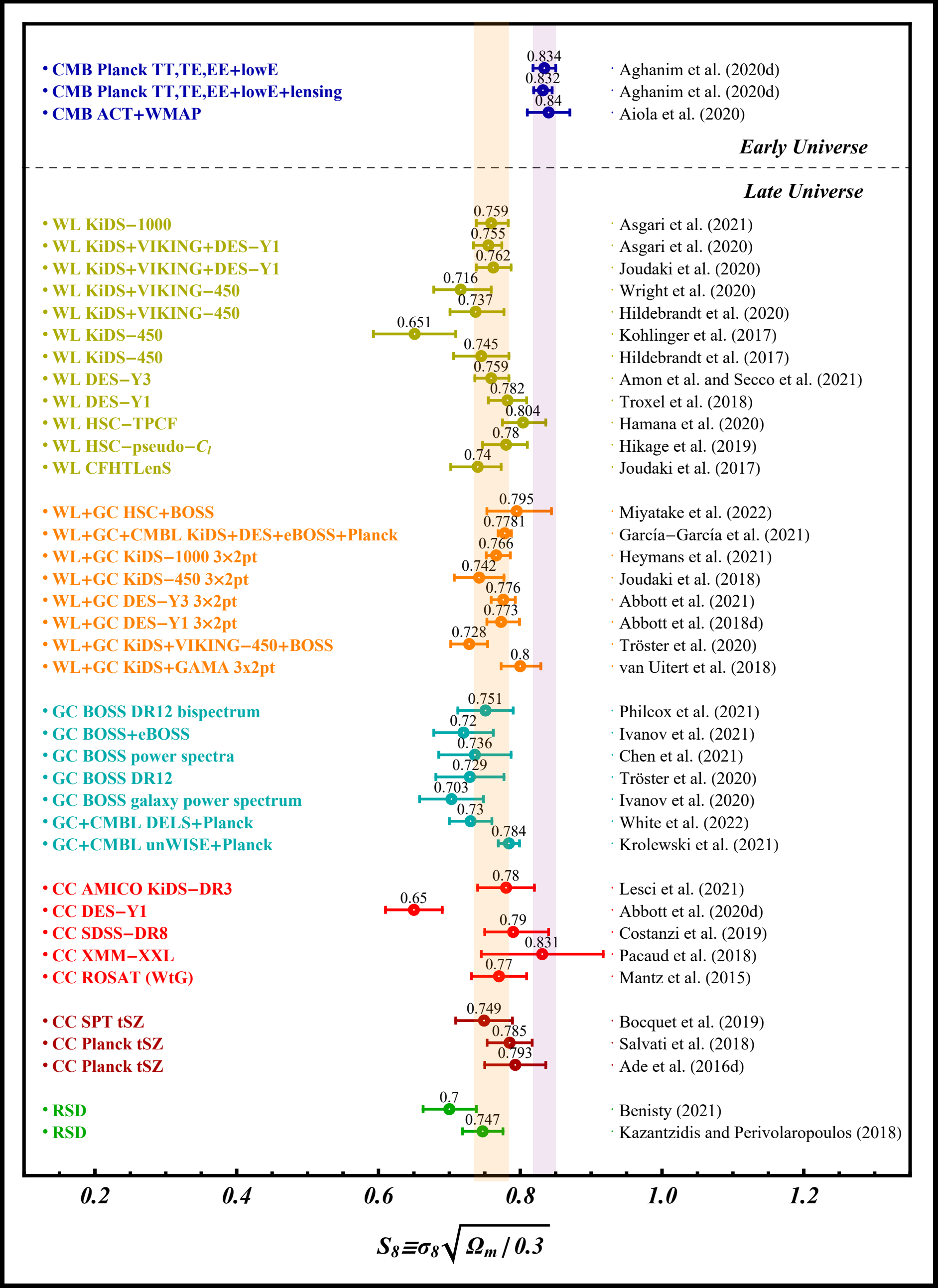

Abdalla et al., *JHEAp* 34 (2022) 49-211

See Di Valentino et al. *Astropart.Phys.* 131 (2021) 102604 and Abdalla et al., arXiv:2203.06142 [astro-ph.CO] for a summary of the possible candidates proposed to solve the S8 tension.

Early solutions to the H0 tension

Actually, a dark energy model that merely changes the value of rd would not completely resolve the tension, since it will affect the inferred value of Ωm and transfer the tension to it.

This is a plot illustrating that achieving a full agreement between CMB, BAO and SH0ES through a reduction of rd requires a higher value of $\Omega_m h^2$.

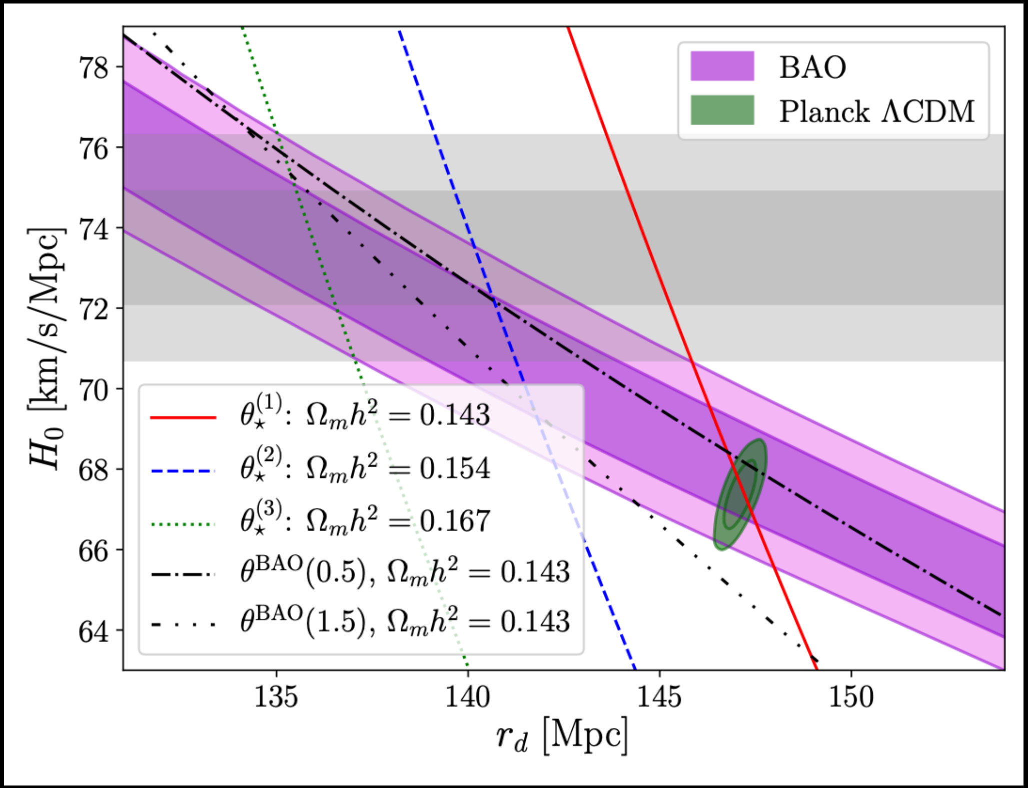

Jedamzik et al., Commun.in Phys. 4 (2021) 123

Early solutions to the H0 tension

Model 2 is defined by the simultaneous fit to BAO and CMB acoustic peaks at $\Omega_m h^2 = 0.155$, while model 3 has $\Omega_m h^2 = 0.167$

The sound horizon problem should be considered not only in the plane H0–rd, but it should be extended to the parameters triplet H0–rd–Ωm.

The figure shows that when attempting to find a full resolution of the Hubble tension, with CMB, BAO and SH0ES in agreement with each other, one exacerbates the tension with DES, KiDS and HSC.

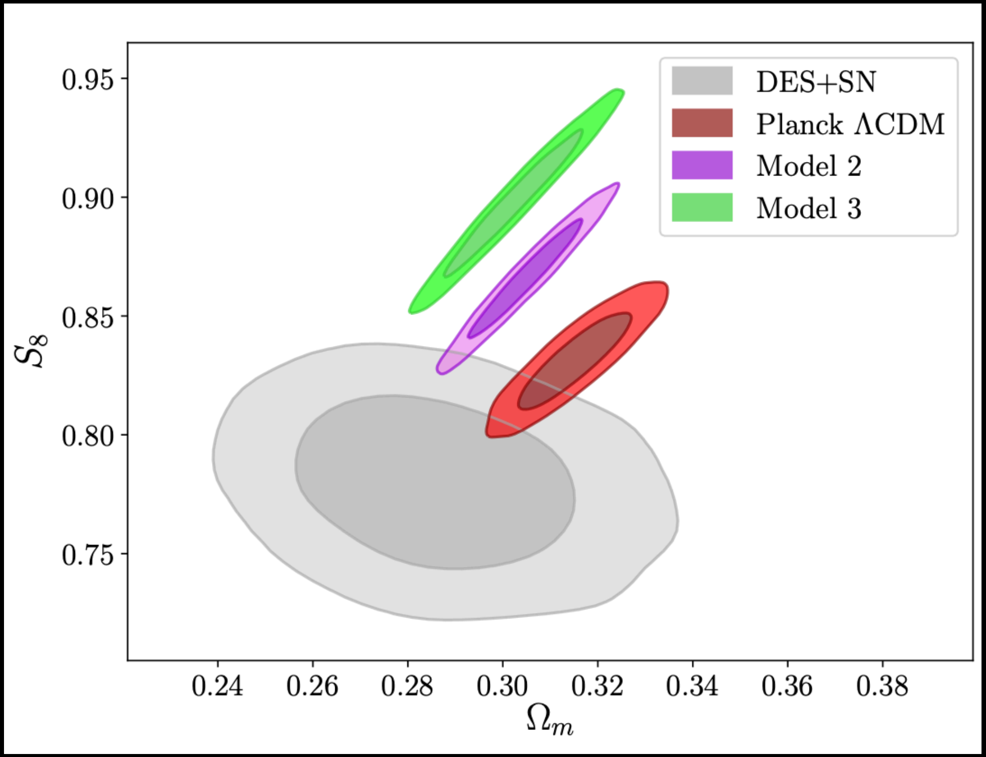

Jedamzik et al., Commun.in Phys. 4 (2021) 123

Successful models?

This is the density of the proposed cosmological models:

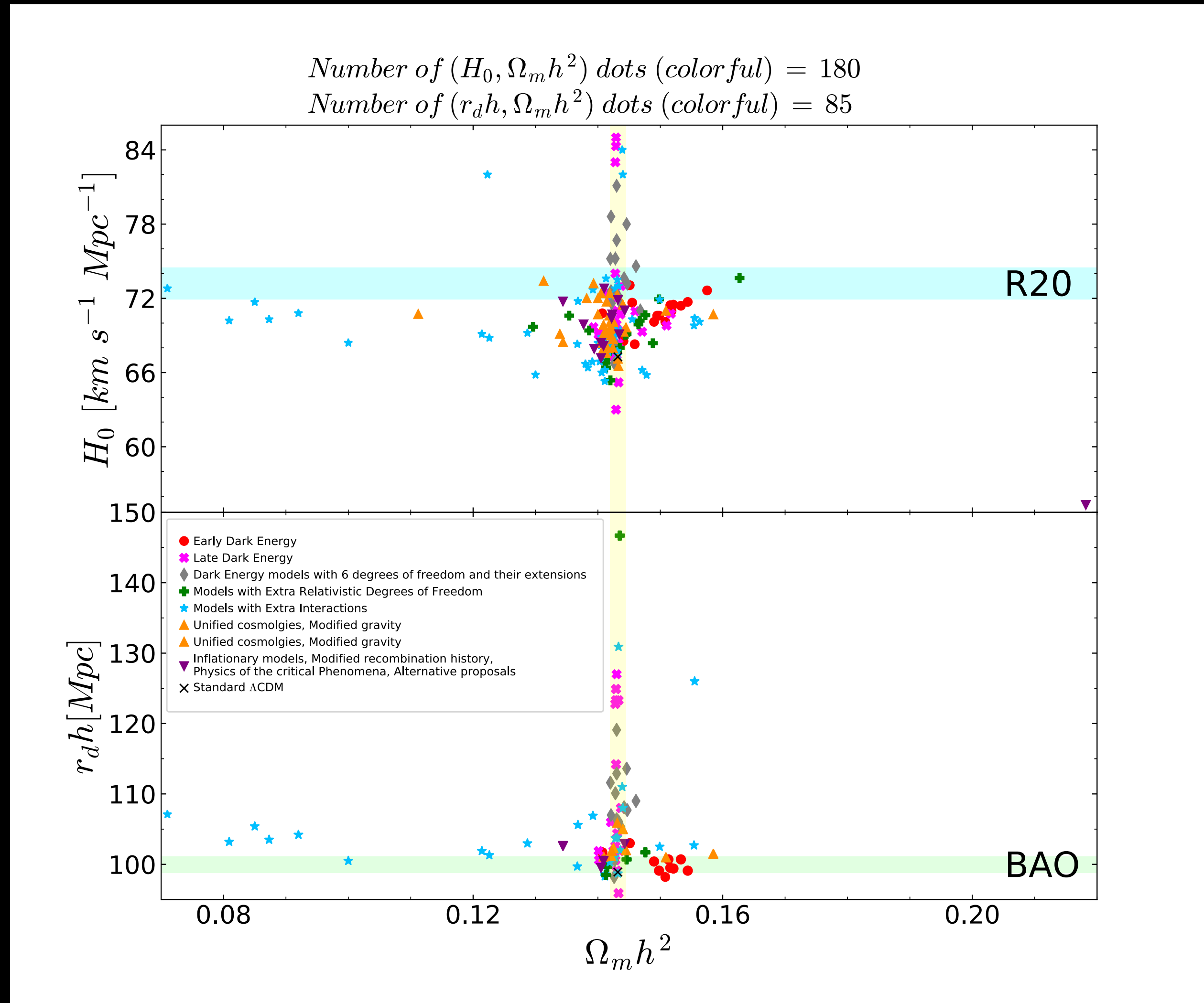

At the moment no specific proposal makes a strong case for being highly likely or far better than all others !!!

Di Valentino et al., Class.Quant.Grav. (2021), arXiv:2103.01183 [astro-ph.CO]

What about the interacting DM-DE models?

The IDE case

In the standard cosmological framework, DM and DE are described as separate fluids not sharing interactions beyond gravitational ones.
At the background level, the conservation equations for the pressureless DM and DE components can be decoupled into two separate equations with an inclusion of an arbitrary function, Q, known as the coupling or interacting function:

$$
\begin{aligned}
\dot{\rho}_c + 3\mathcal{H}\rho_c &= Q\,, \\
\dot{\rho}_x + 3\mathcal{H}(1+w)\rho_x &= -Q\,,
\end{aligned}
$$

and we assume the phenomenological form for the interaction rate:

$$Q = \xi \mathcal{H} \rho_x$$

proportional to the dark energy density ρ_x and the conformal Hubble rate $\mathcal{H}$, via a negative dimensionless parameter ξ quantifying the strength of the coupling, to avoid early-time instabilities.

Gavela et al. J. Cosmol. Astropart. Phys. 07 (2009) 034

The IDE case

In this scenario of IDE the tension on H0 between the Planck satellite and SH0ES is completely solved. The coupling could affect the value of the present matter energy density Ω_m. Therefore, if within an interacting model Ω_m is smaller (because for negative ξ the dark matter density will decay into the dark energy one), a larger value of H0 would be required in order to satisfy the peaks structure of CMB observations, which accurately determine the value of $\Omega_m h^2$.

Parameter	*Planck*	*Planck*+*R19*
$\Omega_b h^2$	0.02239 ± 0.00015	0.02239 ± 0.00015
$\Omega_c h^2$	< 0.105	< 0.0615
n_s	0.9655 ± 0.0043	0.9656 ± 0.0044
$100\theta_s$	$1.0458^{+0.0033}_{-0.0021}$	1.0470 ± 0.0015
τ	0.0541 ± 0.0076	0.0534 ± 0.0080
ξ	$-0.54^{+0.12}_{-0.28}$	$-0.66^{+0.09}_{-0.13}$
H_0 [km s^{-1} Mpc^{-1}]	$72.8^{+3.0}_{-1.5}$	$74.0^{+1.2}_{-1.0}$

TABLE I. Mean values with their 68% C.L. errors on selected cosmological parameters within the $\xi\Lambda$CDM model, considering either the *Planck* 2018 legacy dataset alone, or the same dataset in combination with the *R19* Gaussian prior on H_0 based on the latest local distance measurement from *HST*. The quantity quoted in the case of $\Omega_c h^2$ is the 95% C.L. upper limit.

Di Valentino et al., Phys.Dark Univ. 30 (2020) 100666

The IDE case

Therefore we can safely combine the two datasets together, and we obtain a non-zero dark matter-dark energy coupling ξ at more than FIVE standard deviations.

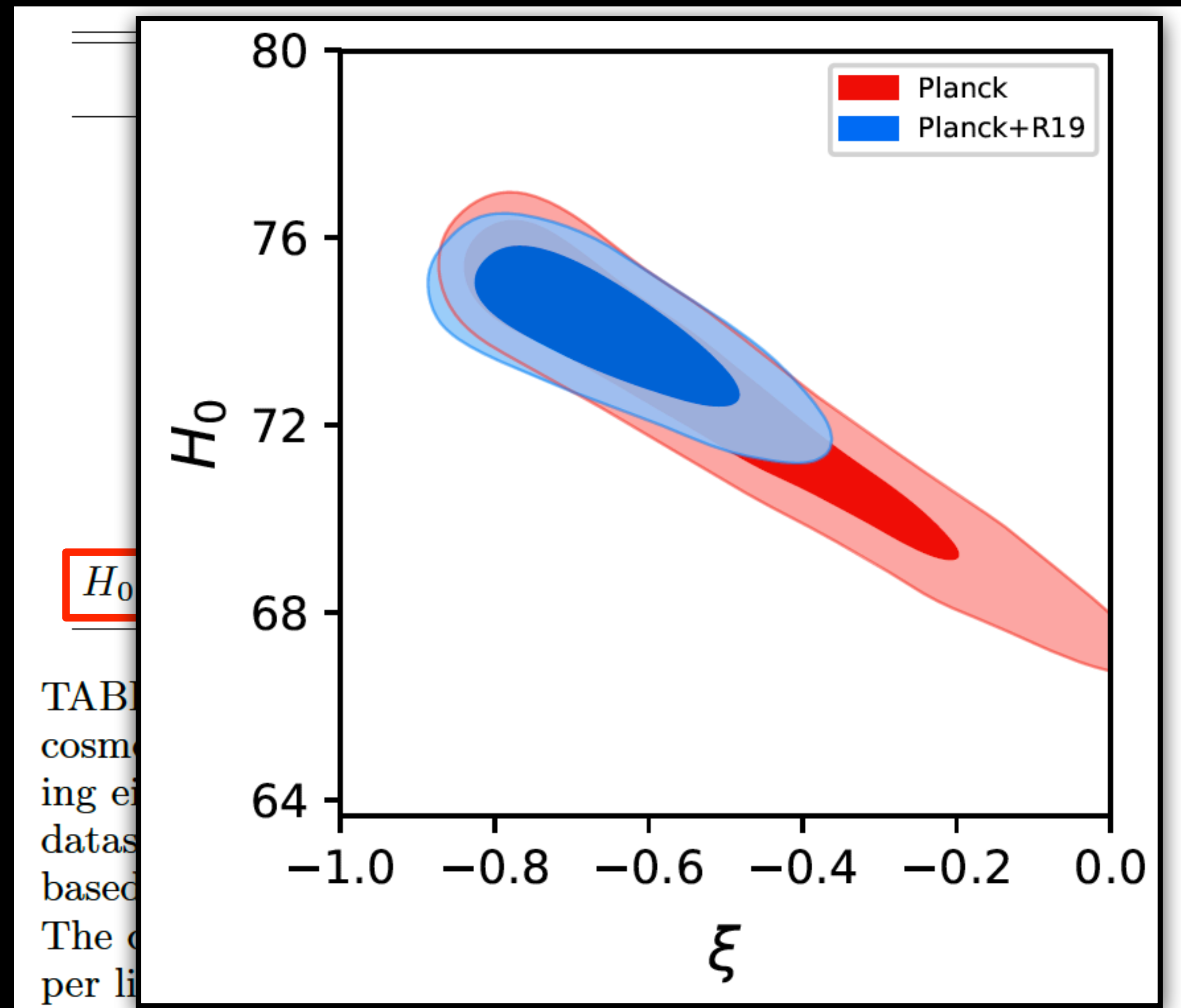

Di Valentino et al., Phys.Dark Univ. 30 (2020) 100666

The IDE case

Moreover, we find a shift of the clustering parameter σ_8 towards a higher value, compensated by a lowering of the matter density Ω_m, both with relaxed error bars.
The reason is that once a coupling is switched on and
Ω_m becomes smaller,
the clustering parameter σ_8 must be larger to have a proper normalization of the (lensing and clustering) power spectra.

This model can therefore significantly reduce the significance of the S8 tension
(See also Lucca, *Phys.Dark Univ.* 34 (2021) 100899)

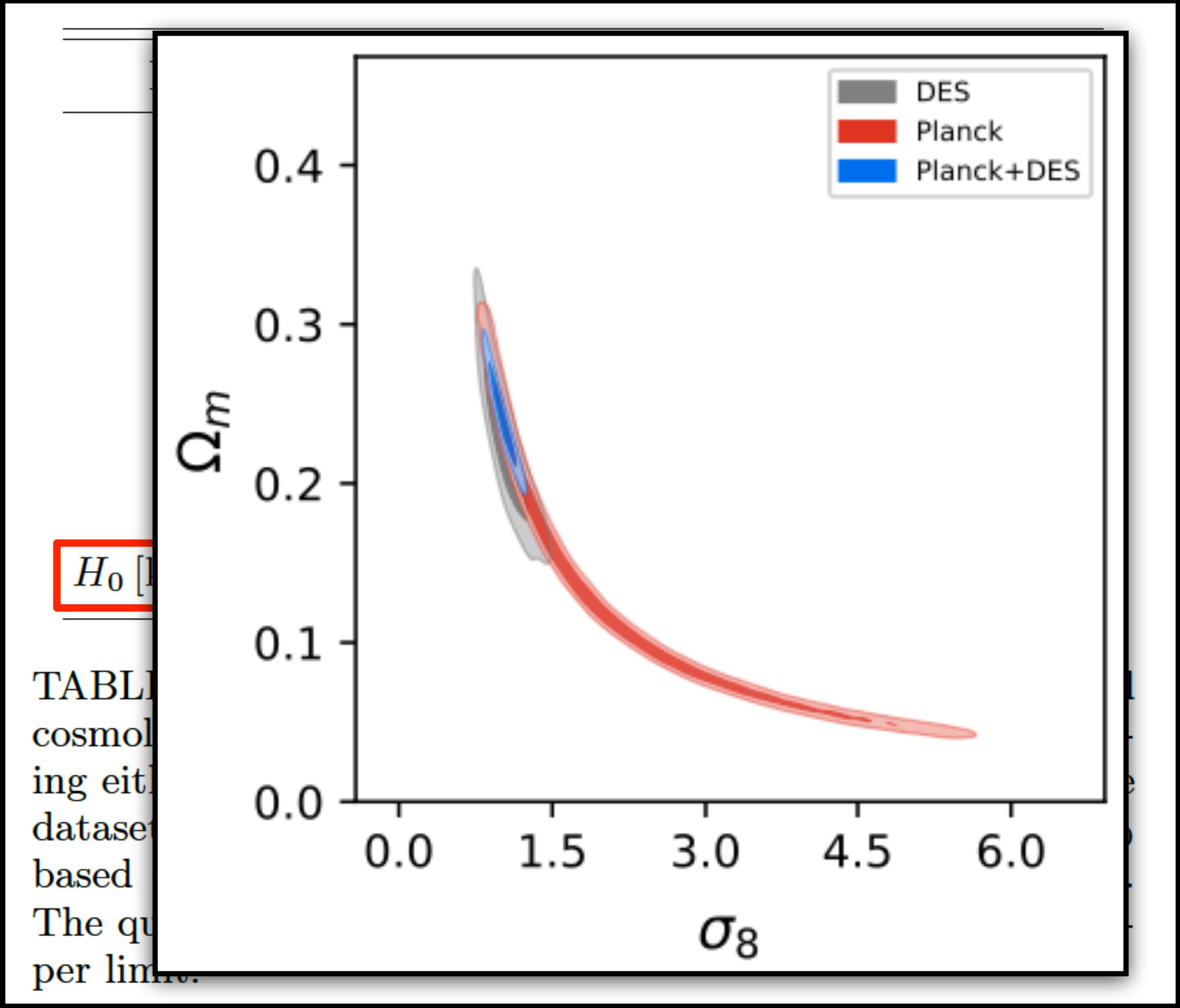

Di Valentino et al., Phys.Dark Univ. 30 (2020) 100666

Bayes factor

Anyway it is clearly interesting to quantify the better accordance of a model with the data respect to another by using the marginal likelihood also known as the Bayesian evidence.

The Bayesian evidence weights the simplicity of the model with the improvement of the fit of the data. In other words, because of the Occam's razor principle, models with additional parameters are penalised, if don't improve significantly the fit.

Given two competing models M_0 and M_1 it is useful to consider the ratio of the likelihood probability (the Bayes factor):

$$ln\mathcal{B} = p(\boldsymbol{x}|M_0)/p(\boldsymbol{x}|M_1)$$

According to the revised Jeffrey's scale by Kass and Raftery 1995, the evidence for M_0 (against M_1) is considered as "weak" if $|\ln B| > 1.0$, "moderate" if $|\ln B| > 2.5$, and "strong" if $|\ln B| > 5.0$.

The IDE case

Computing the Bayes factor for the IDE model with respect to ΛCDM for the Planck dataset we find lnB = 1.2, i.e. a weak evidence for the IDE model. If we consider Planck + SH0ES we find the extremely high value lnB=10.0, indicating a strong evidence for the IDE model.

Parameter	*Planck*	*Planck*+*R19*
$\Omega_b h^2$	0.02239 ± 0.00015	0.02239 ± 0.00015
$\Omega_c h^2$	< 0.105	< 0.0615
n_s	0.9655 ± 0.0043	0.9656 ± 0.0044
$100\theta_s$	$1.0458^{+0.0033}_{-0.0021}$	1.0470 ± 0.0015
τ	0.0541 ± 0.0076	0.0534 ± 0.0080
ξ	$-0.54^{+0.12}_{-0.28}$	$-0.66^{+0.09}_{-0.13}$
$H_0\,[\mathrm{km\,s^{-1}\,Mpc^{-1}}]$	$72.8^{+3.0}_{-1.5}$	$74.0^{+1.2}_{-1.0}$

TABLE I. Mean values with their 68% C.L. errors on selected cosmological parameters within the $\xi\Lambda$CDM model, considering either the *Planck* 2018 legacy dataset alone, or the same dataset in combination with the *R19* Gaussian prior on H_0 based on the latest local distance measurement from *HST*. The quantity quoted in the case of $\Omega_c h^2$ is the 95% C.L. upper limit.

Di Valentino et al., Phys.Dark Univ. 30 (2020) 100666

fake IDE detection

Parameters	Fiducial model	Planck	Planck+BAO	PICO	PRISM
$\Omega_b h^2$	0.02236	0.02238 ± 0.00015	0.02230 ± 0.00014	0.022364 ± 0.000029	0.022361 ± 0.000019
$\Omega_c h^2$	0.1202	$0.056^{+0.025}_{-0.047}$	$0.101^{+0.019}_{-0.006}$	$0.100^{+0.019}_{-0.008}$	$0.103^{+0.016}_{-0.007}$
$100\theta_{MC}$	1.04090	$1.0451^{+0.0021}_{-0.0032}$	$1.0419^{+0.0005}_{-0.0011}$	$1.04206^{+0.0005}_{-0.0011}$	$1.04191^{+0.00042}_{-0.00094}$
τ	0.0544	$0.0528^{+0.010}_{-0.009}$	0.0517 ± 0.0098	$0.0543^{+0.0016}_{-0.0019}$	$0.0542^{+0.0017}_{-0.0019}$
n_s	0.9649	0.9652 ± 0.0041	0.9624 ± 0.0036	0.9571 ± 0.0014	0.9657 ± 0.0012
$\ln(10^{10}A_s)$	3.045	$3.041^{+0.020}_{-0.018}$	3.042 ± 0.019	$3.0436^{+0.0030}_{-0.0034}$	3.0435 ± 0.0032
ξ	0	$-0.48^{+0.16}_{-0.30}$	> -0.223	> -0.220	> -0.195

Di Valentino & Mena, Mon.Not.Roy.Astron.Soc. 500 (2020) 1, L22-L26, arXiv:2009.12620

For a mock Planck-like experiment, due to the strong correlation present between the standard and the exotic physics parameters, there is a dangerous detection at more than 3σ for a coupling between dark matter and dark energy different from zero, even if the fiducial model has $\xi = 0$:

$-0.85 < \xi < -0.02$ at 99% CL

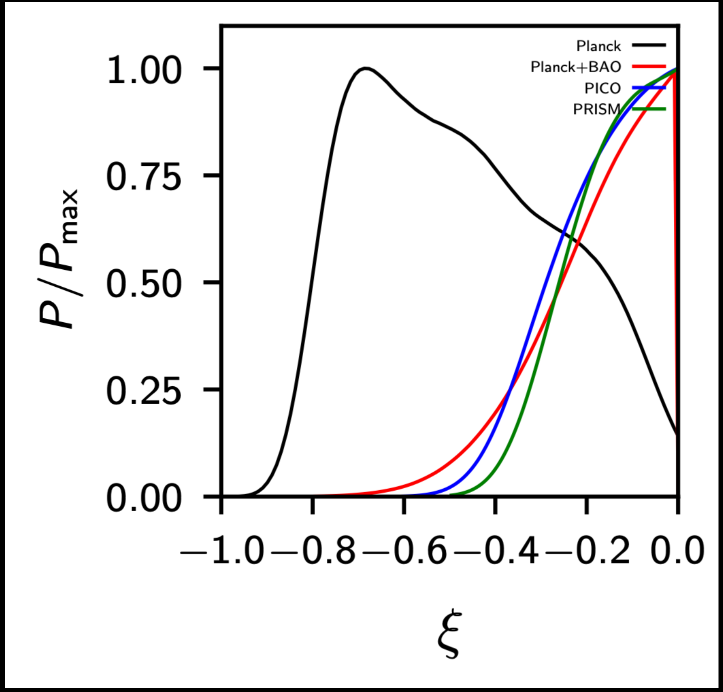

Mock experiments

fake IDE detection

Parameters	Fiducial model	Planck	Planck+BAO	PICO	PRISM
$\Omega_b h^2$	0.02236	0.02238 ± 0.00015	0.02230 ± 0.00014	0.022364 ± 0.000029	0.022361 ± 0.000019
$\Omega_c h^2$	0.1202	$0.056^{+0.025}_{-0.047}$	$0.101^{+0.019}_{-0.006}$	$0.100^{+0.019}_{-0.008}$	$0.103^{+0.016}_{-0.007}$
$100\theta_{MC}$	1.04090	$1.0451^{+0.0021}_{-0.0032}$	$1.0419^{+0.0005}_{-0.0011}$	$1.04206^{+0.0005}_{-0.0011}$	$1.04191^{+0.00042}_{-0.00094}$
τ	0.0544	$0.0528^{+0.010}_{-0.009}$	0.0517 ± 0.0098	$0.0543^{+0.0016}_{-0.0019}$	$0.0542^{+0.0017}_{-0.0019}$
n_s	0.9649	0.9652 ± 0.0041	0.9624 ± 0.0036	0.9571 ± 0.0014	0.9657 ± 0.0012
$\ln(10^{10} A_s)$	3.045	$3.041^{+0.020}_{-0.018}$	3.042 ± 0.019	$3.0436^{+0.0030}_{-0.0034}$	3.0435 ± 0.0032
ξ	0	$-0.48^{+0.16}_{-0.30}$	> -0.223	> -0.220	> -0.195

Di Valentino & Mena, Mon.Not.Roy.Astron.Soc. 500 (2020) 1, L22-L26, arXiv:2009.12620

The inclusion of mock BAO data,
a mock dataset built using the same fiducial cosmological model than that of the CMB,
helps in breaking the degeneracy,
providing a lower limit for the coupling ξ
in perfect agreement with zero.

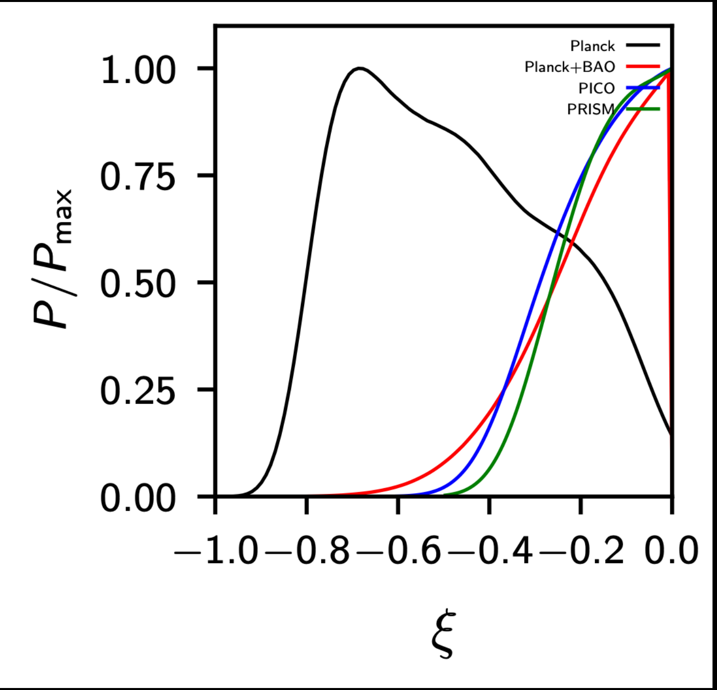

Mock experiments

The IDE case

Constraints at 68% cl.

Parameter	$CMB+BAO$	$CMB+FS$	$CMB+BAO+FS$
ω_c	$0.094^{+0.022}_{-0.010}$	$0.101^{+0.015}_{-0.009}$	$0.115^{+0.005}_{-0.001}$
ξ	$-0.22^{+0.18}_{-0.09}[> -0.48]$	> -0.35	> -0.12
H_0 [km/s/Mpc]	$69.55^{+0.98}_{-1.60}$	$69.04^{+0.84}_{-1.10}$	$68.02^{+0.49}_{-0.60}$
Ω_m	$0.243^{+0.054}_{-0.030}$	$0.261^{+0.038}_{-0.025}$	$0.299^{+0.015}_{-0.007}$

Nunes, Vagnozzi, Kumar, Di Valentino, and Mena, *Phys.Rev.D* 105 (2022) 12, 123506

The addition of low-redshift measurements, as BAO data, still hints to the presence of a coupling, albeit at a lower statistical significance. Also for this data sets the Hubble constant value is larger than that obtained in the case of a pure ΛCDM scenario, enough to bring the H0 tension at 2.1σ with SH0ES.

Baryon Acoustic Oscillations

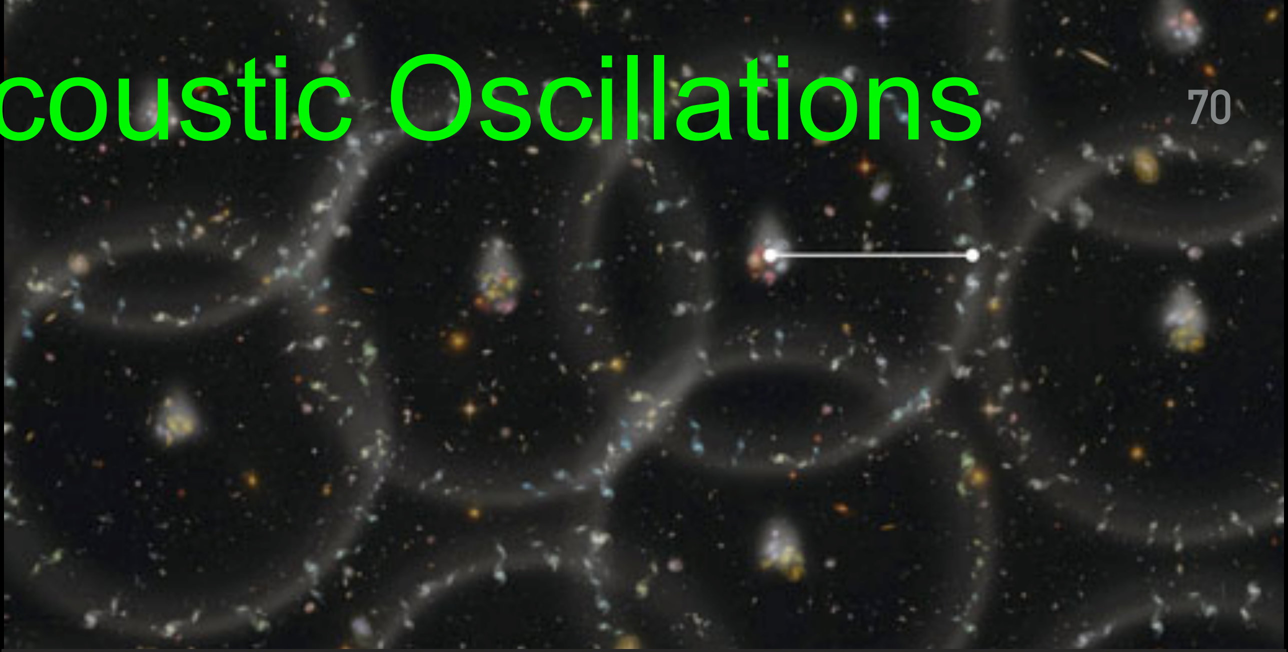

BAO is formed in the early universe, when baryons are strongly coupled to photons, and the gravitational collapse due to the CDM is counterbalanced by the radiation pressure. Sound waves that propagate in the early universe imprint a characteristic scale on the CMB. Since the scale of these oscillations can be measured at recombination, BAO is considered a "standard ruler". These fluctuations have evolved and we can observe BAO at low redshifts in the distribution of galaxies.

Since the data reduction process leading to these measurements involves making certain assumptions about the fiducial cosmology, this makes BAO measurements dependent on the cosmological model being used.

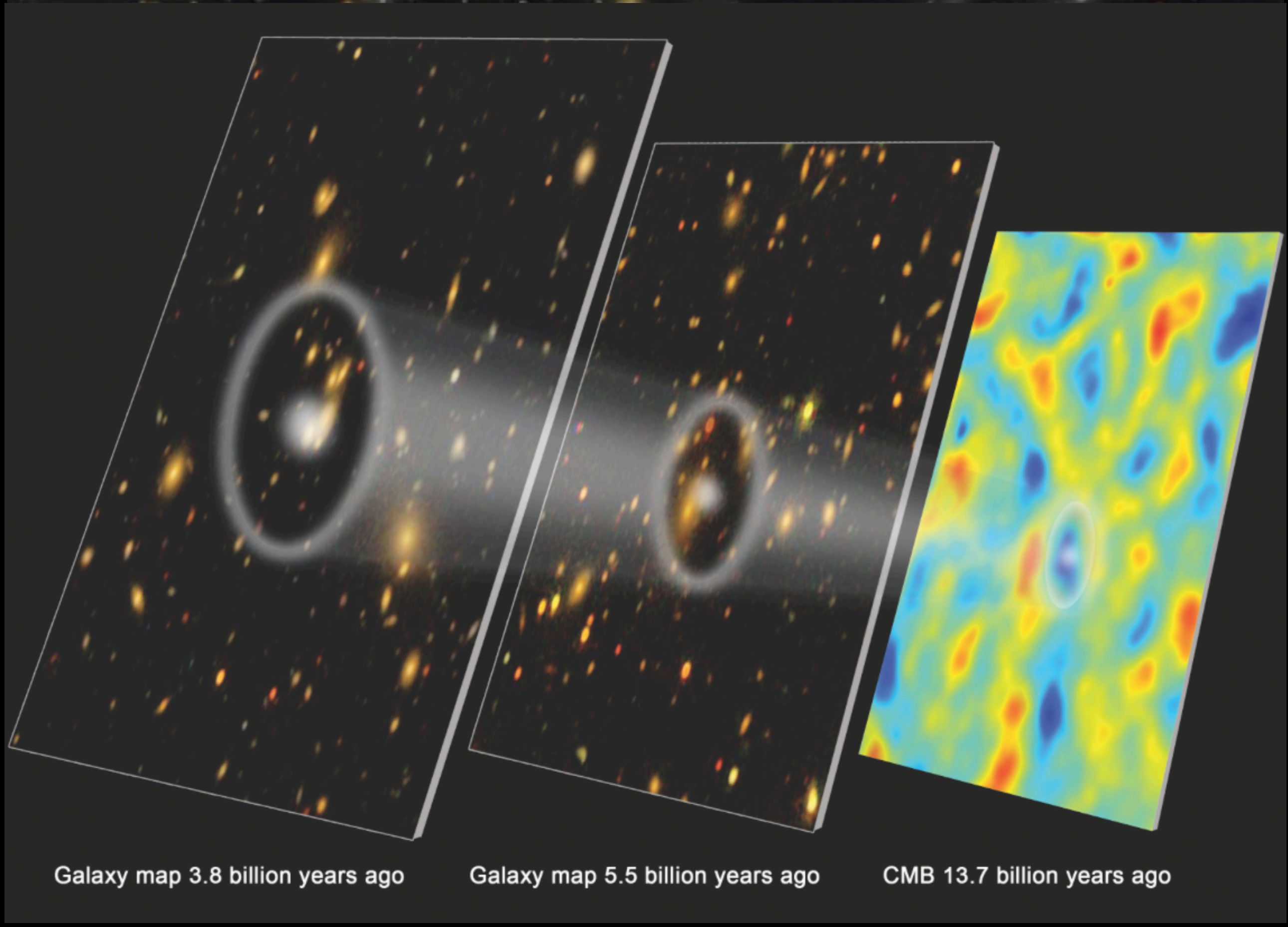

Baryon Acoustic Oscillations

In other words, the tension between Planck+BAO and SH0ES could be due to a statistical fluctuation in this case.

Actually, BAO data are extracted under the assumption of ΛCDM, and the modified scenario of interacting dark energy could affect the result.

In fact, the full procedure which leads to the BAO datasets carried out by the different collaborations might be not necessarily valid in extended DE models with important perturbations in the non-linear scales.

BAO datasets (both the pre- and post- reconstruction measurements) might need to be revised in a non-trivial manner when applied to constrain more exotic dark energy cosmologies.

Baryon Acoustic Oscillations

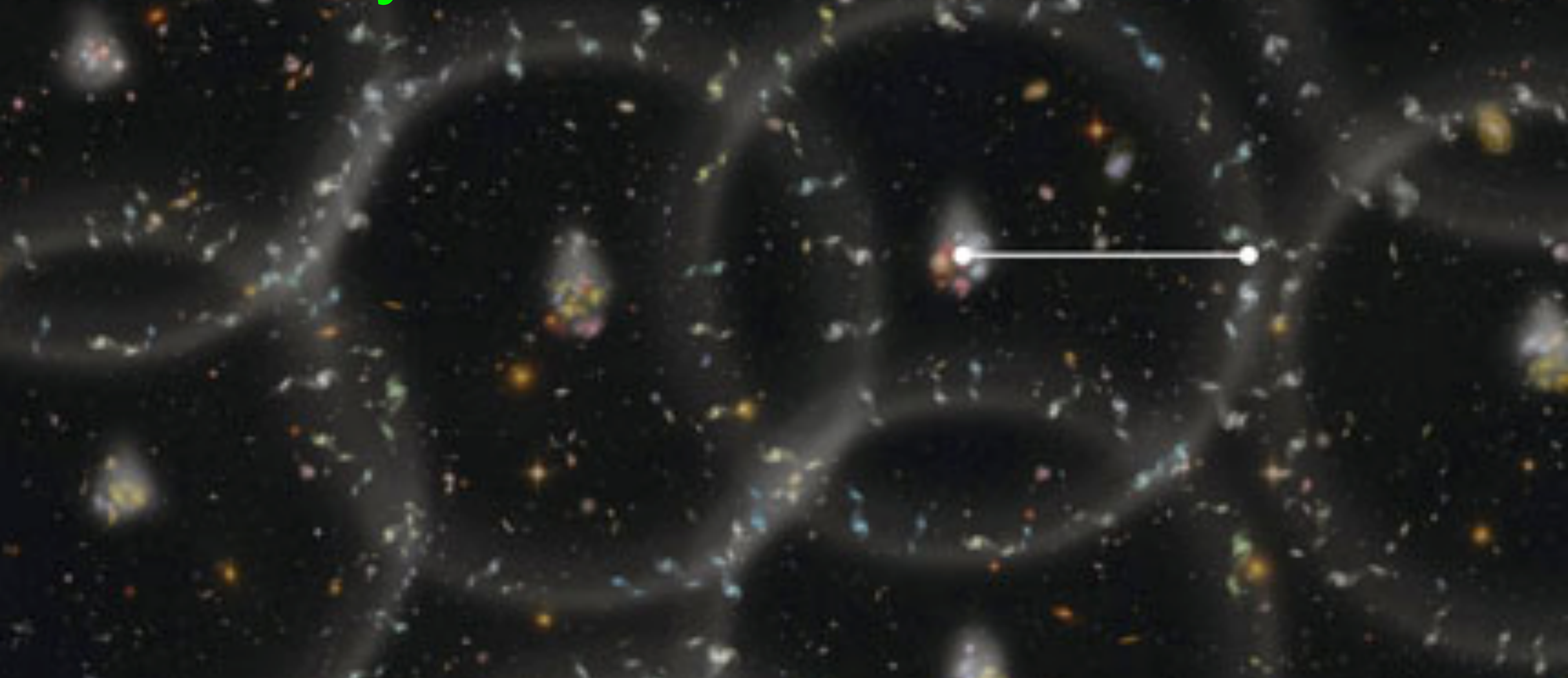

The problem is that for 3D BAO data one needs to reconstruct the comoving distance and this is done assuming a fiducial model.

We can try to see what happens using 2D BAO measurements, that are less model dependent because they are obtained working on spherical shells with redshift thickness Δz and only considering their angular distribution.

The IDE case

Parameter	Planck	+ lensing	Planck + BAO	+ lensing	Planck + BAOtr	+ lensing	Planck + BAOtr + H_0	+ lensing
H_0 [Km/s/Mpc]	67.32 ± 0.62	67.32 ± 0.53	67.65 ± 0.44	67.60 ± 0.43	69.01 ± 0.51	68.85 ± 0.55	69.88 ± 0.48	69.65 ± 0.44
S_8	0.832 ± 0.016	0.834 ± 0.013	0.825 ± 0.012	0.827 ± 0.011	0.794 ± 0.013	0.802 ± 0.012	0.774 ± 0.013	$0.7871^{+0.0095}_{-0.011}$
r_s [Mpc]	147.06 ± 0.30	147.04 ± 0.27	$147.21^{+0.23}_{-0.26}$	147.13 ± 0.23	147.75 ± 0.26	147.64 ± 0.26	148.06 ± 0.25	147.91 ± 0.24

A comparison between the 3D BAO data, model dependent and obtained assuming ΛCDM, and the 2D BAO measurements, less model dependent, shows almost the same results for the ΛCDM scenario.

Bernui, Di Valentino, Giarè, Kumar, and Nunes, *Phys.Rev.D* 107 (2023) 10, 103531

The IDE case

Parameter		Planck	+ lensing	Planck + BAO	+ lensing	Planck + BAOtr	+ lensing	Planck + BAOtr + H_0	+ lensing
ξ	68% CL	$-0.43^{+0.28}_{-0.21}$	$-0.40^{+0.23}_{-0.20}$	> -0.207	> -0.210	$-0.683^{+0.088}_{-0.11}$	$-0.683^{+0.087}_{-0.12}$	-0.58 ± 0.11	-0.53 ± 0.11
	95% CL	(> -0.775)	$(-0.40^{+0.40}_{-0.32})$	(> -0.389)	(> -0.411)	$(-0.68^{+0.21}_{-0.19})$	$(-0.68^{+0.23}_{-0.20})$	$(-0.58^{+0.22}_{-0.21})$	$(-0.53^{+0.19}_{-0.20})$
	99% CL	$[> -0.819]$	$[> -0.743]$	$[> -0.486]$	$[> -0.527]$	$[-0.68^{+0.29}_{-0.23}]$	$[-0.68^{+0.37}_{-0.27}]$	$[-0.58^{+0.31}_{-0.29}]$	$[-0.53^{+0.39}_{-0.25}]$
H_0 [Km/s/Mpc]		$71.7^{+2.3}_{-2.7}$	71.6 ± 2.1	$68.93^{+0.79}_{-1.2}$	$69.08^{+0.74}_{-1.3}$	$75.2^{+1.2}_{-0.75}$	$75.3^{+1.3}_{-0.75}$	73.99 ± 0.88	$73.45^{+0.71}_{-0.59}$
S_8		$1.109^{+0.063}_{-0.28}$	$1.053^{+0.079}_{-0.21}$	$0.891^{+0.025}_{-0.062}$	$0.893^{+0.021}_{-0.065}$	$1.49^{+0.24}_{-0.29}$	1.49 ± 0.26	$1.23^{+0.11}_{-0.22}$	$1.15^{+0.10}_{-0.14}$
r_s [Mpc]		147.08 ± 0.30	147.12 ± 0.27	147.03 ± 0.25	147.05 ± 0.25	147.32 ± 0.27	147.35 ± 0.29	$147.31^{+0.25}_{-0.29}$	$147.32^{+0.26}_{-0.29}$
$\ln B_{ij}$		0.85	−0.17	1.60	0.60	−9.22	−11.68	−14.04	−15.21

A comparison between the 3D BAO data,
model dependent and obtained assuming ΛCDM,
and the 2D BAO measurements, less model dependent,
shows completely different results for the IDE model.
There is a strong evidence for the coupling at more than 99% CL,
solving at the same time the H0 tension with SH0ES.

Bernui, Di Valentino, Giarè, Kumar, and Nunes, *Phys.Rev.D* 107 (2023) 10, 103531

The IDE case

Parameter		Planck	ck + BAOtr + H_0	+ lensing
ξ	68% CL	$-0.43^{+0.}_{-0.}$	-0.58 ± 0.11	-0.53 ± 0.11
	95% CL	$(> -0.77$	$(-0.58^{+0.22}_{-0.21})$	$(-0.53^{+0.19}_{-0.20})$
	99% CL	$[> -0.81$	$[-0.58^{+0.31}_{-0.29}]$	$[-0.53^{+0.39}_{-0.25}]$
H_0 [Km/s/Mpc]		$71.7^{+2.}_{-2.}$	73.99 ± 0.88	$73.45^{+0.71}_{-0.59}$
S_8		$1.109^{+0.0}_{-0.2}$	$1.23^{+0.11}_{-0.22}$	$1.15^{+0.10}_{-0.14}$
r_s [Mpc]		147.08 ± 0	$147.31^{+0.25}_{-0.29}$	$147.32^{+0.26}_{-0.29}$
$\ln B_{ij}$		0.85	-14.04	-15.21

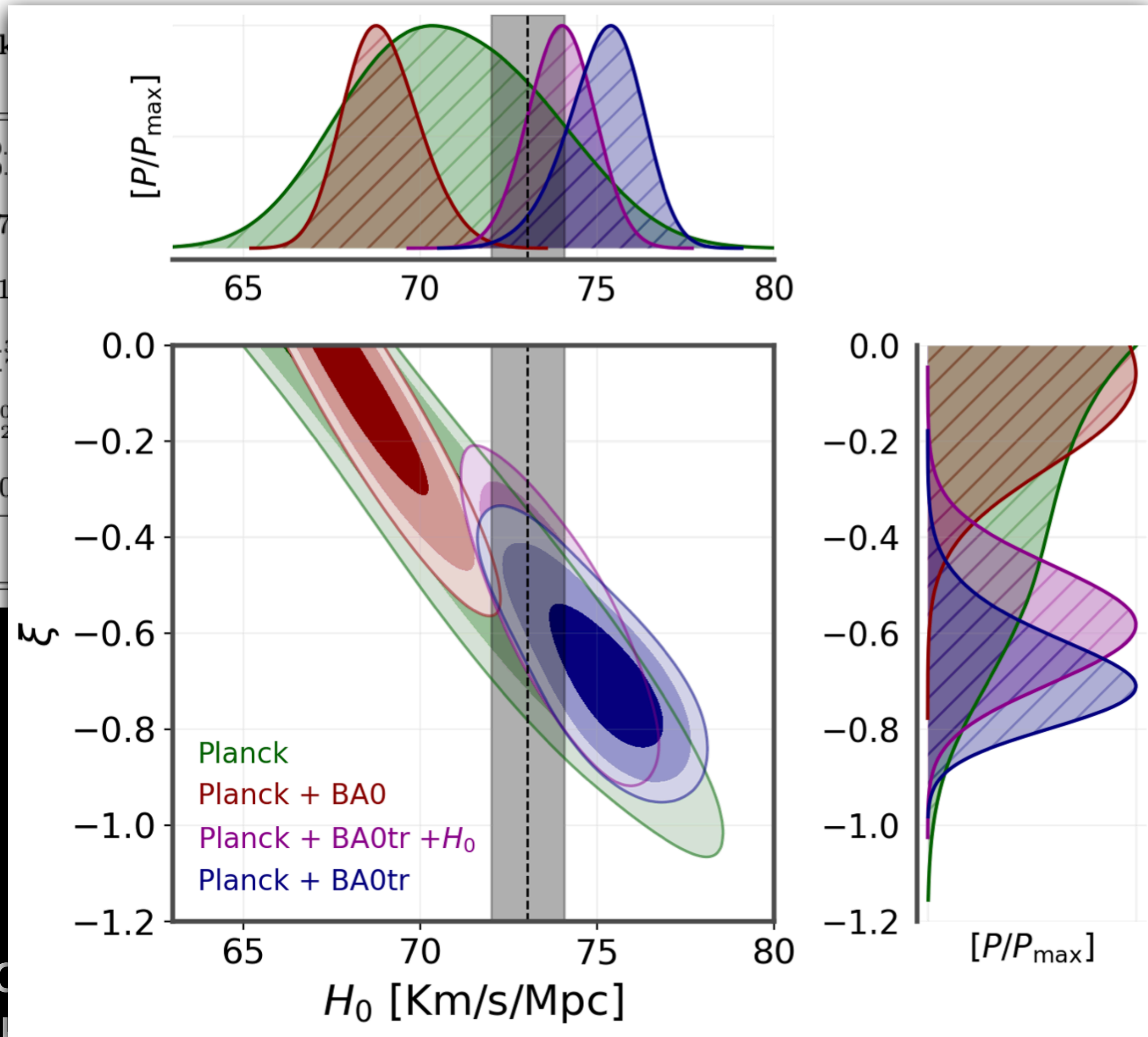

M,
anc … ndent,
sl … odel.

There is a strong evidence for the coupling at more than 99% CL, solving at the same time the H0 tension with SH0ES.

Bernui, Di Valentino, Giarè, Kumar, and Nunes, *Phys.Rev.D* 107 (2023) 10, 103531

The IDE case

Table II. Constraints at 68% CL on the parameters of the ΛCDM model.

Parameter	CMB	CMB+BAO-3D	CMB+BAO-2D (ON)	CMB+BAO-2D (M&M)
$10^2 \times \Omega_b h^2$	2.236 ± 0.015	2.245 ± 0.013	2.263 ± 0.014	2.246 ± 0.014
$\Omega_c h^2$	0.1202 ± 0.0014	0.11911 ± 0.00096	0.1165 ± 0.0011	0.11877 ± 0.00097
H_0	67.32 ± 0.62	67.84 ± 0.43	69.01 ± 0.51	67.96 ± 0.44
$\tau_{\rm reio}$	0.0536 ± 0.0081	0.0590 ± 0.0070	0.0606 ± 0.0081	0.0567 ± 0.0080
$\log(10^{10} A_s)$	3.043 ± 0.016	3.053 ± 0.015	3.049 ± 0.017	3.047 ± 0.016
n_s	0.9646 ± 0.0045	0.9677 ± 0.0037	0.9742 ± 0.0038	0.9688 ± 0.0037

A comparison between the 3D BAO data
and the 2D BAO measurements Menote & Marra arXiv:2112.10000,
from the same BOSS DR12 and eBOSS DR16,
gives exactly the same results for the ΛCDM scenario.

Giarè, Di Valentino, et al. in preparation

The IDE case

Table I. Constraints at 68% (95%) CL on the parameters of the IDE model.

Parameter	**CMB**	**CMB+BAO-3D**	**CMB+BAO-2D (ON)**	**CMB+BAO-2D (M&M)**
$10^2 \times \Omega_b h^2$	2.239 ± 0.015	2.236 ± 0.013	2.248 ± 0.014	2.237 ± 0.014
$\Omega_c h^2$	$0.067^{+0.042}_{-0.031}$ (< 0.115)	$0.101^{+0.016}_{-0.012}$	$0.022^{+0.014}_{-0.019}$	$0.089^{+0.019}_{-0.016}$
H_0	71.6 ± 2.1	$68.92^{+0.96}_{-1.2}$	$75.2^{+1.1}_{-0.96}$	69.9 ± 1.1
$\tau_{\rm reio}$	0.0534 ± 0.0079	0.0544 ± 0.0079	0.0556 ± 0.0082	0.0537 ± 0.0078
$\log(10^{10} A_s)$	3.042 ± 0.016	3.045 ± 0.016	3.044 ± 0.017	3.044 ± 0.016
n_s	0.9655 ± 0.0045	0.9650 ± 0.0037	0.9695 ± 0.0040	0.9657 ± 0.0039
ξ	$-0.40^{+0.23}_{-0.20}$ (> -0.775)	$> -0.207 (> -0.389)$	$-0.683^{+0.088}_{-0.11}$	$-0.26^{+0.18}_{-0.12}$ (> -0.505)

A comparison between the 3D BAO data
and the 2D BAO measurements Menote & Marra arXiv:2112.10000,
from the same BOSS DR12 and eBOSS DR16,
gives different H0 values for the IDE scenario.

Giarè, Di Valentino, et al. in preparation

IDE from ACT

Parameter	Planck	ACT	ACT+WMAP	ACT+Planck
$\Omega_\mathrm{b}h^2$	0.02237 ± 0.00015	0.02153 ± 0.00032	0.02238 ± 0.00020	0.02238 ± 0.00013
$\Omega_\mathrm{c}h^2$	$0.067^{+0.042}_{-0.031}\,(< 0.115)$	$< 0.0754\,(< 0.111)$	$0.070^{+0.046}_{-0.021}\,(< 0.117)$	$0.067^{+0.042}_{-0.030}\,(< 0.115)$
H_0	71.6 ± 2.1	$72.6^{+3.4}_{-2.6}$	$71.3^{+2.6}_{-3.2}$	$71.4^{+2.5}_{-2.8}$
τ_reio	0.0534 ± 0.0079	0.063 ± 0.015	0.061 ± 0.014	0.0533 ± 0.0073
$\log(10^{10}A_\mathrm{s})$	3.042 ± 0.016	3.046 ± 0.030	3.064 ± 0.028	3.047 ± 0.014
n_s	0.9655 ± 0.0045	1.010 ± 0.016	$0.9741^{+0.0066}_{-0.0064}$	0.9699 ± 0.0038
ξ	$-0.40^{+0.23}_{-0.20}$	$-0.46^{+0.20}_{-0.28}$	$-0.38^{+0.35}_{-0.14}$	$-0.40^{+0.27}_{-0.23}$
$\ln \mathcal{B}_{ij}$	-0.17	-0.07	0.06	-0.25

Zhai, Giarè, van de Bruck, Di Valentino, et al, *JCAP* 07 (2023) 032

Let’s now consider different combinations of CMB datasets.

IDE from ACT

Parameter	Planck	ACT	ACT+WMAP	ACT+Planck
$\Omega_b h^2$	0.02237 ± 0.00015	0.02153 ± 0.00032	0.02238 ± 0.00020	0.02238 ± 0.00013
$\Omega_c h^2$	$0.067^{+0.}_{-0.}$ [illegible]	[illegible]	[illegible] 7)	$0.067^{+0.042}_{-0.030}$ (< 0.115)
H_0	71. [illegible]	[illegible]	[illegible]	$71.4^{+2.5}_{-2.8}$
τ_{reio}	0.053 [illegible]	[illegible]	[illegible]	0.0533 ± 0.0073
$\log(10^{10} A_s)$	3.04 [illegible]	[illegible]	[illegible]	3.047 ± 0.014
n_s	0.965 [illegible]	[illegible]	[illegible]	0.9699 ± 0.0038
ξ	−0. [illegible]	[illegible]	[illegible]	$-0.40^{+0.27}_{-0.23}$
$\ln \mathcal{B}_{ij}$	- [illegible]	[illegible]	[illegible]	-0.25

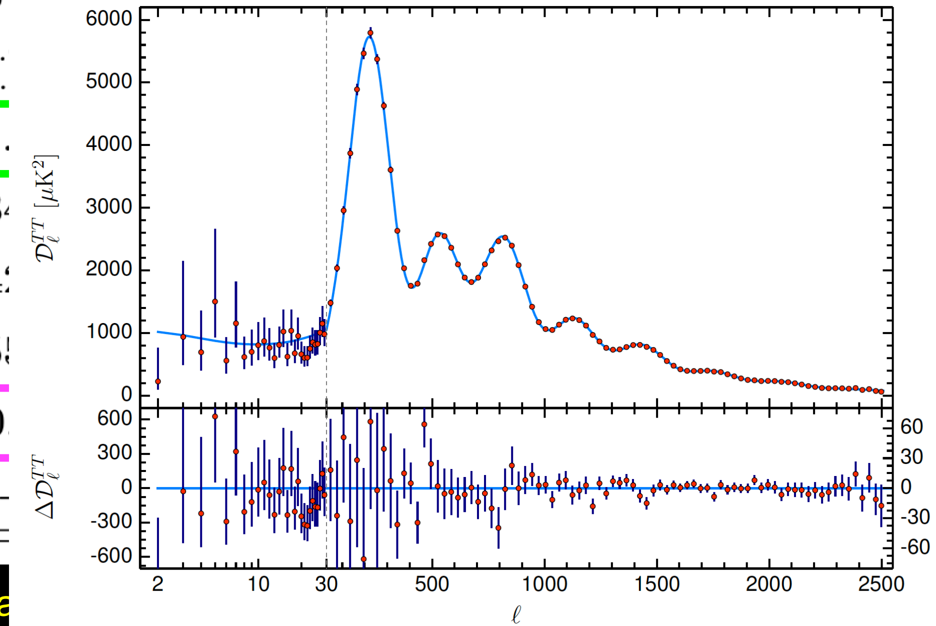

Zha[illegible] [illegible]) 032

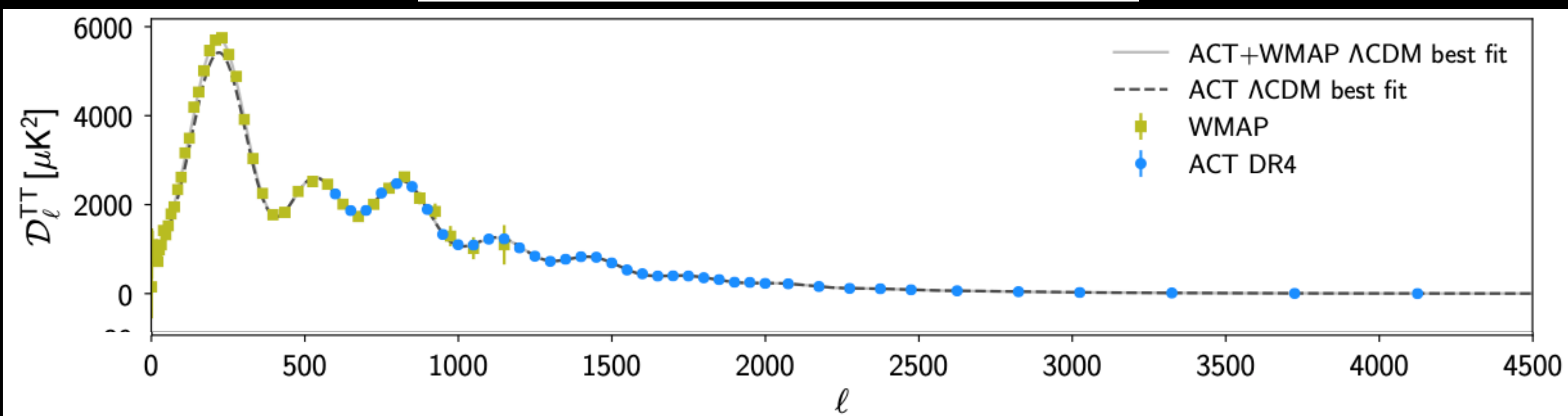

IDE from ACT

Parameter	Planck	ACT	ACT+WMAP	ACT+Planck
$\Omega_b h^2$	0.02237 ± 0.00015	0.02153 ± 0.00032	0.02238 ± 0.00020	0.02238 ± 0.00013
$\Omega_c h^2$	$0.067^{+0.042}_{-0.031}\,(< 0.115)$	$< 0.0754\,(< 0.111)$	$0.070^{+0.046}_{-0.021}\,(< 0.117)$	$0.067^{+0.042}_{-0.030}\,(< 0.115)$
H_0	71.6 ± 2.1	$72.6^{+3.4}_{-2.6}$	$71.3^{+2.6}_{-3.2}$	$71.4^{+2.5}_{-2.8}$
$\tau_{\rm reio}$	0.0534 ± 0.0079	0.063 ± 0.015	0.061 ± 0.014	0.0533 ± 0.0073
$\log(10^{10} A_s)$	3.042 ± 0.016	3.046 ± 0.030	3.064 ± 0.028	3.047 ± 0.014
n_s	0.9655 ± 0.0045	1.010 ± 0.016	$0.9741^{+0.0066}_{-0.0064}$	0.9699 ± 0.0038
ξ	$-0.40^{+0.23}_{-0.20}$	$-0.46^{+0.20}_{-0.28}$	$-0.38^{+0.35}_{-0.14}$	$-0.40^{+0.27}_{-0.23}$
$\ln \mathcal{B}_{ij}$	-0.17	-0.07	0.06	-0.25

Zhai, Giarè, van de Bruck, Di Valentino, et al, *JCAP* 07 (2023) 032

If we consider different combinations of CMB datasets, they provide similar results, favoring IDE with a 95% CL significance in the majority of the cases.
Remarkably, such a preference remains consistent
when cross-checked through independent probes,
while always yielding a value of the expansion rate H0 consistent with the local distance ladder measurements.

IDE from ACT

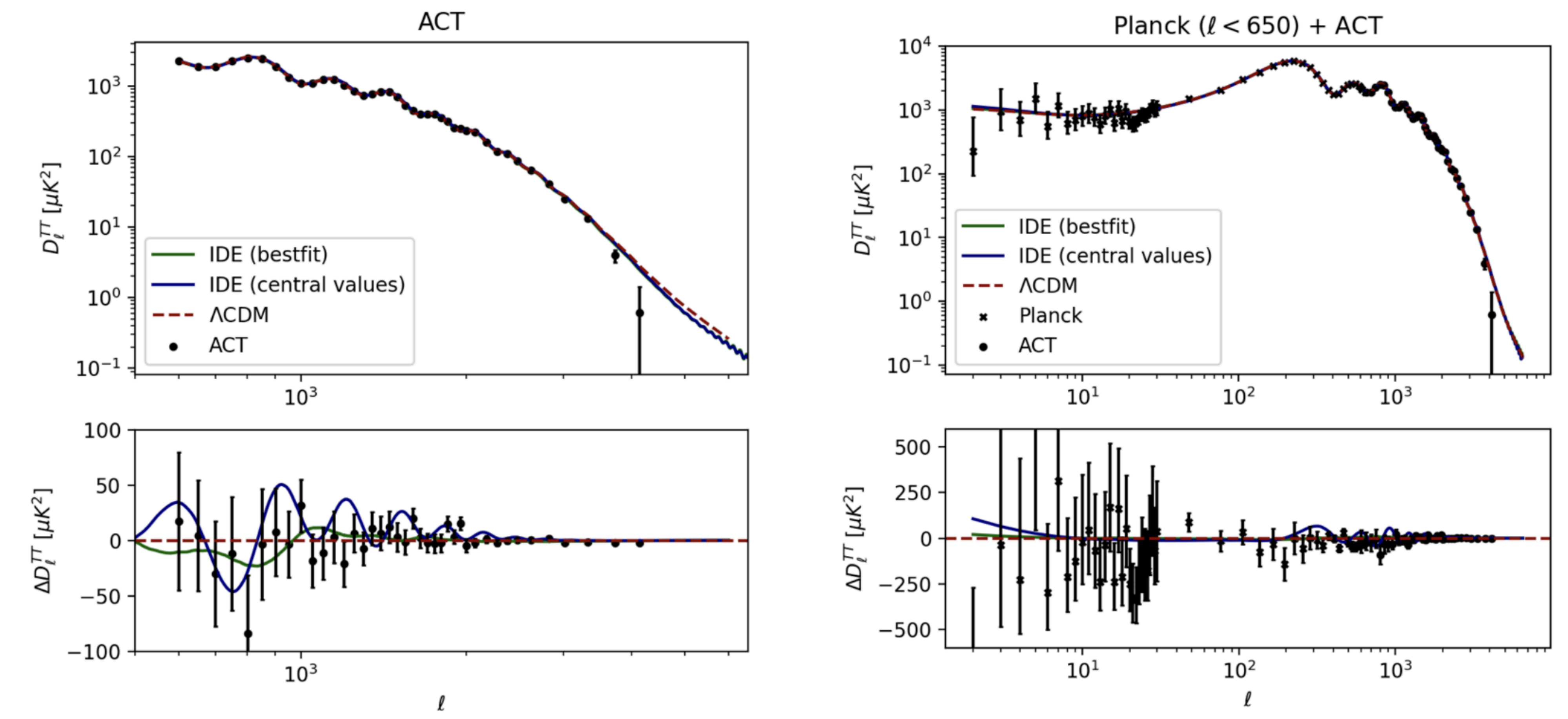

Zhai, Giarè, van de Bruck, Di Valentino, et al, *JCAP* 07 (2023) 032

It is easy to observe that the preference for ξ < 0 is primarily driven by the high multipole ACT CMB data that have a reduced amplitude. These data are also responsible for the improvement of the fit in the context of IDE models compared to the minimal ΛCDM, indicating that it is a genuine effect rather than one caused by parameter degeneracies.

Let’s see another example at late time…

Constraints at 68% cl.

Sign- switching cosmological constant

The Λ_sCDM model is inspired by the recent conjecture that the universe went through a spontaneous AdS-dS transition characterized by a sign - switching cosmological constant:

$$\Lambda \quad \rightarrow \quad \Lambda_s \equiv \Lambda_{s0}\,\mathrm{sgn}[z_\dagger - z],$$

Akarsu, Di Valentino et al., *arXiv:2307.10899*

Data set	Planck	Planck+BAOtr	Planck+BAOtr +PP	Planck+BAOtr +PP&SH0ES	Planck+BAOtr +PP&SH0ES+KiDS-1000
Model	Λ_sCDM	Λ_sCDM	Λ_sCDM	Λ_sCDM	Λ_sCDM
	ΛCDM	ΛCDM	ΛCDM	ΛCDM	ΛCDM
$z_\dagger$	unconstrained	$1.70^{+0.09}_{-0.19}(1.65)$	$1.87^{+0.13}_{-0.21}(1.75)$	$1.70^{+0.10}_{-0.13}(1.67)$	$1.72^{+0.09}_{-0.12}(1.70)$
	$--$	$--$	$--$	$--$	$--$
M_B[mag]	$--$	$--$	$-19.317^{+0.021}_{-0.025}(-19.311)$	$-19.290 \pm 0.017(-19.278)$	$-19.282 \pm 0.017(-19.280)$
	$--$	$--$	$-19.407 \pm 0.013(-19.411)$	$-19.379 \pm 0.012(-19.373)$	$-19.372 \pm 0.011(-19.369)$
H_0[km/s/Mpc]	$70.77^{+0.79}_{-2.70}(71.22)$	$73.30^{+1.20}_{-1.00}(73.59)$	$71.72^{+0.73}_{-0.92}(71.97)$	$72.82 \pm 0.65(73.20)$	$73.16 \pm 0.64(73.36)$
	$67.39 \pm 0.55(67.28)$	$68.84 \pm 0.48(68.61)$	$68.55 \pm 0.44(68.54)$	$69.57 \pm 0.42(69.73)$	$69.83 \pm 0.37(69.96)$
Ω_m	$0.2860^{+0.0230}_{-0.0099}(0.2796)$	$0.2643^{+0.0072}_{-0.0090}(0.2618)$	$0.2768^{+0.0072}_{-0.0063}(0.2759)$	$0.2683 \pm 0.0052(0.2646)$	$0.2646 \pm 0.0052(0.2622)$
	$0.3151 \pm 0.0075(0.3163)$	$0.2958 \pm 0.0061(0.2984)$	$0.2995 \pm 0.0056(0.2992)$	$0.2869 \pm 0.0051(0.2849)$	$0.2837 \pm 0.0045(0.2816)$
S_8	$0.801^{+0.026}_{-0.016}(0.791)$	$0.777 \pm 0.011(0.772)$	$0.791 \pm 0.011(0.794)$	$0.783 \pm 0.010(0.777)$	$0.774 \pm 0.009(0.773)$
	$0.832 \pm 0.013(0.835)$	$0.802 \pm 0.011(0.804)$	$0.808 \pm 0.010(0.804)$	$0.788 \pm 0.010(0.784)$	$0.781 \pm 0.008(0.782)$
χ^2_{min}	2778.06	2793.38	4219.68	4097.32	4185.34
	2780.52	2820.30	4235.18	4138.26	4226.50
$\ln\mathcal{B}_{ij}$	-1.28	-12.65	-7.52	-19.47	-19.77

Constraints at 68% cl.

Sign- switching cosmological constant

Λ_sCDM, for all data combinations including the BAOtr data,
is very strongly favored over ΛCDM in terms of Bayesian evidence.
The favoured transition redshift is z_t~1.7.

Akarsu, Di Valentino et al., *arXiv:2307.10899*

Data set	Planck	Planck+BAOtr	Planck+BAOtr +PP	Planck+BAOtr +PP&SH0ES	Planck+BAOtr +PP&SH0ES+KiDS-1000
Model	Λ_sCDM ΛCDM	Λ_sCDM ΛCDM	Λ_sCDM ΛCDM	Λ_sCDM ΛCDM	Λ_sCDM ΛCDM
$z_\dagger$	unconstrained −−	$1.70^{+0.09}_{-0.19}(1.65)$ −−	$1.87^{+0.13}_{-0.21}(1.75)$ −−	$1.70^{+0.10}_{-0.13}(1.67)$ −−	$1.72^{+0.09}_{-0.12}(1.70)$ −−
M_B[mag]	−− −−	−− −−	$-19.317^{+0.021}_{-0.025}(-19.311)$ $-19.407 \pm 0.013(-19.411)$	$-19.290 \pm 0.017(-19.278)$ $-19.379 \pm 0.012(-19.373)$	$-19.282 \pm 0.017(-19.280)$ $-19.372 \pm 0.011(-19.369)$
H_0[km/s/Mpc]	$70.77^{+0.79}_{-2.70}(71.22)$ $67.39 \pm 0.55(67.28)$	$73.30^{+1.20}_{-1.00}(73.59)$ $68.84 \pm 0.48(68.61)$	$71.72^{+0.73}_{-0.92}(71.97)$ $68.55 \pm 0.44(68.54)$	$72.82 \pm 0.65(73.20)$ $69.57 \pm 0.42(69.73)$	$73.16 \pm 0.64(73.36)$ $69.83 \pm 0.37(69.96)$
Ω_m	$0.2860^{+0.0230}_{-0.0099}(0.2796)$ $0.3151 \pm 0.0075(0.3163)$	$0.2643^{+0.0072}_{-0.0090}(0.2618)$ $0.2958 \pm 0.0061(0.2984)$	$0.2768^{+0.0072}_{-0.0063}(0.2759)$ $0.2995 \pm 0.0056(0.2992)$	$0.2683 \pm 0.0052(0.2646)$ $0.2869 \pm 0.0051(0.2849)$	$0.2646 \pm 0.0052(0.2622)$ $0.2837 \pm 0.0045(0.2816)$
S_8	$0.801^{+0.026}_{-0.016}(0.791)$ $0.832 \pm 0.013(0.835)$	$0.777 \pm 0.011(0.772)$ $0.802 \pm 0.011(0.804)$	$0.791 \pm 0.011(0.794)$ $0.808 \pm 0.010(0.804)$	$0.783 \pm 0.010(0.777)$ $0.788 \pm 0.010(0.784)$	$0.774 \pm 0.009(0.773)$ $0.781 \pm 0.008(0.782)$
χ^2_{min}	2778.06 2780.52	2793.38 2820.30	4219.68 4235.18	4097.32 4138.26	4185.34 4226.50
$\ln\mathcal{B}_{ij}$	−1.28	−12.65	−7.52	−19.47	−19.77

Sign- switching cosmological constant

We see that there is no H_0 tension in the present analyses of Λ_sCDM with all data combinations including the BAOtr data.
Also the S8 tension is completely solved.

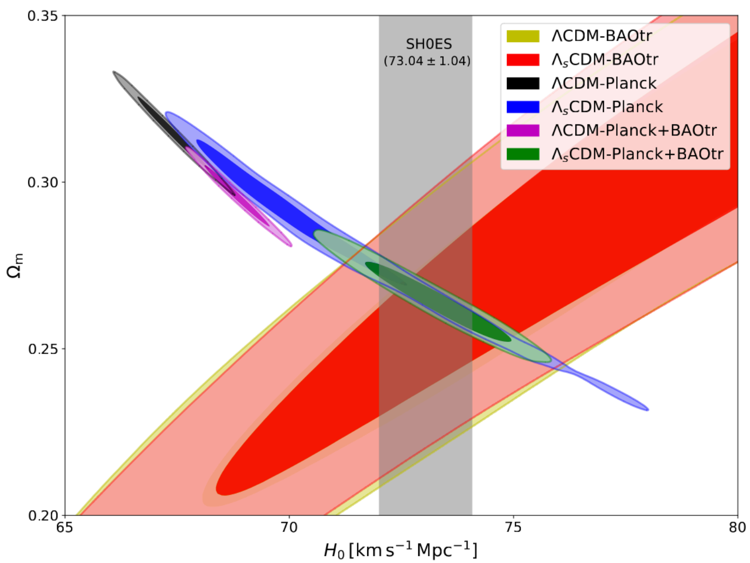

FIG. 2. 2D contours at 68%, and 95% CL in the H_0-Ω_m plane for the Λ_sCDM and ΛCDM models from the Planck and/or BAOtr data. It deserves mention that, in case of Λ_sCDM, the Planck and BAOtr contours intersect right on the vertical band of SH0ES measurement.

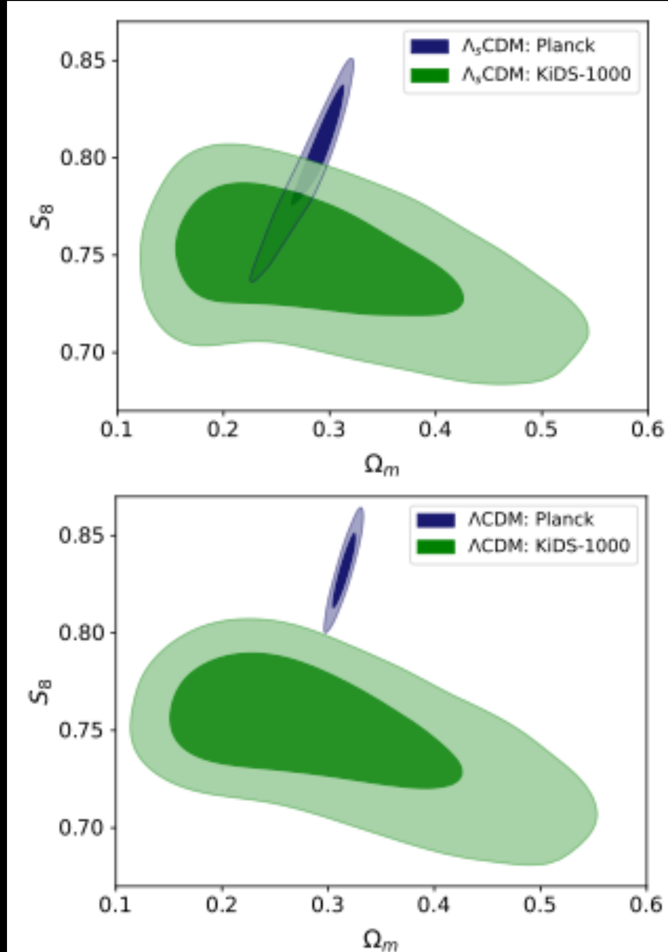

Akarsu, Di Valentino et al., *arXiv:2307.10899*

Sign- switching cosmological constant

We see that there is no H_0 tension in the present analyses of Λ_sCDM with all data combinations including the BAOtr data.

arXiv > astro-ph > arXiv:2402.07716

Search...

Help | Advanc

Astrophysics > Cosmology and Nongalactic Astrophysics

[Submitted on 12 Feb 2024]

Λ_sCDM cosmology from a type-II minimally modified gravity

Ozgur Akarsu, Antonio De Felice, Eleonora Di Valentino, Suresh Kumar, Rafael C. Nunes, Emre Ozulker, J. Alberto Vazquez, Anita Yadav

We have successfully integrated Λ_sCDM, a promising model for alleviating cosmological tensions, into a theoretical framework by endowing it with a specific Lagrangian from the VCDM model, a type-II minimally modified gravity. In this theory, we demonstrate that an auxiliary scalar field with a linear potential induces an effective cosmological constant, enabling the realization of an abrupt mirror AdS-dS transition in the late universe through a piecewise linear potential. To eliminate the sudden singularity in this setup and ensure stable transitions, we smooth out this potential. Realized within the VCDM theory, the Λ_sCDM model facilitates two types of rapid smooth mirror AdS-dS transitions: (i) the agitated transition, associated with a smooth jump in the potential, where Λ_s, and consequently H, exhibits a bump around the transition's midpoint; and (ii) the quiescent transition, associated with a smooth change in the slope of the potential, where Λ_s transitions gracefully. These transitions are likely to leave distinct imprints on the background and perturbation dynamics, potentially allowing the observational data to distinguish between them. This novel theoretical framework propels Λ_sCDM into a fully predictive model capable of exploring the evolution of the Universe including the late-time AdS-dS transition epoch, and extends the applicability of the model. We believe further research is crucial in establishing Λ_sCDM as a leading candidate or guide for a new concordance cosmological model.

$H_0\,[\mathrm{km\,s^{-1}\,Mpc^{-1}}]$

FIG. 2. 2D contours at 68%, and 95% CL in the H_0-Ω_m plane for the Λ_sCDM and ΛCDM models from the Planck and/or BAOtr data. It deserves mention that, in case of Λ_sCDM, the Planck and BAOtr contours intersect right on the vertical band of SH0ES measurement.

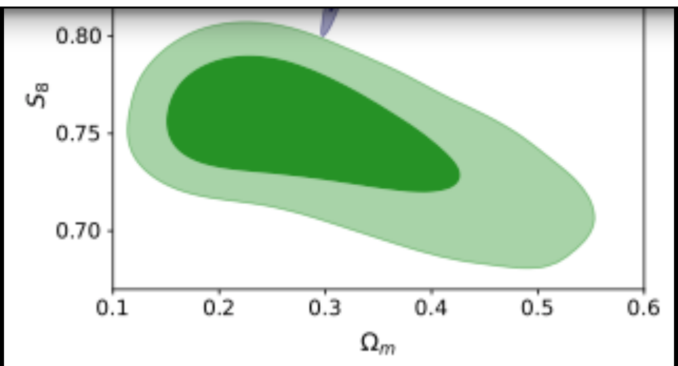

Akarsu, Di Valentino et al., *arXiv:2307.10899*

…but the excess of lensing in Planck could explain S8…

A_L internal anomaly

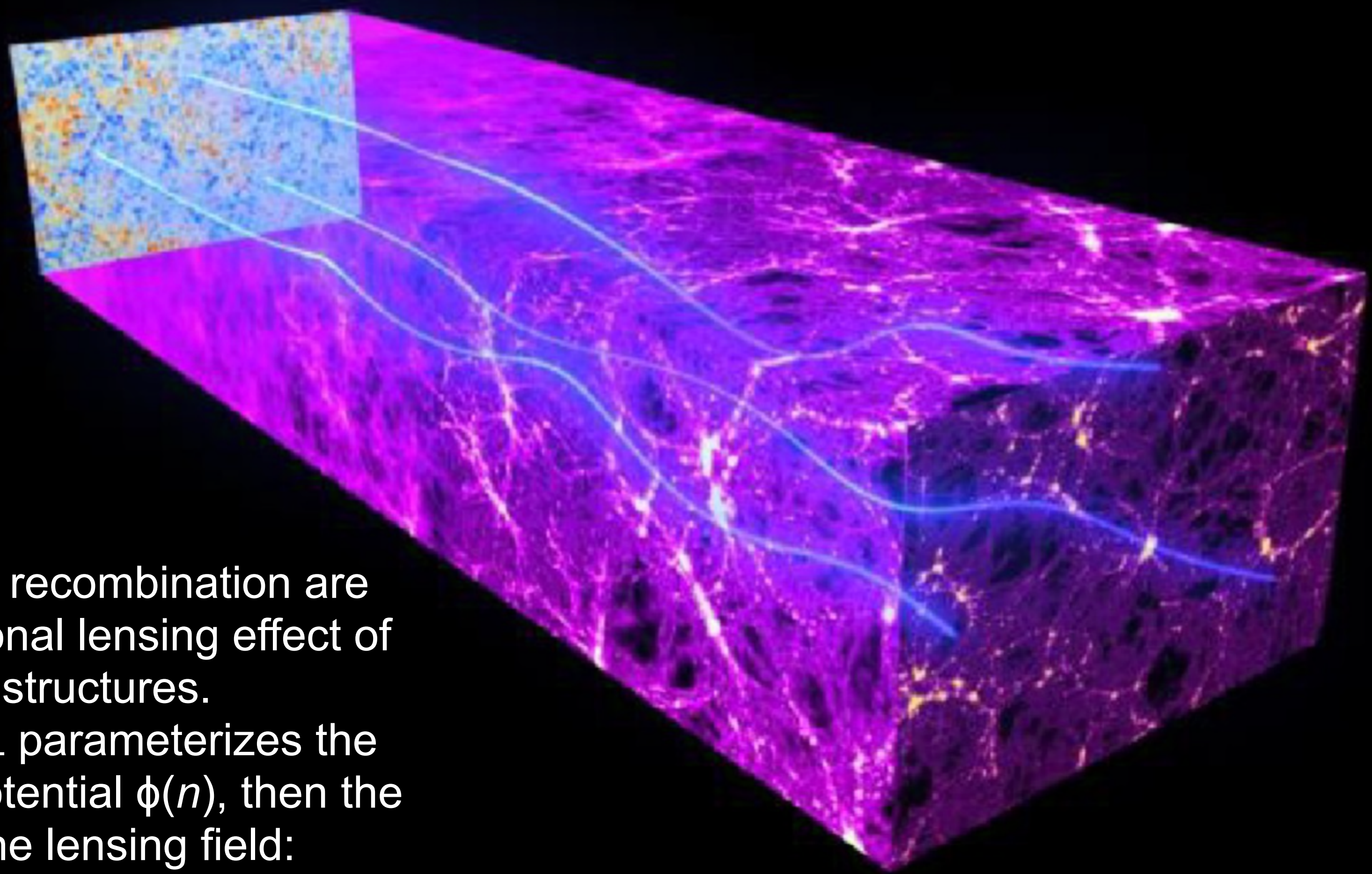

CMB photons emitted at recombination are deflected by the gravitational lensing effect of massive cosmic structures.
The lensing amplitude A_L parameterizes the rescaling of the lensing potential ϕ(*n*), then the power spectrum of the lensing field:

$$C_\ell^{\phi\phi} \rightarrow A_{\rm L} C_\ell^{\phi\phi}$$

The gravitational lensing deflects the photon path by a quantity defined by the gradient of the lensing potential ϕ(*n*), integrated along the line of sight *n*, remapping the temperature field.

A_L internal anomaly

Its effect on the power spectrum is the smoothing of the acoustic peaks, increasing AL.

Interesting consistency checks is if the amplitude of the smoothing effect in the CMB power spectra matches the theoretical expectation AL = 1 and whether the amplitude of the smoothing is consistent with that measured by the lensing reconstruction.

If AL =1 then the theory is correct, otherwise we have a new physics or systematics.

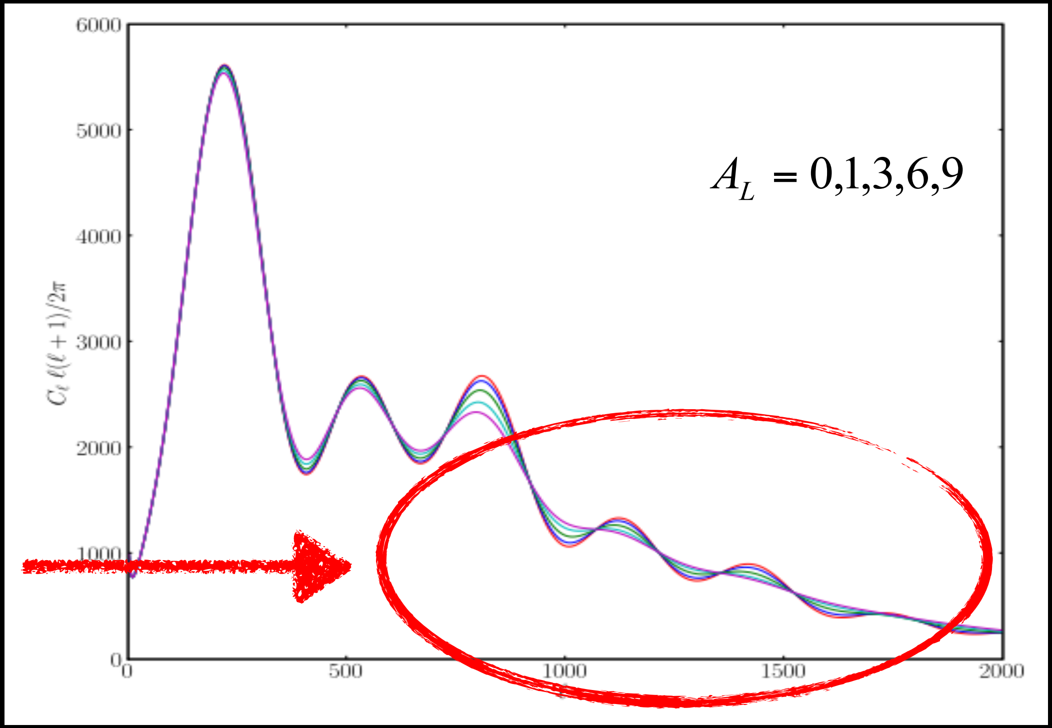

Calabrese et al., Phys. Rev. D, 77, 123531

A_L : a failed consistency check

The Planck lensing-reconstruction power spectrum is consistent with the amplitude expected for ΛCDM models that fit the CMB spectra, so the Planck lensing measurement is compatible with AL = 1.

However, the distributions of AL inferred from the CMB power spectra alone indicate a preference for AL > 1.

The joint combined likelihood shifts the value preferred by the TT data downwards towards AL = 1, but the error also shrinks, increasing the significance of AL > 1 to 2.8σ.

The preference for high AL is not just a volume effect in the full parameter space, with the best fit improved by $\Delta\chi^2 \sim 9$ when adding AL for TT+lowE and 10 for TTTEEE+lowE.

Planck 2018, Astron.Astrophys. 641 (2020) A6

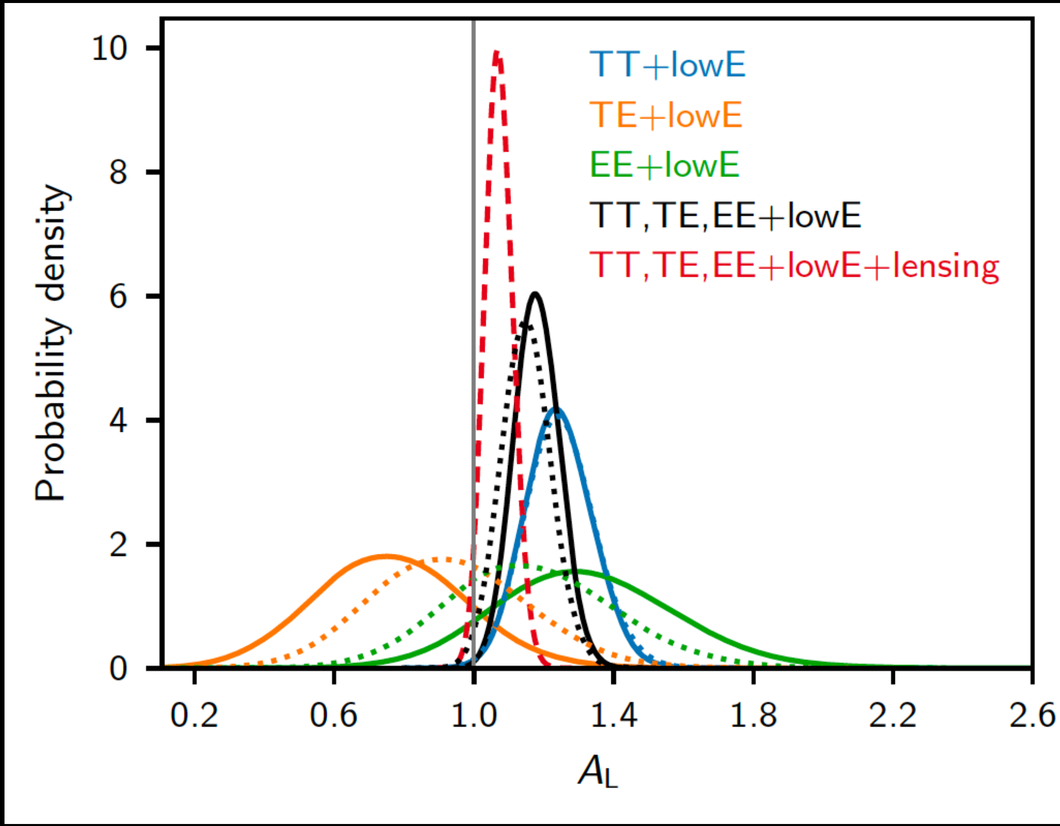

$$A_L = 1.243 \pm 0.096 \quad (68\,\%,\ \textit{Planck}\ \mathrm{TT+lowE}),$$
$$A_L = 1.180 \pm 0.065 \quad (68\,\%,\ \textit{Planck}\ \mathrm{TT,TE,EE+lowE}),$$

A_L can explain internal tension

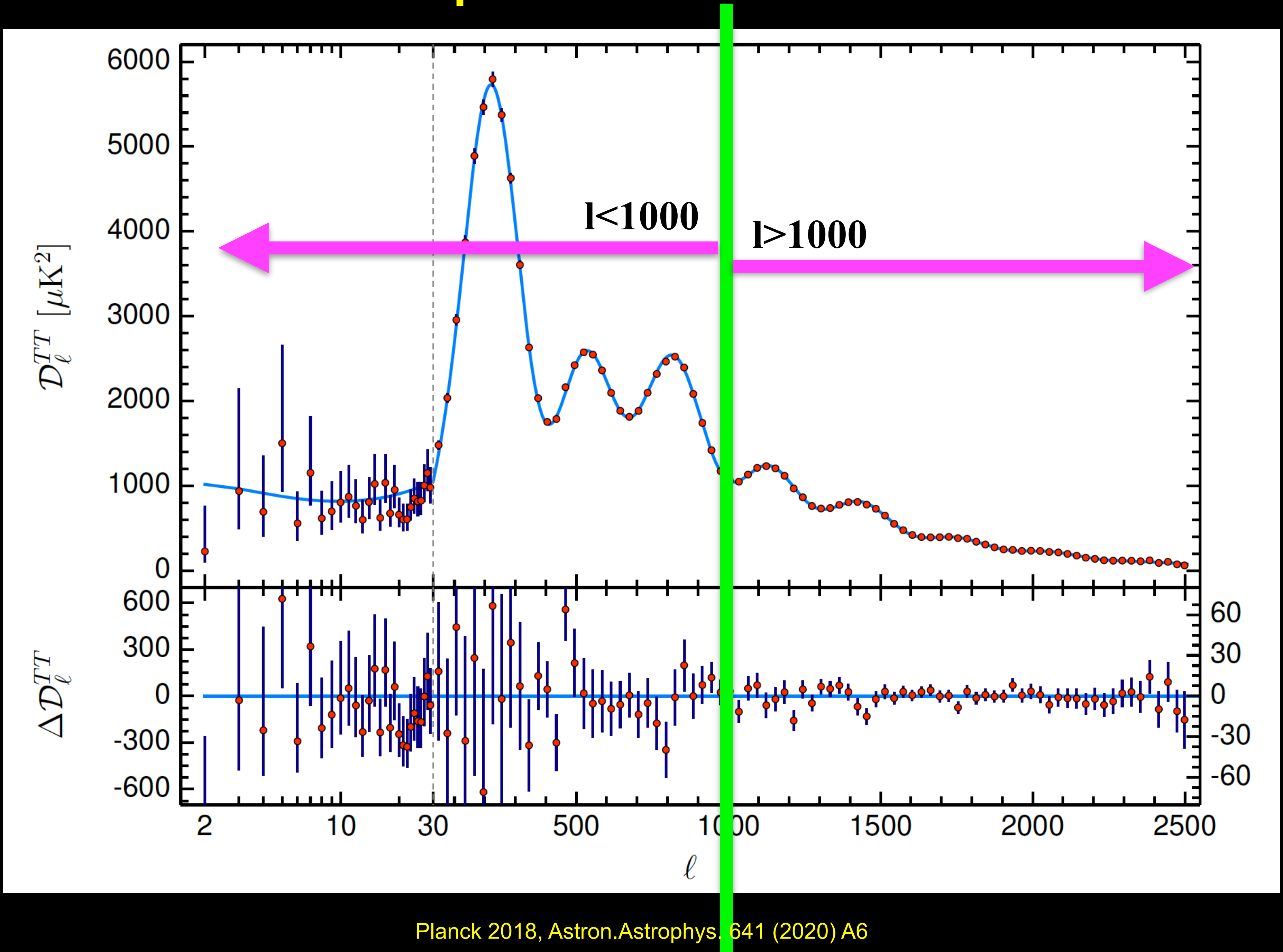

Planck 2018, Astron.Astrophys. 641 (2020) A6

A_L can explain internal tension

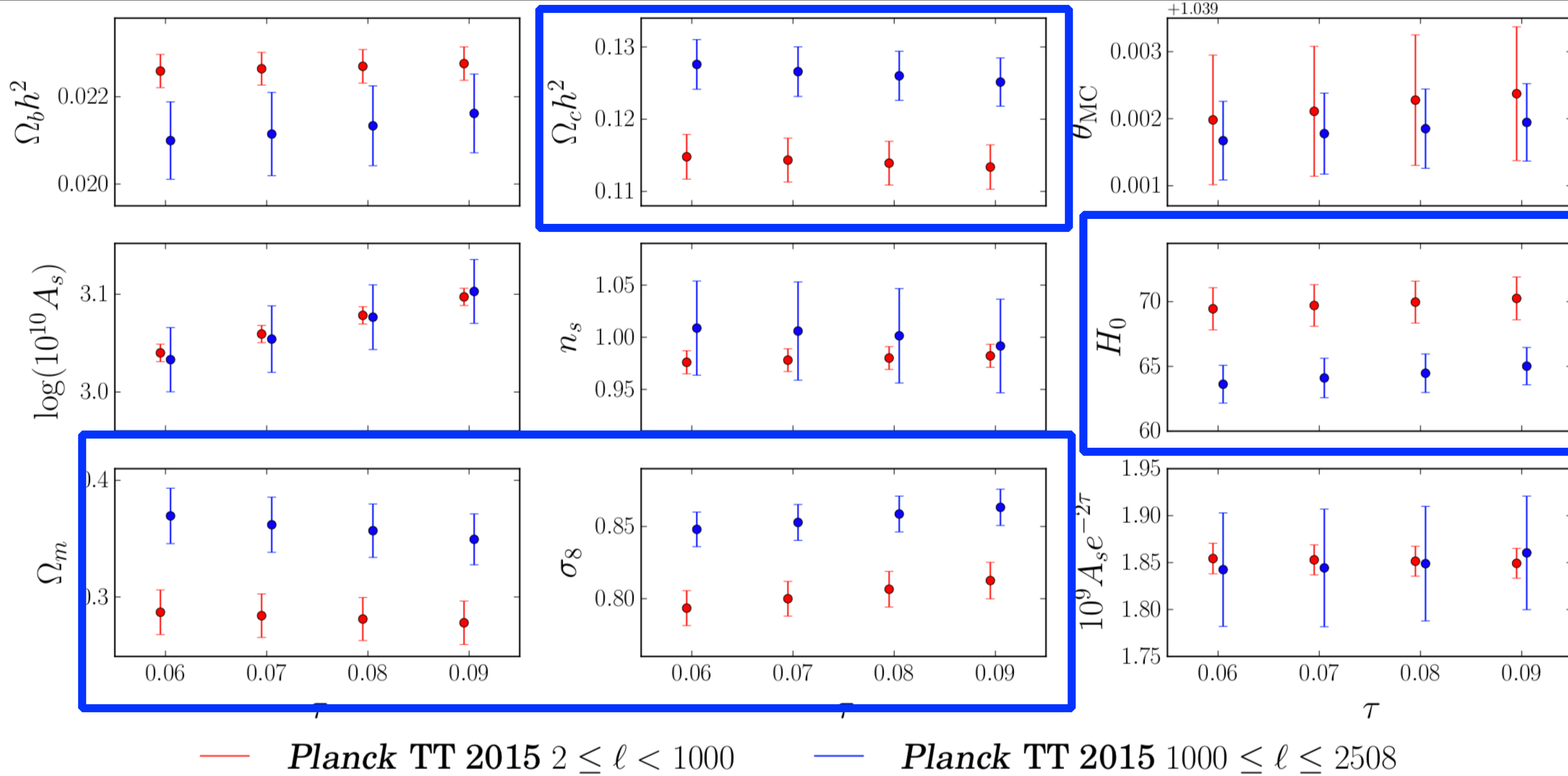

Marginalized 68.3% confidence ΛCDM parameter constraints from fits to the l < 1000 and l ≥ 1000 Planck TT 2015 spectra. Tension at more than 2σ level appears in $\Omega_c h^2$ and derived parameters, including H0, Ωm, and σ8.

Addison et al., Astrophys.J. 818 (2016) no.2, 132

A_L can explain internal tension

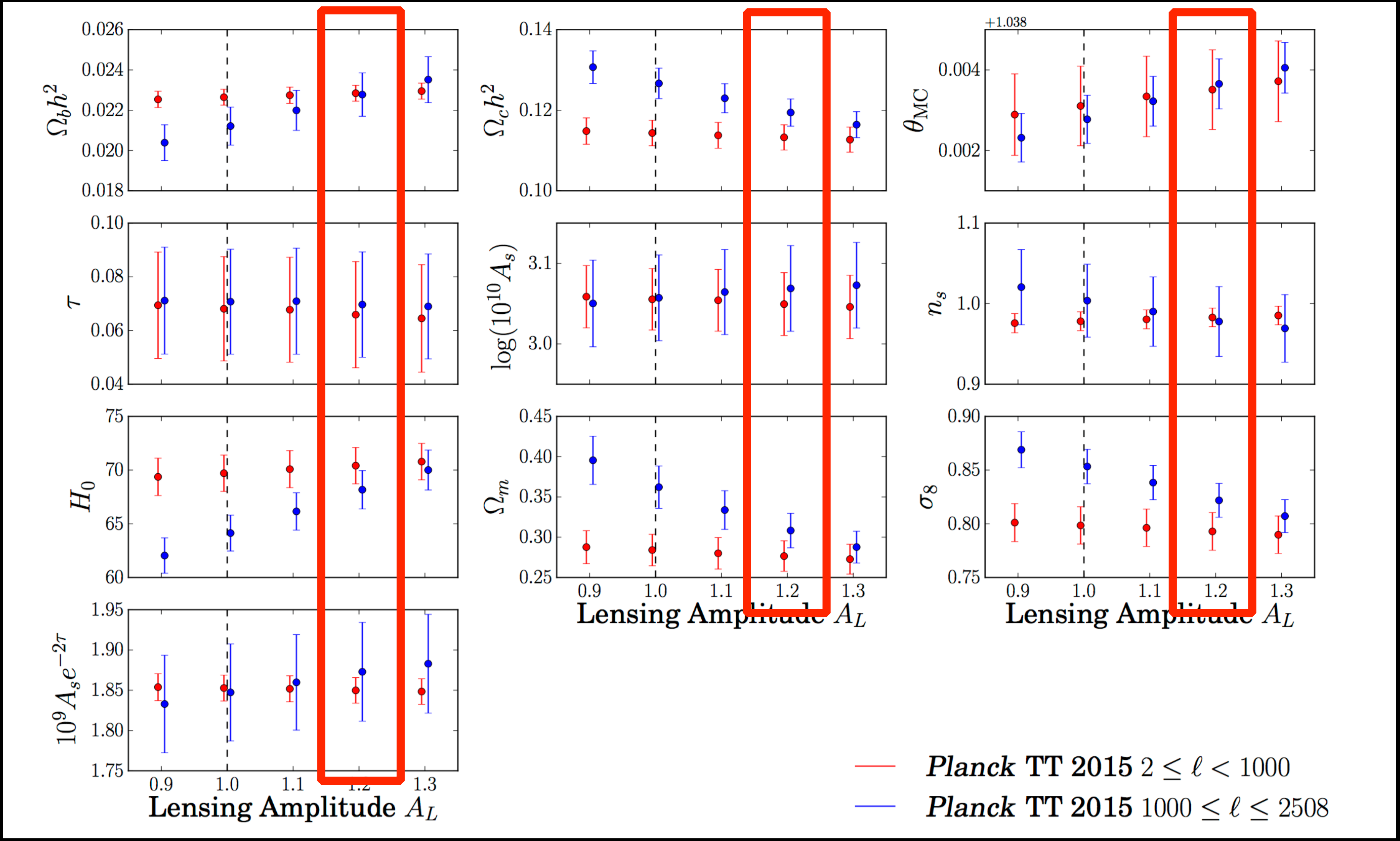

Increasing AL smooths out the high order acoustic peaks, improving the agreement between the two multipole ranges.

Addison et al., Astrophys.J. 818 (2016) no.2, 132

A_L can explain the S8 tension

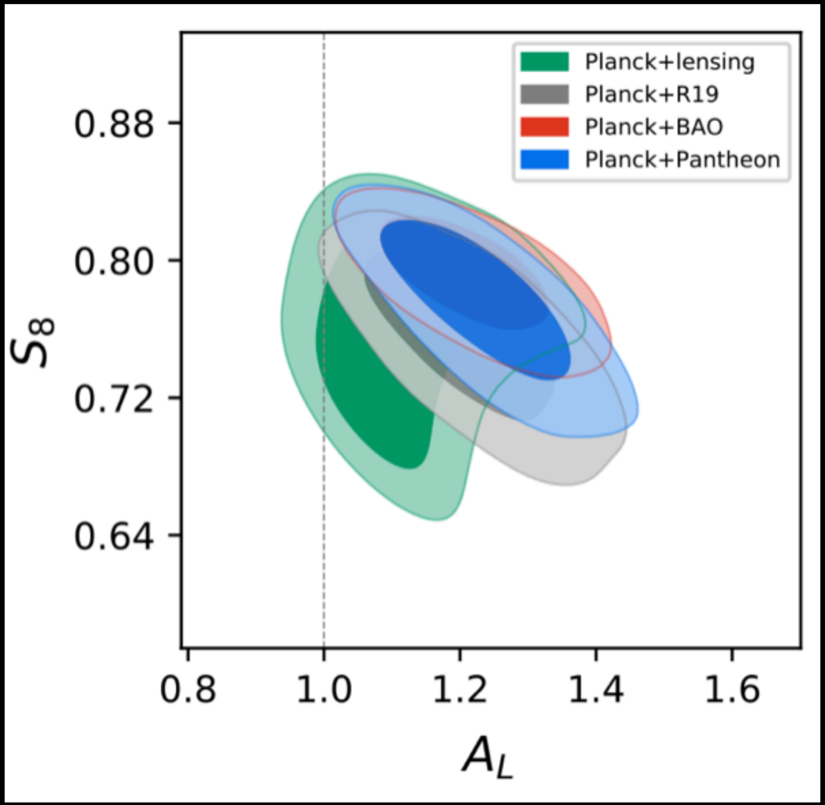

Di Valentino, Melchiorri and Silk, JCAP 2001 (2020) no.01, 013

A_L that is larger than the expected value at about 3 standard deviations even when combining the Planck data with BAO and supernovae type Ia external datasets.

Alternative CMB are not in significant tension

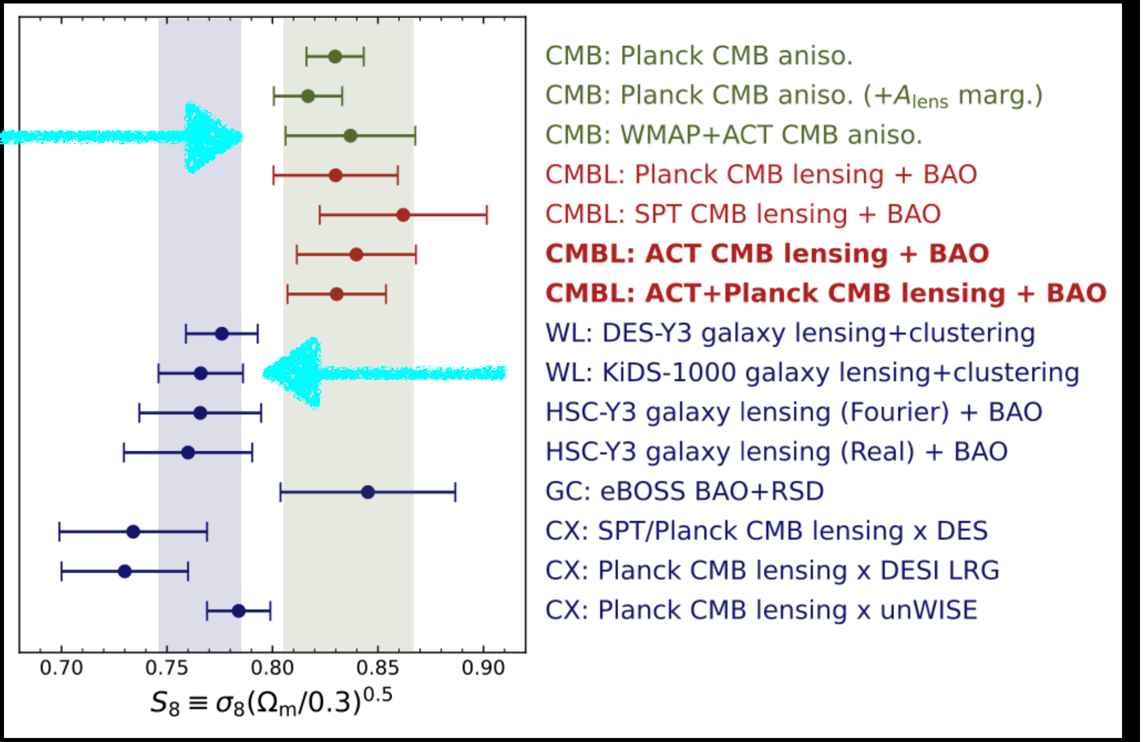

ACT collaboration, arXiv:2304.05203

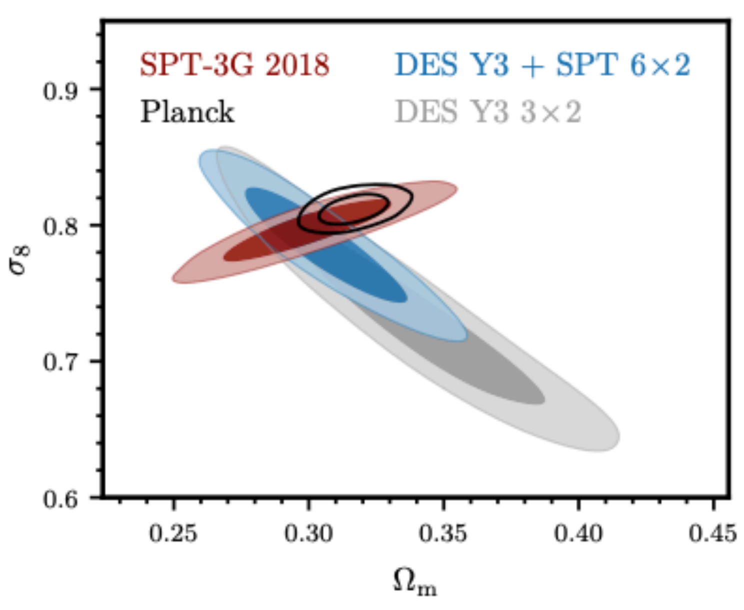

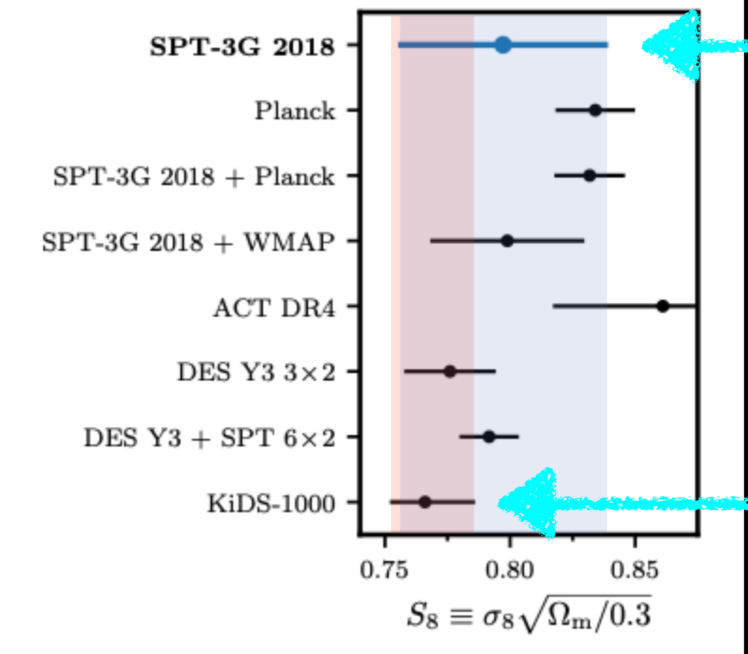

SPT-3G collaboration, arXiv:2212.05642

DES Y3 + KiDS-1000

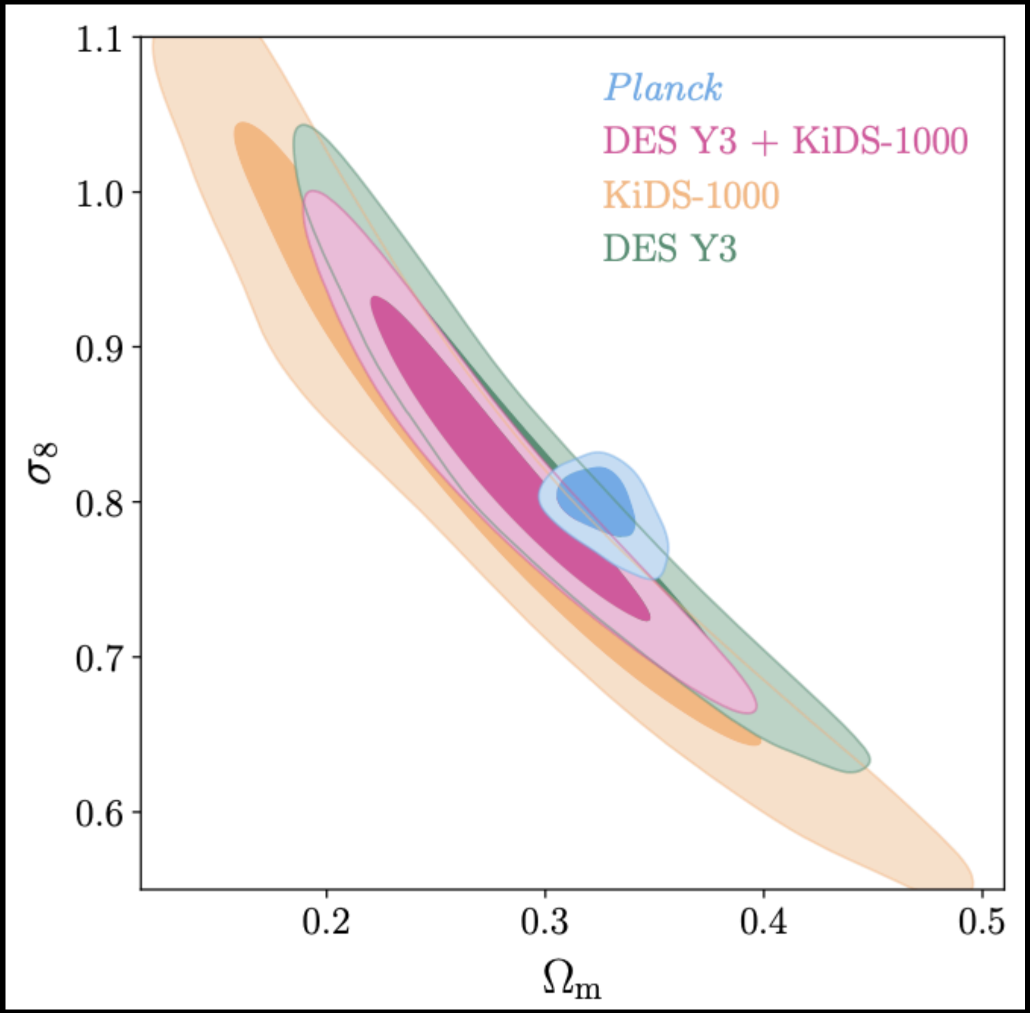

DES Y3 + KiDS-1000 collaborations, arXiv:2305.17173 [astro-ph.CO]

There is no more S8 tension, showing now an agreement at about 1.7σ between Planck assuming ΛCDM and this combined analysis.

$S_8 = 0.790^{+0.018}_{-0.014}$

DES Y3 + KiDS-1000 collaborations, arXiv:2305.17173 [astro-ph.CO]

A_L for different data releases

Table 1. Posterior A_L Constraints from Analyses of Planck Temperature and Polarization Data since 2018 Release

Reference	Data Version	Likelihood	Data Combination	A_L	'Nσ' Preference for $A_L > 1$
Planck Collaboration VI (2020)	PR3/2018	plik	TTTEEE+lowl/lowE	1.180 ± 0.065	2.8σ
	PR3/2018	plik	TT+lowl/lowE	1.243 ± 0.096	2.5σ
Rosenberg et al. (2022)	PR3/2018	CamSpec	TTTEEE+lowl/lowE	1.146 ± 0.061	2.4σ
	PR3/2018	CamSpec	TT+lowl/lowE	1.215 ± 0.089	2.4σ
	PR4/NPIPE	CamSpec	TTTEEE+lowl/lowE	1.095 ± 0.056	1.7σ
	PR4/NPIPE	CamSpec	TT+lowl/lowE	1.198 ± 0.084	2.4σ
Tristram et al. (2023)	PR4/NPIPE	HiLLiPoP	TTTEEE+lowl/LoLLiPoP[a]	1.036 ± 0.051	0.7σ
	PR4/NPIPE	HiLLiPoP	TT+lowl/LoLLiPoP	1.068 ± 0.081	0.8σ

Addison et al., arXiv:2310.03127 [astro-ph.CO]

$S_8 = 0.834 \pm 0.016$

H0 = 67.36 ± 0.54 km/s/Mpc

Planck 2018, Aghanim et al., arXiv:1807.06209 [astro-ph.CO]

$S_8 = 0.819 \pm 0.014$

H0 = 67.64 ± 0.52 km/s/Mpc

Tristram et al., arXiv:2309.10034 [astro-ph.CO]

But…
assuming General Relativity,
is there a physical explanation
for A_L?

Astronomy & Astrophysics manuscript no. ms
September 24, 2019

Planck 2018 results. VI. Cosmological parameters

Planck Collaboration: N. Aghanim[54], Y. Akrami[15,57,59], M. Ashdown[65,5], J. Aumont[95], C. Baccigalupi[78], M. Ballardini[21,41], A. J. Banday[95,8], R. B. Barreiro[61], N. Bartolo[29,62], S. Basak[85], R. Battye[64], K. Benabed[55,90], J.-P. Bernard[95,8], M. Bersanelli[32,45], P. Bielewicz[75,78], J. J. Bock[63,10], J. R. Bond[7], J. Borrill[12,93], F. R. Bouchet[55,90], F. Bou...
J.-F. Cardoso[55,90], J. Carron[23], A. Challinor[58,65,11], H. C. Chi...
F. Cuttaia[41], P. de Bernardis[31], G. de Zotti[42], J. Delabrouil...
A. Ducout[66], X. Dupac[35], S. Dusini[62], G. Efstathiou[65]...
J. Fergusson[11], R. Fernandez-Cobos[61], F. Finelli[41,47], F. For...
S. Galli[55,90†], K. Ganga[2], R. T. Génova-Santos[60,16], M. ...
A. Gruppuso[41,47], J. E. Gudmundsson[94,25], J. Hamann[86], ...
Z. Huang[83], A. H. Jaffe[53], W. C. Jones[25], A. Karakci[59], ...
N. Krachmalnicoff[78], M. Kunz[14,54,3], H. Kurki-Suonio[24,40], ...
M. Le Jeune[2], P. Lemos[58,65], J. Lesgourgues[56], F. Levri...
M. López-Caniego[35], P. M. Lubin[28], Y.-Z. Ma[77,80,74], J. ...
A. Marcos-Caballero[61], M. Maris[43], P. G. Martin[7], M. Mar...
P. R. Meinhold[28], A. Melchiorri[31,50], A. Mennella[32,45], ...
D. Molinari[30,41,48], L. Montier[95,8], G. Morgante[41], A. Mo...
B. Partridge[39], G. Patanchon[2], H. V. Peiris[22], F. Perrot...
J. P. Rachen[18], M. Reinecke[72], M. Remazeilles[64], A. ...
B. Ruiz-Granados[60,16], L. Salvati[54], M. Sandri[41], M. Savelain...
R. Sunyaev[72,91], A.-S. Suur-Uski[24,40], J. A. Tauber[36], D. ...
L. Valenziano[41], J. Valiviita[24,40], B. Van Tent[69], L. Vibert[54,...
S. D. M. W...
(*Affiliation*...

arXiv:1807.06209v2 [astro-ph.CO] 20 Sep 2019

We present cosmological parameter results from the final f...
isotropies, combining information from the temperature an...
improved measurements of large-scale polarization allow th...
cant gains in the precision of other correlated parameters. Im...
many parameters, with residual modelling uncertainties estim...
spatially-flat 6-parameter ΛCDM cosmology having a power...
from polarization, temperature, and lensing, separately and i...
baryon density $\Omega_b h^2 = 0.0224 \pm 0.0001$, scalar spectral inde...
68 % confidence regions on measured parameters and 95 %...
$100\theta_* = 1.0411 \pm 0.0003$. These results are only weakly depe...
in many commonly considered extensions. Assuming the ba...
Hubble constant $H_0 = (67.4 \pm 0.5)\,\mathrm{km\,s^{-1}Mpc^{-1}}$; matter densi...
We find no compelling evidence for extensions to the base-ΛCDM model. Combining with baryon acoustic oscillation (BAO) measurements (and
considering single-parameter extensions) we constrain the ef...
the Standard Model prediction $N_{\rm eff} = 3.046$, and find that th...
to prefer higher lensing amplitudes than predicted in base ΛC...
from the ΛCDM model; however, this is not supported by t...
BAO data. The joint constraint with BAO measurements on s...
with Type Ia supernovae (SNe), the dark-energy equation of...
constant. We find no evidence for deviations from a purely...
Keck Array data, we place a limit on the tensor-to-scalar ra...
deuterium abundances for the base-ΛCDM cosmology are in...
agreement with BAO, SNe, and some galaxy lensing obser...
including galaxy clustering (which prefers lower fluctuation...
measurements of the Hubble constant (which prefer a high...
favoured by the *Planck* data.

Key words. Cosmology: observations – Cosmology: theory – Cosmic background radiation – cosmological parameters

Page 40

$$\Omega_K = -0.044^{+0.018}_{-0.015} \quad (68\,\%, \textit{Planck}\ \text{TT,TE,EE+lowE}), \qquad (46b)$$

a detection of curvature at about 3.4σ

an apparent detection of curvature at well over $2\,\sigma$. The 99 % probability region for the TT,TE,EE+lowE result is $-0.095 < \Omega_K < -0.007$, with only about 1/10000 samples at $\Omega_K \geq 0$. This is not entirely a volume effect, since the best-fit χ^2 changes by $\Delta\chi^2_{\rm eff} = -11$ compared to base ΛCDM when adding the one additional curvature parameter. The reasons for the pull towards

*Corresponding author: G. Efstathiou, gpe@ast.cam.ac.uk
†Corresponding author: S. Galli, gallis@iap.fr
‡Corresponding author: A. Lewis, antony@cosmologist.info

*Corresponding author: G. Efstathiou, gpe@ast.cam.ac.uk
†Corresponding author: S. Galli, gallis@iap.fr
‡Corresponding author: A. Lewis, antony@cosmologist.info

Curvature of the universe

Curvature of the universe

Can Planck provide an unbiased and reliable estimate of the curvature of the Universe?
This may not be the case since a "geometrical degeneracy" is present with Ωm.
When precise CMB measurements at arc-minute angular scales are included, since gravitational lensing depends on the matter density, its detection breaks the geometrical degeneracy. The Planck experiment with its improved angular resolution offers the unique opportunity of a precise measurement of curvature from a single CMB experiment.
We simulated Planck, finding that such experiment could constrain curvature with a 2% uncertainty, without any significant bias towards closed models.

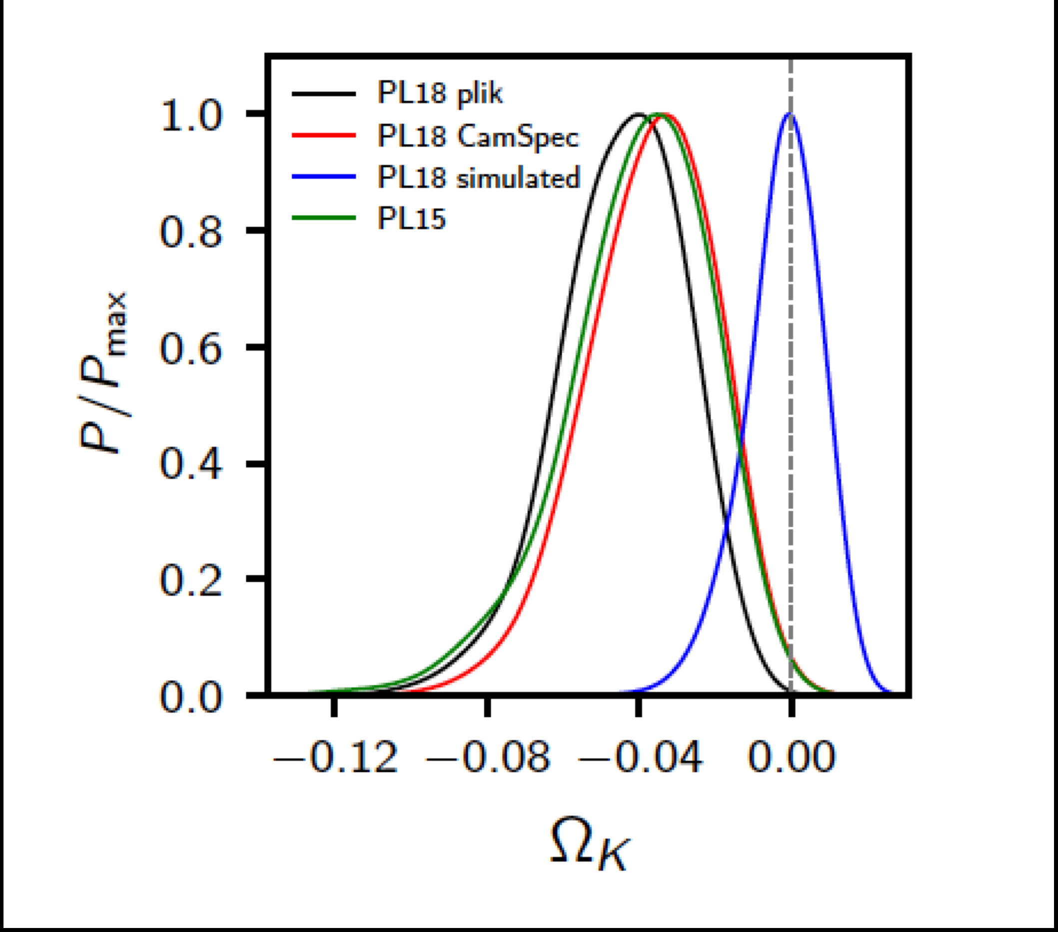

Di Valentino, Melchiorri and Silk, *Nature Astron.* 4 (2019) 2, 196-203

Curvature of the universe

Planck favours a closed Universe ($\Omega k<0$) with 99.985% probability.
A closed Universe with $\Omega K = -0.0438$ provides a better fit to PL18 with respect to a flat model.

This is not entirely a volume effect, since the best-fit $\Delta\chi^2$ changes by -11 compared to base ΛCDM when adding the one additional curvature parameter.
The improvement is due also to the fact that closed models could also lead to a large-scale cut-off in the primordial density fluctuations in agreement with the observed low CMB anisotropy quadrupole.

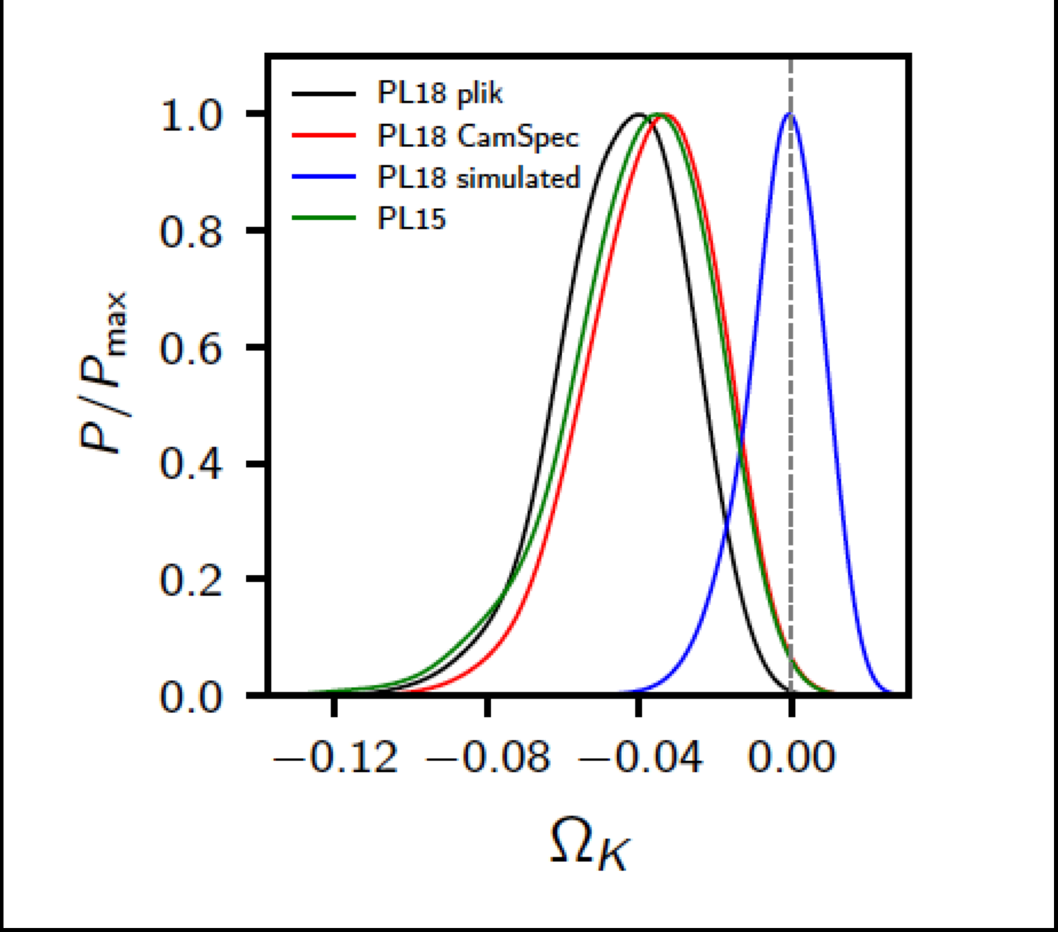

Di Valentino, Melchiorri and Silk, *Nature Astron.* 4 (2019) 2, 196-203

Low CMB anisotropy quadrupole

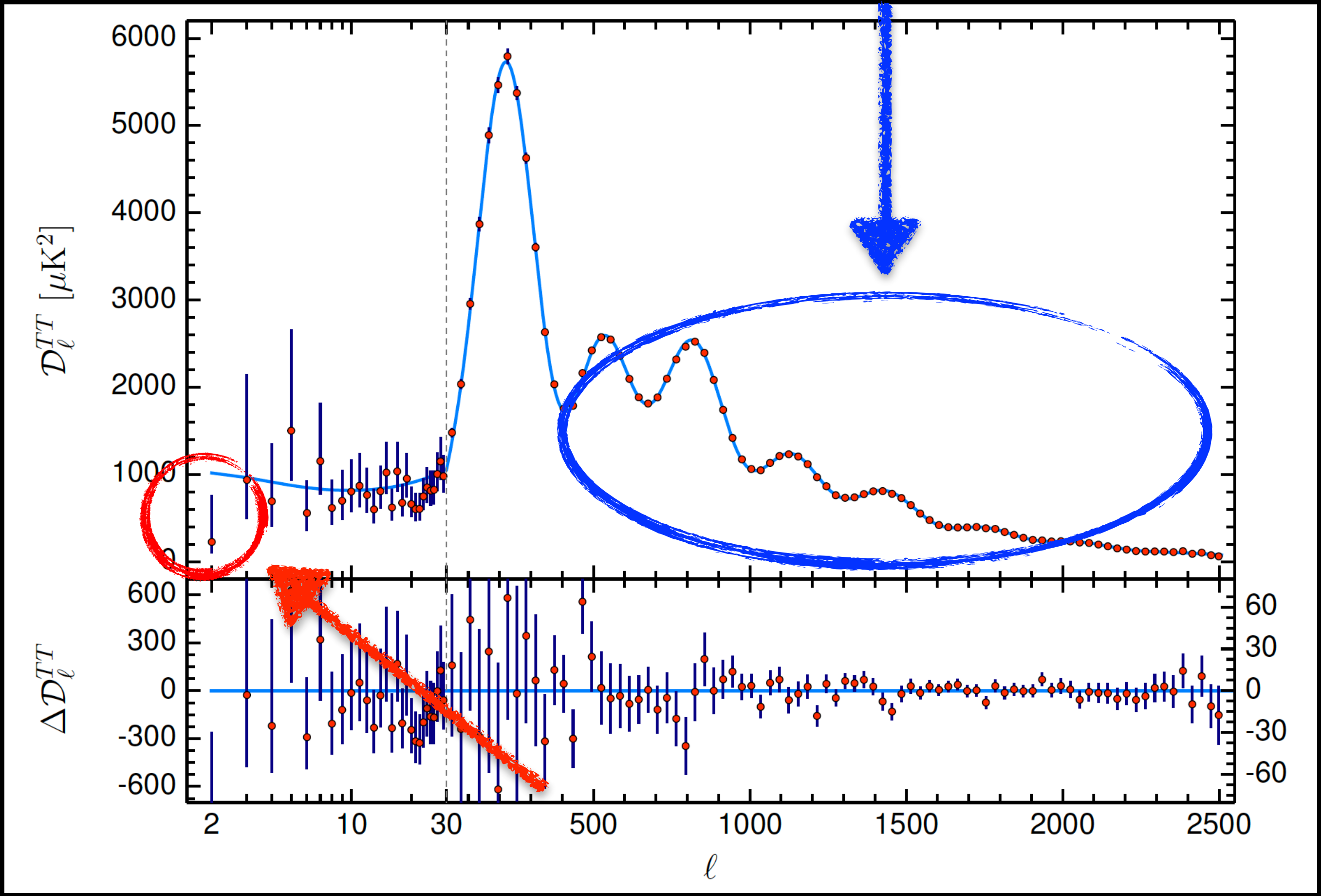

Planck 2018, Astron.Astrophys. 641 (2020) A6

A model with $\Omega_K < 0$ is slightly preferred with respect to a flat model with $A_L > 1$, because closed models better fit not only the damping tail, but also the low-multipole data, especially the quadrupole.

Astrophysics

[Submitted on 5 Mar 2003 (v1), last revised 30 Jul 2003 (this version, v2)]

Is the Low CMB Quadrupole a Signature of Spatial Curvature?

G. Efstathiou (University of Cambridge)

The temperature anisotropy power spectrum measured with the Wilkinson Microwave Anisotropy Probe (WMAP) at high multipoles is in spectacular agreement with an inflationary Lambda-dominated cold dark matter cosmology. However, the low order multipoles (especially the quadrupole) have lower amplitudes than expected from this cosmology, indicating a need for new physics. Here we speculate that the low quadrupole amplitude is associated with spatial curvature. We show that positively curved models are consistent with the WMAP data and that the quadrupole amplitude can be reproduced if the primordial spectrum truncates on scales comparable to the curvature scale.

Comments:	4 pages, Latex, 2 figs, revised version accepted by MNRAS
Subjects:	**Astrophysics (astro-ph)**
Journal reference:	Mon.Not.Roy.Astron.Soc. 343 (2003) L95
DOI:	10.1046/j.1365-8711.2003.06940.x
Cite as:	arXiv:astro-ph/0303127
	(or arXiv:astro-ph/0303127v2 for this version)

Submission history

From: George Efstathiou [view email]
[v1] Wed, 5 Mar 2003 23:30:33 UTC (21 KB)
[v2] Wed, 30 Jul 2003 10:16:45 UTC (22 KB)

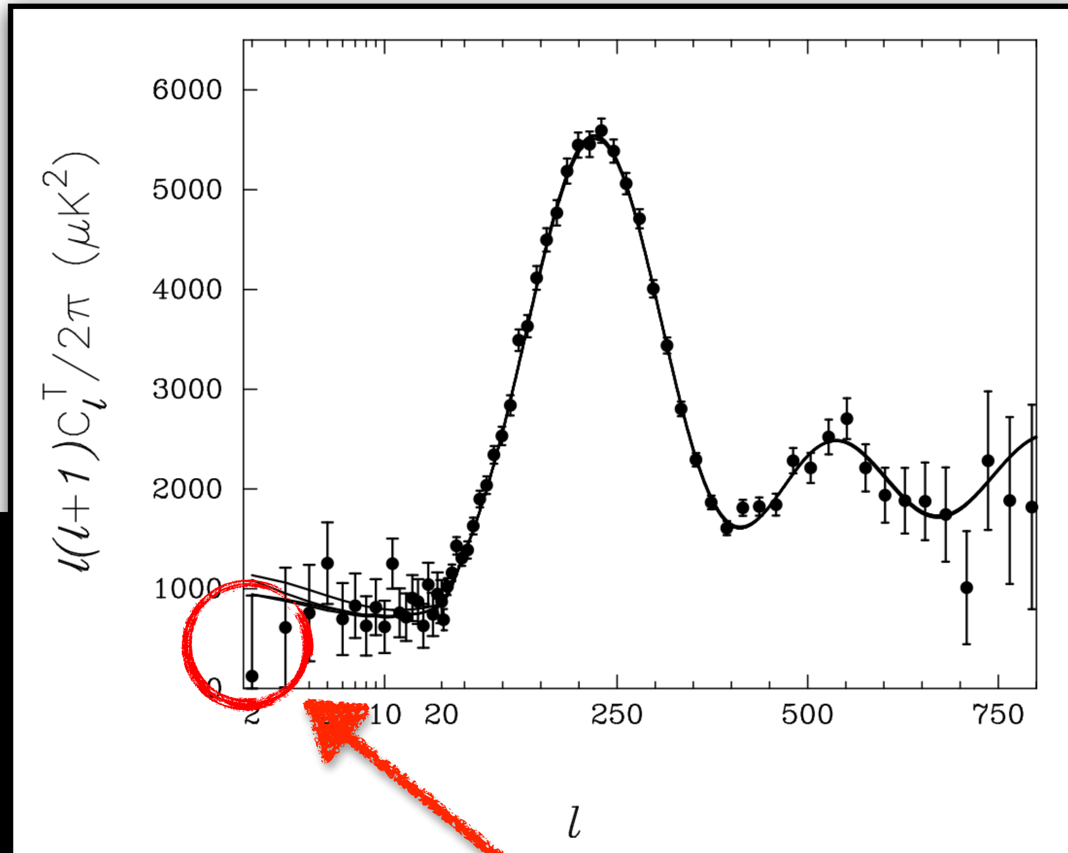

A lower quadrupole than predicted by the ΛCDM was already present in WMAP, and a closed universe to explain this effect was already taken into account.

What about CMB lensing?

Closed models predict substantially higher lensing amplitudes than in ΛCDM, because the dark matter content can be greater, leading to a larger lensing signal. The reasons for the pull towards negative values of Ω_K are essentially the same as those that lead to the preference for $A_L > 1$.

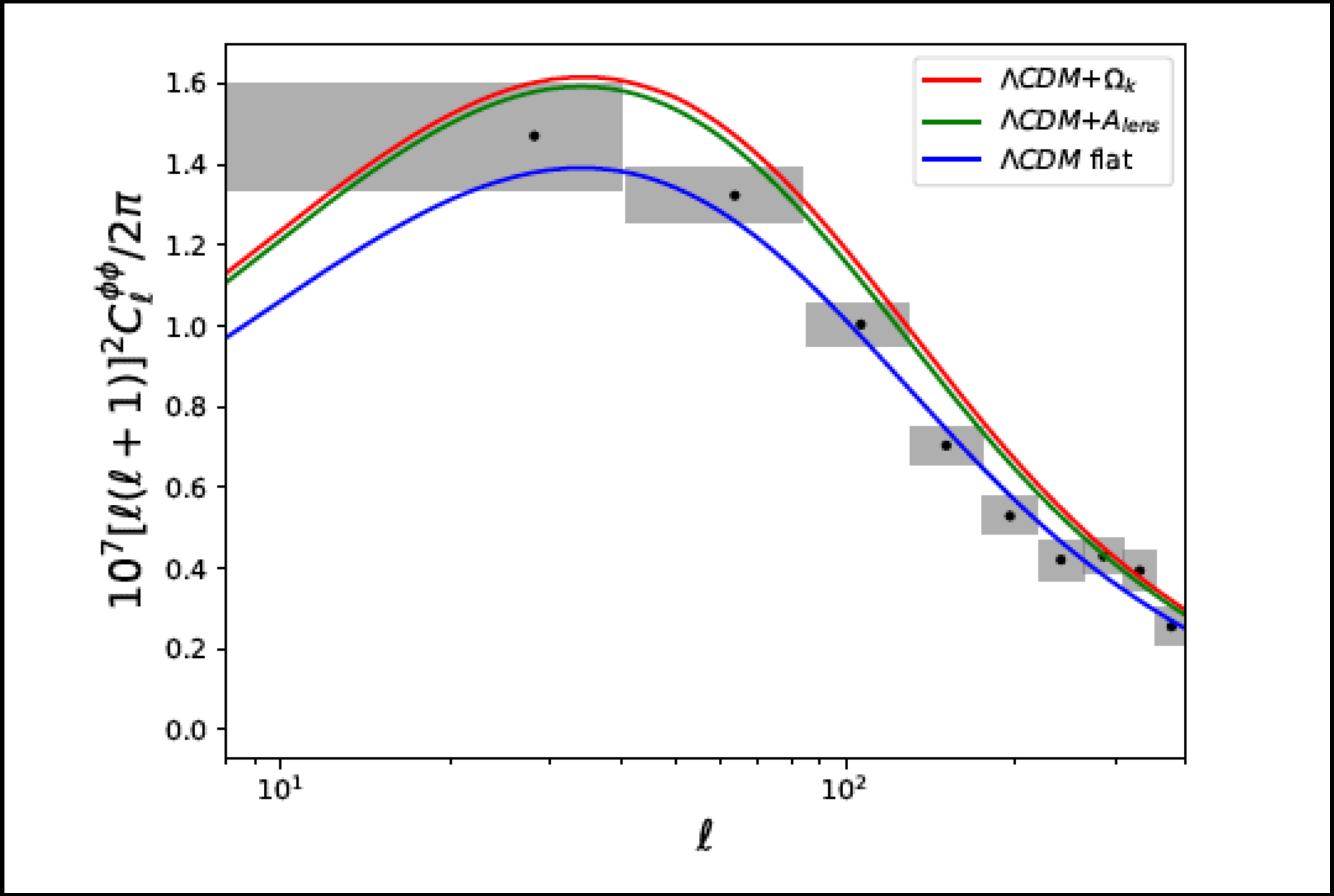

Di Valentino, Melchiorri and Silk, *Nature Astron.* 4 (2019) 2, 196-203

A closed universe (Friedmann 1922) can explain A_L!

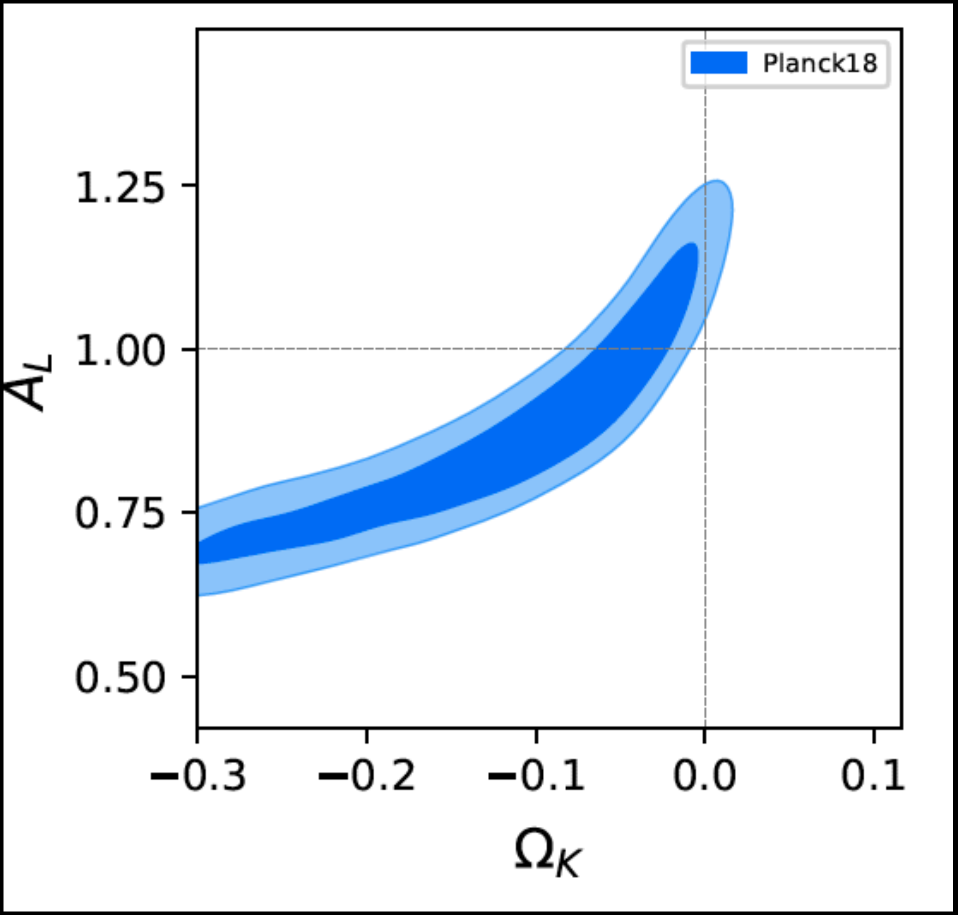

Di Valentino, Melchiorri and Silk, *Nature Astron.* 4 (2019) 2, 196-203

A degeneracy between curvature and the AL parameter is clearly present. A closed universe can provide a robust physical explanation to the enhancement of the lensing amplitude. In fact, the curvature of the Universe is not new physics beyond the standard model, but it is predicted by the General Relativity, and depends on the energy content of the Universe.

A closed universe (Friedmann 1922) can explain A_L!

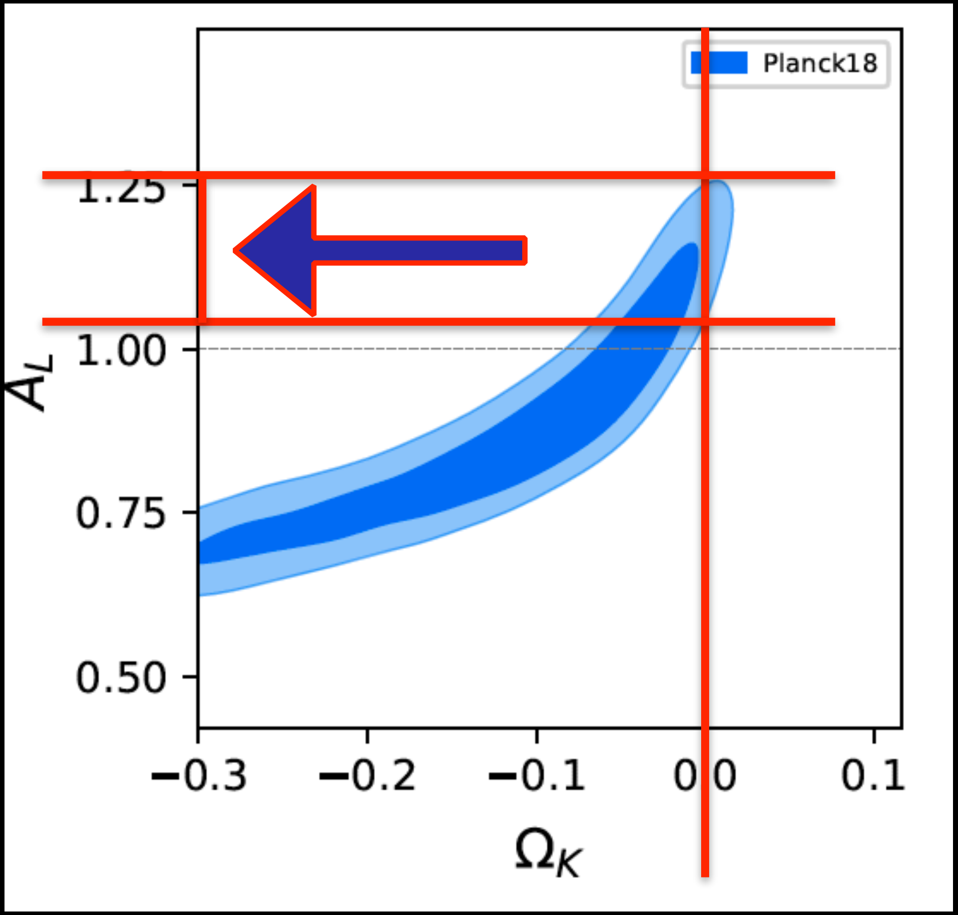

Di Valentino, Melchiorri and Silk, *Nature Astron.* 4 (2019) 2, 196-203

A degeneracy between curvature and the AL parameter is clearly present. A closed universe can provide a robust physical explanation to the enhancement of the lensing amplitude. In fact, the curvature of the Universe is not new physics beyond the standard model, but it is predicted by the General Relativity, and depends on the energy content of the Universe.

A closed universe (Friedmann 1922) can explain A_L!

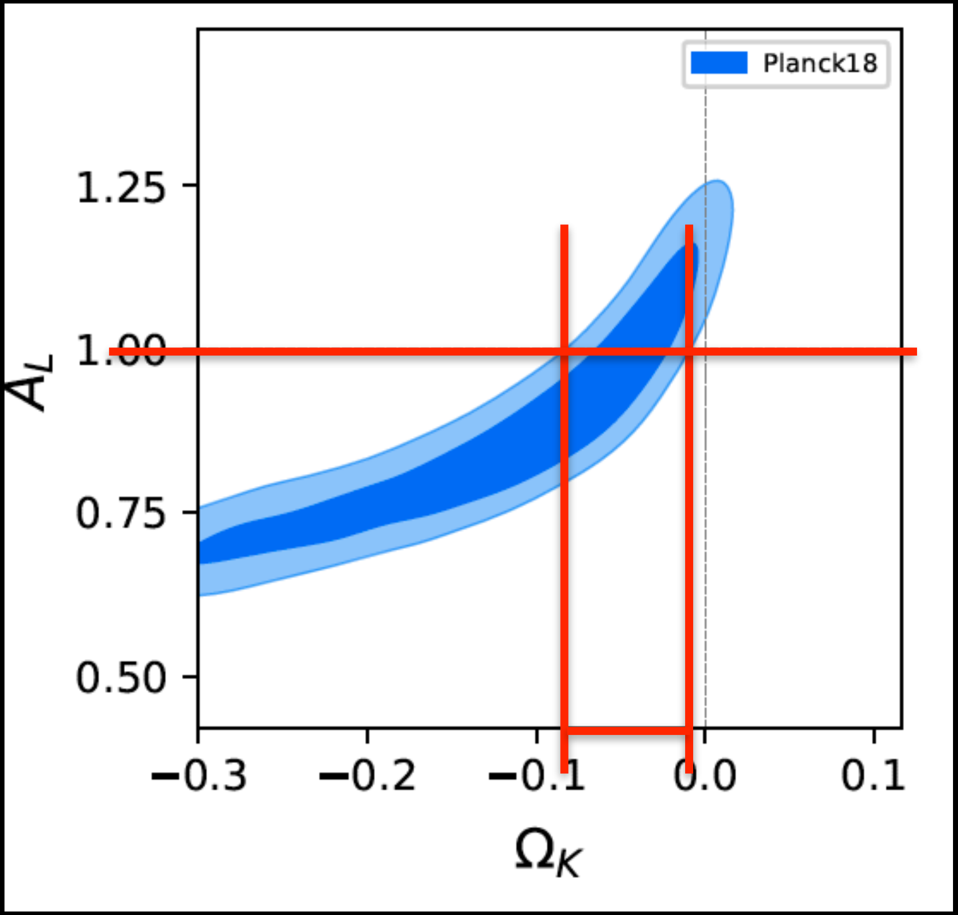

Di Valentino, Melchiorri and Silk, *Nature Astron.* 4 (2019) 2, 196-203

A degeneracy between curvature and the AL parameter is clearly present. A closed universe can provide a robust physical explanation to the enhancement of the lensing amplitude. In fact, the curvature of the Universe is not new physics beyond the standard model, but it is predicted by the General Relativity, and depends on the energy content of the Universe.

The evolution over time of the geometry of the universe is described by Einstein's equations:

$$R_{\mu\nu} - \frac{1}{2}g_{\mu\nu}R = \frac{8\pi G}{c^2}T_{\mu\nu} + \Lambda g_{\mu\nu}$$

which relate the purely geometric properties of space-time, with the distribution of energy of the universe. For this it is sufficient to know the energy content of the Universe to determine its geometry and vice-versa.

Adopting a 4-dimensional coordinate system for the space-time and the Cosmological Principle, i.e. a universe homogeneous and isotropic at large scales, the resulting metric is the Friedmann-Lemaitre-Robertson-Walker (FLRW), that describes the distance between two events in space-time.

$$ds^2 = c^2dt^2 - a^2(t)\left[\frac{dr^2}{1-kr^2} + r^2\left(d\theta^2 + sin^2\theta d\varphi^2\right)\right]$$

The evolution over time of the geometry of the universe is described by Einstein's equations:

$$R_{\mu\nu} - \frac{1}{2}g_{\mu\nu}R = \frac{8\pi G}{c^2}T_{\mu\nu} + \Lambda g_{\mu\nu}$$

which relate the purely geometric properties of space-time, with the distribution of energy of the universe. For this it is sufficient to know the energy content of the Universe to determine its geometry and vice-versa.

Adopting a 4-dimensional coordinate system for the space-time and the Cosmological Principle, i.e. a universe homogeneous and isotropic at large scales, the resulting metric is the Friedmann-Lemaitre-Robertson-Walker (FLRW), that describes the distance between two events in space-time.

$$ds^2 = c^2 dt^2 - a^2(t)\left[\frac{dr^2}{1-kr^2} + r^2\left(d\theta^2 + sin^2\theta d\varphi^2\right)\right]$$

The evolution over time of the geometry of the universe is described by Einstein's equations:

$$R_{\mu\nu} - \frac{1}{2}g_{\mu\nu}R = \frac{8\pi G}{c^2}T_{\mu\nu} + \Lambda g_{\mu\nu}$$

which relate the purely geometric properties of space-time, with the distribution of energy of the universe. For this it is sufficient to know the energy content of the Universe to determine its geometry and vice-versa.

The curvature parameter k can be positive, null or negative, depending on the value of the curvature of the universe: positive, flat or negative.

Adopting a 4-dimensional coordinate system for the space-time and the Cosmological Principle, i.e. a universe homogeneous and isotropic at large scales, the resulting metric is the Friedmann-Lemaitre-Robertson-Walker (FLRW), that describes the distance between two events in space-time.

$$ds^2 = c^2 dt^2 - a^2(t)\left[\frac{dr^2}{1-kr^2} + r^2\left(d\theta^2 + sin^2\theta d\varphi^2\right)\right]$$

The evolution over time of the geometry of the universe is described by Einstein's equations:

$$R_{\mu\nu} - \frac{1}{2} g_{\mu\nu} R = \frac{8\pi G}{c^2} T_{\mu\nu} + \Lambda g_{\mu\nu}$$

which relate the purely geometric properties of space-time, with the distribution of energy of the universe. For this it is sufficient to know the energy content of the Universe to determine its geometry and vice-versa.

Combining together the FLRW metric and Einstein's equations we obtain the Friedmann equations that describe the expansion history of the universe:

1st
$$H^2 = \left(\frac{\dot{a}}{a}\right)^2 = \frac{8\pi G}{3}\rho - \frac{k}{a^2} + \frac{\Lambda}{3}$$

2nd
$$\frac{\ddot{a}}{a} = -\frac{4\pi G}{3}(\rho + 3P) + \frac{\Lambda}{3}$$

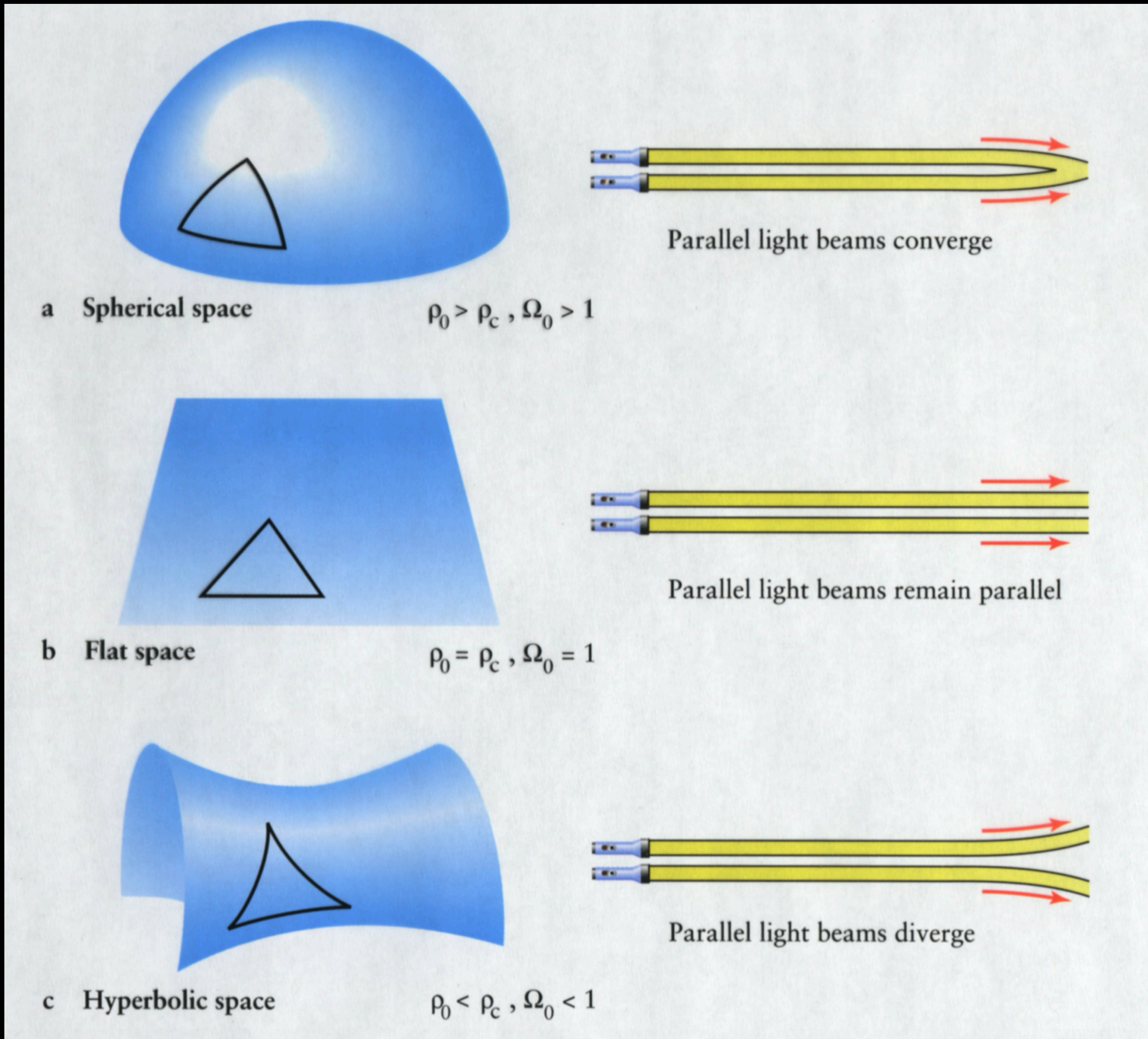

Figure: http://w3.phys.nthu.edu.tw

If we divide the 1[st] Friedmann equation, for the critical density (density of a flat universe), we obtain today:

$$\Omega = \sum_i \Omega_i = \Omega_m + \Omega_\Lambda + \Omega_r = 1 - \Omega_k$$

From this equation it is possible to estimate the curvature of the universe, independently measuring the various contributions to the total density parameter Ω.

$$\begin{cases} \Omega > 1 & \Omega_k < 0 \\ \Omega = 1 & \Omega_k = 0 \\ \Omega < 1 & \Omega_k > 0 \end{cases}$$

→ k>0 : closed Universe

→ k=0 : flat Universe

→ k<0 : open Universe

What about Planck+BAO?

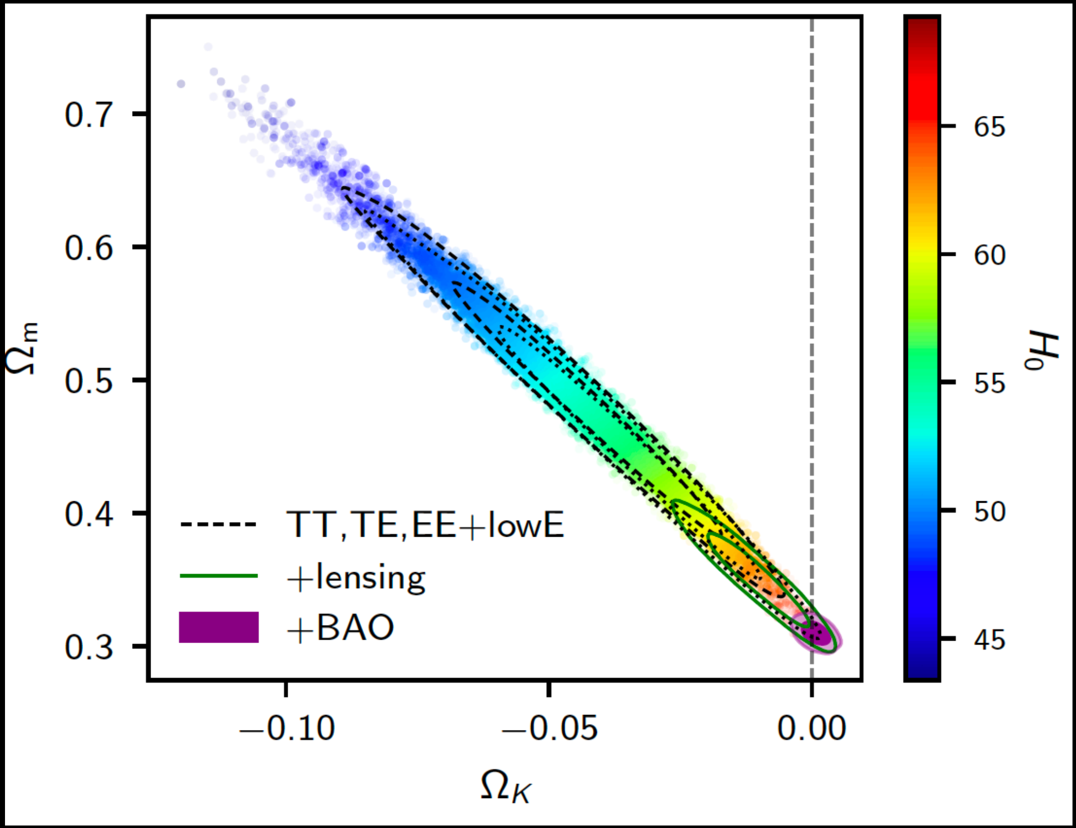

Planck 2018, Astron.Astrophys. 641 (2020) A6

Adding BAO data, a joint constraint is very consistent with a flat universe.

$$\Omega_K = 0.0007 \pm 0.0019 \quad (68\,\%, \text{TT,TE,EE+lowE +lensing+BAO}).$$

Given the significant change in the conclusions from Planck alone, it is reasonable to investigate whether they are actually consistent. In fact, a basic assumption for combining complementary datasets is that these ones must be consistent, i.e. they must plausibly arise from the same cosmological model.

BAO tension

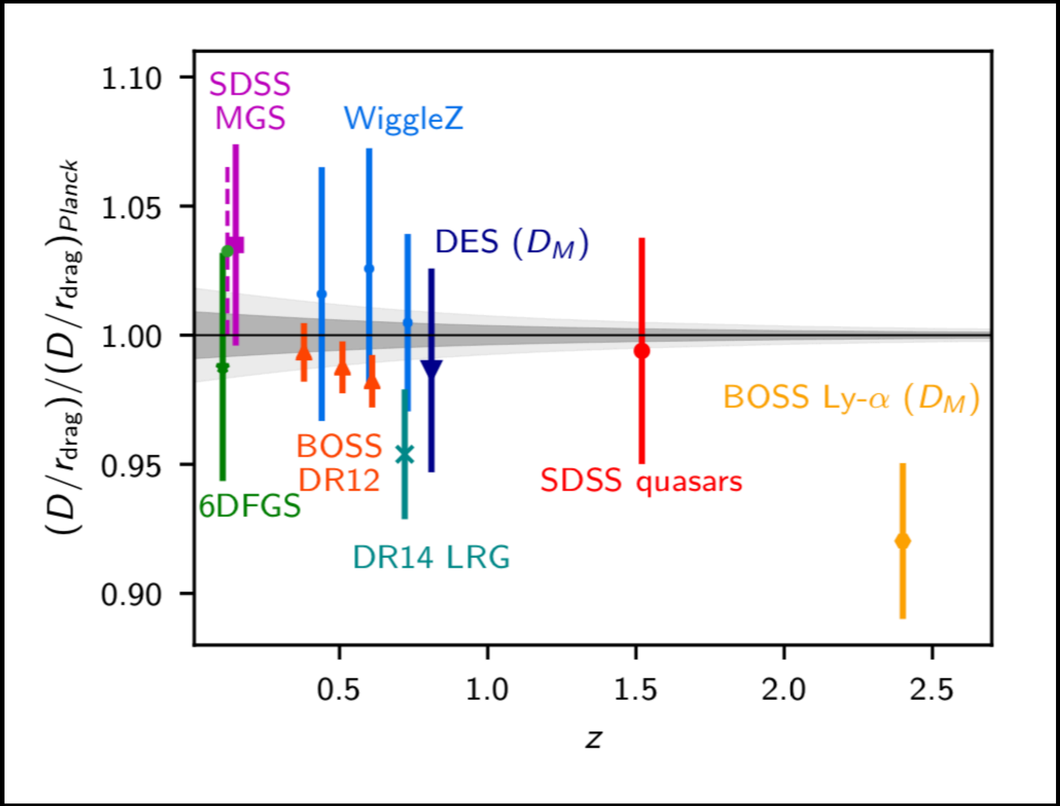

Planck 2018, Astron.Astrophys. 641 (2020) A6

This is a plot of the acoustic-scale distance ratio, DV(z)/rdrag, as a function of redshift, taken from several recent BAO surveys, and divided by the mean acoustic-scale ratio obtained by Planck adopting a model. rdrag is the comoving size of the sound horizon at the baryon drag epoch, and DV, the dilation scale, is a combination of the Hubble parameter H(z) and the comoving angular diameter distance DM(z).

In a ΛCDM model the BAO data agree really well with the Planck measurements…

BAO tension

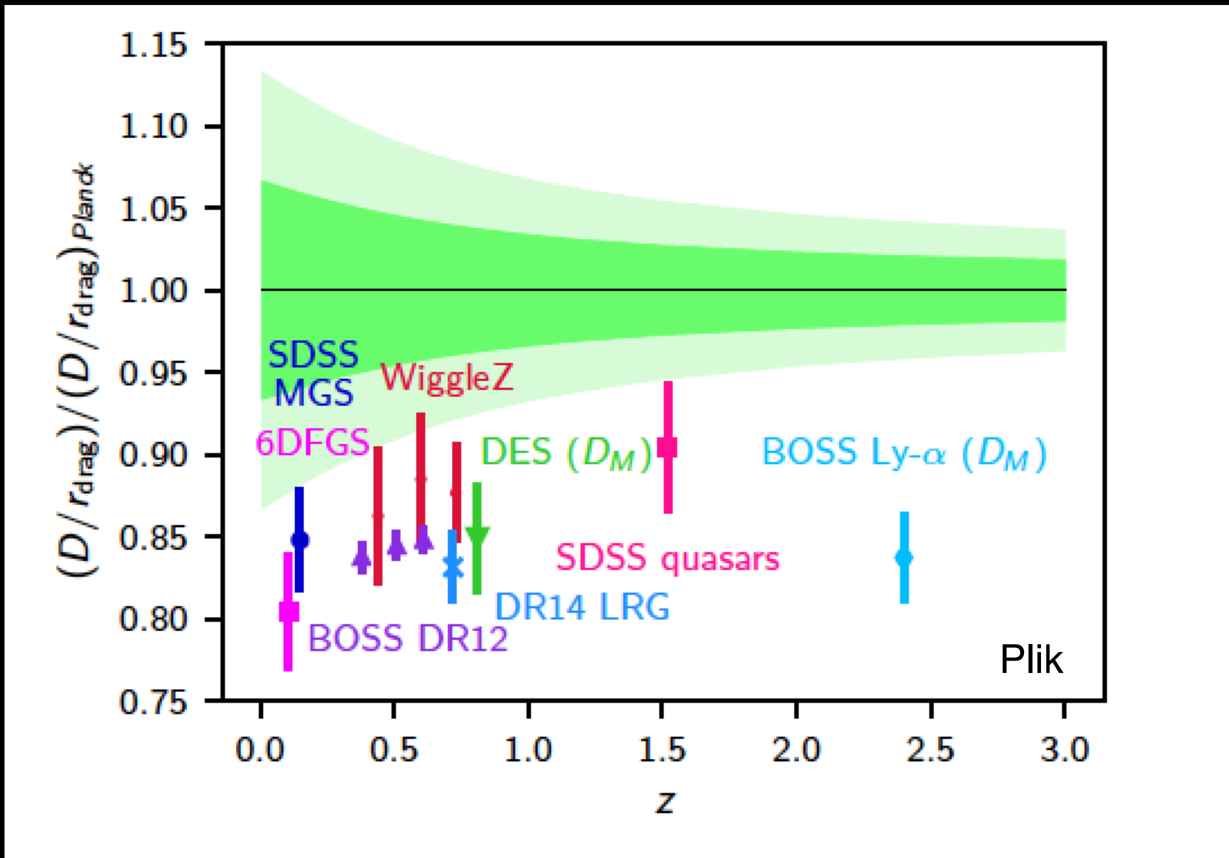

Di Valentino, Melchiorri and Silk, *Nature Astron.* 4 (2019) 2, 196-203

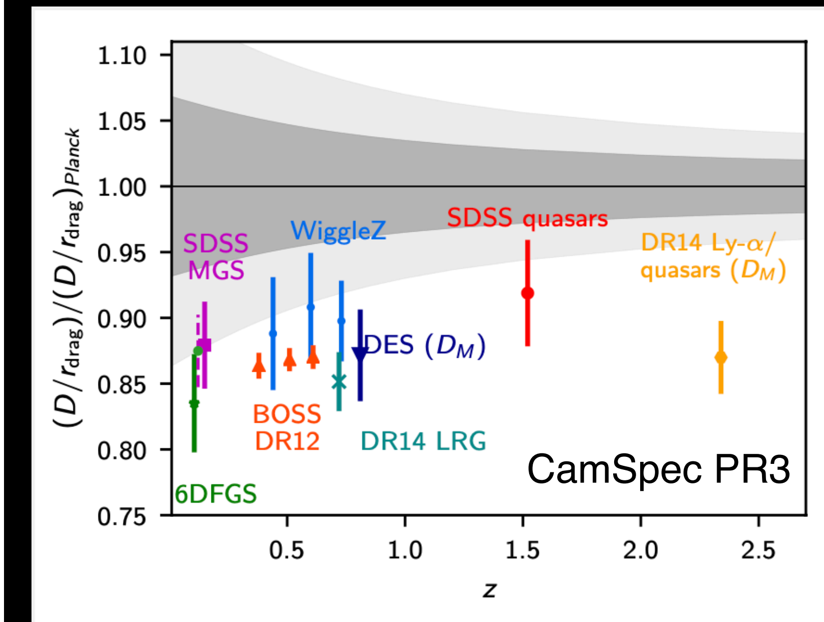

Di Valentino et al., in preparation

… but when we let curvature to vary

there is a striking disagreement between Planck spectra and BAO measurements!

BAO tension

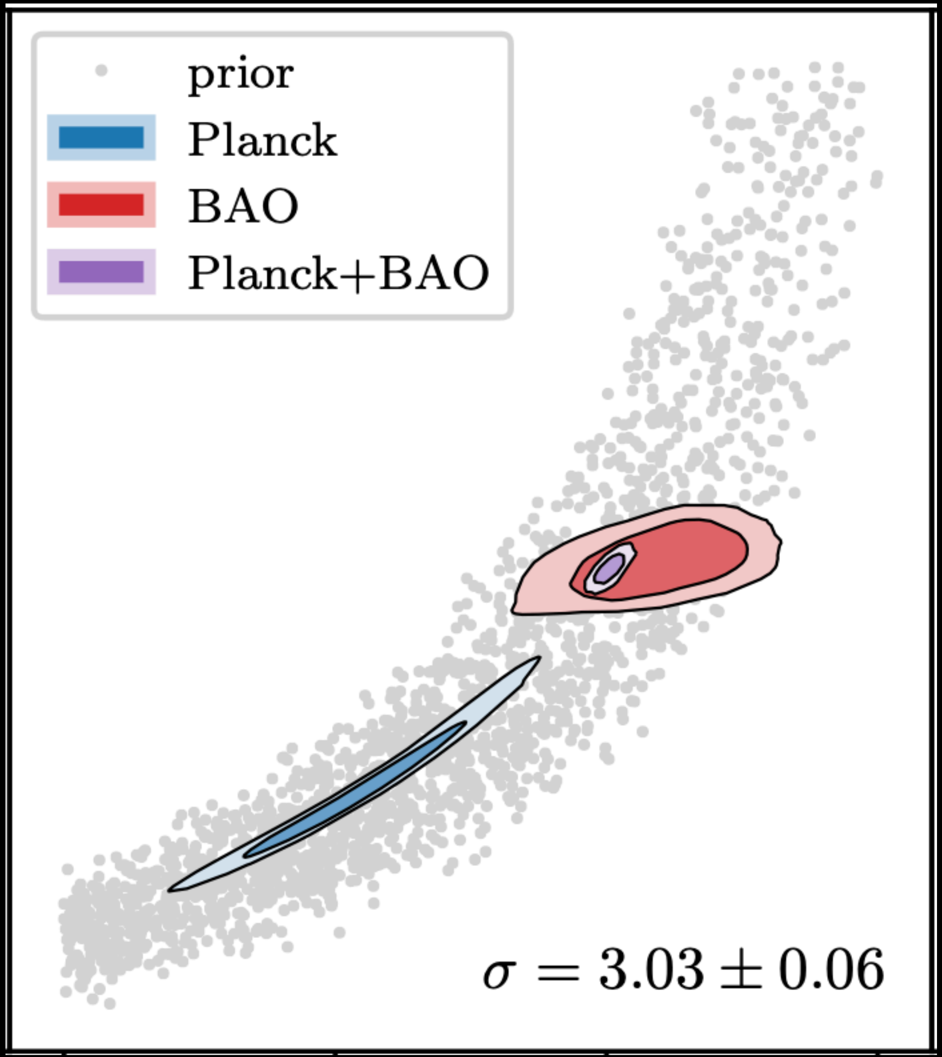

In agreement with
Handley, Phys.Rev.D 103 (2021) 4, L041301

What about Planck+FS?

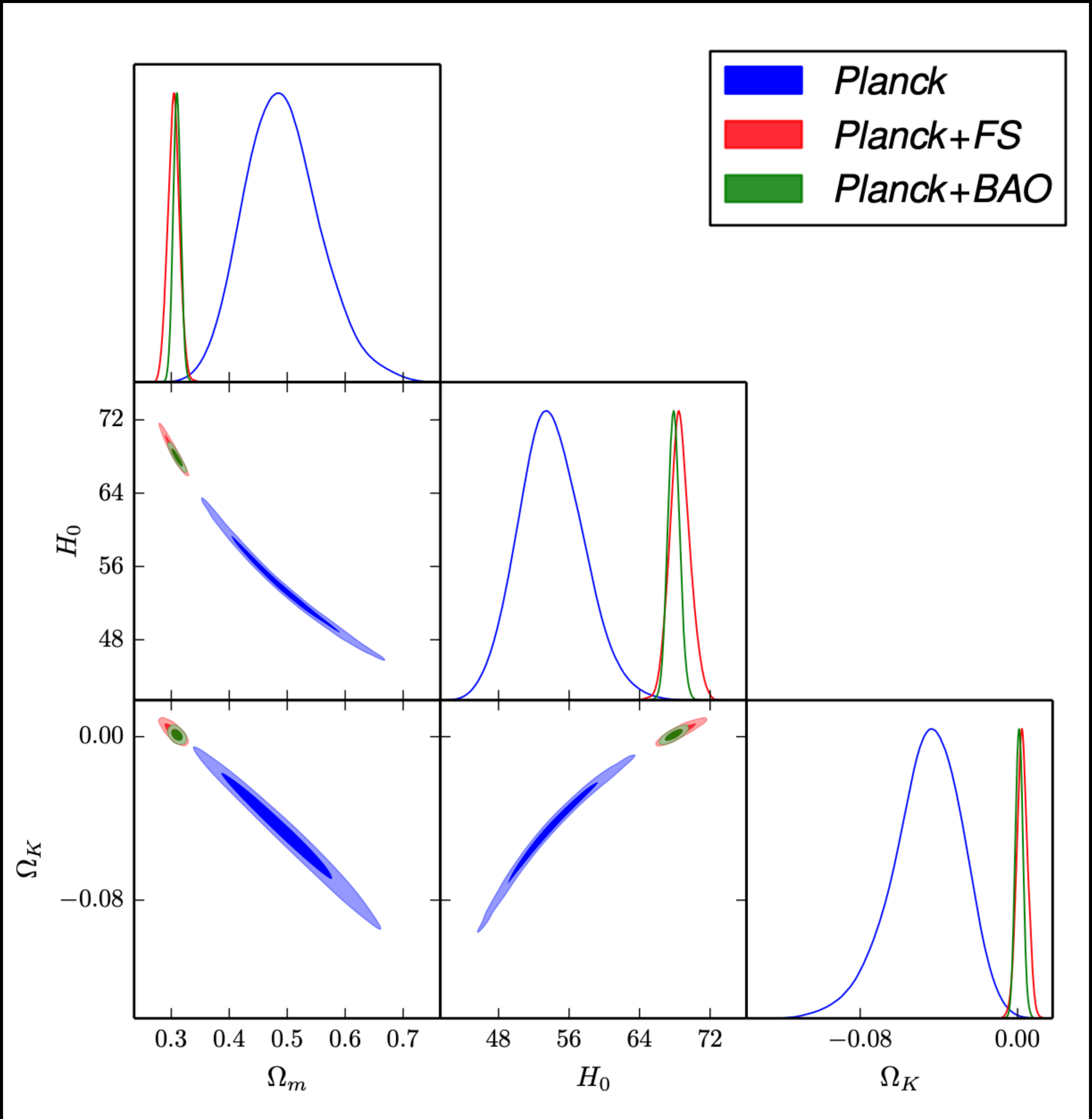

The strong disagreement between Planck and BAO it is evident in this triangular plot, as well as that with the full-shape (FS) galaxy power spectrum measurements from the BOSS DR12 CMASS sample, at an effective redshift $z_{eff} = 0.57$.

Vagnozzi, Di Valentino, et al., *Phys.Dark Univ.* 33 (2021) 100851

ΛCDM+ Ω_k: a 7 parameter standard model

As it has been convincingly pointed out in Anselmi et al., arXiv:2207.06547,
in absence of any theoretical arguments,
we cannot use observations that suggest small Ω_k to enforce $\Omega_k=0$.
The common practice of assuming $\Omega_k=0$ places
the onus on proponents of “curved ΛCDM"
to provide sufficient evidence that $\Omega_k \neq 0$,
and this is required as an additional parameter.
Given the current tensions in cosmological parameters and
CMB anomalies this choice is at least open to debate.
So it would be preferable to have the standard cosmological
phenomenological model with at least 7 parameters.

Curvature can explain internal tension

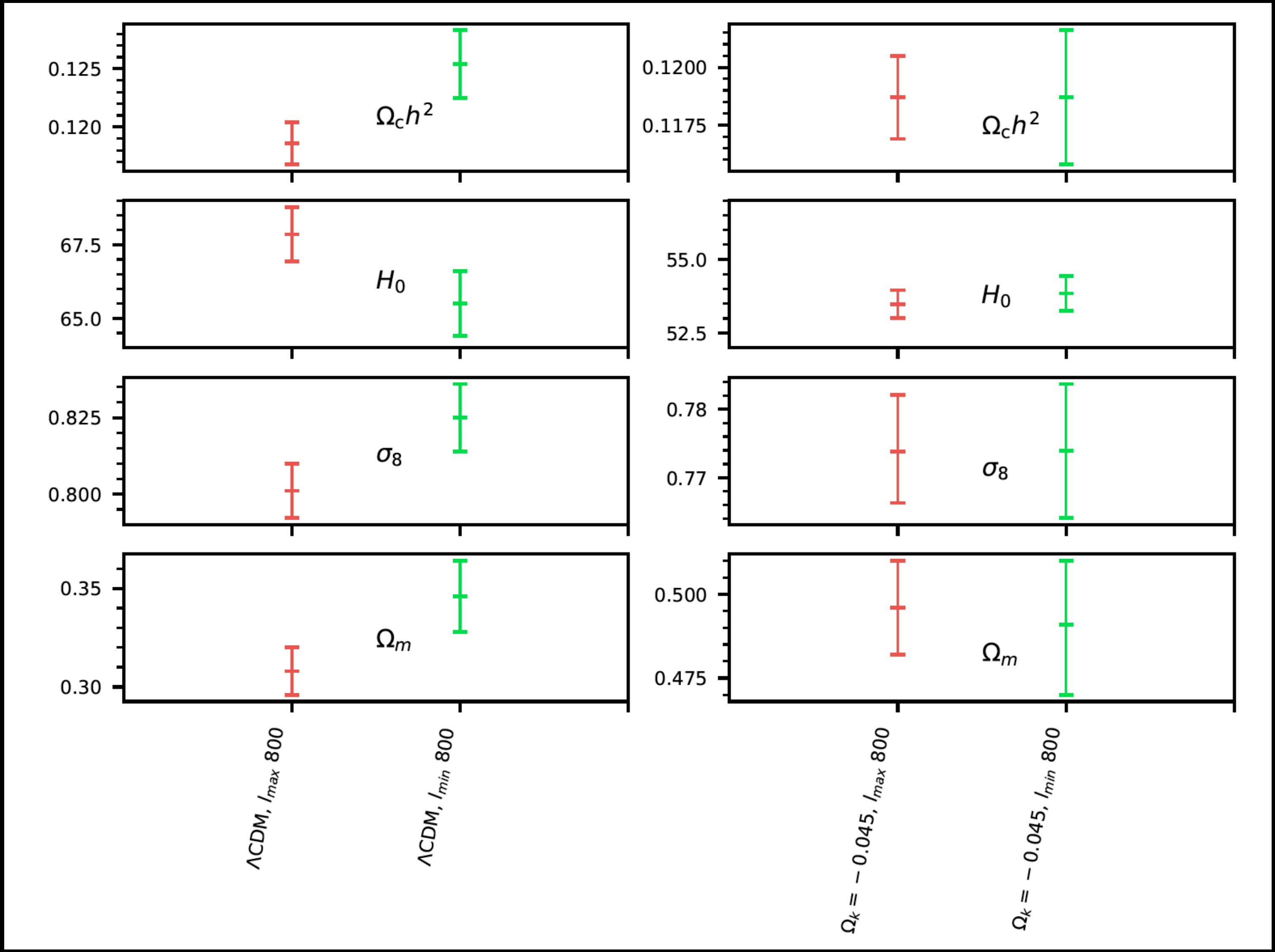

Di Valentino, Melchiorri and Silk, *Nature Astron.* 4 (2019) 2, 196-203

In a closed Universe with ΩK = –0.045, the cosmological parameters derived in the two different multipole ranges are now fully compatible.

Curvature can't explain external tensions

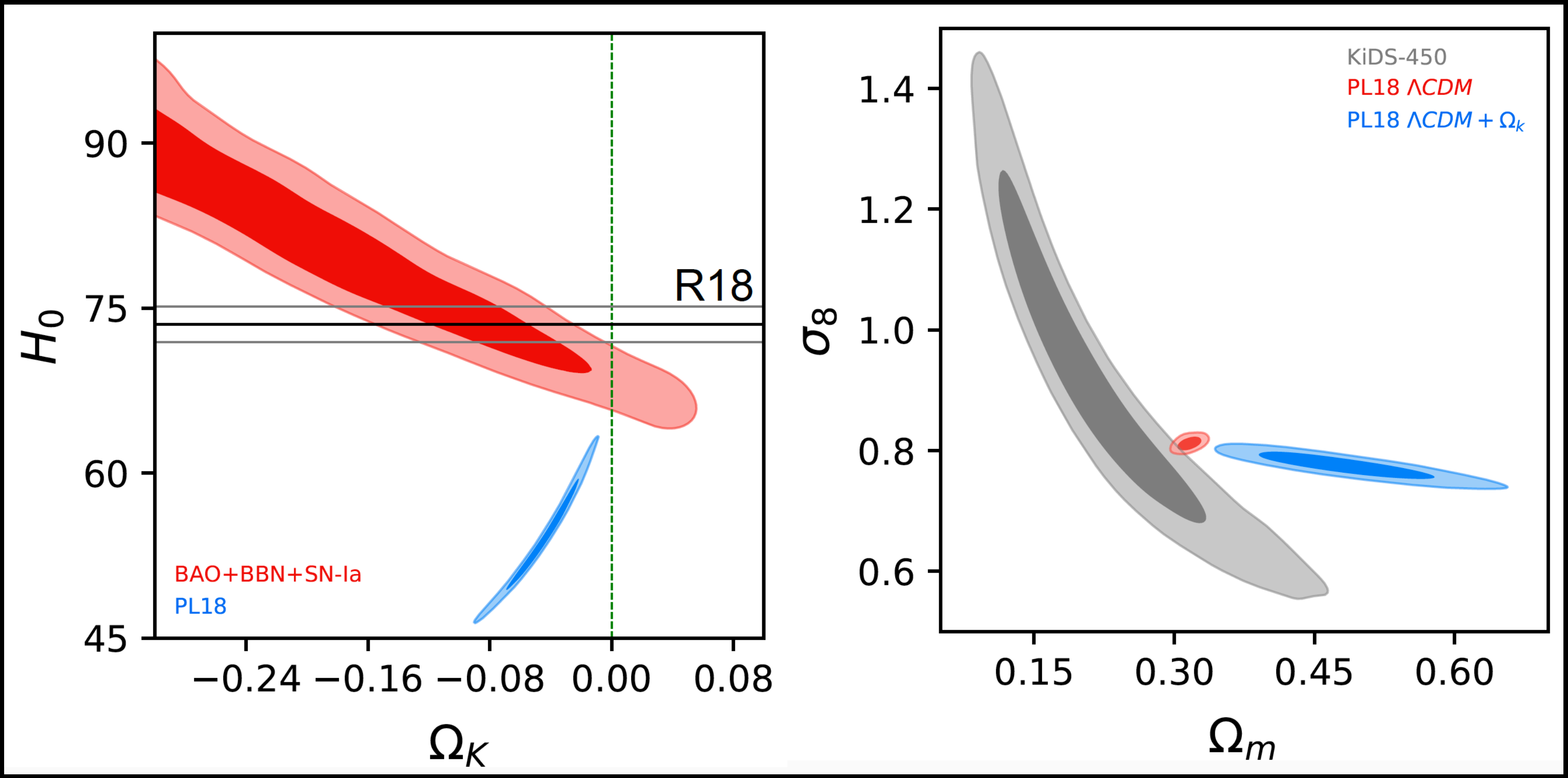

Di Valentino, Melchiorri and Silk, *Nature Astron.* 4 (2019) 2, 196-203

Varying Ωκ, both the well known tensions on H0 and S8 are exacerbated.
In a ΛCDM + ΩK model, Planck gives $H0 = 54.4^{+3.3}_{-4.0}$ km/s/Mpc at 68% cl., increasing the tension with SH0ES at 5.5σ, and S8 in disagreement at about 3.8σ with KiDS-450, and more than 3.5σ with DES.

What about non-CMB data?

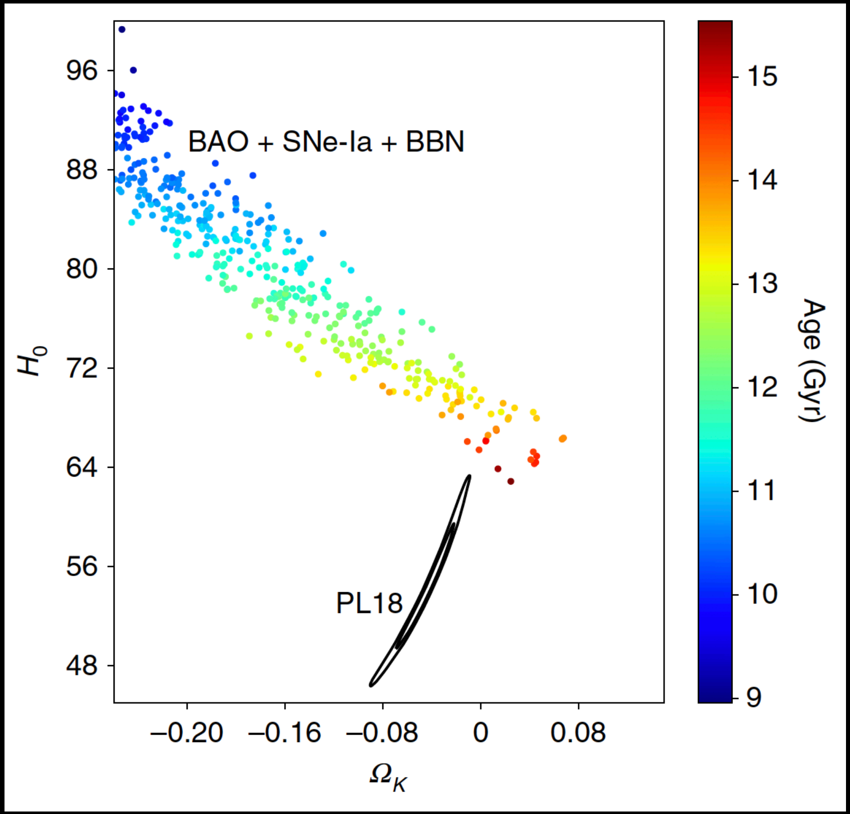

Di Valentino, Melchiorri and Silk, *Nature Astron.* 4 (2019) 2, 196-203

It is now interesting to address the compatibility of Planck with combined datasets, like BAO + type-Ia supernovae + big bang nucleosynthesis data.

In principle, each dataset prefers a closed universe,

but BAO+SN-Ia+BBN gives H0 = 79.6 ± 6.8 km/s/Mpc at 68%cl, perfectly consistent with SH0ES, but at 3.4σ tension with Planck.

What about non-CMB data?

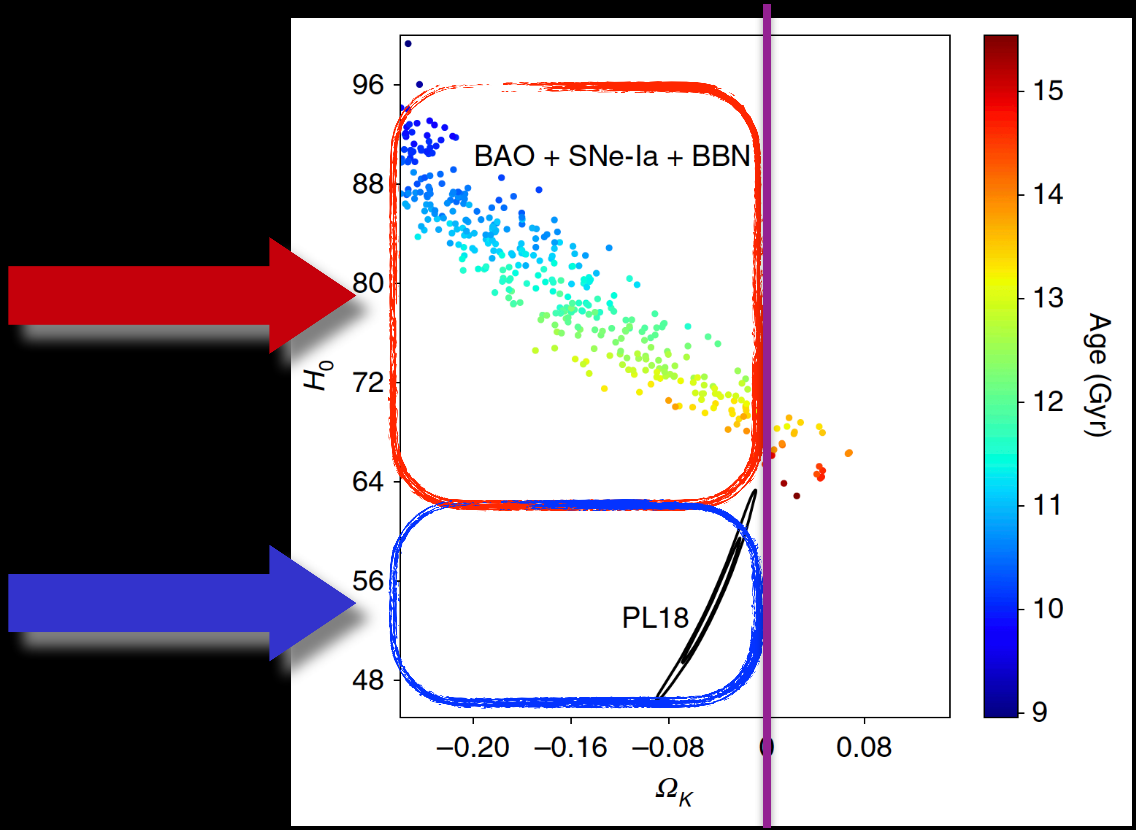

Di Valentino, Melchiorri and Silk, *Nature Astron.* 4 (2019) 2, 196-203

It is now interesting to address the compatibility of Planck with combined datasets, like BAO + type-Ia supernovae + big bang nucleosynthesis data.
In principle, each dataset prefers a closed universe,
but BAO+SN-Ia+BBN gives H0 = 79.6 ± 6.8 km/s/Mpc at 68%cl, perfectly consistent with SH0ES, but at 3.4σ tension with Planck.

BAO+SNIa+BBN+R18 gives Ωk = −0.091 ± 0.037 at 68%cl.

EFTofLSS to investigate FS data

	$\ln(10^{10}A_s)$	h	$\Omega_{cdm}h^2$	Ω_m	Ω_k	n_s	$2*\log(\mathcal{L})$
Flat, fixed n_s	$2.85^{+0.11}_{-0.12}$ (3.03)	$0.667^{+0.011}_{-0.011}$ (0.672)	$0.114^{+0.005}_{-0.004}$ (0.115)	$0.307^{+0.010}_{-0.011}$ (0.304)	-	-	367.2
Curved, fixed n_s	$2.55^{+0.21}_{-0.22}$ (2.77)	$0.686^{+0.015}_{-0.016}$ (0.665)	$0.115^{+0.004}_{-0.005}$ (0.111)	$0.291^{+0.014}_{-0.013}$ (0.302)	$-0.089^{+0.049}_{-0.046}$ (−0.042)	-	366.3
Flat, varying n_s	$2.80^{+0.14}_{-0.13}$ (2.97)	$0.669^{+0.012}_{-0.011}$ (0.668)	$0.117^{+0.009}_{-0.008}$ (0.114)	$0.312^{+0.017}_{-0.014}$ (0.304)	-	$0.950^{+0.04}_{-0.051}$ (0.972)	367.1
Curved, varying n_s	$2.19^{+0.29}_{-0.28}$ (2.62)	$0.707^{+0.021}_{-0.021}$ (0.686)	$0.127^{+0.011}_{-0.009}$ (0.116)	$0.300^{+0.016}_{-0.014}$ (0.295)	$-0.152^{+0.059}_{-0.053}$ (−0.089)	$0.878^{+0.053}_{-0.055}$ (0.932)	364.8

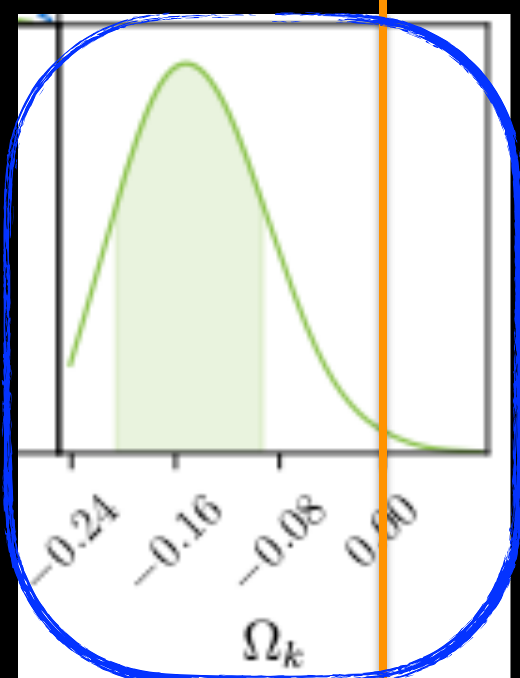

Glanville et al., *arXiv:2205.05892*

In this paper they use EFTofLSS to simultaneously constrain measurements from the 6dFGS, BOSS, and eBOSS catalogues, in order to remove some of the assumptions of flatness that enter into other large-scale structure analyses. Fitting the FS data with a BBN prior they measure a >2σ preference for a closed universe.

Beyond six parameters: extending ΛCDM+Ωk

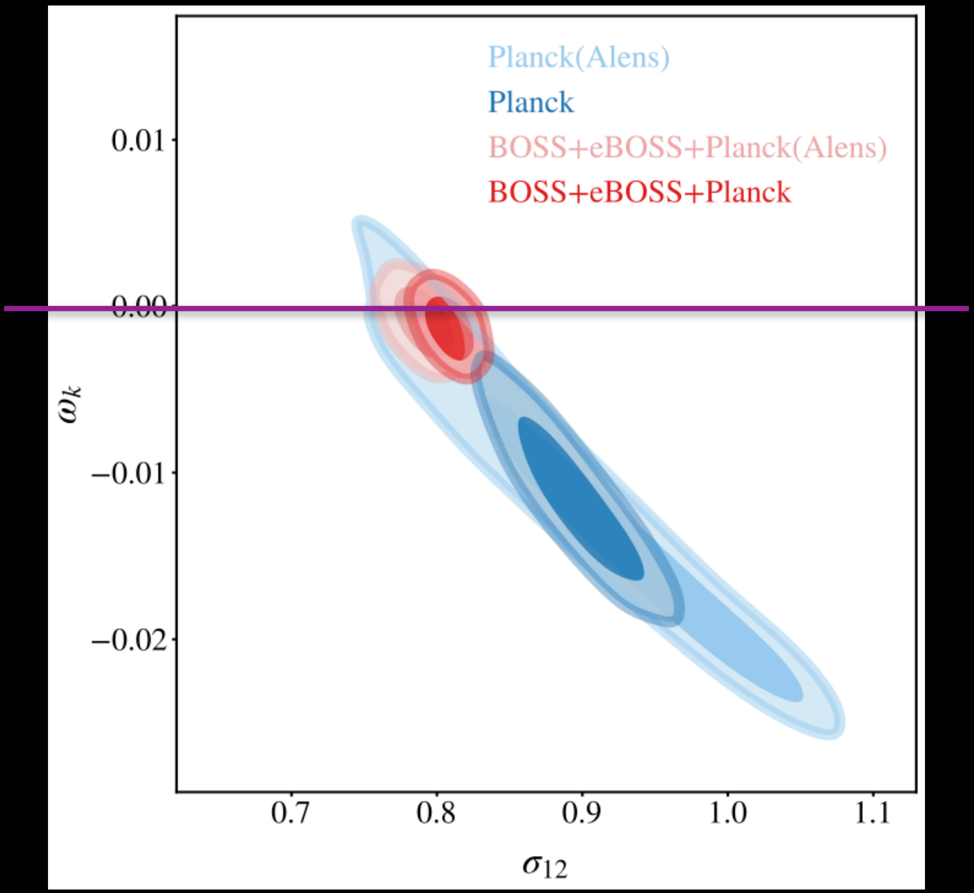

Semenaite et al., arXiv:2210.07304

A similar result has been obtained by analysing a wKCDM model, and the parameter $\omega_K = \Omega_k h^2$ that gives

$$\omega_K = -0.0116^{+0.0029}_{-0.0036}$$

i.e. a 4σ preference for a closed universe.

Evidence for a phantom closed Universe at more than 99% CL!!

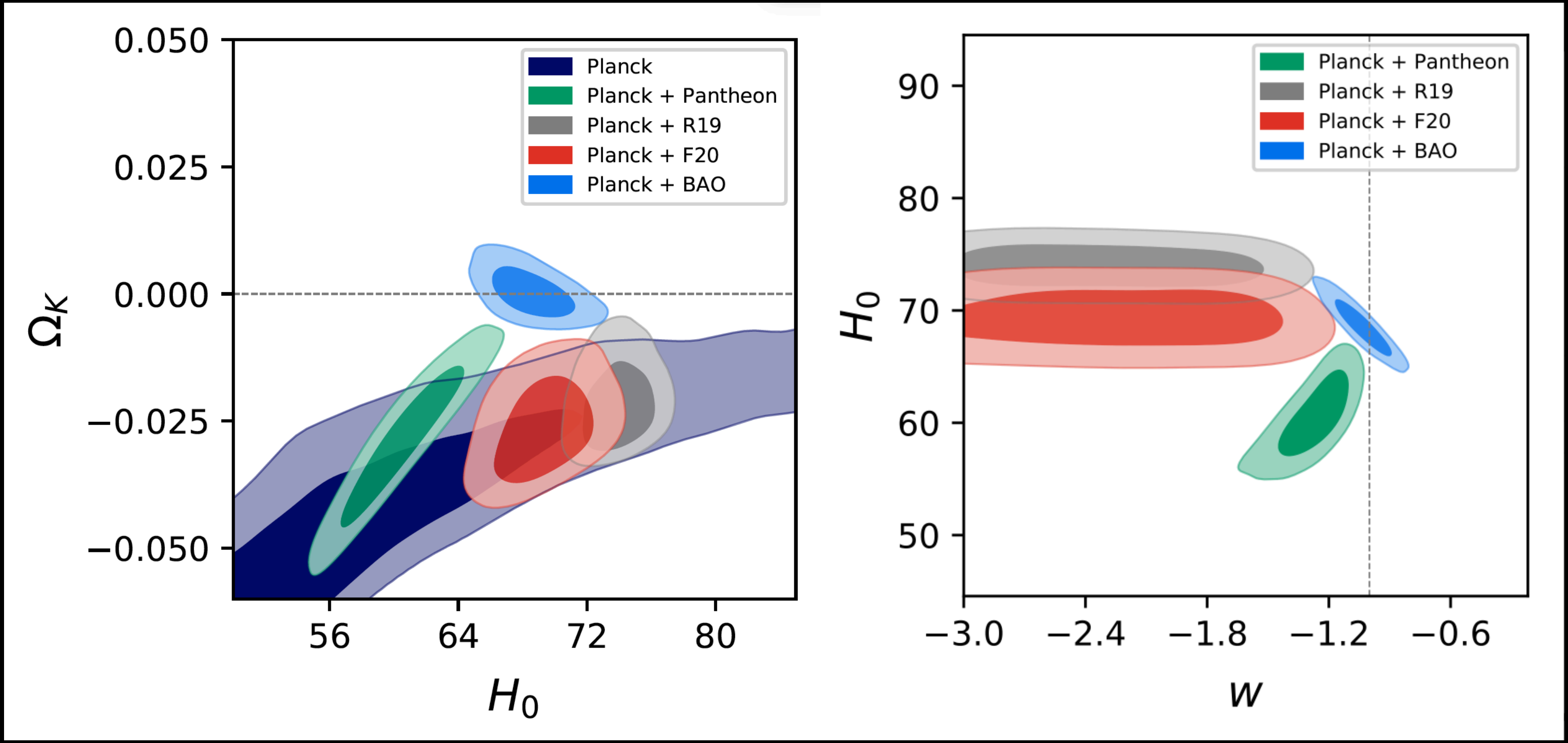

It is interesting to note that if a closed universe increases the fine-tuning of the theory, the removal of a cosmological constant reduces it. It is, therefore, difficult to decide whether a phantom closed model is less or more theoretically convoluted than ΛCDM.

Di Valentino, Melchiorri and Silk, ApJ Letters, 908, L9 (2021), arXiv:2003.04935

So… is the Universe closed?

SPT-3G gives at 68% CL:

$$\Omega_K = 0.001^{+0.018}_{-0.019}$$

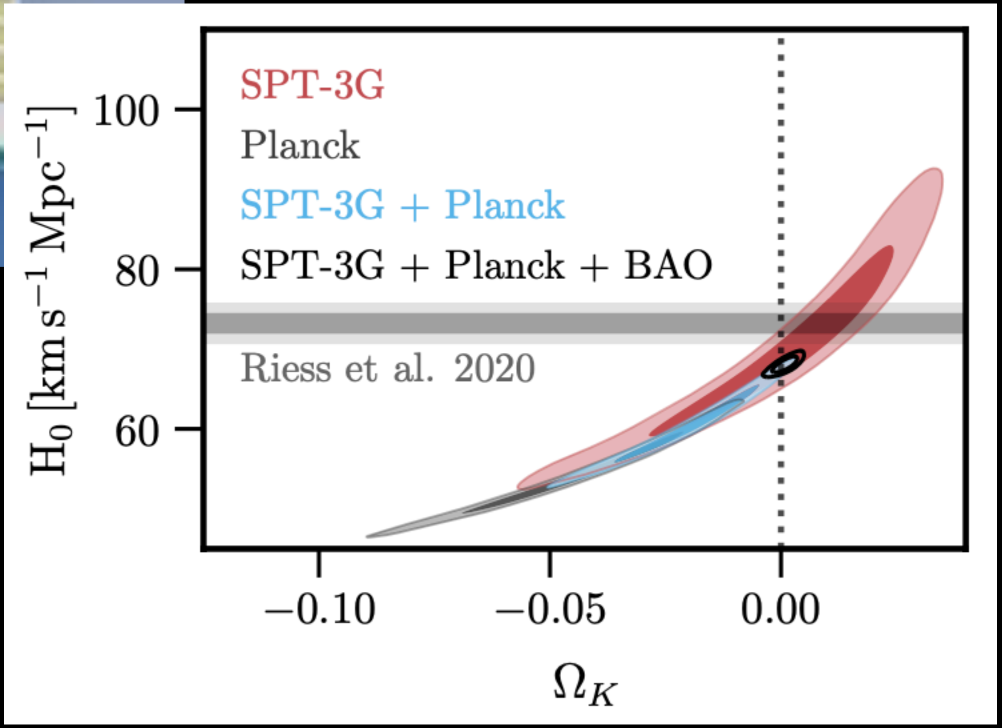

SPT-3G, arXiv:2103.13618 [astro-ph.CO]

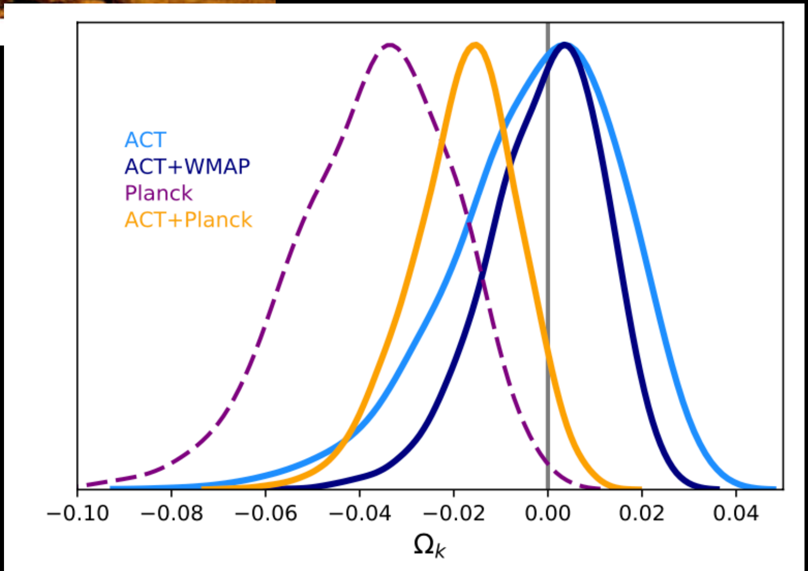

ACT-DR4 2020, Aiola et al., arXiv:2007.07288 [astro-ph.CO]

ACT-DR4 + WMAP gives at 68% CL

$\Omega_k = -0.001 \pm 0.012$

What about Planck PR4 (NPIPE) with CamSpec?

arXiv > astro-ph > arXiv:2205.10869

Search...

Help | Advar

Astrophysics > Cosmology and Nongalactic Astrophysics

[Submitted on 22 May 2022 (v1), last revised 11 Nov 2022 (this version, v2)]

CMB power spectra and cosmological parameters from Planck PR4 with CamSpec

Erik Rosenberg, Steven Gratton, George Efstathiou

We present angular power spectra and cosmological parameter constraints derived from the Planck PR4 (NPIPE) maps of the Cosmic Microwave Background. NPIPE, released by the Planck Collaboration in 2020, is a new processing pipeline for producing calibrated frequency maps from Planck data. We have created new versions of the CamSpec likelihood using these maps and applied them to constrain LCDM and single-parameter extensions. We find excellent consistency between NPIPE and the Planck 2018 maps at the parameter level, showing that the Planck cosmology is robust to substantial changes in the mapmaking. The lower noise of NPIPE leads to ~10% tighter constraints, and we see both smaller error bars and a shift toward the LCDM values for beyond-LCDM parameters including Omega_K and A_Lens.

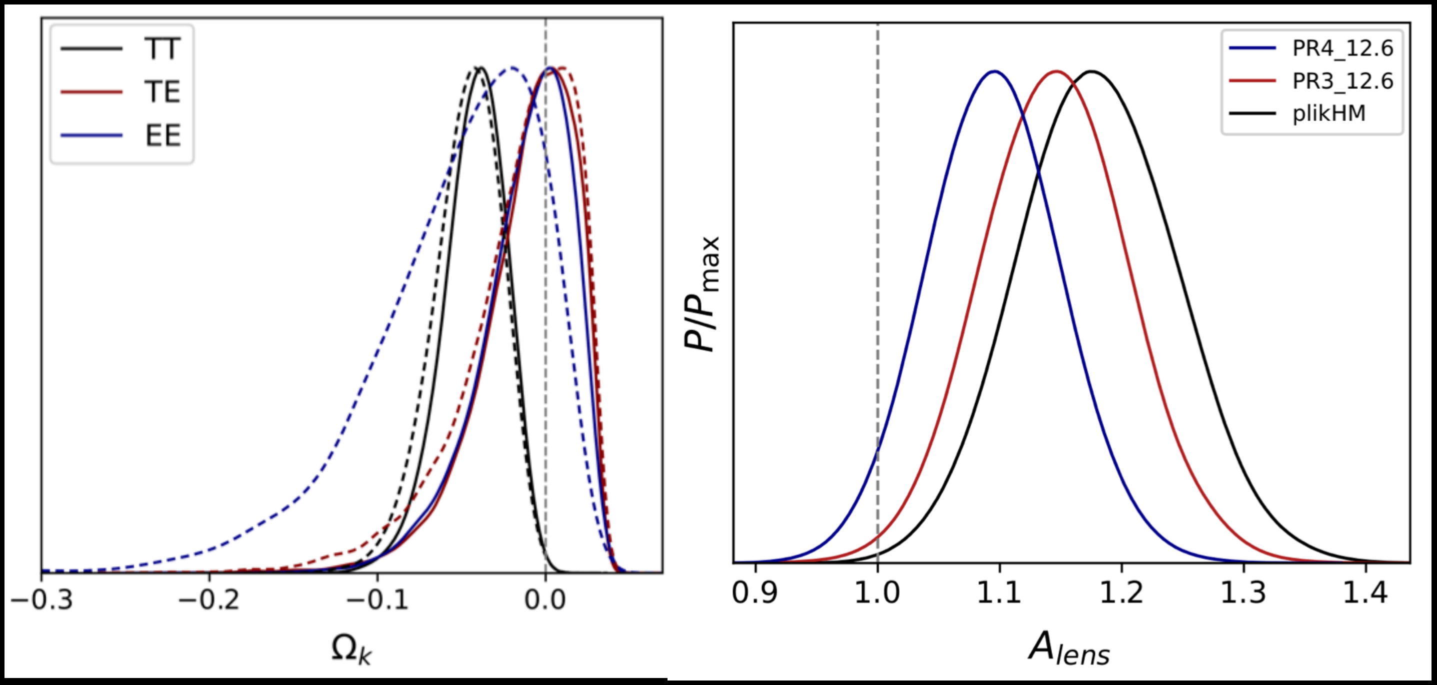

Planck PR4 (NPIPE) with CamSpec

PR4_12.6	A_L	Ω_K	$N_{\rm eff}$	m_ν
TTTEEE	1.095 ± 0.056	$-0.025^{+0.013}_{-0.010}$	3.00 ± 0.21	< 0.161
TT	1.198 ± 0.084	$-0.042^{+0.022}_{-0.016}$	$2.98^{+0.28}_{-0.35}$	< 0.278
TE	0.96 ± 0.15	$-0.010^{+0.035}_{-0.015}$	$3.11^{+0.38}_{-0.42}$	< 0.400
EE	0.995 ± 0.15	$-0.012^{+0.034}_{-0.017}$	4.6 ± 1.3	< 2.37
PR3_12.6	A_L	Ω_K	$N_{\rm eff}$	m_ν
TTTEEE	1.146 ± 0.061	$-0.035^{+0.016}_{-0.012}$	$2.94^{+0.20}_{-0.23}$	< 0.143
TT	1.215 ± 0.089	$-0.047^{+0.024}_{-0.017}$	$2.89^{+0.28}_{-0.32}$	< 0.248
TE	0.96 ± 0.17	$-0.015^{+0.043}_{-0.015}$	$2.96^{+0.42}_{-0.49}$	< 0.504
EE	1.15 ± 0.20	$-0.053^{+0.063}_{-0.029}$	$2.46^{+0.94}_{-1.7}$	-

…but this new likelihood is not really solving the problem of AL/ΩK, that is mainly coming from the TT power spectrum.
And the constraints coming from TT are not changing in the 2 releases…

Rosenberg et al., arXiv:2205.10869

Planck PR4 (NPIPE) with CamSpec

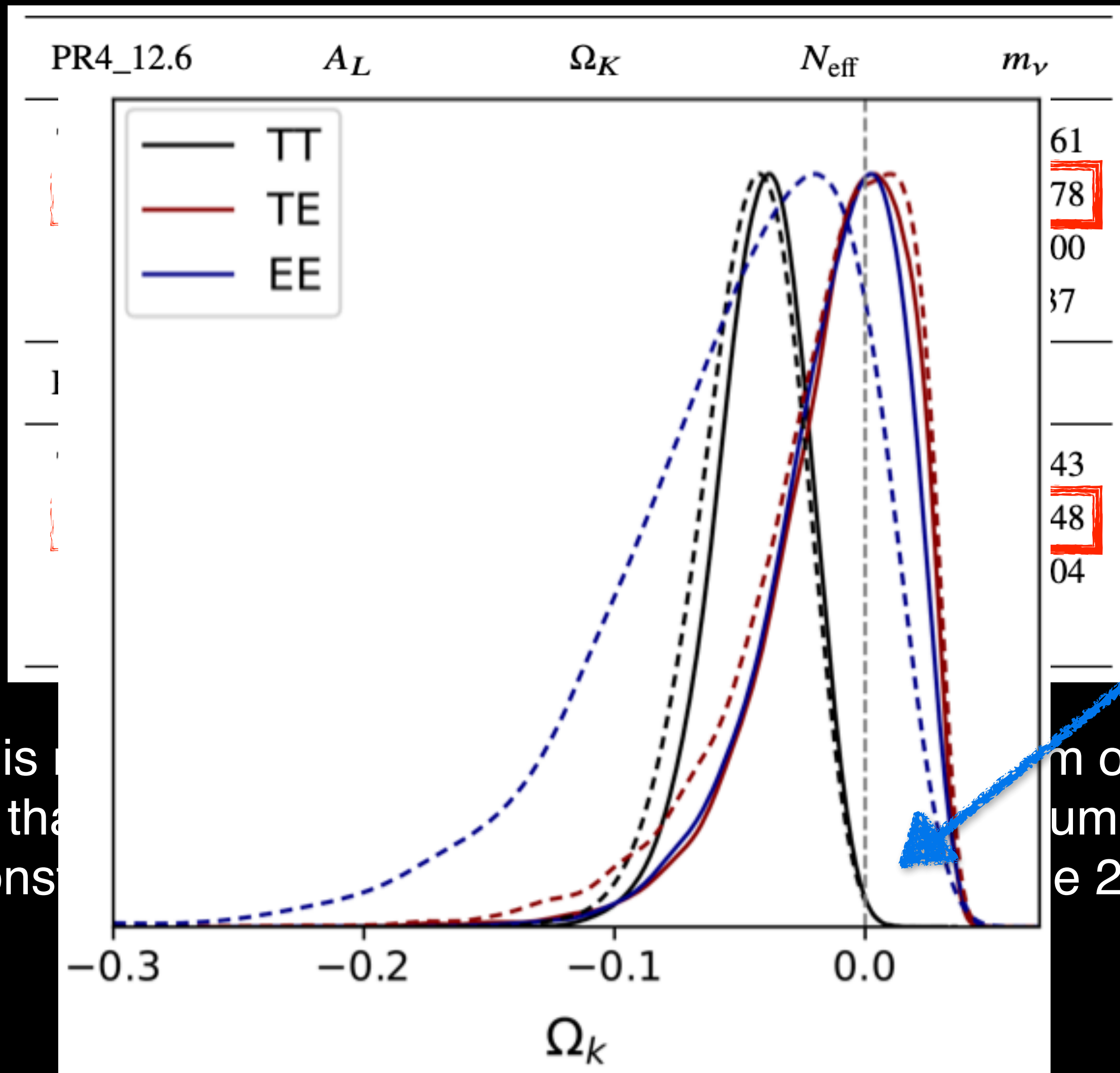

…but this r … m of AL/ΩK,
tha … um.
And the cons … e 2 releases…

Rosenberg et al., arXiv:2205.10869

Planck PR4 (NPIPE) with CamSpec

PR4_12.6	A_L	Ω_K	$N_{\rm eff}$	m_ν
TTTEEE	1.095 ± 0.056	$-0.025^{+0.013}_{-0.010}$	3.00 ± 0.21	< 0.161
TT	1.198 ± 0.084	$-0.042^{+0.022}_{-0.016}$	$2.98^{+0.28}_{-0.35}$	< 0.278
TE	0.96 ± 0.15	$-0.010^{+0.035}_{-0.015}$	$3.11^{+0.38}_{-0.42}$	< 0.400
EE	0.995 ± 0.15	$-0.012^{+0.034}_{-0.017}$	4.6 ± 1.3	< 2.37
PR3_12.6	A_L	Ω_K	$N_{\rm eff}$	m_ν
TTTEEE	1.146 ± 0.061	$-0.035^{+0.016}_{-0.012}$	$2.94^{+0.20}_{-0.23}$	< 0.143
TT	1.215 ± 0.089	$-0.047^{+0.024}_{-0.017}$	$2.89^{+0.28}_{-0.32}$	< 0.248
TE	0.96 ± 0.17	$-0.015^{+0.043}_{-0.015}$	$2.96^{+0.42}_{-0.49}$	< 0.504
EE	1.15 ± 0.20	$-0.053^{+0.063}_{-0.029}$	$2.46^{+0.94}_{-1.7}$	-

…but this new likelihood is not really solving the problem of AL/ΩK, that is mainly coming from the TT power spectrum.
And the constraints coming from TT are not changing in the 2 releases…

The constraints derived from the EE power spectrum are instead those pulling all the parameters towards ΛCDM and thus alleviating the tensions.

Rosenberg et al., arXiv:2205.10869

Planck PR4 (NPIPE) with CamSpec

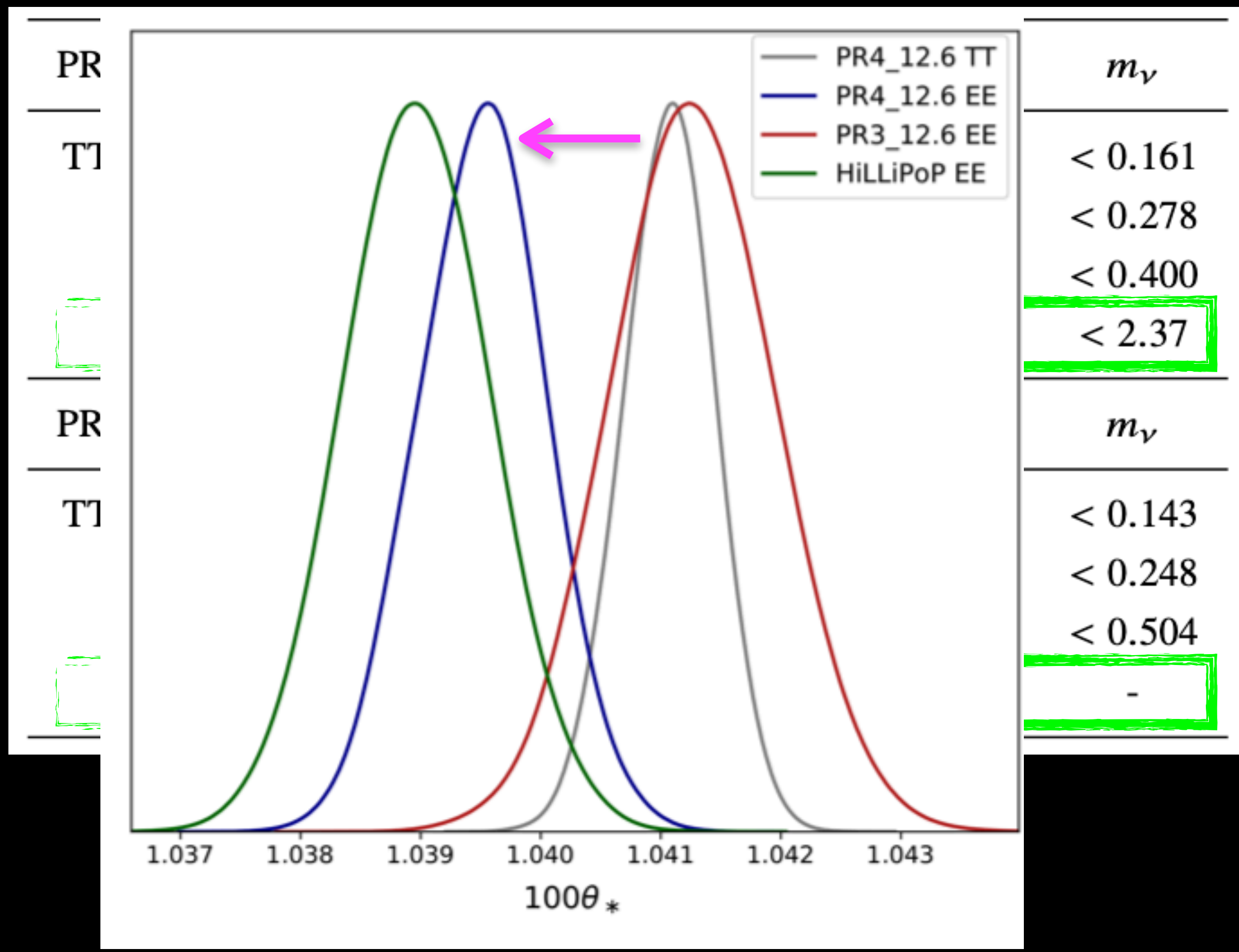

However, this change in EE is producing a significant shift of the acoustic scale parameter θ, and an internal tension at 2.8σ between TT and EE, that becomes more than 3.2-3.3σ when AL/ΩK vary.

Rosenberg et al., arXiv:2205.10869

Planck PR4 (NPIPE) with CamSpec

	ℓ range	N_D	$\hat{\chi}^2$	$(\hat{\chi}^2 - 1)/\sqrt{2/N_D}$
TT 143x143	30 – 2000	1971	1.021	0.67
TT 143x217	500 – 2500	2001	0.985	-0.47
TT 217x217	500 – 2500	2001	1.002	0.05
TT All	30 – 2500	5973	1.074	4.07
TE	30 – 2000	1971	1.055	1.73
EE	30 – 2000	1971	1.026	0.82
TEEE	20 – 2000	3942	1.046	2.02
TTTEEE	30 – 2500	9915	1.063	4.46

Table 1. χ^2 of the different components of the PR4_12.6 likelihood with respect to the TTTEEE best-fit model. N_D is the size of the data vector. $\hat{\chi}^2 = \chi^2/N_D$ is the reduced χ^2. The last column gives the number of standard deviations of $\hat{\chi}^2$ from unity.

..but more significantly, the reduced χ2 values show a more than 4σ tension of the data with the best-fit obtained by TTTEEE assuming a ΛCDM model.

Should we really prioritize
enhancing the agreement with the ΛCDM model over preventing
an internal inconsistency and a worse fit of the data?

Rosenberg et al., arXiv:2205.10869

The role of the optical depth: can the anomalies such as lensing and curvature recast a wrong calibration of τ?

The optical depth

During the cosmic reionization, CMB photons undergo Thomson scattering off free electrons at scales smaller than the horizon size.
As a result, they deviate from their original trajectories, reaching us from a direction different from the one set during recombination.
Similarly to recombination, this introduces a novel 'last scattering' surface at later times and produces distinctive imprints in the angular power spectra of temperature and polarization anisotropies.
A well-known effect of reionization is an enhancement of the spectrum of CMB polarization at large angular scales alongside a suppression of temperature anisotropies occurring at smaller scales.
The distinctive polarization bump produced by reionization on large scales dominates the signal in the EE spectrum whose amplitude strongly depends on the total integrated optical depth to reionization:

$$\tau = \sigma_{\rm T} \int_0^{z_{\rm rec}} dz\, \bar{n}_e(z)\, \frac{dr}{dz},$$

where σ_T is the Thomson scattering cross-section, $\bar{n}_e(z)$ is the free electron proper number density at redshift z, and dr/dz is the line-of-sight proper distance per unit redshift.
For this reason, precise observations of E-mode polarization on large scales are crucial.

Giarè, Di Valentino, Melchiorri, arXiv:2312.06482 [astro-ph.CO]

The optical depth

Thanks to large-scale polarization measurements released by the Planck satellite, we have achieved an unprecedented level of accuracy, constraining the optical depth at reionization down to $\tau = 0.054 \pm 0.008$ at 68% CL.
Measuring τ to such a level of precision holds implications that extend beyond reionization models. For example, the constraints on the Hubble parameter H_0 and the scalar spectral index n_s both improve by approximately 22% when incorporating Planck large-scale polarization data in the analysis.
However, as often happens when dealing with high-precision measurements at low multipoles, there are certain aspects that remain less than entirely clear:

- The detected signal in the EE spectrum is extremely small, on scales where cosmic variance sets itself a natural limit on the maximum precision achievable, and even minor undetected systematic errors could have a substantial impact on the results.

- Small, undetected foreground effects could play a role in determining polarization measurements.

- Measurements of temperature and polarization anisotropies at large angular scales exhibit a series of anomalies. For example, the TE spectrum at low multipoles shows an excess variance compared to simulations, for reasons that are not understood, and is commonly disregarded for cosmological data analyses.

Giarè, Di Valentino, Melchiorri, arXiv:2312.06482 [astro-ph.CO]

The optical depth

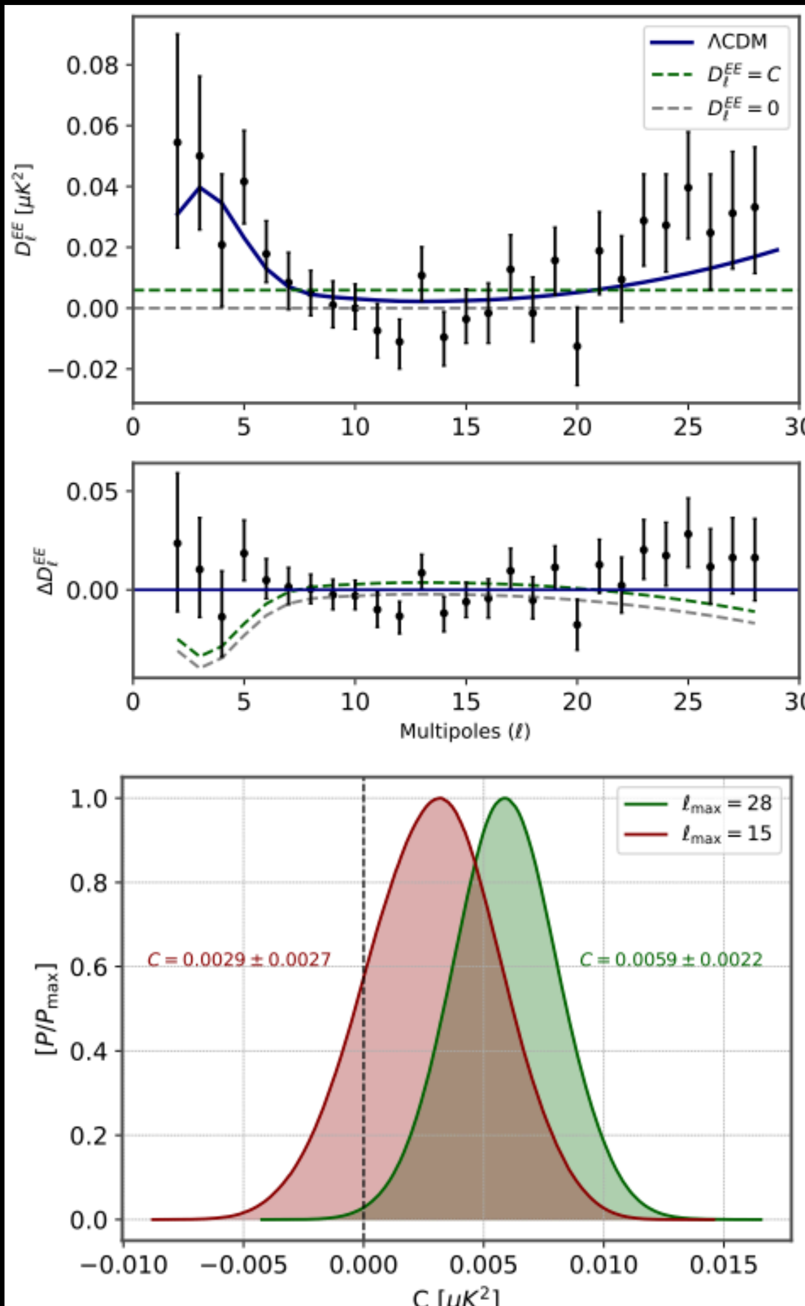

We perform a fit to measurements of the low multipoles EE data assuming a constant instead of the expected reionization bump, and this is compatible with the data with a p-value of p=0.063, above the threshold value typically adopted to reject the hypothesis.

And if we focus only on data-points at $2 \leq l \leq 15$, i.e. those scale that contribute more when determining τ because it is where the reionization bump in polarization manifests itself more prominently, the case C = 0 (i.e., no signal at all) falls basically within the 1σ range.

Therefore we argue the concern that, when dealing with measurements so close to the absence of a signal and experimental sensitivity, any statistical fluctuation or lack of understanding of the foregrounds could be crucial and potentially have implications in the measurement of τ.

Giarè, Di Valentino, Melchiorri, arXiv:2312.06482 [astro-ph.CO]

Planck new physics depends on the optical depth

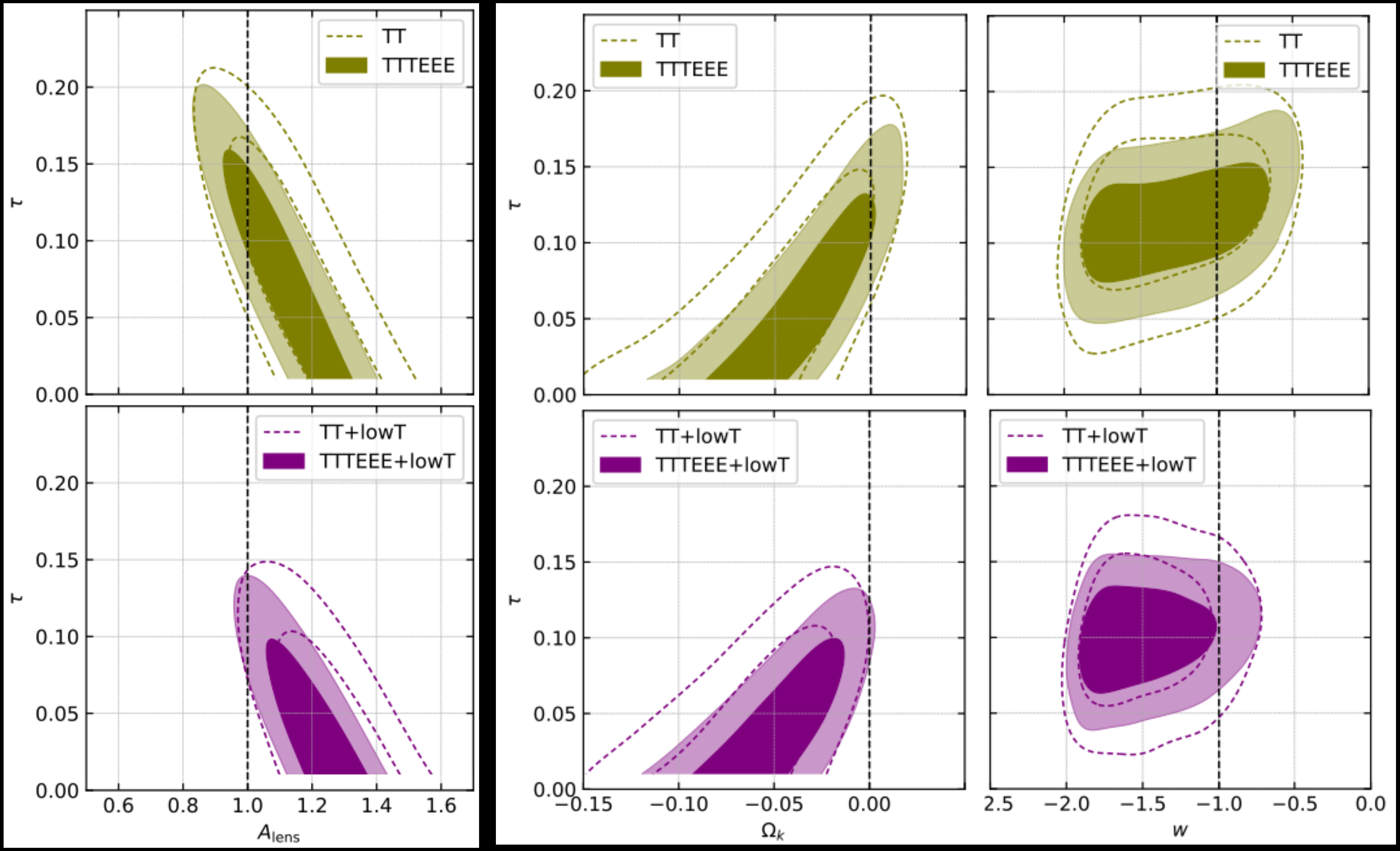

Excluding the lowE data everything is consistent with LCDM.

Giarè, Di Valentino, Melchiorri, arXiv:2312.06482 [astro-ph.CO]

Is it possible to achieve competitive constraints on τ without exclusively relying on large-scale CMB polarization?

lowE independent optical depth

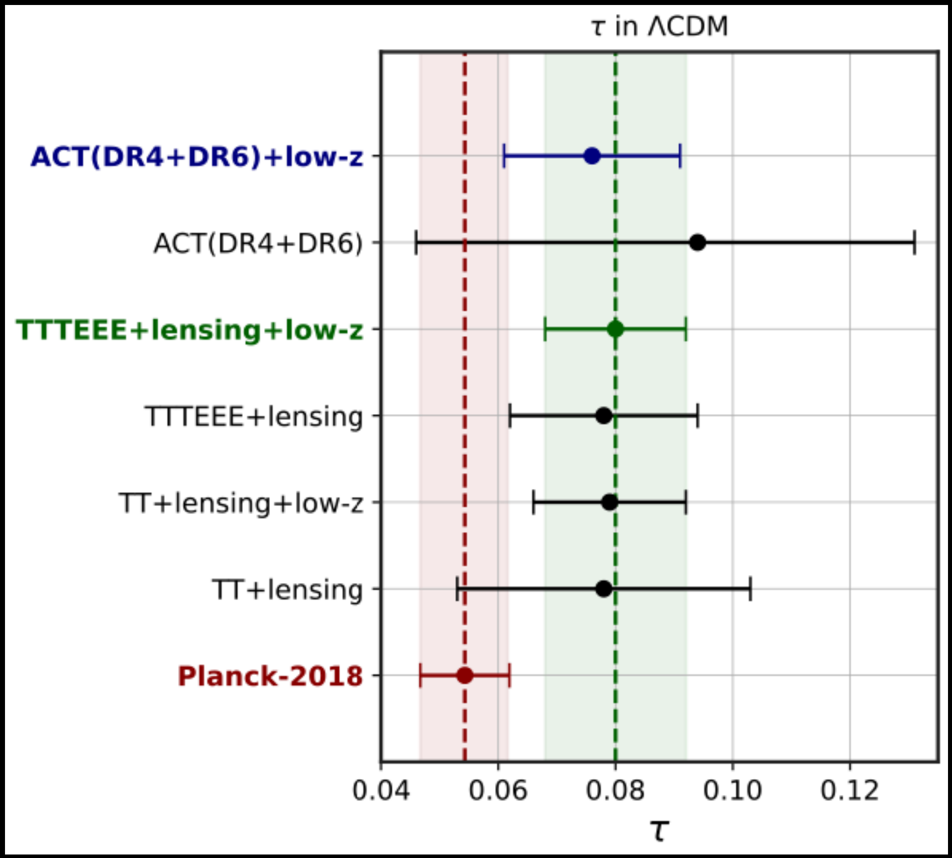

By using different combinations of Planck temperature and polarization data at $l > 30$, ACT and Planck reconstructions of the lensing potential, BAO measurements from BOSS and eBOSS surveys, and Type-Ia supernova data from the Pantheon-Plus sample, we can constrain τ independently.

The most constraining limit $\tau = 0.080 \pm 0.012$ comes from TTTEEE+lensing+low-z.

Using only ACT- based temperature, polarization, and lensing data, from ACT(DR4+DR6)+low-z we got $\tau = 0.076 \pm 0.015$ which is entirely independent of Planck.

Giarè, Di Valentino, Melchiorri, arXiv:2312.06482 [astro-ph.CO]

lowE independent optical depth

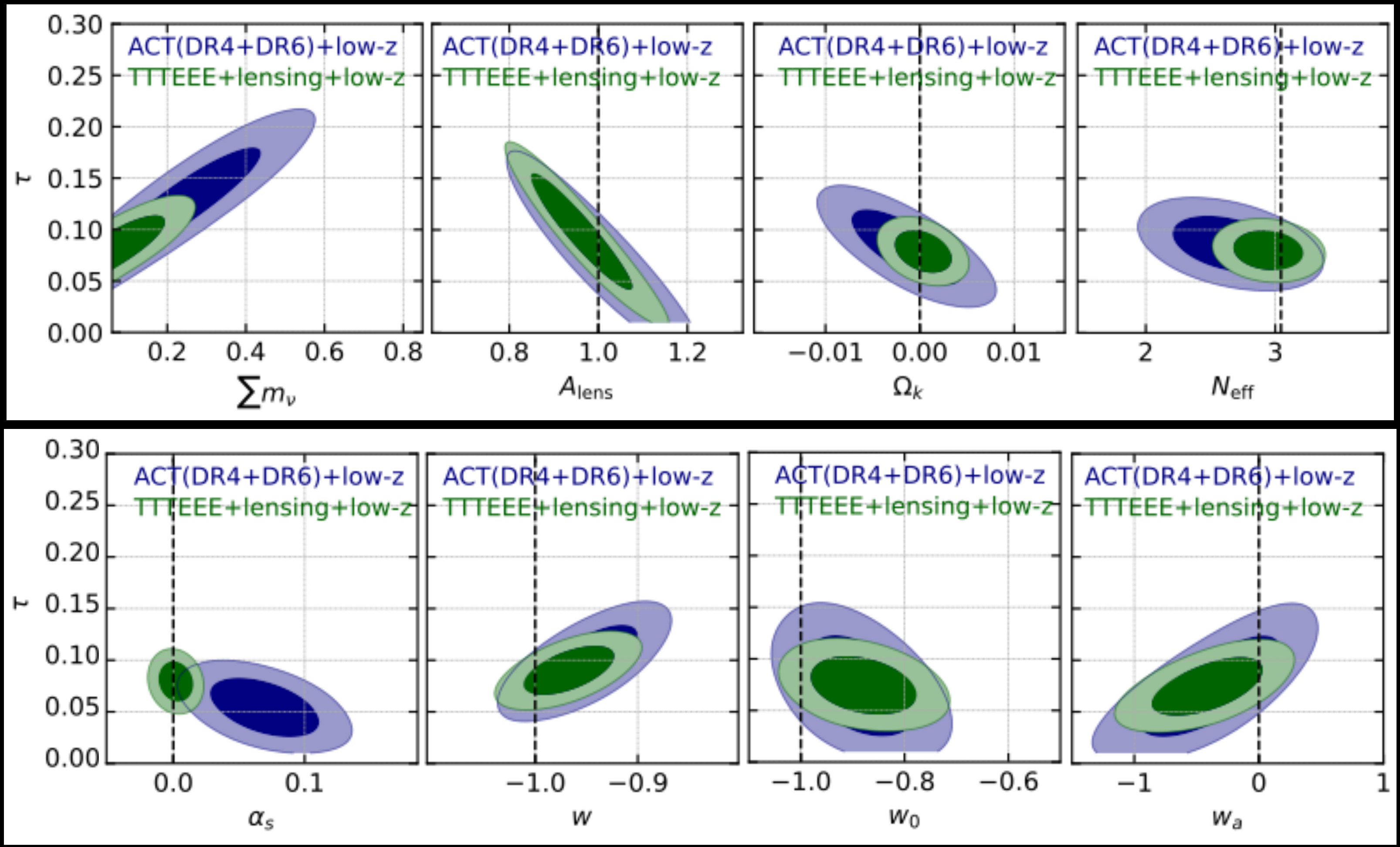

Considering our best combinations to constrain τ the typical LCDM extensions are all in agreement with the expected values.

Giarè, Di Valentino, Melchiorri, arXiv:2312.06482 [astro-ph.CO]

What about the alternative CMB experiments?

Harrison-Zel'dovich scale-invariant spectrum?

Dataset	Scalar Spectral Index (n_s)
	ΛCDM
ACT	1.009 ± 0.015
ACT+BAO (DR12)	1.006 ± 0.013
ACT+BAO (DR16)	1.006 ± 0.014
ACT+DESy1	1.007 ± 0.013
ACT+SPT+BAO (DR12)	0.996 ± 0.012
Planck	0.9649 ± 0.0044
Planck+BAO (DR12)	0.9668 ± 0.0038
Planck+BAO (DR16)	0.9677 ± 0.0037
Planck ($2 \leq \ell \leq 650$)	0.9655 ± 0.0043
Planck ($\ell > 650$)	0.9634 ± 0.0085

Giarè, Renzi, Mena, Di Valentino, and Melchiorri, MNRAS 521 (2023) 2, 2911

ACT shows a preference for a larger spectral index consistent with a Harrison-Zel'dovich scale-invariant spectrum ns=1 of primordial density perturbations introducing a tension with a significance of 2.7σ with the results from the Planck satellite.

Harrison-Zel'dovich scale-invariant spectrum?

Dataset	Scalar Spectral Index (n_s)
	ΛCDM
ACT	1.009 ± 0.015
ACT+BAO (DR12)	1.006 ± 0.013
ACT+BAO (DR16)	1.006 ± 0.014
ACT+DESv1	1.007 ± 0.013

In ACT-DR4 2020, arXiv:2007.07288 [astro-ph.CO] this discrepancy was interpreted as a consequence of the lack of information concerning the first acoustic peak of the temperature power spectrum.

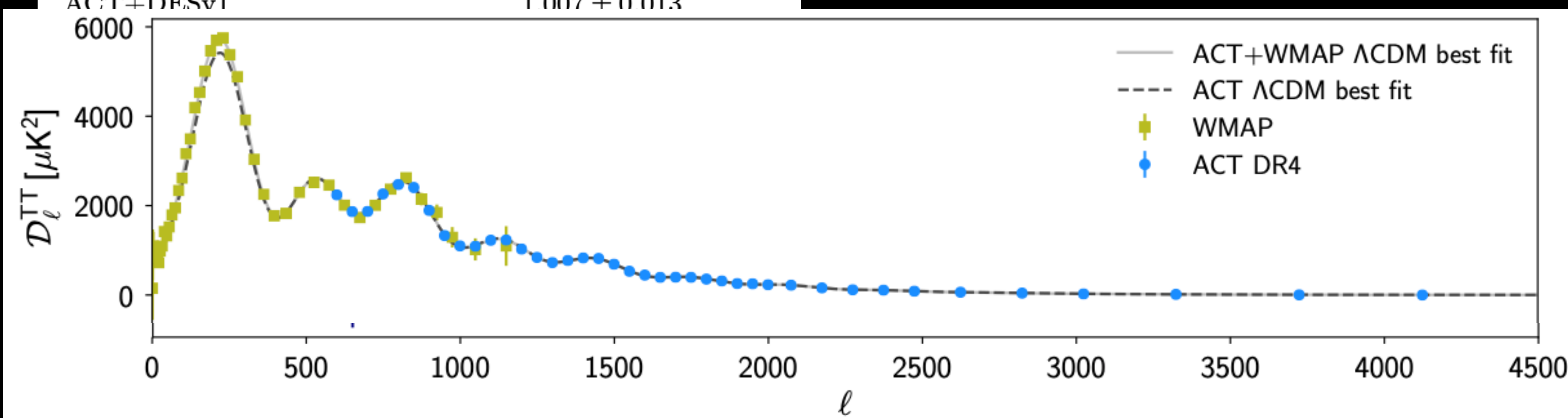

Harrison-Zel'dovich scale-invariant spectrum?

Dataset	Scalar Spectral Index (n_s)
	ΛCDM
ACT	1.009 ± 0.015
ACT+BAO (DR12)	1.006 ± 0.013
ACT+BAO (DR16)	1.006 ± 0.014
ACT+DESy1	1.007 ± 0.013
ACT+SPT+BAO (DR12)	0.996 ± 0.012
Planck	0.9649 ± 0.0044
Planck+BAO (DR12)	0.9668 ± 0.0038
Planck+BAO (DR16)	0.9677 ± 0.0037
Planck ($2 \leq \ell \leq 650$)	0.9655 ± 0.0043
Planck ($\ell > 650$)	0.9634 ± 0.0085

Giarè, Renzi, Mena, Di Valentino, and Melchiorri, MNRAS 521 (2023) 2, 2911

In ACT-DR4 2020, arXiv:2007.07288 [astro-ph.CO] this discrepancy was interpreted as a consequence of the lack of information concerning the first acoustic peak of the temperature power spectrum.

To verify this origin of the discrepancy in the CMB values of ns, we have performed two separate analyses of the Planck observations, splitting the likelihood into low 2< l < 650 and high l > 650 multipoles. We find that the discrepancy still persists at the level of 3σ (2σ) for low (high) multiple temperature data.

Planck data still prefer a value of the scalar spectral index smaller than unity at ~4.3σ when the information about the first acoustic peak is removed.

We tested some models of inflation regarded as well - established benchmark scenarios and found out that they are ruled out by ACT at more than 3σ.

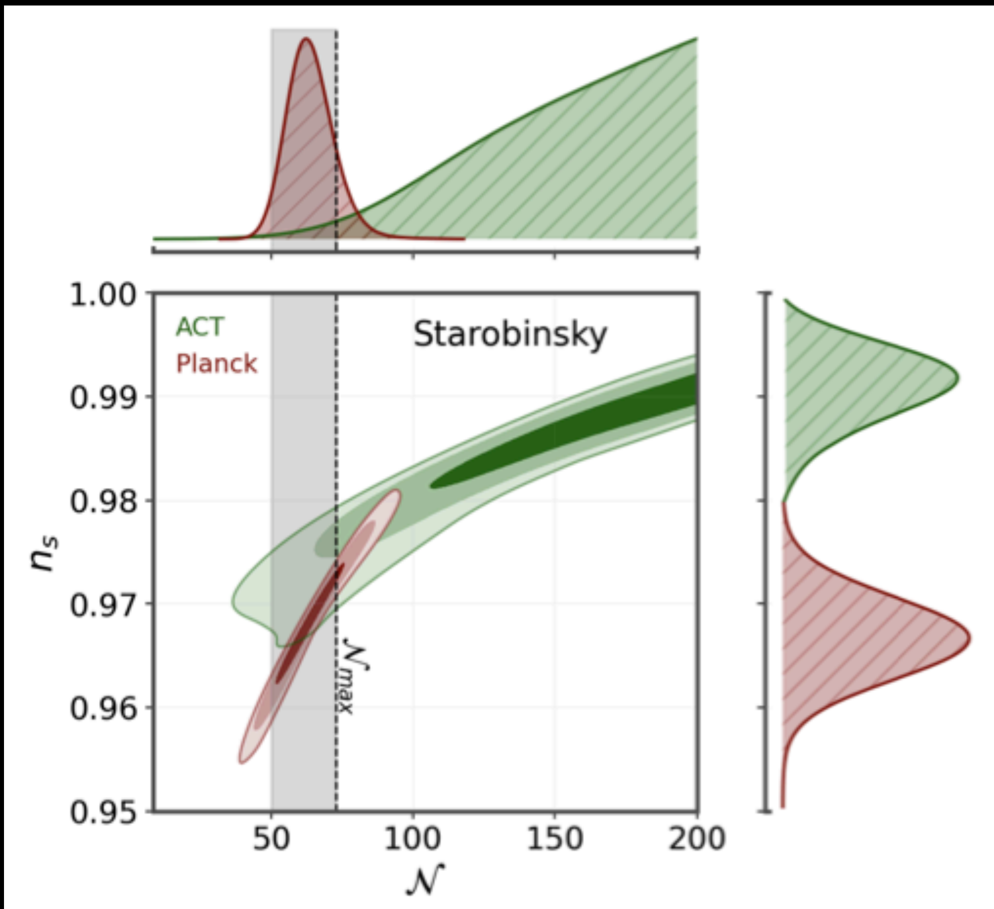

Giarè, Pan, Di Valentino, Yang, de Haro, and Melchiorri, *JCAP* 09 (2023) 019

In the plot we show for example the 2D contours at 68%, 95%, and 99% CL and 1D posteriors in the (n_s, N_{efolds}) plane for the Starobinsky model.
The grey vertical band refers to the typical range of folds expansion $N_{efolds} \in [50, N_{max}]$, expected in standard inflation.
The upper limit, $N_{max} \leq 73$, is represented by the black dashed line.

Very similar results are obtained for all the other potentials, and in particular for ACT we find the following values for the number of e-folds at 68% (95%) CL:

- $\mathcal{N} > 138$ ($\mathcal{N} > 92.8$) for the Starobinsky model;
- $\mathcal{N} > 134$ ($\mathcal{N} > 88.6$) for α-Attractor models;
- $\mathcal{N} > 257$ ($\mathcal{N} > 208$) for Polynomial inflation;
- $\mathcal{N} > 177$ ($\mathcal{N} > 105$) for the SUSY potential.

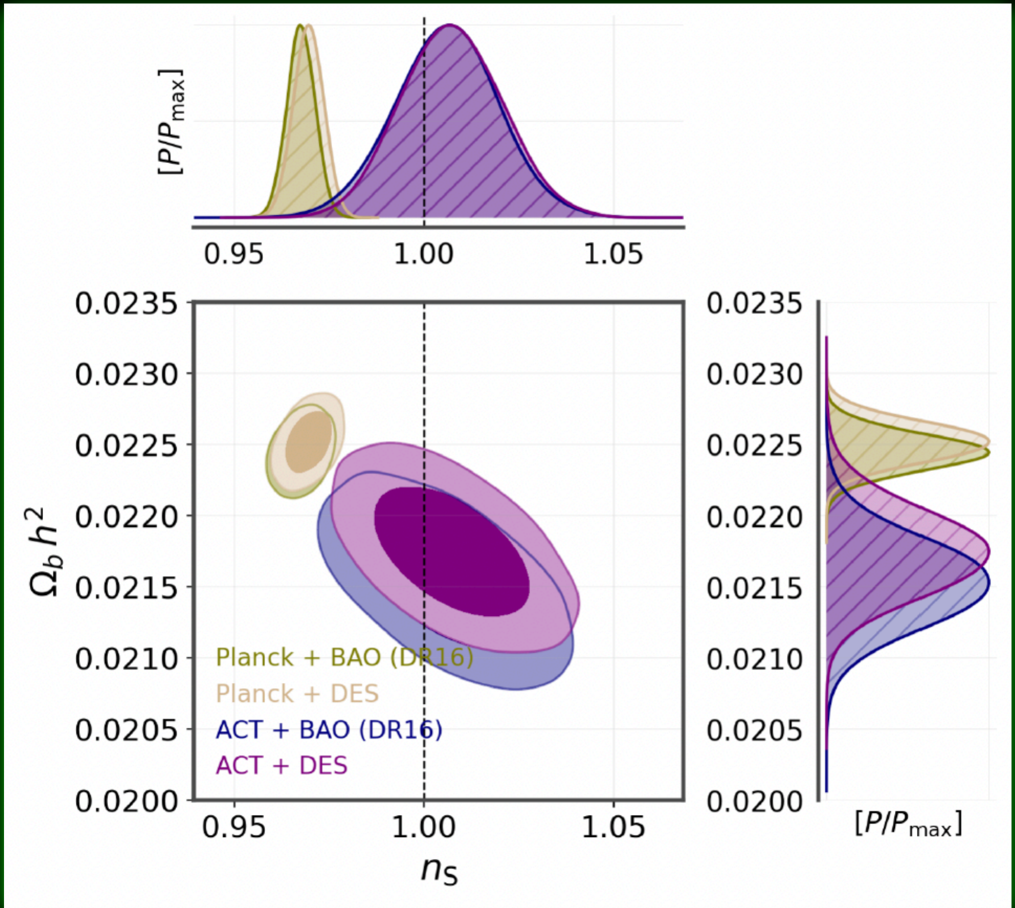

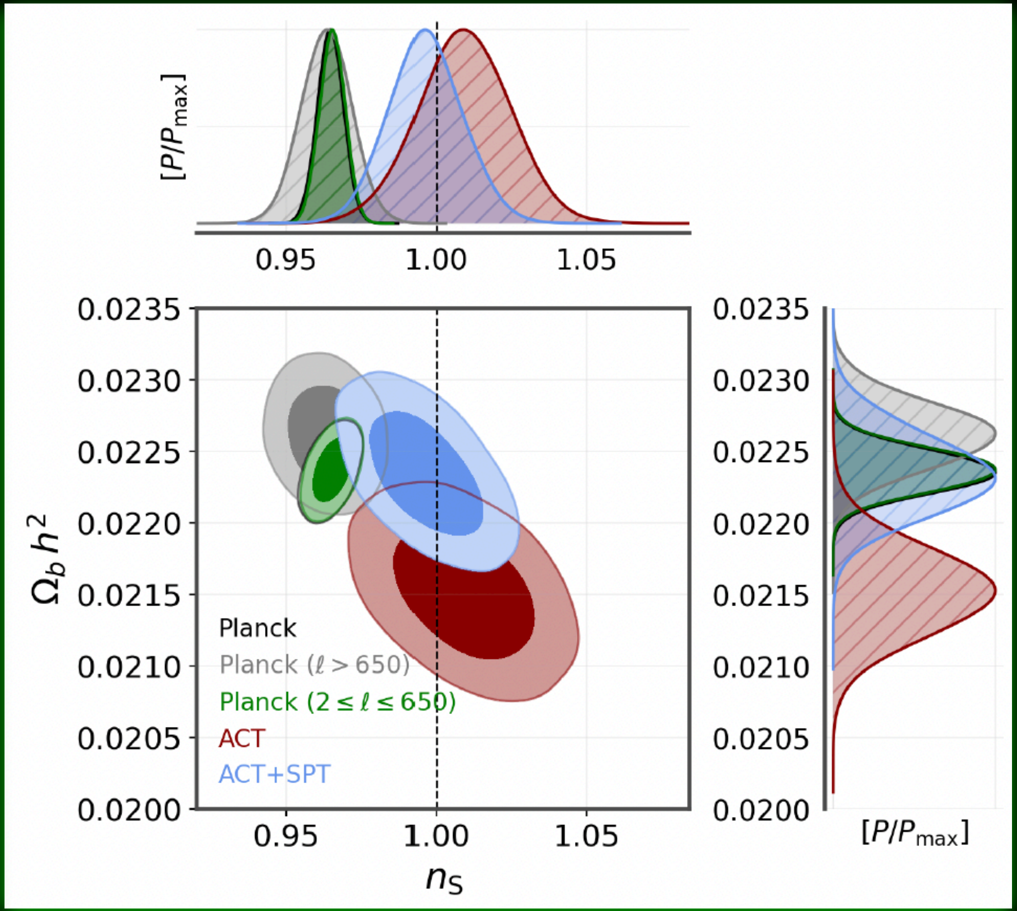

Giarè, Renzi, Mena, Di Valentino, and Melchiorri, MNRAS 521 (2023) 2, 2911

Such preference remains robust under the addition of large scale structure information,
and in the two-dimensional plane it can be definitely noted that
the direction of the $\Omega_b h^2$ - ns degeneracy is opposite for ACT and Planck,
and the disagreement here is significantly exceeding 3σ.
This tension is partially driven by the ACT polarization data,
as we can see replacing it with the SPT polarization measurements, but while the tension is
relaxed in the plane $\Omega_b h^2$ - ns, this combination is still preferring ns=1.

Quantifying global CMB tension

Handley and Lemos, arXiv:2007.08496 [astro-ph.CO]

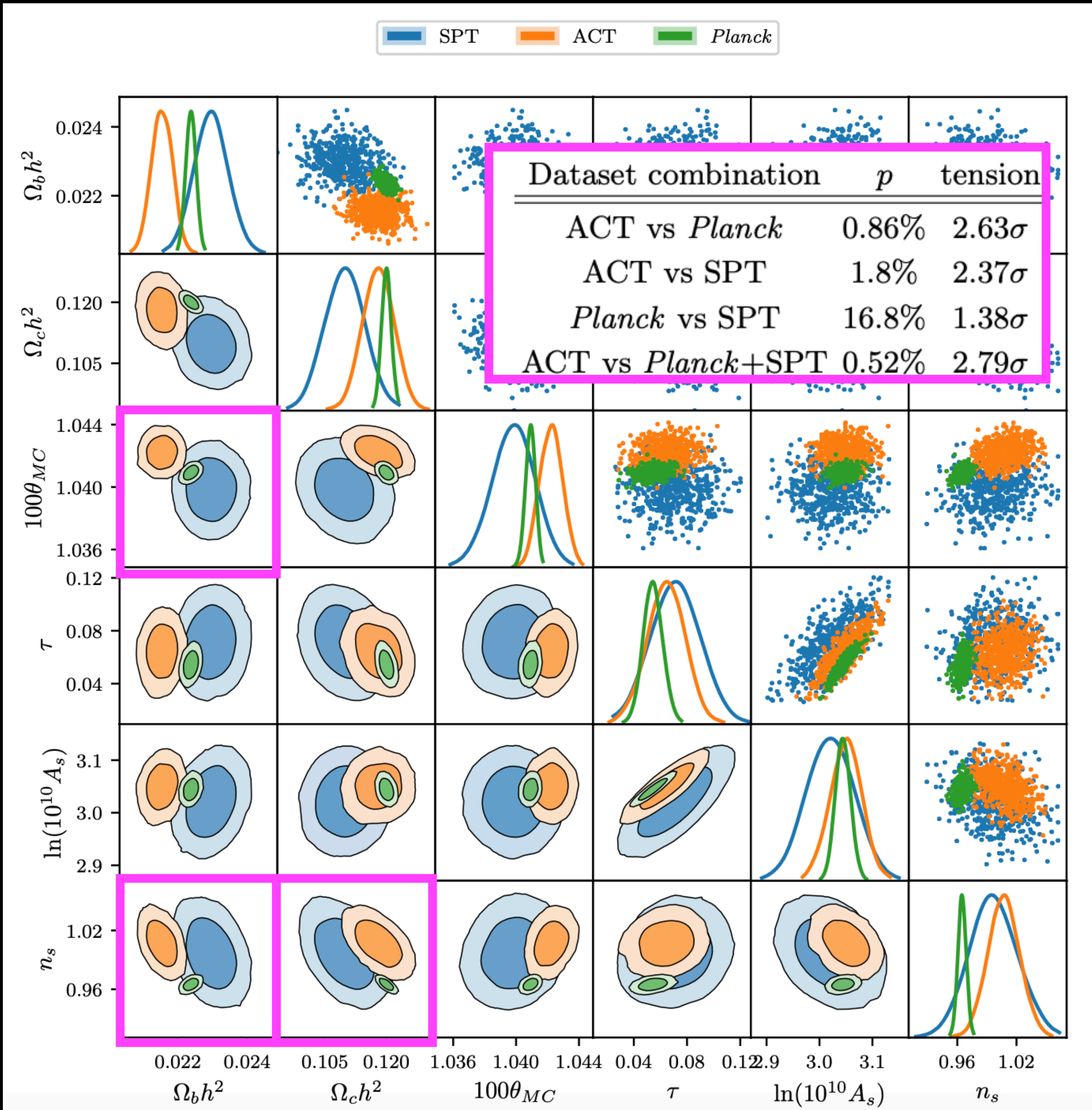

Dataset combination	p	tension
ACT vs *Planck*	0.86%	2.63σ
ACT vs SPT	1.8%	2.37σ
Planck vs SPT	16.8%	1.38σ
ACT vs *Planck*+SPT	0.52%	2.79σ

Global tensions between CMB datasets.

For each pairing of datasets this is the tension probability p that such datasets would be this discordant by (Bayesian) chance, as well as a conversion into a Gaussian-equivalent tension.

Between Planck and ACT there is a 2.6σ tension.

Assuming ΛCDM

ACT-DR4 vs Planck: EDE

Constraints on EDE ($n = 3$)

Parameter	ACT DR4 TT+TE+EE, τ	ACT DR4 TT+TE+EE, *Planck* 2018 TT ($\ell_{\rm max} = 650$), τ	ACT DR4 TT+TE+EE, *Planck* 2018 TT ($\ell_{\rm max} = 650$), *Planck* 2018 lensing, BAO, τ	*Planck* 2018 TT+TE+EE (from Ref. [38])	ACT DR4 TT+TE+EE, *Planck* 2018 TT+TE+EE (no low-ℓ EE), τ
$f_{\rm EDE}$	$0.142^{+0.039}_{-0.072}$	$0.129^{+0.028}_{-0.055}$	$0.091^{+0.020}_{-0.036}$	< 0.087	< 0.124
$\log_{10}(z_c)$	< 3.70	< 3.43	< 3.36	$3.66^{+[illegible]}_{-0.28}$	$3.54^{+[illegible]}_{-0.20}$
θ_i	> 0.24	< 2.89	< 2.82	> 0.36	> 0.51
$\Omega_c h^2$	$0.1307^{+0.0054}_{-0.0120}$	$0.1291^{+0.0051}_{-[illegible]}$	$0.1286^{+0.0027}_{-[illegible]}$	$0.1234^{+0.0019}_{-0.0038}$	$0.1244^{+0.0025}_{-[illegible]}$
H_0 [km/s/Mpc]	$74.5^{+2.5}_{-4.4}$	$74.4^{+2.2}_{-3.0}$	$70.9^{+1.0}_{-2.0}$	$68.29^{+0.73}_{-1.20}$	$69.17^{+0.83}_{-1.70}$
Ω_m	$0.276^{+[illegible]}_{-0.023}$	0.274 ± 0.017	0.3000 ± 0.0072	0.3145 ± 0.0086	0.3084 ± 0.0084
σ_8	$0.831^{+0.027}_{-0.043}$	$0.827^{+0.029}_{-0.035}$	$0.829^{+0.013}_{-0.021}$	$0.820^{+0.009}_{-0.013}$	$0.838^{+0.013}_{-0.015}$
S_8	0.796 ± 0.049	$0.791^{+0.040}_{-0.046}$	$0.828^{+0.015}_{-0.018}$	0.839 ± 0.018	0.850 ± 0.017

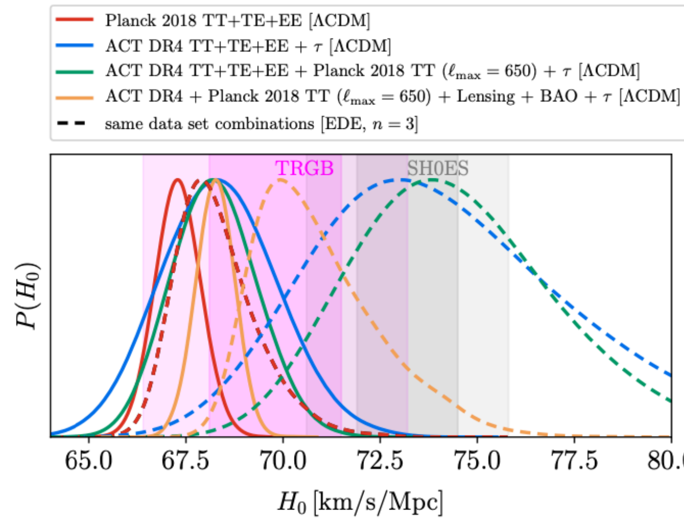

ACT collaboration, Hill et al. arXiv:*2109.04451*

Considering ACT only data or combined with Planck TT up to multipoles 650, there is an evidence for EDE > 3σ, solving completely the Hubble tension.

The evidence for EDE > 3σ persists with the inclusion of Planck lensing + BAO data, but shifting H0 towards a lower value.

Once the full Planck data are considered, the evidence for EDE disappears and H0 is again in tension with SH0ES.

The Planck damping tail is in disagreement with EDE different from zero.

ACT-DR4 vs Planck: α_s and β_s

Forconi, Giarè, Di Valentino and Melchiorri, *Phys.Rev.D* 104 (2021) 10, 103528

Parameter	Planck18	ACTPol + WMAP
$\Omega_b h^2$	0.02235 ± 0.00017	0.02195 ± 0.00025
$\Omega_c h^2$	0.1207 ± 0.0015	0.1190 ± 0.0029
[illegible]	[illegible]1	1.04174 ± 0.00066
[illegible]	[illegible]6	0.061 ± 0.013
$\log(10^{10} A_S)$	3.053 ± 0.018	3.051 ± 0.026
n_s	0.9612 ± 0.0054	0.9680 ± 0.0082
α_s	0.001 ± 0.010	0.035 ± 0.012
β_s	0.012 ± 0.013	0.035 ± 0.013

$$\alpha_s \doteq \left[\frac{dn_s}{d\log k}\right]_{k=k_*} \qquad \beta_s \doteq \left[\frac{d\alpha_s}{d\log k}\right]_{k=k_*}$$

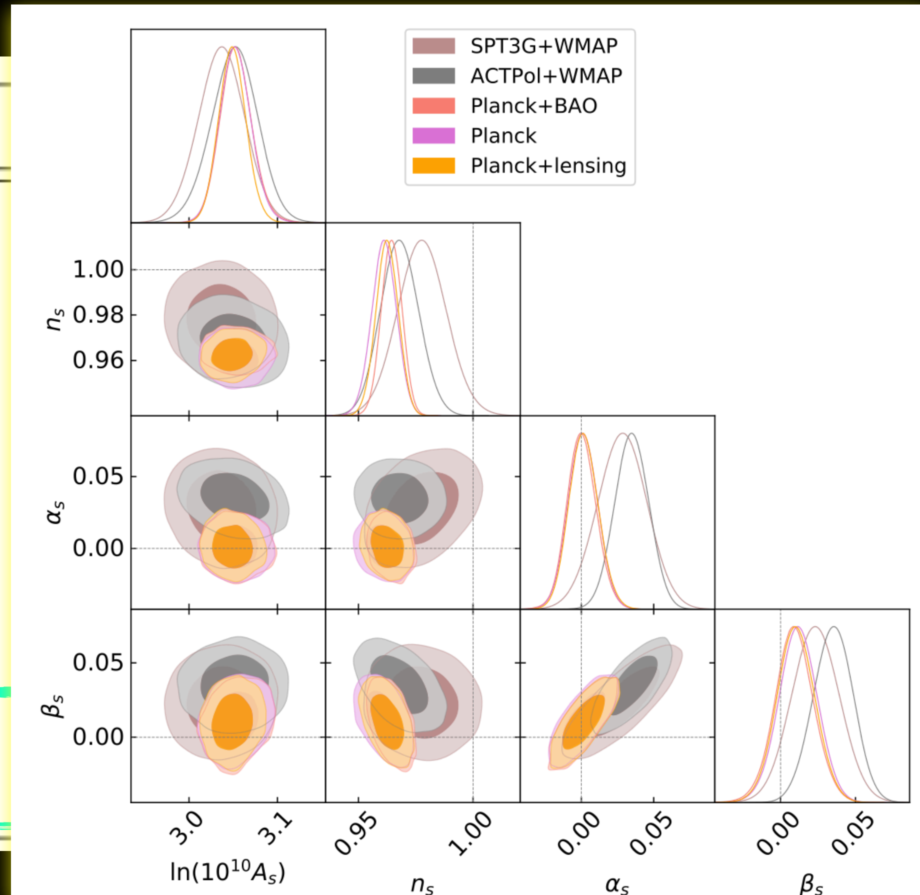

ACT-DR4 and SPT-3G are in agreement one with each other, but in disagreement with Planck, for the value of the running of the scalar spectral index α_s and of the running of the running β_s.

In particular ACT-DR4 + WMAP prefer both a non vanishing running α_s and running of the running β_s at the level of 2.9σ and 2.7σ, respectively.

Alternative CMB vs Planck: Σmν

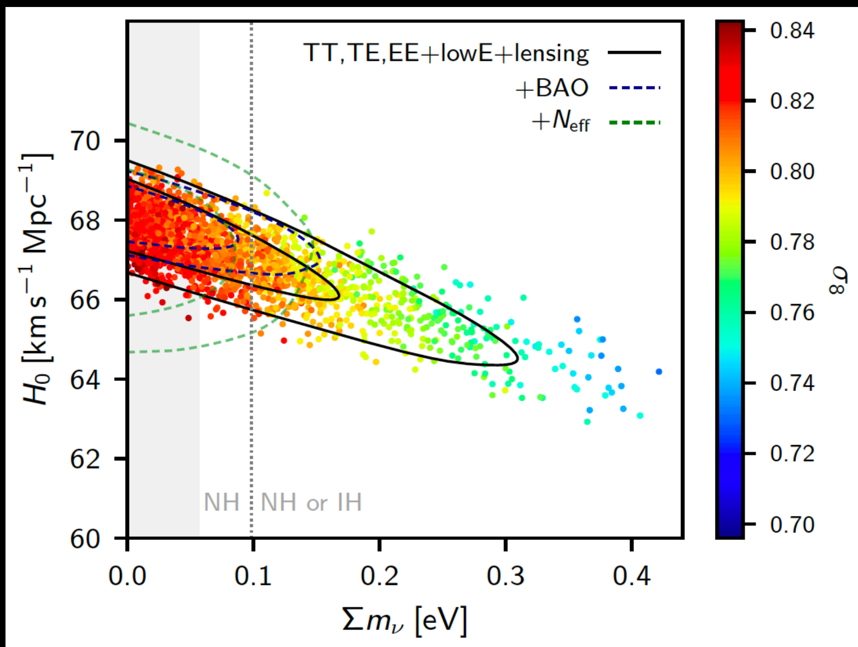

$$\sum m_\nu < 0.24 \text{ eV} \quad (95\,\%,\ \text{TT,TE,EE+lowE+lensing})$$

Planck 2018 collaboration, arXiv:1807.06209 [astro-ph.CO]

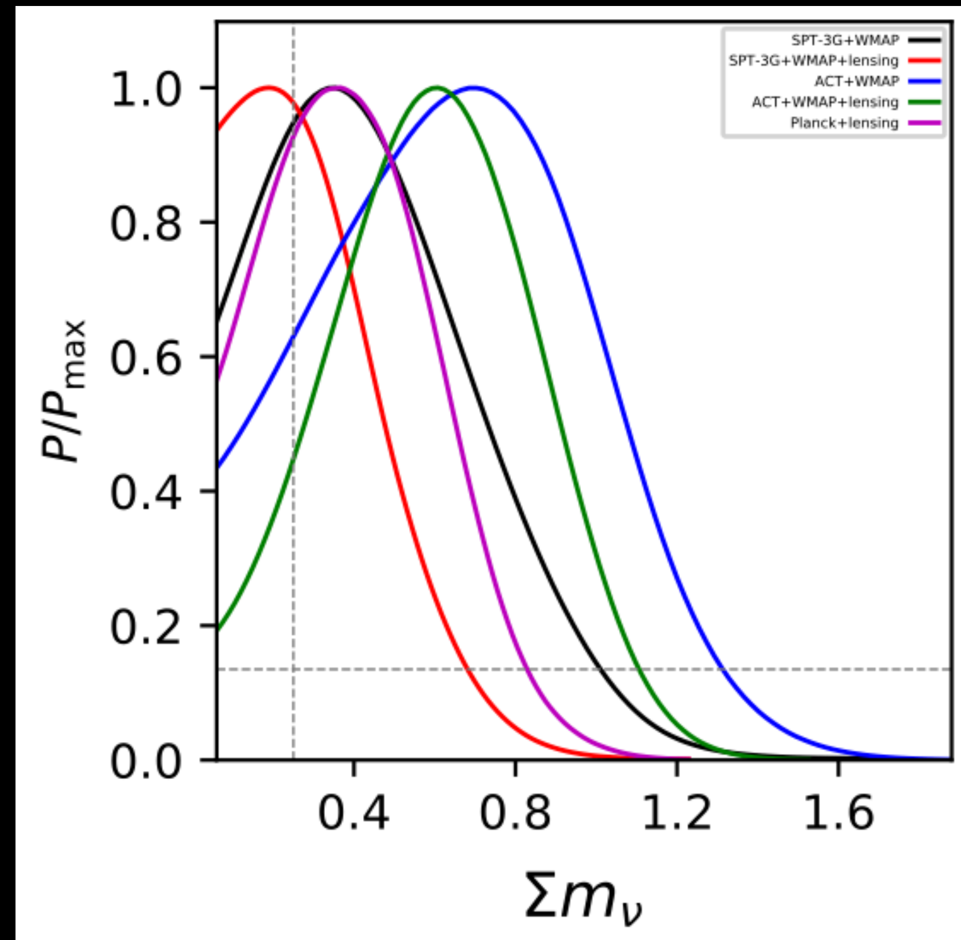

Di Valentino and Melchiorri, 2022 *ApJL* **931** L18

While we have only an upper limit for Planck on the total neutrino mass, ACT-DR4, when combined with WMAP and lensing, prefers a neutrino mass different from zero at more than 95% CL.

Constraints at 68% CL

Dataset	Σm_ν [eV]
ACT-DR4+WMAP+Lensing	0.60 ± 0.25
Planck+Lensing ($+A_{\rm lens}$)	$0.41^{+0.17}_{-0.25}$

Quantifying global CMB tension

Cosmological model	d	χ^2	p	$\log S$	Tension
ΛCDM	6	16.3	0.012	-5.17	$2.51\,\sigma$
$\Lambda\text{CDM} + A_{\text{lens}}$	7	18.5	0.00977	-5.77	$2.58\,\sigma$
$\Lambda\text{CDM} + N_{\text{eff}}$	7	13	0.0719	-3	$1.80\,\sigma$
$\Lambda\text{CDM} + \Omega_k$	7	16.5	0.0209	-4.75	$2.31\,\sigma$
wCDM	7	16.8	0.0187	-4.9	$2.35\,\sigma$
$\Lambda\text{CDM} + \sum m_\nu$	7	20.7	0.00421	-6.86	$2.86\,\sigma$
$\Lambda\text{CDM} + \alpha_s$	7	20.6	0.00448	-6.78	$2.84\,\sigma$
$w\text{CDM} + \Omega_k$	8	17.6	0.0249	-4.78	$2.24\,\sigma$
$\Lambda\text{CDM} + \Omega_k + \sum m_\nu$	8	21.2	0.00651	-6.62	$2.72\,\sigma$
$w\text{CDM} + \Omega_k + \sum m_\nu$	9	19.8	0.0195	-5.38	$2.34\,\sigma$
$w\text{CDM} + \Omega_k + \sum m_\nu + N_{\text{eff}}$	10	18.8	0.0434	-4.38	$2.02\,\sigma$
$w\text{CDM} + \Omega_k + \sum m_\nu + \alpha_s$	10	22	0.015	-6.01	$2.43\,\sigma$
$w\text{CDM} + \Omega_k + N_{\text{eff}} + \alpha_s$	10	20.9	0.0218	-5.45	$2.29\,\sigma$
$w\text{CDM} + \sum m_\nu + N_{\text{eff}} + \alpha_s$	10	31.1	0.000575	-10.5	$3.44\,\sigma$
$w\text{CDM} + \Omega_k + \sum m_\nu + N_{\text{eff}} + \alpha_s$	11	24.7	0.0102	-6.83	$2.57\,\sigma$

Di Valentino et al., MNRAS 520 (2023) 1, 210-215

$\Lambda\text{CDM} + N_{\text{eff}}$	Planck	–	2.92 ± 0.19
	ACT-DR4	–	$2.35^{+0.40}_{-0.47}$

If we now study the global agreement between Planck and ACT in various cosmological models that differ by the inclusion of different combinations of additional parameters, we can use the Suspiciousness statistic, to quantify their global "CMB tension".

We find that the 2.5σ tension within the baseline ΛCDM is reduced at the level of 1.8σ when Neff is significantly less than 3.044, while it ranges between 2.3σ and 3.5σ in all the other extended models.

Concluding

At this point, given the quality of all the analyses at play,
probably these tensions are indicating a problem with the underlying cosmology and our understanding of the Universe,
rather than the presence of systematic effects.

Many models have been proposed to solve the H0 tension.
However, looking for a solution by changing the standard model of cosmology is challenging because of some additional complications:

1. The sound horizon problem
2. The S8 tension
3. The correlation between the parameters and possible fake detection
4. The hidden model dependence of some of the datasets (such as BAO)
5. The Planck AL problem
6. The role of the optical depth
7. The inconsistency between the different CMB experiments

Therefore, this is presenting a serious limitation to the precision cosmology.

These cosmic discordances
call for new observations and stimulate the investigation of alternative theoretical models and solutions.

MENU

Thank you!

e.divalentino@sheffield.ac.uk

COSMOVERSE • COST ACTION CA21136

Addressing observational tensions in cosmology with systematics and fundamental physics

https://cosmoversetensions.eu/

WG1 – Observational Cosmology and systematics

Unveiling the nature of the existing cosmological tensions and other possible anomalies discovered in the future will require a multi-path approach involving a wide range of cosmological probes, various multiwavelength observations and diverse strategies for data analysis.

READ MORE

WG2 – Data Analysis in Cosmology

Presently, cosmological models are largely tested by using well-established methods, such as Bayesian approaches, that are usually combined with Monte Carlo Markov Chain (MCMC) methods as a standard tool to provide parameter constraints.

READ MORE

WG3 – Fundamental Physics

Given the observational tensions among different data sets, and the unknown quantities on which the model is based, alternative scenarios should be considered.

READ MORE